University of Alberta

Structural and Functional Analysis of Calreticulin and Calnexin

By

Jody Groenendyk ©

A thesis submitted to the Faculty of Graduate Studies and Research in partial fulfillment of the requirements for the degree of Doctor of Philosophy

Medical Sciences - Pediatrics

Edmonton, Alberta

Fall, 2006

Library and Archives Canada

Published Heritage Branch

395 Wellington Street
Ottawa ON K1A 0N4
Canada

Bibliothèque et Archives Canada

Direction du Patrimoine de l'édition

395, rue Wellington
Ottawa ON K1A 0N4
Canada

Your file Votre référence
ISBN: 978-0-494-23037-4
Our file Notre référence
ISBN: 978-0-494-23037-4

NOTICE:
The author has granted a non-exclusive license allowing Library and Archives Canada to reproduce, publish, archive, preserve, conserve, communicate to the public by telecommunication or on the Internet, loan, distribute and sell theses worldwide, for commercial or non-commercial purposes, in microform, paper, electronic and/or any other formats.

The author retains copyright ownership and moral rights in this thesis. Neither the thesis nor substantial extracts from it may be printed or otherwise reproduced without the author's permission.

AVIS:
L'auteur a accordé une licence non exclusive permettant à la Bibliothèque et Archives Canada de reproduire, publier, archiver, sauvegarder, conserver, transmettre au public par télécommunication ou par l'Internet, prêter, distribuer et vendre des thèses partout dans le monde, à des fins commerciales ou autres, sur support microforme, papier, électronique et/ou autres formats.

L'auteur conserve la propriété du droit d'auteur et des droits moraux qui protège cette thèse. Ni la thèse ni des extraits substantiels de celle-ci ne doivent être imprimés ou autrement reproduits sans son autorisation.

In compliance with the Canadian Privacy Act some supporting forms may have been removed from this thesis.

While these forms may be included in the document page count, their removal does not represent any loss of content from the thesis.

Conformément à la loi canadienne sur la protection de la vie privée, quelques formulaires secondaires ont été enlevés de cette thèse.

Bien que ces formulaires aient inclus dans la pagination, il n'y aura aucun contenu manquant.

Canada

ABSTRACT

Calreticulin and calnexin perform a unique function in the ER, in conjunction with ERp57, to work together to specifically chaperone nascent glycoproteins, facilitating their delivery to their target location in a functionally competent manner. In this study, we investigate the functional importance of specific amino acid residues in calreticulin and calnexin. An essential His153 is identified by mutational analysis to be involved in the coordination of Zn^{2+} in the N-domain of calreticulin, necessary for the chaperone function of calreticulin. Trp244 and Trp302 are also identified as essential residues, *in vivo* and *in vitro*, for the chaperone function of calreticulin. Two amino acids, Glu351 and Trp302, are important for calnexin function. Amino acid residues involved in calreticulin-ERp57 interactions are also identified. Asp241 and Trp244 are critical for binding to ERp57 and residues Glu239 and Glu243 exhibite significant reduction in ERp57 binding. A similar conserved amino acid residue in calnexin, Glu351 (calreticulin Glu243) did not demonstrate the same disturbance in ERp57 binding, indicating that calreticulin and calnexin may interact with ERp57 in different manners. Interestingly, Trp302, an amino acid residue in a globular N-domain of calreticulin, also affects ERp57 binding. Mutation of this conserved amino acid residue in calnexin demonstrated enhanced ERp57 binding, presumably as a result of structural changes in the conformation of the protein. We also show that Zn^{2+} plays an important role as a structural molecule in the N-domain of calreticulin. Ca^{2+} binding to calreticulin and calnexin affect stability in both proteins. Nucleotide binding to calnexin and calreticulin demonstrated structural dependence on this interaction.

A role for calnexin in ER stress-induced apoptosis is investigated. We showed that calnexin-deficient human T-lymphoblasts and calnexin-deficient mouse embryonic

fibroblasts have reduced Bap31 cleavage as well as increased resistance to apoptosis. In the ER, calnexin formed functional complexes with Bap31 and caspase 12 which are involved in the proper transmission of ER stress-induced apoptotic signals. The multiple functions of the proteins localized to the ER and disruption of ER Ca^{2+} homeostasis results not only in organellar disease but will have detrimental effects at cellular and systemic levels as well.

ACKNOWLEDGEMENTS

I would like to thank my supervisor, Dr. Marek Michalak. You have always been a great boss, supervisor and friend. You are always there to bounce ideas off and constantly enthusiastic. The reason I am still here after 15 years is because of you. The reason I enjoy my work is because of you! Thank you! You are the best!

I would like to thank the members of my supervisory committee, Dr. R. Chris Bleackley and Dr. Larry Fliegel. You were always helpful and I benefited greatly from your constructive input and knowledge.

I would also like to thank all the people over the years that have kept me sane and made the lab a great deal of fun. Thank you Monika, you have been through the same things that I have, always with a smile! Thank you Sandi for being my roommate and always being here. You are so enjoyable to be around! Thank you Helen for being there to talk to. You and I have so much in common! Thank you Yuan, Alison and Asia, you have many years of enjoyment ahead and I look forward to working with you. Thank you to Simone for protein modeling and best wishes at home with your new baby! Thank you, Pam. You are a great student and I hope that I will be a good supervisor for you. We will have fun in the years ahead. As well, I would like to thank Karen, Robert, Shairaz, Nasrin and all the others who have helped to shape the researcher and person that I have become. Thank you to all.

Finally, I would like to acknowledge both the Canadian Institute for Health Research and the Alberta Heritage Foundation for Medical Research for financial support during my Ph.D. studies. I am honoured to be a recipient of such prestigious awards.

TABLE OF CONTENTS

Chapter One — Quality Control in the Endoplasmic Reticulum **1**

Introduction 2

The Endoplasmic Reticulum and Ca^{2+} 5

Role of the Endoplasmic Reticulum in Protein Synthesis and Folding 11

Quality Control of the Secretory Pathway 12

Endoplasmic Reticulum Associated Degradation (ERAD) 18

Calreticulin and Calnexin 21

The N-Domain of Calreticulin and Calnexin 25

The P-Domain of Calreticulin and Calnexin 26

The C-Domain of Calreticulin and Calnexin 27

Calreticulin and Calnexin Deficient Mice 29

Calreticulin and Calnexin, Multifunctional Proteins 30

ERp57 35

Unfolded Protein Response (UPR) 38

ER and Apoptosis 43

Apoptosis and Ca^{2+} 48

Research Objective 51

Research Hypothesis 52

Chapter Two — Materials and Methods **53**

Chemicals and Materials 54

Isolation and Generation of Calreticulin and Calnexin-Deficient Mouse Embryonic Fibroblasts ... 56

Cell Culture 56

Flow Cytometry of Antibody Labeled Wild-type and Calreticulin-Deficient Mouse Embryonic Fibroblasts 57

Western Blot Analysis of Cell Lysates 57

Plasmids and Site-directed Mutagenesis of Calreticulin and Calnexin 60

Generation and Purification of Recombinant Proteins 61

Protein Aggregation Assay of Calreticulin and Calnexin Wild-type and Mutant Proteins 63

Intrinsic Fluorescence Assay of Calreticulin and Calnexin Wild-type and Mutant Proteins 64

Proteolytic Digestion of Calreticulin and Calnexin Wild-type and Mutant Proteins 64

CD Analysis of Calreticulin and Calnexin Wild-type and Mutant Proteins 64
Surface Plasmon Resonance Analysis of Calreticulin and Calnexin Wild-type and Mutant Proteins 65
Analysis of Ca^{2+} Binding to Recombinant Proteins 66
Measurements of Intracellular Ca^{2+} Concentration 67
Generation of the Calnexin-Deficient Mouse 68
Isolation and Purification of DNA 70
PCR Analysis of Wild-type and Calnexin-Deficient Mouse Embryos 70
X-Galactosidase Staining and Western Blot Analysis of Wild-type and Calnexin-Deficient Mouse Embryos 70
Southern Blot Analysis of Wild-type and Calnexin-Deficient Embryos 71
Purification of RNA 72
Apoptosis and Caspase Assays 73
Indirect Immunofluorescence and Electron Microscopy 75
Drug Treatment of Cells 77
Immunoprecipitation 78
Determination of Protein Concentration 79
Chapter Three — Mutational Analysis of Calreticulin **84**
Introduction 85
Results 86
Expression of Mutants in Calreticulin-Deficient Cells 86
Bradykinin-Induced Ca^{2+} Release in Cells Expressing Calreticulin Mutants 90
Effect of Calreticulin Mutants on Thermal Aggregation of MDH and IgY 95
Structural Analysis of Calreticulin Mutants 100
Association of ERp57 with Calreticulin 114
Discussion 119
Chapter Four — Mutational Analysis of Calnexin **130**
Introduction 131
Results 132
Cascade Blue Analysis of S-Cnx 132
CD Analysis of Purified S-Cnx 134
Limited Trypsin Digestion of S-Cnx and Mutants 137

Intrinsic Fluorescence of S-Cnx and Mutants 139
The Ability of S-Cnx to Prevent Aggregation 139
Protein Interaction of S-Cnx and Mutants with ERp57 142
Interaction of Calnexin and Mutants with ATP 145
Discussion 148
Chapter Five — Calnexin and Apoptosis 153
Introduction 154
Results 155
Identification of a Caspase 12-like Protein in Human Leukemic T-cells 155
ER Stress Response in Calnexin-Deficient Cells — CEM and NKR 159
ER Stress Response in Calnexin-Deficient Cells — MEFs 161
Expression of Apoptotic Proteins in Calnexin-Deficient Cells after ER Stress-Induced Apoptosis — CEM and NKR 163
Expression of Apoptotic Proteins in Calnexin-Deficient Cells after ER Stress-Induced Apoptosis — MEFs 165
ER Stress-Induced Apoptosis in Calnexin-Deficient Cells 168
ER Ca^{2+} Homeostasis in Calnexin-Deficient Cells 171
Ca^{2+} Homeostasis in the Absence of Calnexin 174
The Effects of Caspase Inhibitors on Ca^{2+} Signaling in Human Leukemic T-cells 177
Bap31 in Calnexin-Deficient Cells 179
The Effect of Caspase Inhibitors on Bap31 Cleavage in Human Leukemic T-cells 182
Interaction between Bap31, Caspase 12 and Calnexin 184
Intracellular Localization of Caspase 12, Calnexin and Bap31 in Wild-type CEM and MEFs 188
Discussion 192
Chapter Six — Structural and Functional Analysis of Calreticulin and Calnexin 197
3D Model of Calreticulin and Calnexin 201
Amino Acid Residues Necessary for the Structure and Function of Calreticulin and Calnexin 202
In Vivo and In Vitro Functional Analysis 202
Calreticulin and Calnexin Interaction with ERp57 203
Site Specific Mutations of Calreticulin and Calnexin with Subsequent Modification of Conformation 206

ER Factors Responsible for Regulating the Conformation of Calreticulin and Calnexin.....206
Specific Amino Acid Mutations that Disrupt Function are Directly involved in Structure and Conformation of the Protein.....208
Conformation of Calreticulin and Calnexin Regulates Function.....209
Contrasts between Calreticulin and Calnexin.....211
Calreticulin and Calnexin during Apoptosis.....212
ER Membrane Protein Bap31 and Apoptosis.....213
The Role of Caspase 12 during Apoptosis.....214
Caspase 12 in Human Leukemic T-cells and Mouse Embryonic Fibroblasts.....215
A Functional Complex between Calnexin, Caspase 12 and Bap31, Regulating ER Stress-Induced Apoptosis.....216
References.....**219**

LIST OF TABLES

Chapter 1

Table 1- 1 — ER-related diseases. 4

Table 1- 2 — Ca^{2+} buffering proteins found in the lumen of the endoplasmic reticulum. 9

Chapter 2

Table 2- 1 — Cell lines generated. 80

Table 2- 2 — Plasmid DNA used in this study. 81

Table 2- 3 — Antibodies used in this study. 82

Table 2- 4 — Primers used in this study. 83

Chapter 3

Table 3- 1 — Provencher-Glochner secondary structural analysis 108

Table 3- 2 — Ca^{2+} binding to recombinant calreticulin 113

Chapter 4

Table 4- 1 — CD analysis of S-Cnx. 135

LIST OF FIGURES

Chapter 1

Figure 1- 1 — N-linked oligosaccharide.....16
Figure 1- 2 — N-linked glycosylation.....17
Figure 1- 3 — ER associated degradation (ERAD).....20
Figure 1- 4 — Amino acid sequence of mouse calreticulin and calnexin.....23
Figure 1- 5 — Model of the domain structure of calreticulin and calnexin.....24
Figure 1- 6 — Crystal structure of calnexin and predicted structure of calreticulin.....28
Figure 1- 7 — Model of interaction between ERp57 and calreticulin.....37
Figure 1- 8 — Unfolded protein response (UPR).....40
Figure 1- 9 — The apoptotic cascade.....45

Chapter 3

Figure 3- 1 — Expression of histidine mutants in calreticulin-deficient mouse embryonic fibroblasts.....88
Figure 3- 2 — Expression of calreticulin mutants in calreticulin-deficient mouse embryonic fibroblasts.....89
Figure 3- 3 — Bradykinin-induced Ca^{2+} release in cells expressing calreticulin mutants. 91
Figure 3- 4 — Bradykinin-induced Ca^{2+} release in cells expressing calreticulin mutants. 94
Figure 3- 5 — Effects of calreticulin mutants on thermal aggregation of MDH, a non-glycosylated substrate.....97
Figure 3- 6 — Effects of calreticulin on thermal aggregation of IgY, a glycosylated substrate.....98
Figure 3- 7 — Effects of Trp302Ala and Trp244Ala calreticulin mutants on thermal aggregation of MDH and IgY.....99
Figure 3- 8 — Conformational changes in His153Ala mutant.....103
Figure 3- 9 — Conformational change in Trp244Ala calreticulin mutant.....104
Figure 3- 10 — Conformational changes in His153Ala revealed by ANS fluorescence.....105
Figure 3- 11 — CD analysis of calreticulin and His153Ala calreticulin mutant.....107
Figure 3- 12 — CD analysis of calreticulin and calreticulin mutants.....109
Figure 3- 13 — Trypsin digestion of calreticulin and His153Ala mutant.....111

Figure 3- 14 — Trypsin digestion of calreticulin and calreticulin mutants. 112
Figure 3- 15 — Analysis of interactions between ERp57 and calreticulin by surface plasmon resonance..... 115
Figure 3- 16 — SPR analysis of the interaction of ATP with calreticulin and mutants. 117
Figure 3- 17 — SPR analysis of the interaction of wild-type calreticulin protein with various nucleotides..... 118
Figure 3- 18 — Putative 3D model of calreticulin..... 122
Figure 3- 19 — Three-dimensional structure of the tip of the P-domain of calreticulin. 125
Figure 3- 20 — Model of interaction of ERp57 and calreticulin and the location of the mutated amino acid residues. 127

Chapter 4

Figure 4- 1 — Cascade blue analysis of structural changes in purified calnexin protein. 133
Figure 4- 2 — CD analysis of purified wild-type and mutant S-Cnx protein. 136
Figure 4- 3 — Trypsin digestion of purified wild-type and mutant calnexin protein. 138
Figure 4- 4 — Intrinsic fluorescence of purified soluble wild-type and mutant calnexin protein..... 140
Figure 4- 5 — Aggregation assay using purified soluble wild-type and mutant calnexin protein..... 141
Figure 4- 6 — SPR analysis of the interaction between S-Cnx and ERp57..... 143
Figure 4- 7 — Model of calnexin and ERp57. 144
Figure 4- 8 — SPR Analysis of the interaction of calnexin with ATP-Mg^{2+}. 146
Figure 4- 9 — SPR Analysis of ATP binding to calnexin..... 147
Figure 4- 10 — Modeling of the crystal structure of S-Cnx and the putative ATP binding site. 152

Chapter 5

Figure 5- 1 — MS/MS analysis of caspase 12 antibody immunoprecipitation. 157
Figure 5- 2 — Construct used to generate calnexin-deficient mouse and identification by Southern blot analysis..... 158
Figure 5- 3 — Expression of ER-associated proteins in CEM and NKR cells..... 160
Figure 5- 4 — Expression of ER proteins in calnexin-deficient MEFs. 162

Figure 5- 5 — Expression of caspase family proteins in CEM and NKR cell lines. 164
Figure 5- 6 — Bax and Bcl-2 in calnexin-deficient cells. 166
Figure 5- 7 — Expression of apoptotic proteins in calnexin-deficient cells. 167
Figure 5- 8 — ER stress-induced apoptosis in calnexin-deficient cells. 169
Figure 5- 9 — Percent apoptosis as measured by Annexin V and PI - FACS analysis. .170
Figure 5- 10 — Immunofluorescence and electron microscope analysis of calnexin-deficient NKR cells. 173
Figure 5- 11 — Electron microscopy of wild-type and calnexin-deficient MEFs. 173
Figure 5- 12 — Total ER Ca^{2+} content of calnexin-deficient NKR cells. 175
Figure 5- 13 — Agonist-induced Ca^{2+} release in calnexin-deficient NKR cells. 176
Figure 5- 14 — Ca^{2+} release induced by thapsigargin and carbachol in calnexin-deficient cells incubated with caspase inhibitors. 178
Figure 5- 15 — Expression of Bap31 in CEM and NKR cells. 180
Figure 5- 16 — Expression of Bap31 and generation of the p20 fragment. 181
Figure 5- 17 — Expression of Bap31 and generation of the p20 fragment. 183
Figure 5- 18 — Bap31 and calnexin complex. 185
Figure 5- 19 — Caspase 12-like protein and Bap31 form a complex in CEM cells. 186
Figure 5- 20 — Caspase 12, Bap31 and calnexin form a complex in MEFs. 187
Figure 5- 21 — Immunofluorescence analysis of CEM cells. 189
Figure 5- 22 — Coimmunolocalization of calnexin, caspase 12 and Bap31. 191
Figure 5- 23 — Model of the regulation of ER stress induced apoptosis. 194

Chapter 6

Figure 6- 1 — Model of the interaction between ERp57 and calreticulin or calnexin with the location of the mutated amino acid residues. 200
Figure 6- 2 — Three-dimensional structure of the tip of the P-domain of calreticulin. 210
Figure 6- 3 — Formation of a complex at the ER membrane between calnexin, Bap31 and caspase 12, in ER stress-induced apoptosis. 218

LIST OF ABBREVIATIONS AND NOMENCLATURE USED

Ac-DEVD-AFC	acetyl-DEVD-7-amino-4-(trifluoromethyl) coumarin
ADP	adenosine diphosphate
αMEM	alpha minimal essential medium
AMP	adenosine monophosphate
ANS	8-anilino-1-naphthalene-sulfonic acid
Apaf1	apoptotic peptidase activating factor-1
APMSF	4-amidino-phenyl)-methane-sulfonyl fluoride
ASK	apoptosis signal regulating kinase
ATF6	activating transcription factor 6
ATP	adenosine triphosphate
Bap31	B-cell receptor-associated protein 31
BiP/GRP78	immunoglobulin heavy chain binding protein
BSA	bovine serum albumin
CAD	caspase activated DNase
CAIN/Cabin1	calcineurin inhibitor/calcineurin binding protein 1
CB	cascade blue
CD	circular dichroism
CFTR	cystic fibrosis transmembrane conductance regulator protein
CHAPS	3-[(3-cholamidopropyl)dimethylammonio]1-propanesulfonate
CHOP	C/EBP homologous protein
Cnx	calnexin
CO_2	carbon dioxide
Crt	calreticulin
CS	citrate synthase
C-terminus	carboxyl terminus
CTL	cytotoxic T-lymphocyte
Cyto *c*	cytochrome *c*
DAG	diacylglycerol
DD	death domain
DED	death effector domain

DEPC	diethyl pyrocarbonate
DISC	death initiator signaling complex
DMEM	Dulbecco's modified eagles medium
DMF	N,N-dimethylformamide
DMSO	dimethyl sulfoxide
Drp1	dynamin related protein 1
DTT	dithiothreitol
E-64	(2*S*,3*S*)-3-(*N*-{(*S*)-1-[*N*-(4-guanidinobutyl)carbamoyl]3 methylbutyl}carbamoyl)oxirane-2-carboxylic acid
ECL	electro chemiluminescence
EDTA	ethylene diamine tetraacetic acid
EGTA	ethylene glycol bis(2-aminoethyl ether)-N,N,N'N'-tetraacetic acid
eIF2α	eukaryotic initiation factor 2α
ER	endoplasmic reticulum
ERAD	endoplasmic reticulum associated degradation
ERp57	endoplasmic reticulum protein 57
ERSE	endoplasmic reticulum stress response element
ES	embryonic stem cells
FADD	Fas Associated protein with Death Domain
FasR	Fas ligand receptor
FCS	fetal calf serum
FITC	fluorescein-5-isothiocyanate
FPLC	fast performance liquid chromatography
Fura 2-AM	acetoxymethyl ester
GDP	guanosine diphosphate
Glc	glucose
GlcNAc	N-acetyl-glucosamine
G-protein	guanosine triphosphate-binding protein
GMEM	glasgow's minimum essential media
GRP78	glucose regulated protein 78
GRP94	glucose regulated protein 94
GT	UDP-glucose glycoprotein glucosyltransferase

GTP	guanosine triphosphate
HA tag	hemagglutinin tag
HACBP	high affinity Ca^{2+} binding protein
His tag	histidine tag
iCAD	inhibitor of caspase activated DNase
$InsP_3$	inositol 1,4,5-triphosphate
IPTG	isopropyl-beta-D-thiogalactopyranoside
IRE1	inositol response element protein 1
JNK	c-Jun kinase
kDa	kilodalton
KDEL	lysine-aspartate-glutamate-leucine
KH_2PO_4	potassium phosphate monobasic
LIF	leukemia inhibitory factor
Man	mannose
MDH	malate dehydrogenase
MEF2	myocyte enhancer factor 2
mg	milligram
µg	microgram
MHC I	major histocompatability complex class I
mM	millimolar
µM	micromolar
M-MLV RT	*moloney murine leukemia virus reverse transcriptase*
MMRRC	Mutant Mouse Regional Resource Centers
MOPS	4-morpholinepropanesulfonic acid
MW	molecular weight
MWCO	molecular weight cut-off
NFAT	nuclear factor of activated T-cells
Ni-NTA	nickel-nitrilotriacetic acid
NK	natural killer cells
nM	nanomolar
PBS	phosphate buffered saline
PCR	polymerase chain reaction

PDI	protein disulfide isomerase
PERK	dsRNA-activated protein kinase-like ER kinase
PI	propidium iodide
PIPES	piperrazine-N,N'-bis(2-ethanesulfonic acid)
PFA	paraformaldehyde
PKC	protein kinase C
PLC-β	phospholipase C beta
PM	plasma membrane
PMSF	phenylmethylsulphonylfluoride
PS	phosphatidylserine
p.s.i.	pounds per square inch
PTP	permeability transition pore
RIPA	radio-immunoprecipitation assay
RNA	ribonucleic acid
RyR	ryanodine receptor
S-Cnx	soluble form of calnexin
SDS-PAGE	sodium dodecyl sulfate-polyacrylamide gel electrophoresis
SERCA2	sarcoplasmic/endoplasmic reticulum Ca^{2+} ATPase isoform 2
SPR	surface plasmon resonance
SR	sarcoplasmic reticulum
SRP	signal recognition particle
SRPR	signal recognition particle receptor
SV40	simian virus 40
TAP	transporter associated with antigen processing
TLCK	tosyl-L-lysine chloromethyl ketone
TNF	tumor necrosis factor
TNFR	tumor necrosis factor receptor
TPCK	tosyl-L-phenylalanine chloromethyl ketone
TRADD	TNF receptor-associated death Domain
TRAF2	TNF receptor-associated factor 2
TUNEL	terminal deoxynucleotidyl transferase biotin-dUTP nick end labeling

UPR	unfolded protein response
VCP	valosin containing protein
VDAC	voltage-dependent anion channel
WT	wild-type
Z-DEVD-FMK	Z-Asp(OMe)-Glu(OMe)-Val-Asp(OMe)-fluoromethyl-ketone caspase 3 inhibitor
Z-IETD-FMK	Z-Ile-Glu(OMe)-Thr-Asp(OMe)- fluoromethyl-ketone caspase 8 inhibitor

AMINO ACID ABBREVIATIONS

A	Ala	Alanine
C	Cys	Cysteine
D	Asp	Aspartate
E	Glu	Glutamate
F	Phe	Phenyalanine
G	Gly	Glycine
H	His	Histidine
I	Iso	Isoleucine
K	Lys	Lysine
L	Leu	Leucine
M	Met	Methionine
N	Asp	Asparagine
P	Pro	Proline
Q	Glu	Glutamine
R	Arg	Arginine
S	Ser	Serine
T	Thr	Threonine
V	Val	Valine
W	Trp	Tryptophan
Y	Tyr	Tyrosine
X		Any amino acid

Chapter One — Quality Control in the Endoplasmic Reticulum

Introduction

Eukaryotic cells contain many diverse organelles, including mitochondria, Golgi, peroxisomes and the endoplasmic reticulum (ER), to name just a few, each liable for a multitude of critical processes necessary for cellular life. One of these organelles, the ER, is responsible for several of the most important functions within a cell. It is the largest membrane bound organelle, containing and managing the majority of intracellular Ca^{2+} necessary for signaling within the cell as well as intracellular homeostasis. Ca^{2+} is regulated by specific Ca^{2+} buffering proteins found in the lumen of the ER. The central role of the ER is also evident in another critical cellular process that is performed within the ER, with the synthesis, folding, modification and assembly of secreted and membrane proteins. Specific protein folding that takes place in the lumen of the ER utilizes a number of proteins termed molecular chaperones that assist with the proper folding of the nascent proteins that progress through the ER. As well, the lumen of the ER facilitates post translational modifications of these nascent proteins, such as N-linked glycosylation and disulfide bond formation. To monitor the folding process, the ER has a sophisticated quality control mechanism as well as a complicated unfolded protein response (UPR) that is activated upon ER stress resulting from an accumulation of misfolded or aggregated proteins. ER-associated degradation (ERAD) is capable of taking care of most of this accumulation, but with extenuating ER stress, the ER has the ability to signal apoptosis. The ER contributes to cellular adaptability in response to many different challenges which include environmental, metabolic and intrinsic demands as well as developmental pathways with their ensuing concerns.

The ER is responsible for the proper folding and transit of nascent proteins destined for membranes or for secretion, as well as maintenance of intracellular Ca^{2+} homeostasis. Therefore, the ER is essential for a number of cellular functions, such as contraction-relaxation, cell motility, cytoplasmic and mitochondrial metabolism, gene expression and cell cycle progression. There are many disease conditions related to a breakdown of these ER processes, including vascular diseases such as myocardial infarction (Brooks, 1997; Brooks, 1999; Jakob et al., 2001b; Sherman and Goldberg, 2001) and atherosclerosis (Graf et al., 2004), neurodegenerative diseases, such as Alzheimer's Disease (Rutkowski and Kaufman, 2004; Soti and Csermely, 2002) and Charcot-Marie Tooth Disease (Shames et al., 2003), systemic diseases, such as Cystic

Fibrosis (Chevet et al., 1999a) and Familial Hypercholesterolemia (Sorensen et al., 2006), prion diseases such as Bovine Spongiform Encephalopathy and the human variant, Creutzfeldt-Jakob Disease (Jeffery et al., 2000), as well as a number of cancer conditions, including malignant melanoma (Dissemond et al., 2004) and breast cancer (Li et al., 2001a) (Table 1- 1).

A number of specific conditions contribute to make the ER a unique compartment, involved in the regulation of Ca^{2+} signaling as well as protein folding, including an elevated concentration of Ca^{2+}, a high presence of folding factors, dependence on Zn^{2+}, as well as rich in energy. Elucidation of the components within the lumen of the ER will be the focus of this introduction.

Table 1- 1 — ER-related diseases.

Name of Disease	Affected Protein	Clinical Phenotype
Cystic Fibrosis	Cystic Fibrosis Transmembrane Regulator	Lung disease
Diabetes Mellitus	Insulin receptor	Diabetes
Tyrosinase deficiency	Tyrosinase	Pigment defect
α1-antichymotrypsin deficiency	α1-antichymotrypsin	Lung and liver disease
α1-chymotrypsin	α1-chymotrypsin	Lung disease
Tay-Sachs disease	β-hexosaminidase	Neurological defect
Charcot-Marie-Tooth disease	Peripheral myelin protein	Neurological disease
β-amyloid deficiency	β-amyloid	Neurodegenerative disease
Atherosclerosis	Apolipoprotein A	Heart disease
Marfan Syndrome	Fibrillin	Connective tissue disorder
Sitosterolemia	Sterol receptor	Metabolic defect
Hypercholesterolemia	LDL receptor	Heart/circulatory defect
Down's syndrome	β-amyloid	Neurological disorder
Scurvy	Collagen	Connective tissue disorder
Fabry disease	α-galactosidase	Circulatory disorder
Polycystic kidney disease	polycystins	Kidney disease
Creutzfeldt-Jakob disease	$Prion_{sc}$ mutation	Neurodegenerative disease
Alzheimer's disease	Amyloid/presenilin protein	Neurodegenerative disease
Breast cancer	Human epidermal growth factor receptor/Heregulin	Breast cancer
Metastatic melanoma	MHC classI	Skin cancer

The Endoplasmic Reticulum and Ca^{2+}

Ca^{2+} is a universal, ubiquitous signaling molecule that influences a variety of developmental and cellular processes, including: fertilization (Kono et al., 1996; Swanson et al., 1997), differentiation (Buonanno and Fields, 1999), proliferation (Berridge, 1995; Lu and Means, 1993) and transcription factor activation (Schulz and Yutzey, 2004). Ca^{2+} directly regulates gene translation and expression, protein and steroid synthesis, modification and folding of proteins, secretion and apoptosis (Berridge et al., 2000; Crabtree, 1999). A number of global cellular functions are also affected by alterations in intracellular Ca^{2+} concentration such as: embryogenesis, learning and memory, contraction and relaxation, membrane excitability, ATP synthesis and metabolism and cell cycle progression (Berridge et al., 2003; Pozzan et al., 1994; Webb and Miller, 2003). The majority of intracellular Ca^{2+} is stored in the lumen of the ER (Demaurex and Frieden, 2003). A decrease in ER Ca^{2+} stores leads to inhibited ER-Golgi trafficking (Ashby and Tepikin, 2001; Di Jeso et al., 1998; Porat and Elazar, 2000), impedes transport of molecules across the nuclear pore (Greber and Gerace, 1995) and disrupts chaperone function (Stevens and Argon, 1999). It appears that any disruption in Ca^{2+} stores within the ER as well as obstruction of Ca^{2+} released from the ER has the potential to activate transcriptional and translational cascades. These cascades ultimately regulate chaperones responsible for protein folding within the ER, proteins responsible for ER stress, UPR and ERAD, as well as proteins involved in the apoptotic pathway (Berridge, 2002; Breckenridge et al., 2003a).

The resting free cytoplasmic Ca^{2+} concentration has to be maintained at a very low level. It is achieved by actively pumping Ca^{2+} from the cytoplasm, either into the ER or out of the cell. Extracellular Ca^{2+} concentration is in excess of 2 mM, free cytoplasmic Ca^{2+} concentration is about 100 nM while the free ER Ca^{2+} concentration is approximately 200 μM, with total ER Ca^{2+} concentration up to 1 mM. Ca^{2+} homeostasis and signaling are maintained by controlling Ca^{2+} release from the ER by the $InsP_3$ receptor ($InsP_3R$) (Taylor and Laude, 2002) and ryanodine receptor (RYR) (Franzini-Armstrong and Protasi, 1997), whereas the ER stores are refilled by the sarco/endoplasmic reticulum Ca^{2+}-ATPase (SERCA) (Ashby and Tepikin, 2001). Ca^{2+} is also transported out of the cytoplasm into the extracellular fluid via the sodium-Ca^{2+} exchanger (NCX) (Li et al., 2000) and the plasma membrane Ca^{2+}-ATPase (PMCA)

(Greeb and Shull, 1989). The Ca^{2+} present in the ER stores serves as a source of easily releasable Ca^{2+}, but is also important as a regulator of a number of ER enzymes and proteins, including feedback regulation of the IP_3R, the RyR and SERCA.

Within the lumen of the ER are a number of proteins specifically involved in Ca^{2+} signaling and homeostasis. These proteins are termed "Ca^{2+} buffers", responsible for buffering ER luminal Ca^{2+} as well as involved in numerous aspects of ER function (Baumann and Walz, 2001; Bergeron et al., 1994; Corbett and Michalak, 2000; Groenendyk et al., 2004; Groenendyk and Michalak, 2005; High et al., 2000; Jakob et al., 2001b; Meldolesi and Pozzan, 1998; Molinari and Helenius, 2000; Nauseef, 1999; Williams and Watts, 1995). These luminal buffering proteins are specifically retained in the ER by the KDEL C-terminal amino acid retention/retrieval motif (Munro and Pelham, 1987). Ca^{2+} buffering proteins are critical as the total Ca^{2+} concentration of the ER is in the μM to mM range.

Many of these Ca^{2+} buffering proteins universally display high Ca^{2+} binding capacity (10 moles of Ca^{2+} per mole of protein or higher) and low affinity (K_d = 1 mM or higher), while others have a low capacity (1-2 moles of Ca^{2+} per mole of protein) but high affinity (K_d = 1 μM). There are two Ca^{2+} binding motifs found in ER resident Ca^{2+} buffers: long stretches of negatively charged amino acids or EF-hand-like motifs. Regions of acidic amino acids present a negative charge and coordinate the binding of the positively charged Ca^{2+} ion using charge-based interactions (Fliegel et al., 1989). EF-hand motifs bind Ca^{2+} in a high affinity manner and consist of a 29 residue polypeptide containing helix we (helix E), a loop around the Ca^{2+} ion and helix II (helix F), in which five oxygen-containing residues are conserved for coordination of Ca^{2+} binding (Nelson and Chazin, 1998). There are also EF-hand-like motifs, consisting of a helix-loop-helix but not composed of the canonical sequence (de Alba and Tjandra, 2004) that may be involved in binding Ca^{2+} in a high affinity manner (Fliegel et al., 1989).

Calreticulin is a major Ca^{2+} buffering protein in the lumen of the ER (Milner et al., 1992b), utilizing an acidic region as its high capacity Ca^{2+} binding site (Smith and Koch, 1989), with 43 acidic amino acid residues in the last 82 amino acids of the protein, to bind 25 mole of Ca^{2+} per mole of protein with low affinity (K_d = 2 mM) (Baksh and Michalak, 1991). Calreticulin also contains a high affinity (K_d = 10 μM), low capacity (1

mole of Ca^{2+} per mole of protein) binding site contained in the proline-rich arm domain with a potential EF-hand-like helix-loop-helix motif (Baksh and Michalak, 1991). Calreticulin was first identified as a high affinity Ca^{2+} binding protein, binding approximately 50% of ER luminal Ca^{2+} and was initially named HACBP (Baksh and Michalak, 1991; Ostwald and MacLennan, 1974). Calnexin, the membrane bound homolog of calreticulin was first cloned and named by Wada et al. (Wada et al., 1991). It was identified to bind Ca^{2+}, similar to calreticulin (Wada et al., 1991), but only utilizing a high affinity Ca^{2+} binding site, the helix-loop-helix motif. In addition, the acidic C-terminal cytoplasmic domain of calnexin may bind Ca^{2+} under specific Ca^{2+} signaling conditions but this has not been elucidated (Tjoelker et al., 1994). GRP94 (94-kDa) is another abundant Ca^{2+} binding protein in the lumen of the ER (Koch et al., 1986). Like calreticulin, GRP94 has an acidic C-terminal region comprising its low affinity Ca^{2+} binding site. It contains approximately nineteen Ca^{2+} binding sites, four of which have high affinity (K_d = 2 μM) and low capacity (1 mole of Ca^{2+} per mole of protein), fifteen of which have low affinity (K_d = 600 μM), but high capacity (10 mole of Ca^{2+} per mole of protein) and are composed of negatively charged regions (Van et al., 1989). GRP94 is an ER-localized member of the HSP90 family of stress-induced proteins and binds ATP with ATPase activity (Li and Srivastava, 1993). GRP94 was initially discovered as a protein upregulated upon glucose starvation (Kozutsumi et al., 1988). BiP/GRP78 is a 78-kDa ER chaperone that was identified to bind immunoglobulins and coordinate their proper folding (Haas and Wabl, 1983). It is a monomeric protein with two distinct functional domains, an ATP-binding domain and a peptide-binding domain. While BiP/GRP78 has a relatively low capacity for binding Ca^{2+} (1-2 mole of Ca^{2+} per mole of protein), it contributes possibly as much as 25% of the total Ca^{2+} storage capacity of the ER, with elevated expression resulting in an appreciable increase in ER Ca^{2+} storage capacity (Lievremont et al., 1997).

Calsequestrin is one of the best known and studied Ca^{2+} buffering proteins. It was first identified in 1971 by MacLennan and Wong (MacLennan and Wong, 1971) as a protein of the sarcoplasmic reticulum (SR) of striated muscle. Calsequestrin binds with low affinity (K_d = 1 mM), approximately 50 mole of Ca^{2+} per mole of protein. To bind this much Ca^{2+}, calsequestrin utilizes a stretch of forty five acidic negatively charged amino acids in the last seventy five amino acids of the C-terminus which interact with

the positively charged Ca^{2+} molecules (Beard et al., 2004). Calsequestrin plays a major role in buffering free Ca^{2+} inside the SR, as it is responsible for lowering the concentration of free Ca^{2+} inside the SR, thereby decreasing the concentration gradient against which SERCA must work as it transports Ca^{2+} from the cytoplasm back into the SR. Overexpression of calsequestrin in the ER dramatically decreases Ca^{2+} release, increases the Ca^{2+} uptake and the total Ca^{2+} content of the cell (Jones et al., 1998).

The PDI family of proteins is also involved in buffering a large portion of ER luminal Ca^{2+}. PDI is a 58-kDa Ca^{2+} buffering protein of the ER that contains a KDEL ER retention/retrieval signal. It is a high capacity Ca^{2+} binding protein (approximately 20 mole of Ca^{2+} per mole of protein) but with low affinity (K_d = between 2 and 5 mM) (Lebeche et al., 1994). The C-terminus of PDI contains pairs of acidic residues that constitute the low affinity, high capacity Ca^{2+} binding sites (Lebeche et al., 1994). ERcalcistorin/PDI is a 58-kDa calsequestrin-like high capacity, low affinity Ca^{2+} binding protein found in the lumen of the ER. It has 55% identity to PDI, a chaperone with disulfide bond isomerase activity in the ER. On the basis of its identity to PDI, ERcalcistorin/PDI has a putative bifunctional role as a Ca^{2+} storage protein and as an isomerase enzyme. This protein has seven C-terminal acidic amino acid pairs that bind 23 mole of Ca^{2+} per mole of protein with low affinity (K_d = ~1 mM). A high concentration of Ca^{2+} enhances its isomerase activity. ERp72 is a 72-kDa member of the PDI family (Nigam et al., 1994), contains three thioredoxin-like active sites and has PDI-like activity (Kuznetsov et al., 1997). Its amino acid sequence includes an acidic C-terminus that is involved in the high capacity Ca^{2+} binding responsible for binding 12 mole of Ca^{2+} per mole of protein with low affinity (Lucero et al., 1998). ERp57, a 57-kDa PDI-like protein (Hirano et al., 1995), carries out disulfide bond exchange in conjunction/complex with calreticulin or calnexin. Ca^{2+} binding to this protein has not been investigated, but there is a high probability that ERp57 does not bind Ca^{2+} as it has a positively charged C-terminus. Interestingly, the majority of these Ca^{2+} binding proteins also appear to be involved in the folding and quality control of newly synthesized proteins and the prevention of incorrectly folded intermediates with the functions of these chaperones modulated by changes in Ca^{2+} concentration (Molinari and Helenius, 2000). Table 1- 2 demonstrates the variety of proteins within the ER involved in buffering the luminal Ca^{2+} concentration.

Table 1- 2 — Ca^{2+} buffering proteins found in the lumen of the endoplasmic reticulum.

Protein Name	Characteristic of Ca^{2+} binding (mol Ca^{2+} per mole protein)	Putative Ca^{2+} binding sites
Calreticulin	high capacity site = 25 low capacity site = 1	clusters of acidic residues proline-rich helix-loop-helix motif
Calnexin	low capacity site = 1	proline-rich helix-loop-helix motif
Calsequestrin	high capacity site = ~50	clusters of acidic residues
BiP/GRP78	low capacity site = 2	clusters of acidic residues
GRP94	high capacity site = 10 low capacity site = 1	clusters of acidic residues potential helix-loop-helix
PDI	high capacity site = 20	clusters of acidic residues
ERCalcistorin/PDI	high capacity site = 23	clusters of acidic residues
ERp72	high capacity site = 12	clusters of acidic residues
ERp57/ER60/GRP58	not investigated	unknown

Since these proteins bind large amounts of Ca^{2+}, they have the potential to influence many Ca^{2+}-dependent processes in the ER (Corbett and Michalak, 2000; Meldolesi and Pozzan, 1998), including modulation of the quality and competence of protein folding (Booth and Koch, 1989; Corbett and Michalak, 2000; Lodish and Kong, 1990; Lodish et al., 1992). The majority of these Ca^{2+} buffering proteins are also involved in the folding and quality control of newly synthesized proteins with the prevention of incorrectly folded intermediates and are termed molecular chaperones (Molinari and Helenius, 2000). GRP94, a Ca^{2+} buffering protein in the ER, is regulated by free Ca^{2+} concentration in the ER, with a decrease in ER Ca^{2+} concentration induced by thapsigargin, a specific inhibitor of SERCA, resulted in an upregulation of GRP94 (Li et al., 1993; Van et al., 1989). As well, a loss of binding of actin and calmodulin to GRP94 was observed when Ca^{2+} was depleted (Koyasu et al., 1989). GRP94 also functions as a molecular chaperone (Meunier et al., 2002), binding only advanced folding intermediates or misfolded proteins that have previously associated with BiP/GRP78. It appears that GRP94 is a chaperone specific for advanced intermediates in protein biosynthesis (Argon and Simen, 1999) and that it works downstream of, or in conjunction with other chaperones. BiP/GRP78, another important Ca^{2+} binding molecular chaperone, assists in the folding of newly-synthesized polypeptides by binding to exposed hydrophobic side chains and subsequently coordinating formation of their correct conformation. BiP/GRP78 has an ATP binding site and this ATPase activity is essential for its chaperone function. As BiP/GRP78 is also a Ca^{2+} buffering protein of the ER, its association with nascent polypeptides is stabilized by the high concentrations of Ca^{2+} in the ER lumen. BiP/GRP78 is upregulated upon Ca^{2+} depletion (Li et al., 1993) with its ATPase activity altered with reduced ER Ca^{2+} concentration (Csermely et al., 1995). PDI is an abundant and widely-distributed ER luminal protein with its major function being disulfide bond formation in newly synthesized proteins (Edman et al., 1985). Changes in Ca^{2+} concentration also affect PDI function (Primm et al., 1996), resulting in conformational changes as well as protein interactions with calreticulin abolished with decreased ER Ca^{2+} concentration (Baksh et al., 1995a). ERp72, a PDI-like protein containing the thioredoxin fold and active site is induced under conditions of ER stress, including Ca^{2+} depletion (Linden et al., 1998), while high Ca^{2+} concentrations were observed to augment chaperone function of ERcalcistorin/PDI (Lucero and Kaminer,

1999). Another PDI-like protein, ERp57 was also observed to be affected by luminal Ca^{2+} concentration with binding to calreticulin lost upon changes in luminal Ca^{2+} concentration (Corbett et al., 1999). Recently, an interaction between ERp57 and SERCA was observed to be Ca^{2+}-dependent, with ERp57 potentially responsible for the redox state of the luminal cysteines of SERCA, leading to regulation of ER Ca^{2+} homeostasis (Li and Camacho, 2004). It appears that proteins that bind and store Ca^{2+} are also intrinsically regulated by free luminal Ca^{2+} concentration. Changes in ER Ca^{2+} concentration perform an important signaling function in the lumen and these Ca^{2+} buffering proteins have the ability to sense this change, resulting in modification of protein interactions within the ER.

Role of the Endoplasmic Reticulum in Protein Synthesis and Folding

The ER is the first compartment in the secretory pathway. mRNA encoding proteins that traverse the eukaryotic secretory pathway are initially targeted to the ER where the mRNA is translated and the protein is transported through the membrane by the translocon (Rapoport et al., 1996). As the protein emerges in the ER lumen, maturation and processing of the polypeptide chain occurs, including cleavage of the signal sequence (Johnson and van Waes, 1999), transfer and modification of N-linked glycans and disulfide bond formation, all occurring co-translationally. As well, it is within the ER that hetero and homo-oligomeric, as well as complex proteins are folded and assembled. As nascent glycoproteins are translocated into the lumen of the ER, they associate with a number of Ca^{2+}-dependent molecular chaperones (Helenius and Aebi, 2004) responsible for the appropriate folding of nascent proteins and the prevention of improperly folded proteins (Molinari and Helenius, 2000). Some molecular chaperones, a classical one being BiP, perform their function by binding reversibly to hydrophobic segments that are exposed in the nascent unfolded protein, thereby stabilizing the folding intermediate, preventing aggregation and slowing down the folding rate, allowing the protein to find its lowest energy conformation. This results in an increased yield of correctly folded proteins and their multi-protein complexes and also an increase in the rate of correctly folding intermediates. For a protein to perform its function, it must be folded into a distinct three dimensional conformation.

It has been believed for many years that various polypeptides can fold spontaneously *in vitro* and will reform their native conformation by themselves. This was uniquely demonstrated using denatured RNase that was allowed to fold without the help of any factors or enzymes *in vitro* which gave rise to a biologically active enzyme. This implied that the conformation was inherent in the amino acid sequence and was subsequently termed Anfinsen's Dogma (Anfinsen, 1961). Interestingly, it took about twenty minutes for this to occur, which was too slow to be biologically relevant (Goldberger et al., 1963). This finding supported the hypothesis that factors or enzymes are needed to enhance the folding process. Levinthal's paradox (Karplus, 1997; Levinthal, 1968) states that if an amino acid can assume ten different conformations, the total number of potential conformations in a polypeptide chain of one hundred amino acids would be 10^{100}. For proper folding to occur *in vitro,* one needs several non-physiological parameters, including lower temperature, low protein concentration (compared to *in vivo*) and long incubation times. This demonstrates that for a protein to find its native conformation, it will need help from external factors or enzymes. This can be seen *in vivo* as all proteins somehow fold and assemble properly, forming biologically active molecules. But folding *in vivo* also has concerns, including physical crowding and high total protein concentration, both of which can induce aggregation. Therefore, protein folding *in vivo* demands factors and enzymes that prevent aggregation and slow down the conformation sampling process and do this in a biologically relevant time frame. This protein folding *in vivo* is facilitated by proteins termed molecular chaperones which are part of a system named quality control.

Quality Control of the Secretory Pathway

Essentially, quality control is defined as a collection of activities designed to ensure adequate quality and is used for design analysis and inspection for defects (Webster-Miriam Dictionary). Within the ER, this translates into the association of nascent unfolded proteins with molecular chaperones and enzymes including BiP/GRP78, calreticulin, calnexin, GRP94 and the thiol oxidoreductases PDI and ERp57, all involved in generating a conformationally competent and functional protein. Each of these factors has their own unique mechanism to prevent the transport of conformationally incompetent proteins out of the ER. BiP/GRP78 and GRP94 have the

ability to recognize exposed hydrophobic regions common to nascent unfolded proteins, assisting in the folding and assembly (Argon and Simen, 1999; Gething, 1999), while calreticulin and calnexin interact with nascent glycoproteins via their polypeptide and lectin binding ability (Helenius et al., 1997; Saito et al., 1999). PDI and ERp57 both thiol oxidoreductases, utilize the oxidizing environment of the ER to generate disulfide linkages (Molinari and Helenius, 1999; Noiva, 1999; Oliver et al., 1997), with the formation of these intra- and inter-chain disulfide bonds an integral part of the maturation of most secretory and membrane bound proteins in the ER. These chaperones and folding enzymes are maintained in the ER by sharing a retention/retrieval signal that localizes them to the ER. ER resident luminal proteins contain a C-terminal amino acid sequence of Lys-Asp-Glu-Leu (KDEL) or a variation of this (Nilsson and Warren, 1994), while integral ER membrane proteins contain a Lys-Lys-X-X (KKXX), both of which determine that this protein will either be retained in the ER or retrieved back to the ER (Griffiths et al., 1994; Nilsson and Warren, 1994). Soluble ER resident proteins are trapped by binding to the KDEL receptor expressed in the cis-Golgi and retrieved to the ER.

About 30% of all cellular proteins are synthesized into the ER, where they interact with molecular chaperones and are transported as cargo through the ER to intracellular destinations as well as to the plasma membrane and the extracellular environment (Ghaemmaghami et al., 2003). The majority of proteins that traverse the ER contain N-linked glycosylation sites which function within the cell as a tag used for correct protein folding, efficient quality control, degradation, lysosomal sorting and transport (Helenius and Aebi, 2001; Helenius and Aebi, 2004). This N-linked glycosylated protein is recognized by the quality control mechanism (Ellgaard and Helenius, 2003), which manages the proper processing of glycoproteins that shuttle through the ER (Helenius and Aebi, 2004). These nascent glycoproteins undergo quality control which involves recognition of the N-linked glycan linked nascent polypeptide by either calreticulin or calnexin or both (Bedard et al., 2005; Groenendyk and Michalak, 2005), to ensure that only conformationally competent proteins are transported out of the ER. Proteins that are destined for secretion or for the cell surface are then transported to the Golgi apparatus where further processing of their carbohydrate occurs. Proteins are then either transported to the cell surface or packaged into secretory

vesicles for secretion. If the protein is unable to fold properly, it is targeted for degradation by the proteosomal pathway (Ellgaard and Frickel, 2003). If it is not degradable, these misfolded or unfolded proteins accumulate and trigger a variety of signaling pathways to control ensuing ER stress (Groenendyk and Michalak, 2005; Schroder and Kaufman, 2005a).

Synthesis of the oligosaccharide that is N-linked to the nascent protein is generated on the cytoplasmic side of the ER by the addition of the sugars to a lipid anchor termed dolichylphosphate (DP) (Gahmberg and Tolvanen, 1996; Helenius and Aebi, 2004). Initially two N-acetylglucosamine residues and five mannose residues are added to DP, with the oligosaccharide then flipped to the lumen of the ER. In the ER lumen, four more mannose residues and three glucose residues are added. This oligosaccharide is composed of $Glc_3Man_9GlcNAc_2$ (Figure 1- 1). As the nascent protein traverses the translocon as an extended chain (Whitley et al., 1996) and emerges in the lumen of the ER, an enzyme, OST (oligosaccharyl transferase), closely associated with the translocon (Knauer and Lehle, 1999; Shibatani et al., 2005; Silberstein and Gilmore, 1996) recognizes a specific sequence in the protein, NXS/T (asparagine-X-serine/threonine) (Breuer et al., 2001) when it is 12 to 14 amino acids away from the membrane/translocon (Popov et al., 1997) and attaches the oligosaccharide to the amino acid asparagine via an amide linkage (Figure 1- 2). This close association is very important as these proteins are co-translationally translocated into the ER lumen while being co- and post-translationally modified by N-linked glycosylation (Scheper et al., 2003). Two ER luminal enzymes then modify the oligosaccharide by cleaving the terminal glucose residues. Glucosidase we removes an initial glucose residue (Kalz-Fuller et al., 1995) while glucosidase II cleaves two further glucose residues (Hammond et al., 1994; Ray et al., 1991) (Figure 1- 2). Prior to glucosidase II cleaving the third glucose residue, the glycoprotein is recognized by the quality control cycle, which manages the proper processing of glycoproteins that shuttle through the ER (Helenius and Aebi, 2004) (Figure 1- 2). Quality control consists of a number of molecular chaperones, including calnexin and calreticulin, that assist during the folding of nascent proteins, as well as sensing misfolded proteins, attempting to refold them and if this is not possible, targeting them for degradation (Ellgaard and Helenius, 2003). ERp57 also carries out an important function during this cycle as it associates with calreticulin (Oliver et al., 1997),

calnexin and nascent proteins (Molinari and Helenius, 1999) and functions as an oxidoreductase, generating disulfide linkages, vital during protein folding in the ER. Once the protein has been properly folded, the third glucose is removed by glucosidase II, the protein is released from the quality control cycle and the protein is transported out of the ER. In some cases, this third glucose is prematurely removed and this misfolded or unfolded protein is recognized by an enzyme, UGGT (UDP-glucose glycoprotein glucosyltransferase), which replaces the deleted glucose with a new glucose residue (Fernandez et al., 1998; Parodi, 2000) (Figure 1- 2). UGGT may serve as a folding sensor and is identified to specifically reglucosylate incompletely folded glycoproteins (Trombetta and Helenius, 2000), thereby forcing these incompletely folded glycoproteins to remain in the calreticulin/calnexin cycle until they have attained their proper conformation and are no longer recognized by UGGT. This quality control cycle serves as an efficient retention method as unfolded glycoproteins cannot be released from these chaperones unless they are deglucosylated by glucosidase II (Trombetta and Helenius, 2000). Prolonged interaction with calnexin targets a protein for degradation (Jakob et al., 1998; Otteken and Moss, 1996). This misfolded protein is recognized by α1,2-mannosidase I, which specifically cleaves mannose residues (Frenkel et al., 2003), allowing recognition by the ER-associated degradation machinery (Hos okawa et al., 2001). This quality control cycle may happen numerous times until the protein is folded correctly, or if the quality control is unable to fold the protein, these misfolded and unfolded proteins accumulate and result in a variety of signaling pathways being activated to control ensuing ER stress, including ERAD and UPR.

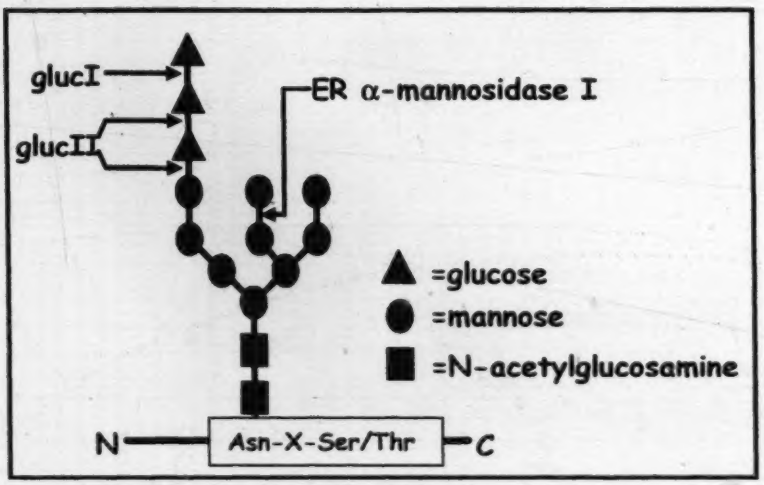

Figure 1- 1

Figure 1- 1 — N-linked oligosaccharide.

The N-linked oligosaccharide is composed of two N-acetylglucosamine residues followed by nine mannose residues in a three branch conformation. This is followed by the addition of three glucose residues on one of the branches. Glucosidase I and II (gluc I and gluc II) are involved in the cleavage of these glucose residues, while ER α-mannosidase I cleaves one of the mannose residues. Asn, asparagine; X, any amino acid; Ser, serine; Thr, threonine.

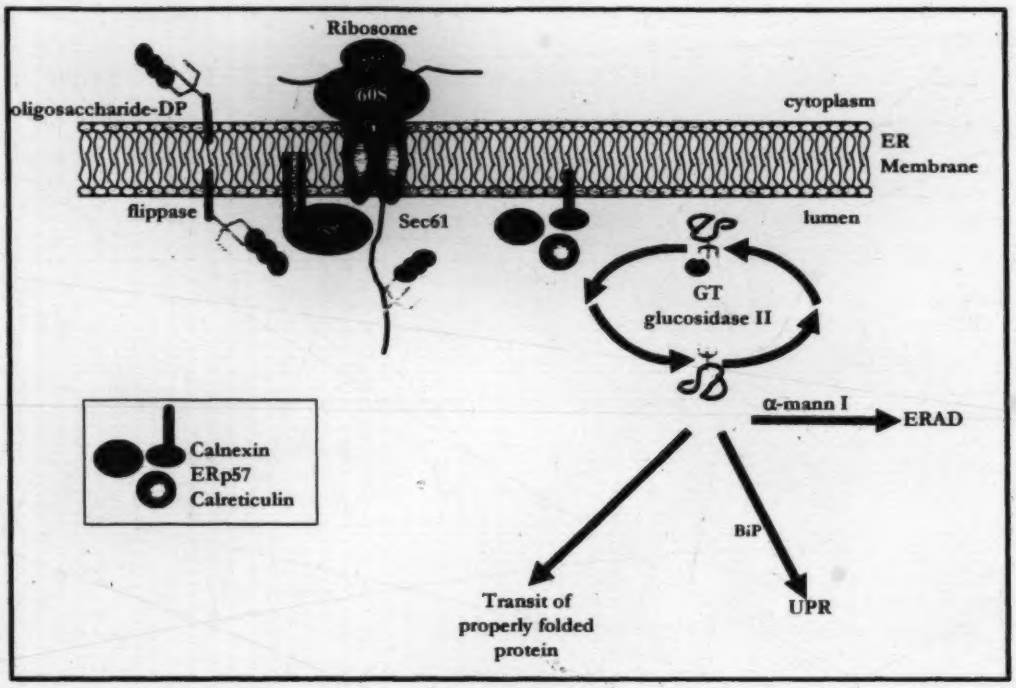

Figure 1- 2

Figure 1- 2 — N-linked glycosylation.

The oligosaccharide is first generated in the cytoplasm and is linked to a membrane bound anchor, DP (dolichylphosphate), followed by flipping to the lumen of the ER, where it is linked to the asparagine in the specific sequence, NXS/T of a nascent protein by the enzyme OST (oligosaccharyl transferase). This nascent protein then associates with ER quality control, including calnexin, calreticulin, ERp57 and UGGT (glucosyl transferase). These enzymes and chaperones cooperate to fold a nascent glycoprotein. If this protein does not fold after repeated cycles of interaction with quality control, it undergoes cleavage of a mannose residue by α-1,2 mannosidase I and it is targeted for ERAD. The accumulation of misfolded protein triggers UPR and interaction of BiP/GRP78 with the misfolded proteins. If the protein folds properly, it exits the ER and transits to other locations within the cell. Sec61, translocon; GT, UGGT; α-mann I, α-1,2 mannosidase I; ERAD, ER associated degradation; UPR, unfolded protein response.

Endoplasmic Reticulum Associated Degradation (ERAD)

ERAD is a process by which misfolded ER proteins are detected and prevented from progressing along the secretory pathway by ER-resident factors and directed to translocation machinery for retrotranslocation into the cytoplasm, where they undergo ubiquitin- and proteasome-dependent degradation (Figure 1- 3). The retrotranslocation machinery, named Derlin1, forms a complex with cytoplasmic VCP (valosin containing protein), also termed AAA ATPase p97 (Ye et al., 2005), as distinct from the Sec61 translocon (Lilley and Ploegh, 2004; Lilley and Ploegh, 2005; Ye et al., 2004). The Derlin translocon complexes with the deglucosylation enzyme, N-glycanase (Katiyar et al., 2005) which removes the oligosaccharide, transfers the misfolded polypeptide from the lumen of the ER back to the cytoplasm for degradation by the proteasome, with this machinery an essential constituent of ERAD (Oda et al., 2006) (Figure 1- 3).

Many specific components of the ERAD pathway are induced by the UPR. Indeed, the UPR is required for efficient ERAD, as UPR transcription induces upregulation of the Derlin retrotranslocation channel (Oda et al., 2006). Excess unfolded protein in the ER triggers the UPR to upregulate ERAD machinery and thereby eliminate misfolded product (Jarosch et al., 2003; Meusser et al., 2005). As one function of UPR is upregulation of proteins involved in ERAD, transcription of genes encoding these proteins involves activation of the UPR element (UPRE) site in their promoter (Yamamoto et al., 2004). ERAD is triggered when misfolded glycoproteins are targeted by the ER α1,2-mannosidase we which cleaves one or more mannose residues in the middle branch of the oligosaccharide (Figure 1- 3). Trimming of these mannose residues effectively prevents reglucosylation by UGGT, thereby disrupting any interaction with calnexin in an attempt to refold the protein (Eriksson et al., 2004). Mannose trimmed oligosaccharides are specifically recognized by EDEM (ER degradation enhancing 1,2-mannosidase-like protein) (Eriksson et al., 2004; Spiro, 2004) which appears to accept the protein from calnexin (Oda et al., 2003) and transport it to the Derlin retrotranslocation machinery (Hosokawa et al., 2001; Jakob et al., 2001a; Oda et al., 2006) (Figure 1- 3). EDEM, a mannosidase-like chaperone, recognizes the α-mannosidase we cleaved glycoprotein exhibiting the $Man_8GlcNAc_2$ sugar (Spiro, 2004) and regulates the extraction of this misfolded glycoprotein from the calnexin cycle (Olivari et al., 2005). The misfolded protein is then retro-translocated into the cytoplasm

where it is deglucosylated by N-glycanase (Katiyar et al., 2005), unfolded (Prakash and Matouschek, 2004), poly-ubiquitinated and subsequently targeted to the 26S proteasome for degradation (Tsai et al., 2002) (Figure 1- 3).

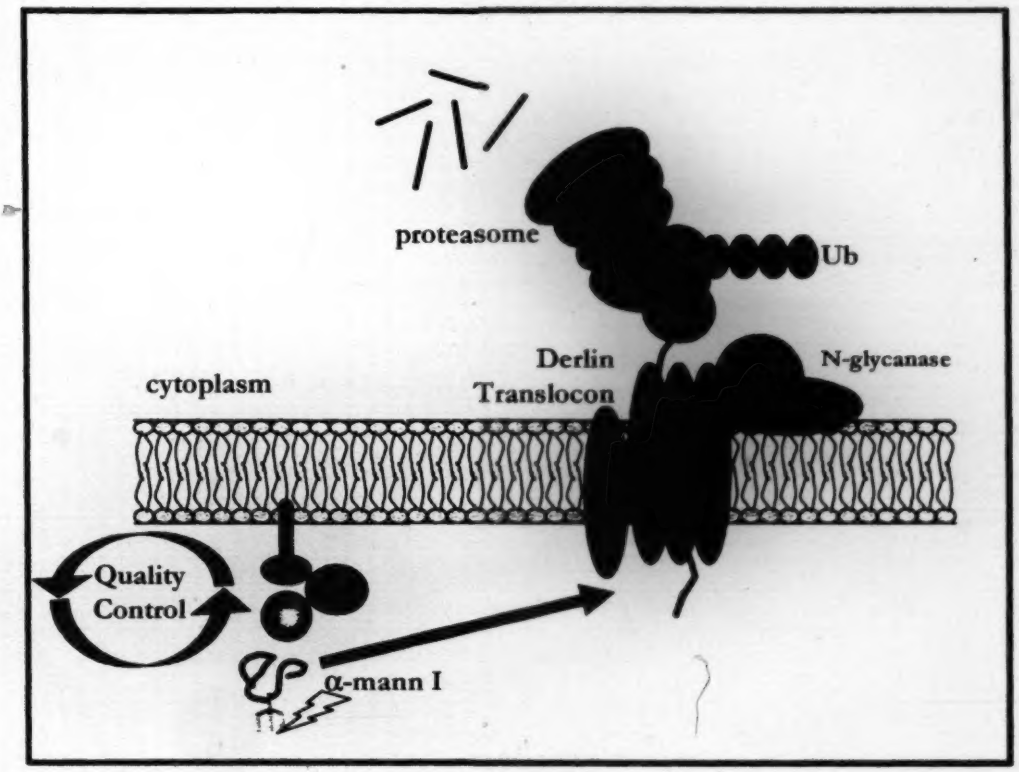

Figure 1- 3

Figure 1- 3 — ER associated degradation (ERAD).

Misfolded proteins are enzymatically cleaved by α-1,2 mannosidase I to remove mannose residues. Truncated oligosaccharides are recognized by the EDEM receptor and retrotranslocated via the Derlin translocon, complexed with the ATPase VCP, deglucosylated by N-glycanase and unfolded by an unknown mechanism. Once in the cytoplasm, the protein is ubiquitinated via the enzymes, E1, E2 and E3, presenting a protein for recognition by the proteasome and resultant degradation. Ub, ubiquitin; α-mannI, α-1,2 mannosidase I; VCP, valosin containing protein.

Calreticulin and Calnexin

Two ER localized proteins, calreticulin (Michalak et al., 1999) and calnexin (Wada et al., 1991), both lectin-like chaperones and members of the protein folding machinery found in the ER, are involved in the recognition of nascent polypeptides and glycoproteins (Ellgaard and Helenius, 2003; Michalak et al., 2002b). Calreticulin and calnexin are homologous proteins that share approximately 40% sequence similarity and 30% sequence identity and as such, contain similar regions, appear to perform similar functions and are classified as a family of proteins. Both calreticulin and calnexin bind glycoproteins as well as non-glycosylated proteins (Leach et al., 2002). Specifically, calreticulin efficiently suppresses the aggregation of both glycosylated and non-glycosylated proteins with the capacity to suppress aggregation via protein-protein interactions in conjunction with an oligosaccharide interaction, increasing overall binding and aggregation suppression capability (Saito et al., 1999). Zn^{2+} and ATP play an important role in the regulation of chaperone function (Saito et al., 1999). In the absence of calreticulin, folding is accelerated and there is significantly more partially folded proteins produced, while in calnexin-deficient cells, folding is severely impaired (Molinari et al., 2004).

In addition to its chaperone function, calreticulin is involved in numerous processes that are necessary for cellular Ca^{2+} homeostasis and intracellular Ca^{2+} signaling, most notably providing the Ca^{2+} necessary for the function of many Ca^{2+}-dependent enzymes, including calcineurin (Groenendyk et al., 2004; Lynch et al., 2005; Michalak et al., 2002a). Calreticulin is also involved in several processes that comprise cellular Ca^{2+} homeostasis such as Ca^{2+} uptake into the ER via SERCA (Camacho and Lechleiter, 1995), Ca^{2+} storage within the ER (Nakamura et al., 2001b) and Ca^{2+} release from the ER (Mesaeli et al., 1999). Calreticulin also influences store operated Ca^{2+} influx at the plasma membrane (Arnaudeau et al., 2002). Calreticulin is 416 amino acids in length and has a molecular weight of 46,567 Da. It contains 109 acidic and 52 basic amino acids (Figure 1- 4). It has an N-terminal cleavable signal sequence that directs it to the ER and an ER KDEL retention/retrieval signal. The protein is composed of three different domains, a globular N-domain, an extended arm P-domain and an acidic C-domain (Figure 1- 5).

Calnexin has a similar amino acid sequence to calreticulin, also binding N-linked glycoproteins and promoting their correct folding (Saito et al., 1999). Calnexin is a 90-

kDa membrane, lectin-like protein (Bergeron et al., 1994) that binds Ca^{2+} with high affinity (Ellgaard and Frickel, 2003; Michalak et al., 2002b; Tjoelker et al., 1994) and binds ATP (Ou et al., 1995). Calnexin is 591 amino acids in length and has an N-terminal cleavable signal sequence that directs it to the ER as well as a C-terminal RKPRRE ER retention/retrieval signal (Figure 1- 4) (Jackson et al., 1990; Rajagopalan et al., 1994). The protein contains three domains, the N-domain, P-domain and C-domain (Figure 1- 5).

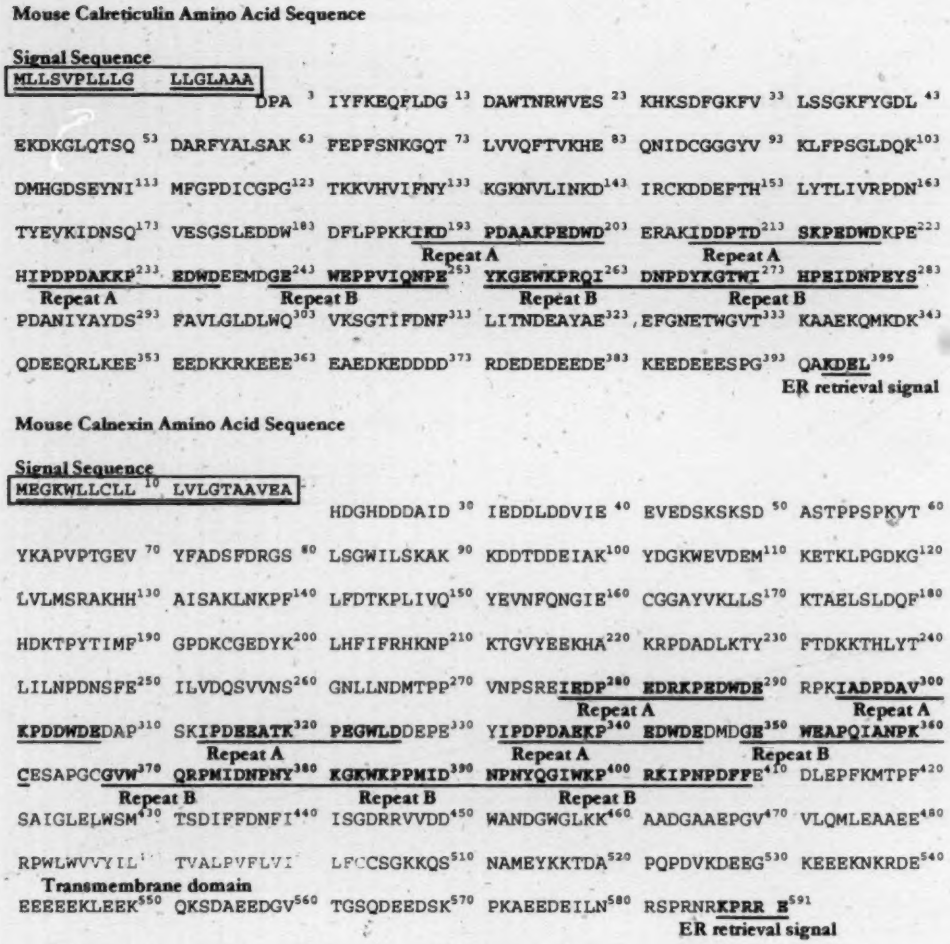
Mouse Calreticulin Amino Acid Sequence
Signal Sequence
MLLSVPLLLG LLGLAAA
DPA 3 IYFKEQFLDG 13 DAWTNRWVES 23 KHKSDFGKFV 33 LSSGKFYGDL 43
EKDKGLQTSQ 53 DARFYALSAK 63 FEPFSNKGQT 73 LVVQFTVKHE 83 QNIDCGGGYV 93 KLFPSGLDQK 103
DMHGDSEYNI 113 MFGPDICGPG 123 TKKVHVIFNY 133 KGKNVLINKD 143 IRCKDDEFTH 153 LYTLIVRPDN 163
TYEVKIDNSQ 173 VESGSLEDDW 183 DFLPPKKIKD 193 PDAAKPEDWD 203 ERAKIDDPTD 213 SKPEDWDKPE 223
Repeat A
Repeat A
HIPDPDAKKP 233 EDWDEEMDGE 243 WEPPVIQNPE 253 YKGEWKPRQI 263 DNPDYKGTWI 273 HPEIDNPEYS 283
Repeat A
Repeat B
Repeat B
Repeat B
PDANIYAYDS 293 FAVLGLDLWQ 303 VKSGTIFDNF 313 LITNDEAYAE 323 EFGNETWGVT 333 KAAEKQMKDK 343
QDEEQRLKEE 353 EEDKKRKEEE 363 EAEDKEDDDD 373 RDEDEDEEDE 383 KEEDEEESPG 393 QAKDEL 399
ER retrieval signal
Mouse Calnexin Amino Acid Sequence
Signal Sequence
MEGKWLLCLL 10 LVLGTAAVEA
HDGHDDDAID 30 IEDDLDDVIE 40 EVEDSKSKSD 50 ASTPPSPKVT 60
YKAPVPTGEV 70 YFADSFDRGS 80 LSGWILSKAK 90 KDDTDDEIAK 100 YDGKWEVDEM 110 KETKLPGDKG 120
LVLMSRAKHH 130 AISAKLNKPF 140 LFDTKPLIVQ 150 YEVNFQNGIE 160 CGGAYVKLLS 170 KTAELSLDQF 180
HDKTPYTIMF 190 GPDKCGEDYK 200 LHFIFRHKNP 210 KTGVYEEKHA 220 KRPDADLKTY 230 FTDKKTHLYT 240
LILNPDNSFE 250 ILVDQSVVNS 260 GNLLNDMTPP 270 VNPSREIEDF 280 EDRKPEDWDE 290 RPKIADPDAV 300
Repeat A
Repeat A
KPDDWDEDAP 310 SKIPDEEATK 320 PEGWLDDEPE 330 YIPDPDAEKP 340 EDWDEDMDGE 350 WEAPQIANPK 360
Repeat A
Repeat A
Repeat B
CESAPGCGVW 370 QRPMIDNPNY 380 KGKWKPPMID 390 NPNYQGIWKP 400 RKIPNPDFFE 410 DLEPFKMTPF 420
Repeat B
Repeat B
Repeat B
SAIGLELWSM 430 TSDIFFDNFI 440 ISGDRRVVDD 450 WANDGWGLKK 460 AADGAAEPGV 470 VLQMLEAAEE 480
RPWLWVVYIL TVALPVFLVI LFCCSGKKQS 510 NAMEYKKTDA 520 PQPDVKDEEG 530 KEEEKNKRDE 540
Transmembrane domain
EEEEEKLEEK 550 QKSDAEEDGV 560 TGSQDEEDSK 570 PKAEEDEILN 580 RSPRNRKPRR E 591
ER retrieval signal

Figure 1- 4

Figure 1- 4 — Amino acid sequence of mouse calreticulin and calnexin.

The amino acid sequence deduced from the nucleotide sequence of mouse cDNA. Calreticulin contains 416 amino acids beginning with an ER signal sequence and ending with an ER retention/retrieval signal KDEL. Amino acid repeat sequences *(A and B)* are indicated by underlining. Calreticulin contains three sets of A and B repeats while calnexin contains four sets. Calnexin additionally contains a transmembrane domain and is localized to the ER membrane. Signal sequence is shown boxed and in light green, the N-domain of both proteins is indicated in blue, the P-domain of both proteins is indicated in red and the C-domain in green. The retrieval signal in both proteins is underlined and the transmembrane domain of calnexin is indicated in orange.

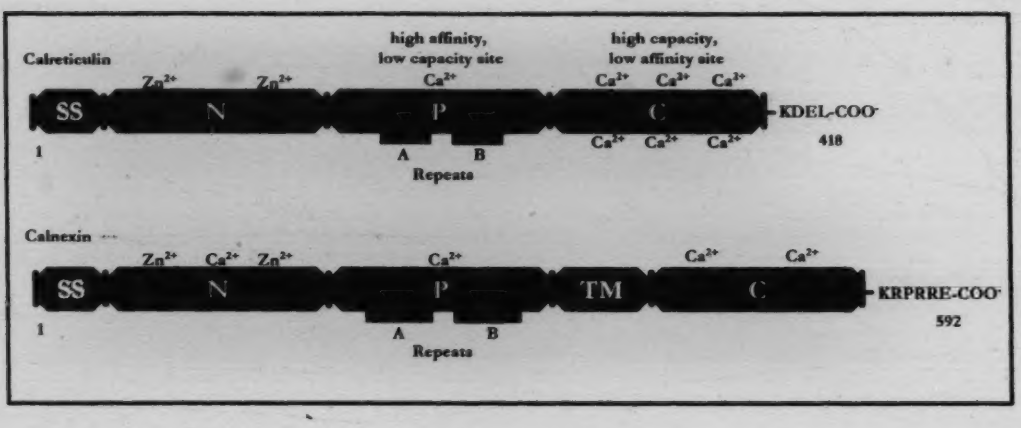

Figure 1- 5

Figure 1- 5 — Model of the domain structure of calreticulin and calnexin.

Calreticulin and calnexin are composed of three similar domains, the N-domain, the P-domain and the C-domain. Both proteins contain a signal sequence that is cleaved upon entering the ER. Calnexin has an additional transmembrane domain that anchors it to the ER membrane with the C-domain exposed to the cytoplasm. Both proteins contain a C-terminal ER retention/retrieval motif (KDEL for calreticulin and KRPRRE for calnexin). The N-domain is the most conserved domain of both proteins and encompasses approximately one-third of the protein. The P-domain is comprised of a proline-rich sequence and contains three or four sets of A and B amino acid repeats, shown in purple and blue. *In vitro*, the P-domain binds Ca^{2+} with high affinity and low capacity (1 mole Ca^{2+} per mole of protein, K_d = 1 μM). The C-domain of both proteins is highly acidic. Calreticulin binds a large amount of Ca^{2+} but with low affinity (25 mole of Ca^{2+} per mole of protein, K_d = 2 mM). Zn^{2+} binding occurs in the N-domain of both proteins. TM, transmembrane; SS, signal sequence; N, amino-terminal domain; P, proline-rich domain; C, carboxyl-terminal domain.

The N-Domain of Calreticulin and Calnexin

X-ray crystallography has further identified the N-terminus of calnexin as a Ca^{2+} binding, globular β-sandwich domain, resembling legume lectins, and in addition, once the crystal was soaked with glucose, exhibites an interaction with this glucose moiety (Schrag et al., 2001). Structural and modeling analysis indicate that the glucose binding pocket contains a centrally located tryptophan residue and several charged amino acid residues (Michalak et al., 2002b; Schrag et al., 2001). Prediction of secondary structure of calreticulin suggest that the N-terminal region also forms a globular domain containing eight anti-parallel β-strands (Fliegel et al., 1989) (Figure 1- 6). The N-domain of calreticulin contains the polypeptide and carbohydrate binding site (Kapoor et al., 2004; Leach et al., 2002), a Zn^{2+} binding site (Baksh et al., 1995b), a disulfide linkage (Andrin et al., 2000) and may also bind ATP (Corbett et al., 2000) (Figure 1- 5). In comparison, the calnexin N-domain contains a high affinity Ca^{2+} binding site, the majority of the glycoprotein binding site as well as a Zn^{2+}-dependent ERp57 binding site (Leach et al., 2002; Tjoelker et al., 1994) (Figure 1- 5).

Polypeptide and oligosaccharide binding regions are located in the N-domain of calreticulin and calnexin with weaker secondary sites located in the P-domain (Leach et al., 2002). Oligosaccharide binding by this region induces conformational change in the proteins, thereby influencing polypeptide binding (Saito et al., 1999), with a requirement for both the N-domain, with the oligosaccharide and polypeptide binding regions, as well as the P-domain, containing the secondary binding sites to generate full chaperone function of both calreticulin and calnexin (Leach et al., 2002). Polypeptide binding is favored under conditions that induce an unfolding conformational event in calnexin while oligosaccharide binding is favored under conditions that enhance the structural stability of the protein (Thammavongsa et al., 2005). Recently, Kapoor et al. (Kapoor et al., 2004) identified two site directed mutants in calreticulin (Tyr109 and Asp135) in the globular N-domain, that abolish interaction of the protein with sugar substrates. A number of additional residues in calreticulin (Lys111, Tyr128 and Asp317) are also identified to be involved in oligosaccharide binding (Thomson and Williams, 2005). Six interacting amino acid residues in the globular N-domain of calnexin are identified as important for the oligosaccharide binding site (Tyr156, Lys167, Tyr186, Met189, Glu217 and Glu426) (Leach and Williams, 2004). The disulfide linkage found in the N-domain of

both calreticulin and calnexin is important for proper folding and structural integrity of these chaperones.

Structural and functional studies indicate that the N-domain, in conjunction with the P-domain, may form the functional protein folding region responsible for chaperone function of calreticulin and calnexin (Nakamura et al., 2001b). Calnexin and calreticulin also contain a secondary Zn^{2+}-dependent ERp57 binding site in the globular N-domain (Leach et al., 2002), with calreticulin interacting with ERp57 in a Zn^{2+}-dependent manner via a segment located near its N-terminus (Corbett et al., 1999) and in the absence of Zn^{2+}, via a segment within the P-domain (Frickel et al., 2002).

The P-Domain of Calreticulin and Calnexin

The middle region of the calreticulin and calnexin amino acid sequence is proline-rich, suggesting flexibility. This P-domain contains pairs of a fourteen amino acid repeat A (IxDPxA/DxKPEDWDx – Repeat A) and a fourteen amino acid repeat B (GxWxPPxIxNPxYx – Repeat B) (three A and B pairs in calreticulin (Ellgaard et al., 2001a) and four A and B pairs in calnexin (Ohsako et al., 1994)) that might be involved in lectin-like function (Vassilakos et al., 1998) (Figure 1- 4). The P-domain of calreticulin is composed of a flexible, extended, finger-like region stabilized by three antiparallel β-sheets (Ellgaard et al., 2001a) that interacts with ERp57 (Ellgaard et al., 2002; Frickel et al., 2002; Oliver et al., 1999) (Figure 1- 6). *In vitro*, this region of the protein binds Ca^{2+} with high affinity (K_d = 1 μM) but low capacity (1 mole of Ca^{2+} per mole of protein) (Baksh and Michalak, 1991; Tjoelker et al., 1994). The P-domain of calnexin is a 140 Å extended arm and consists of two β-strands folded in a hairpin configuration that contains conserved proline residues and the four tandem repeats (Leach et al., 2002; Schrag et al., 2001). This is similar to what was observed in an NMR structural analysis of calreticulin (Ellgaard et al., 2001a) (Figure 1- 6). Both calreticulin and calnexin facilitate protein folding in conjunction with ERp57 (Leach et al., 2002) and using NMR spectroscopy, the primary ERp57 binding site in calnexin is narrowed down to specific amino acids localized at the tip of the P-domain (Pollock et al., 2004). Both proteins demonstrate an interaction with ERp57 via a secondary Zn^{2+}-dependent site located in the globular domain as identified using GST pull down analysis (Leach et al., 2002).

The C-Domain of Calreticulin and Calnexin

The C-domain of calreticulin contains nineteen pairs of acidic and negatively charged amino acid residues that bind 29% of ER luminal Ca^{2+} with high capacity (25 mole of Ca^{2+} per mole of protein) and low affinity (K_d = 2 mM) (Figure 1- 4). Ca^{2+} binding to the C-domain of calreticulin affect calreticulin-protein interactions. The C-domain of calnexin contains a transmembrane α-helix, an ER retention/retrieval amino acid sequence, responsible for retaining it in the ER, as well as a negatively charged cytoplasmic tail that binds Ca^{2+} with moderate affinity (Tjoelker et al., 1994) (Figure 1-5). The C-domain also contains numerous consensus sites for phosphorylation by protein kinase C, casein kinase II, proline-directed kinase and mitogen-activated kinase (Chevet et al., 1999b; Delom and Chevet, 2006; Roderick et al., 2000; Tjoelker et al., 1994; Wong et al., 1998). These phosphorylation-dependent events may regulate interactions of calnexin with various proteins, including SERCA (Roderick et al., 2000), the translocon and ribosomal proteins (Chevet et al., 1999b; Delom and Chevet, 2006) and MHC class I molecules (Margolese et al., 1993).

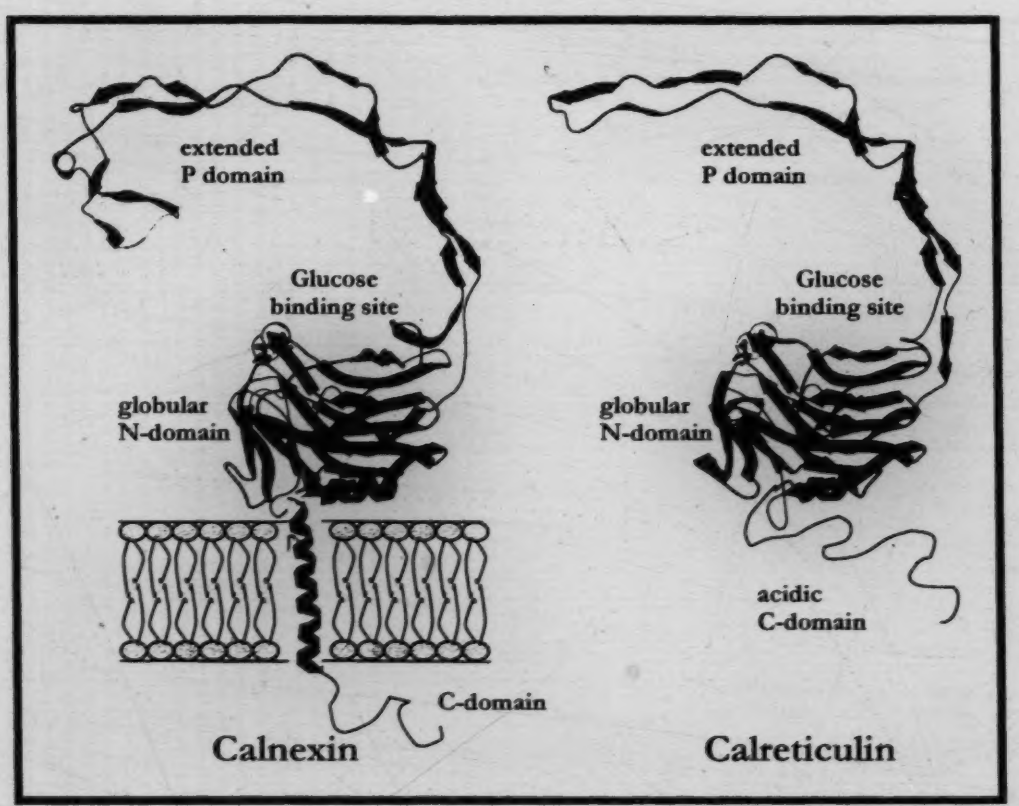

Figure 1- 6

Figure 1- 6 — Crystal structure of calnexin and predicted structure of calreticulin.

The crystal structure of calnexin was solved by Schrag et al. (Schrag et al., 2001) A globular N-domain is composed of β-sheet secondary structure *(blue)*. The extended P-domain *(red)* contains matched pairs of β-sheet motifs with a disulfide linkage at the tip of the P-domain of calnexin only. Calnexin also contains a transmembrane domain and cytoplasmic C-terminus. Yellow balls correspond to the S-S disulfide linkage in the N-domain. Modified from: Ca^{2+} signaling and calcium binding chaperones of the endoplasmic reticulum. Cell Calcium. 2002 Nov-Dec;32(5-6):269-78.

Calreticulin and Calnexin Deficient Mice

Calreticulin-deficient mice are embryonic lethal at approximately day 14.5, due to a disruption in the Ca^{2+} signaling important during cardioembryogenesis, resulting in impaired heart development (Mesaeli et al., 1999). This confirms the essential reliance on Ca^{2+} buffering within the lumen of the ER, necessary for proper Ca^{2+} signaling during development. As calreticulin is 35% conserved across most species and given the role of calreticulin in a number of cellular process such as protein folding and Ca^{2+} homeostasis, it is not surprising that calreticulin-deficiency is embryonic lethal in mice (Mesaeli et al., 1999) and cells derived from calreticulin-deficient embryos have impaired Ca^{2+} handling ability as well as compromised protein folding and quality control (Knee et al., 2003; Mesaeli et al., 1999; Nakamura et al., 2001b), indicating the importance of these two functions of calreticulin. The major effects of calreticulin-deficiency are observed in the heart (Mesaeli et al., 1999) and calreticulin-deficient embryos dying at day 14.5 as a result of improper development of the ventricular wall (Mesaeli et al., 1999). Subsequent studies show that calreticulin is highly expressed in embryonic heart where it performs an important role by providing the Ca^{2+} necessary during cardiac growth and differentiation (Mesaeli et al., 2001; Mesaeli et al., 1999). IP_3-mediated Ca^{2+} release from the ER is inhibited in calreticulin-deficient cells, further confirming the importance of this function of calreticulin (Mesaeli et al., 1999; Nakamura et al., 2001b). Calreticulin deficiency affects the function of calcineurin, a Ca^{2+}-calmodulin activated serine/threonine phosphatase (Liu et al., 1991). Calcineurin plays an important role in the regulation of skeletal and cardiac muscle growth and differentiation (Chin et al., 1998; Michalak et al., 2002a; Molkentin et al., 1998; Wu et al., 2000), memory processes (Mansuy et al., 1998; Winder et al., 1998; Zhuo et al., 1999) and apoptosis (Asai et al., 1999; Krebs, 1998; Shibasaki and McKeon, 1995). To narrow down the specific role of calreticulin in the calcineurin signaling pathway, transgenic calreticulin-deficient mice were generated that express cardiac specific, constitutively active calcineurin (Guo et al., 2002). These transgenic mice are observed to rescue the lethal phenotype, essentially circumventing the necessity for Ca^{2+} release from the ER required for the activation of calcineurin, documenting a physiologically relevant relationship between calreticulin and calcineurin-dependent pathways. These results demonstrate the importance of both

calreticulin and calcineurin in the Ca^{2+}-dependent signaling pathways that are essential for normal cardiac development.

Further studies on cells derived from calreticulin-deficient embryos indicat that protein folding in the ER is also compromised, resulting in the accumulation of misfolded protein and the activation of the unfolded protein response (Knee et al., 2003; Molinari et al., 2004). Deficiency in calreticulin results in modification of the process and outcome of glycoprotein production and the fidelity of quality control. Effects seen are acceleration in the folding rate, reduction in the folding efficiency and an increase in the retention of misfolded glycoprotein (Knee et al., 2003; Molinari et al., 2004). In summary, calreticulin deficiency compromises overall quality control with a global effect, more than just a disruption in Ca^{2+} signaling.

Considering functional and structural similarities between calreticulin and calnexin, it is surprising that calnexin-deficient mice are viable postnatally. Calnexin-deficient mice are significantly smaller than their siblings with an abnormal gait and limb coordination. The majority of physical differences are presented in the nervous system, with a reduction in the number of large myelinated nerve fibers, potentially responsible for the gait disturbances (Denzel et al., 2002). A mammalian cell line deficient in calnexin expression has also been isolated that was initially derived as a subclone (CEM-NK_R) from a human T-lyphoblastoid cell line (CEM) that has developed resistance to natural killer (NK) cell mediated lysis (Howell et al., 1985). It was later established that CEM-NK_R (depicted as NKR) fails to express calnexin (Scott and Dawson, 1995). Even though calnexin is clearly demonstrated to interact with major histocompatibility complex class 1 (MHC class I) heavy chains, in NKR calnexin-deficient cells, there is no decrease in the expression levels of MHC class I on the cell surface and no alteration in the transport rate of MHC class I to the cell membrane (Prasad et al., 1998; Sadasivan et al., 1995).

Calreticulin and Calnexin, Multifunctional Proteins

Historically, both the chaperone function and the Ca^{2+} binding capacity of calreticulin are demonstrated to be involved in a wide variety of cellular systems, including MHC class I assembly and secretion (Elliott and Williams, 2005; Wright et al., 2004), cytolytic T lymphocytes (CTL) natural killer cells (Burns et al., 1992; Porcellini et

al., 2006; Smyth et al., 2001), autoimmunity (Rokeach et al., 1991; Tanaka et al., 2006), spermiogenesis (Nakamura et al., 1992a; Nakamura et al., 1992b) and cell motility (Coppolino and Dedhar, 1999; Tran et al., 2002).

MHC class I complexes are found at the membrane of most nucleated cells and play a vital role during the immune response of an organism. Their task is to present peptides at the cell surface for recognition by a cytotoxic natural killer cell followed by cell lysis and death. These peptides, usually about nine amino acids in length, are generated by the proteasome in the cytoplasm, including peptides from intracellular proteins as well as foreign proteins. This heterotrimeric complex is assembled in the ER with the assistance of a number of chaperones and factors and consists of a polymorphic glycosylated heavy chain, non-polymorphic β2 microglobulin and a peptide. The peptide loading complex consisting of the peptide transporter TAP (transporter associated with antigen processing), ERp57, calreticulin and tapasin, is integral to this process (Elliott and Williams, 2005). Calnexin and calreticulin are identified to be part of the peptide loading complex for MHC class I polypeptide complexes (Hochstenbach et al., 1992; Sadasivan et al., 1996). Both calreticulin and calnexin promote this assembly as well as retaining incompletely assembled complexes in the ER (Harris et al., 1998). ERp57 is also a part of this complex in conjunction with calreticulin and calnexin (Hughes and Cresswell, 1998; Morrice and Powis, 1998; Peaper et al., 2005). There might be a sequential interaction of chaperones and factors to generate a properly assembled MHC class I multiprotein complex. Initially, TAP and tapasin associate with each other and are recognized by calnexin and ERp57 in a glycan-independent manner to form an intermediate complex with the heavy chain. This intermediate complex binds the MHC class I-β2 dimers, with calnexin released followed by calreticulin interaction, generating the MHC class I loading complex. The complex is ready for peptide loading and once bound, the MHC class I-β2 dimer is dissociated and the MHC-peptide complex is transported to the cell surface (Diedrich et al., 2001; Harris et al., 1998). The majority of key molecules involved in the immune response traverse the ER and are highly glycosylated along the way. Glycosylation of the proteins involved in the immune system are necessary for stability, but are also involved in recognition events. Oligosaccharides attached to glycoproteins in the junction between T-cells and antigen-presenting cells

help to orient the two binding membranes, provide protease protection and restrict nonspecific protein-protein interactions (Rudd et al., 2001).

CTL cells are cytolytic cells that release specific factors; Ca^{2+} activated perforin and granzymes (proteases), upon interaction with target cells with the final result being the target cell undergoing lysis and apoptosis. Calreticulin colocalizes with perforin in the secretory granules (lysosome-like vesicles) of the CTL's. It appears the Ca^{2+} binding capacity of calreticulin is involved in the protection of CTL cells, with chelation of Ca^{2+} necessary for inactivation of perforin, involved in penetrating the plasma membrane of a target cell (Dupuis et al., 1993). Porcellini et al. demonstrates the dependence on calreticulin for shaping the Ca^{2+} signaling, responsible for modulating the T-cell adaptive immune response (Porcellini et al., 2006), with induction of auto-immune diseases, while Sipione et al. discovered using calreticulin-deficient cells, that calreticulin is not critical for the cytolytic activity of the granzymes and perforin, but that it is required for efficient targeting and contact of the CTL to the target cell (Sipione et al., 2005). Calreticulin may also be involved in autoimmunity, as antibodies against calreticulin are found in patients with systemic lupus erythematosus (Ben-Chetrit, 1993; Rokeach et al., 1991). Autoantibodies to calreticulin are identified in polychondritis, a systemic inflammatory disease where the body generates autoimmunity to cartilage-related components (Tanaka et al., 2006). Calreticulin may play an important role during integrin-mediated adhesion events (Tran et al., 2002). Calreticulin binds integrin and may couple integrins with Ca^{2+} channels on the cell surface (Kwon et al., 2000).

Calnexin interacts with a wide variety of proteins, including the LDL receptor (Sorensen et al., 2006), rhodopsin (Rosenbaum et al., 2006), G-protein coupled receptors (Lanctot et al., 2006), acetylcholine receptors (Wanamaker and Green, 2005), PMP22 (Dickson et al., 2002; Fontanini et al., 2005), ribosomes (Delom and Chevet, 2006), the IP_3R (Joseph et al., 1999) and SERCA (Roderick et al., 2000; Vangheluwe et al., 2005). Calnexin is specifically linked to chaperoning and retaining mutant LDL receptor in the lumen of the ER (Sorensen et al., 2006) with induction of UPR. Calnexin is also required for the maturation of rhodopsin, involved in light sensitivity in the eye, as well as regulating Ca^{2+} necessary for photoreceptor cell light stimulation (Rosenbaum et al., 2006). Missense point mutations in myelin protein PMP22, responsible for Charcot-Marie-Tooth disease, result in the consequent accumulation of the protein in the ER in

conjunction with calnexin and the formation of aggresomes (Dickson et al., 2002; Fontanini et al., 2005). PMP22 is a major component of myelin expressed in the compact layer of myelinated fibers in the peripheral nervous system and is produced predominantly by Schwann cells. PMP22 appeared to interact with calnexin in both an oligosaccharide-dependent (Dickson et al., 2002) and independent manner, via protein-protein interactions (Fontanini et al., 2005). This also occurred during acetylcholine receptor maturation (Wanamaker and Green, 2005). Protein-based and oligosaccharide independent interactions were observed during the interaction of calnexin with G-protein coupled receptors (Lanctot et al., 2006), as well as with proteolipid protein (PLP) (Swanton et al., 2003). It appears that calnexin interacts with these membrane proteins via their transmembrane region, with calnexin facilitating the proper folding and assembly of these proteins. This was also the case for the interaction of calnexin with ribosomal proteins, but via the cytoplasmic tail of calnexin, dependent on the phosphorylation status of calnexin, potentially representing a regulatory mechanism for the lectin-like function of calnexin (Delom and Chevet, 2006). This phosphorylation event may also act as a molecular switch, regulating the interaction of calnexin with SERCA2b, thereby affecting Ca^{2+} signaling and controlling Ca^{2+} sensitive chaperone functions in the ER (Roderick et al., 2000; Vangheluwe et al., 2005).

Calnexin may be involved in numerous protein folding diseases, including Cystic Fibrosis (Amaral, 2004), Sitosterolemia, caused by reduced trafficking of a sterol receptor resulting in sterol accumulation and premature atherosclerosis (Graf et al., 2004) and Charcot-Marie Tooth Disease, caused by misfolded PMP22 (Shames et al., 2003). Significant upregulation of calnexin is observed in breast cancer (Li et al., 2001a), while metastatic melanoma lesions exhibited considerable downregulation of calnexin (Dissemond et al., 2004).

Recent studies indicate that calnexin binding to oligosaccharides requires the structural stability of calnexin (Thammavongsa et al., 2005) and oligosaccharide binding can be lost upon Ca^{2+} depletion (Vassilakos et al., 1998), while polypeptide recognition requires a specific partially unfolded conformation of calnexin as a result of transient Ca^{2+} depletion (Thammavongsa et al., 2005). In conjunction with studies done on calreticulin-deficient cells, calnexin-deficiency also results in compromised quality control, with accumulation of misfolded protein and upregulation of the UPR (Knee et

al., 2003; Molinari et al., 2004). It is demonstrated that calnexin deficiency results in an increased rate of folding, a reduction in the folding efficiency and retention of misfolded protein in the ER (Knee et al., 2003; Molinari et al., 2004). Similar to calreticulin, calnexin deficiency compromises overall quality control resulting in a global effect. As well, recent evidence suggests a new role for calnexin, involved in the regulation of cytoplasmic molecules via the acidic and phosphorylated C-terminus, located in the cytoplasm. Chevet et al. has demonstrated phosphorylation-dependent interaction of the C-terminus of calnexin with ribosomes, manipulating ribosomal activity and localization with the translocon (Chevet et al., 1999b; Delom and Chevet, 2006). Phosphorylated calnexin is implicated to form a complex with the SRP receptor (signal recognition particle), involved in recognition of the signal sequence (Ou et al., 1992). Further evidence verifies the importance of this C-domain with its separate function, as phosphorylation of a specific serine residue acts as a molecular switch regulating the interaction of calnexin with SERCA2b, with an increase in cytoplasmic Ca^{2+} concentration resulting in Ca^{2+}-dependent dephosphorylation (Roderick et al., 2000) (potentially by calcineurin), thereby coupling Ca^{2+} signaling and Ca^{2+}-sensitive chaperone functions in the ER. Most recently, calnexin is identified to perform an important role during rhodopsin maturation, Ca^{2+} regulation and photoreceptor cell survival. Ca^{2+} plays an vital role during light stimulation and therefore regulation of Ca^{2+} homeostasis is critical. Mutations in drosophila calnexin results in severe disruption of rhodopsin expression as well as aberrant cytoplasmic Ca^{2+} levels, indicating a role for calnexin during Ca^{2+} homeostasis, via the two Ca^{2+} binding sites, the P-domain site and the acidic cytoplasmic tail (Rosenbaum et al., 2006). This result is the first indication of the Ca^{2+} binding function of calnexin being important in cellular homeostasis.

Although calreticulin and calnexin share a high degree of structural similarity, the two chaperones demonstrate considerable differences in their substrates and specificities (Bedard et al., 2005; Denzel et al., 2002). This is observed both for different folding intermediates as well as for distinct domains of the same glycoprotein (Hebert et al., 1997). These substrates can be divided into those which interact with calnexin exclusively, including vesicular stomatitis virus G protein (Hammond et al., 1994), the myelin protein PMP22 (Dickson et al., 2002) or the acetylcholine receptor (Keller et al., 1998), or those which interact with calreticulin only, such as coagulation factor V (Pipe

et al., 1998). As evidence from gene knockout studies in mice, the two proteins cannot compensate for one another (Denzel et al., 2002). The tissue expression patterns of both calnexin and calreticulin greatly differ. During development, calreticulin is highly expressed in the heart and significantly downregulated upon maturity, while this same pattern of expression is not observed for calnexin (Mesaeli et al., 1999). Calreticulin and calnexin are multifunctional proteins and even though they appear similar in function and structure, in several ways they are very different from one another.

ERp57

The folding and processing of polypeptides and protein complexes appears to be a coordinated process, as demonstrated by the number of chaperone complexes existing in conjunction with folding intermediates (Kuznetsov et al., 1997; Melnick et al., 1994; Tatu and Helenius, 1997). This cohesive action may hold polypeptides in a specific conformation to allow post-translational modifications. Multi-protein complexes containing calreticulin, calnexin and ERp57 are identified (Bouvier, 2003; Diedrich et al., 2001; Oliver et al., 1999). Calreticulin and calnexin interact with ERp57 (Frickel et al., 2004), via the tip of the P-domain, with ERp57 involved in the catalysis of disulphide bonds in nascent proteins within the ER (Oliver et al., 1999; Zapun et al., 1998) (Figure 1- 7). The interaction of ERp57 and calreticulin or calnexin has historically been demonstrated *in vitro* utilizing RNaseB glycoproteins containing the $Glc_1Man_9GlcNAc_2$ oligosaccharide (Zapun et al., 1998). It is demonstrated that ERp57 catalyzes disulfide linkages found in the glycosylated substrate, versus PDI, which interacts with glycoproteins and nonglycoproteins alike (Zapun et al., 1998). Interestingly, the interaction of ERp57 with either calreticulin or calnexin enhances the disulfide-isomerase activity of ERp57, whereas the same type of interaction with PDI reduces the disulfide-isomerase activity of PDI as well as the peptide binding (Zapun et al., 1998; Zapun et al., 1997). Further studies using NMR spectroscopy demonstrate ERp57 binding to the P-domain of calreticulin with the specific region of the tip of the P-domain identified by chemical shift mapping (Frickel et al., 2002). Truncated calreticulin and calnexin lacking the most distal set of repeats exhibit an impairment in ERp57 binding as analyzed by GST pulldown assays (Leach et al., 2002). This site is further narrowed down using NMR spectroscopy and Yeast 2-Hybrid analysis, to the specific amino acids (Asp342,

Asp344, Asp346, Met347, Asp348 and Glu352) found at the tip of the P-domain of calnexin (Pollock et al., 2004) with Asp344 and Glu352 likely the two most important residues contributing to this interaction (Pollock et al., 2004). The amino acid residues responsible for the interaction with ERp57 are not identified in calreticulin (Figure 1- 7). It appears that a variety of factors act either simultaneously or sequentially during the conformational maturation of nascent proteins.

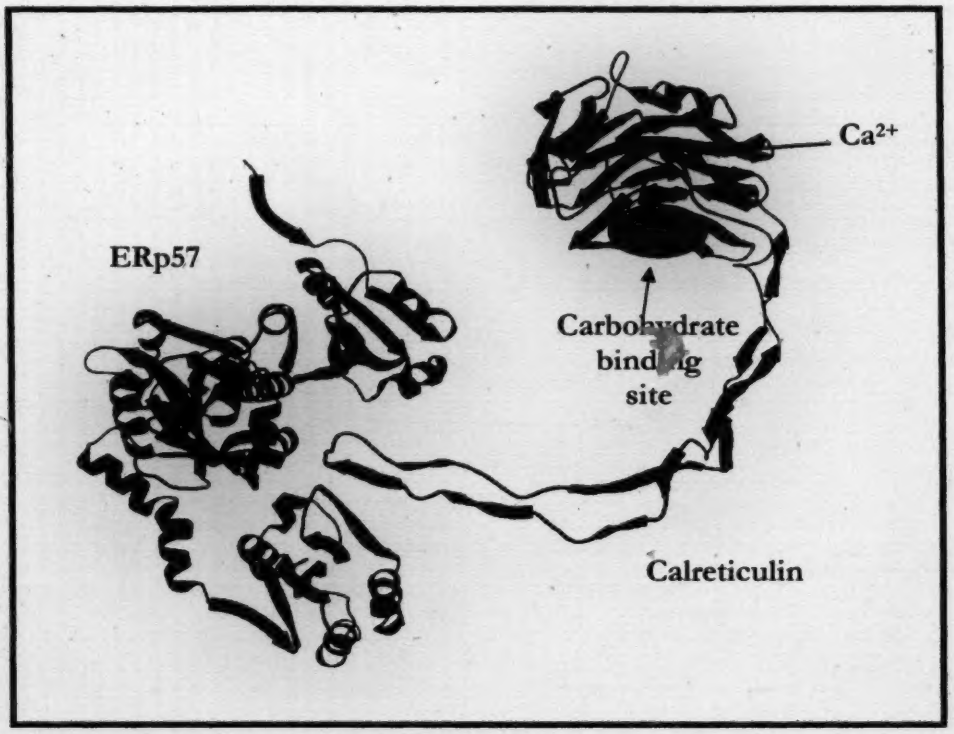

Figure 1- 7

Figure 1- 7 — Model of the interaction between ERp57 and calreticulin.

A 3D model of ERp57 generated based on its similarities to PDI amino acid sequence and 3D structure of calsequestrin. The model indicates that ERp57 may be composed of three domains connected by two loops. The loops may be bent to form a pocket surrounded by two domains. The arginine-rich pocket of the ERp57 structure formed by the three domains may slide over the tip of the P-domain (*in red*) of calreticulin to form structural and functional complexes. Modified from: Ca^{2+} signaling and calcium binding chaperones of the endoplasmic reticulum. Cell Calcium. 2002 Nov-Dec;32(5-6):269-78.

The ER is able to respond to an increase in the unfolded protein situation and return the ER to its normal physiological state by two simple adaptive mechanisms. Immediate first response includes downregulation of the biosynthetic load of the ER via interruption of protein synthesis on a transcriptional and translational level, followed by increased clearance of misfolded or aggregated proteins from the ER by upregulating the ERAD machinery. The second response includes upregulation of the folding capacity of the ER through induction of ER resident molecular chaperones and folding enzymes as well as increasing the size of the ER (Menzel et al., 1997), as seen in yeast. Upon conditions of exacerbated ER stress, after these adaptive mechanisms are employed, with the cell unable to recover its normal state, apoptosis is triggered, presumably to eliminate unhealthy or damaged cells (Schroder and Kaufman, 2005a).

Unfolded Protein Response (UPR)

A build up of misfolded protein leads to a specific ER stress-response, termed UPR, signaling attenuation of gene transcription and protein translation, upregulation in chaperone expression (Schroder and Kaufman, 2005b), inhibited protein synthesis (Brostrom et al., 1996; Harding et al., 1999; Prostko et al., 1995) and facilitated protein degradation (Jeffery et al., 2000). The primary aim of UPR is to limit damage to the cell by adapting the cell to the situation causing the ER stress. However, increased UPR caused by prolonged stress or the additive effect of several inducers may trigger apoptosis of the cell (Ma and Hendershot, 2004).

Three resident transmembrane proteins, in combination with the ER molecular chaperone BiP/GRP78 (Bertolotti et al., 2000), are responsible for the response to ER stress. The UPR mechanism involves transcriptional activation of chaperones and members of the ERAD by the transcription factor ATF6 (activating transcription factor 6) (Shen et al., 2002), in conjunction with the ER membrane kinase and endoribonuclease IRE1 (inositol-requiring 1) (Cox et al., 1993), as well as translational repression of protein synthesis by the ER kinase PERK (dsRNA-activated protein kinase-like ER kinase) (Rutkowski and Kaufman, 2004) (Figure 1- 8).

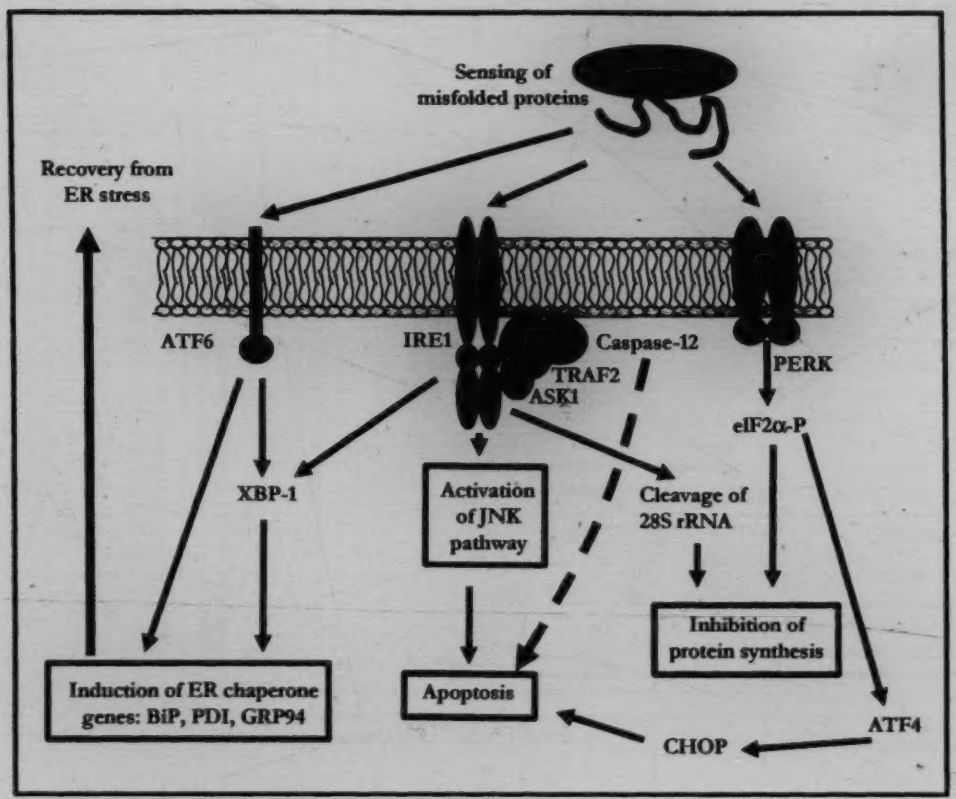

Figure 1- 8

Figure legend on the next page.

Figure 1- 8 — Unfolded protein response (UPR).

Upon an accumulation of misfolded protein in the ER lumen, BiP/GRP78 is sequestered away from three transmembrane proteins, ATF6, IRE1 and PERK. ATF6 is retained in the ER by the interaction with BiP, but it is transported to the Golgi where it undergoes site specific cleavage by SP1 and SP2, releasing an active transcription factor involved in activation of ER chaperone genes, as well as the XBP1 gene. IRE1 dimerizes upon release from BiP, resulting in activation of its ribonuclease activity and cleavage of the mRNA encoding XBP1, producing a truncated transcript encoding a transcription factor. IRE1 forms a complex with TRAF2 and ASK1, resulting in activation of the JNK pathway, eventually signaling to apoptosis. Caspase 12, an ER stress-dependent caspase has also been complexed to TRAF2. Furthermore, IRE1 ribonuclease activity is also involved in inhibition of protein synthesis by cleavage of ribosomal RNA. PERK, upon loss of interaction with BiP, also dimerizes and autoactivates, resulting in the phosphorylation of eIF2 and inhibition of protein synthesis. eIF2 also activates a transcription factor, ATF4, involved in the induction of apoptosis via CHOP induction. The broken arrow demonstrates caspase-dependent signaling of apoptosis upon ER stress. BiP, binding protein; PERK, dsRNA-activated protein kinase-like ER kinase; IRE1, inositol response element 1; TRAF2, TNF receptor associated factor 2; ASK1, apoptosis signaling kinase 1; eIF2α, eukaryotic initiation factor 2 α; JNK, c-JUN kinase; XBP1, X-box binding protein 1; rRNA, ribosomal RNA; ATF4/6, activating transcription factor 4/6; CHOP, C/EBP homologous protein; PDI, protein disulfide isomerase; GRP94, glucose regulated protein 94.

UPR is activated upon an increase of misfolded or unfolded protein in the lumen of the ER. It involves three distinct steps, translational attenuation to avoid further accumulation of unfolded proteins in the ER, transcriptional activation of chaperone and protein folding genes and activation of ERAD in an attempt to rectify the accumulation of misfolded protein. The instant cessation in protein synthesis mediated by PERK reduces the translocation of nascent proteins into the ER lumen. IRE1 and ATF6 mediate the transcriptional activation of genes encoding components that increase protein folding, export and degradation. As this activity requires chaperone transcription and translation, it follows the translational attenuation with a slight delay to allow recovery in protein translation.

ATF6 is a transmembrane protein localized to the ER membrane that upon cleavage becomes a potent transcription factor. Under non-stress conditions, BiP/GRP78 interacts with ATF6, masking its Golgi localization signals (Shen et al., 2002), retaining it in the ER, but upon an accumulation of unfolded nascent proteins, BiP/GRP78 is sequestered away, binding to the hydrophobic sections of these nascent proteins, resulting in ATF6 being transported to the Golgi where it undergoes cleavage by the proteases, S1P and S2P (Shen et al., 2002). This yields a soluble basic leucine zipper (bZIP) transcription factor that translocates to the nucleus and induces target genes by binding directly to the ER stress response element (ERSE) located upstream of the target gene (Yoshida et al., 1998). The classic ERSE is composed of CCAAT(N9)CCACG with N representing a GC rich region (Mao et al., 2006). Several target proteins that are upregulated include BiP/GRP78, calreticulin and calnexin, proteins involved in ERAD, such as the EDEM receptor and XBP1 (X-Box Binding Protein-1) (Mori et al., 1996). BiP/GRP78 is also sequestered away from PERK or IRE1, resulting in their homodimerization and conformational modification that is transmitted across the membrane, leading to activation of their kinase activity (Bertolotti et al., 2000; Schroder and Kaufman, 2006). PERK activation leads to the phosphorylation of the translation initiation factor eIF2α (eukaryotic initiation factor 2α). The inititation factor eIF2α forms a ternary complex with GTP and the initiator $tRNA_{met}$ responsible for initiating the translation of nascent protein (Bertolotti et al., 2000). The activity of eIF2α is controlled by phosphorylation since the phosphorylated

form sequesters eIF2β and prevents GTP-GDP exchange, inhibiting protein synthesis (Nika et al., 2001). IRE1 is a type I ER transmembrane protein that contains a serine-threonine kinase module and a C-terminal endoribonuclease domain in its cytoplasmic region (Tirasophon et al., 1998). When BiP/GRP78 senses the accumulation of unfolded proteins in the ER (Cox et al., 1993), IRE1 is released, allowing homodimerization and autophosphorylation to activate the kinase domain (Figure 1- 8). As well, IRE1 has endoribonuclease activity used to cleave 28 rRNA and inhibit protein synthesis as well as splice and activate XBP1 mRNA, upregulated by ATF6 (Yoshida et al., 2001) (Figure 1-8). A 26-nucleotide intron is excised and an undefined mechanism then re-ligates the 5' and 3' fragments, yielding a spliced XBP1 mRNA with an altered reading frame (Calfon et al., 2002; Yoshida et al., 2001). Similar to activated ATF6 transcription factor, the new XBP1 splice variant binds to the specific promoter, ERSE (Calfon et al., 2002; Lee et al., 2002; Yamamoto et al., 2004; Yoshida et al., 2001). This signals downstream transcriptional upregulation of BiP/GRP78 and other chaperones by the transcription factor XBP1 to compensate for the amount of unfolded protein. However, XBP1 also binds to a second cis-acting promoter motif, termed the UPRE (Yamamoto et al., 2004), specifically upregulating genes involved in ERAD.

Recent evidence has recognized ATF6 as a glycoprotein, with three specific N-linked sites, identified to interact with calreticulin (Hong et al., 2004). ER stress induced by Ca^{2+} depletion triggers the formation of a nascent, partially glycosylated form of ATF6, that has reduced interaction with calreticulin and the ability to traverse to the Golgi at a faster rate, resulting in higher transactivation of the BiP/GRP78 promoter, a major target of the UPR. As an accumulation of under-glycosylated proteins in the ER has the ability to induce UPR, the glycosylation status of ATF6 may serve as a novel sensor of glycoprotein homeostasis, leading to activation of the UPR (Hong et al., 2004). In calreticulin-deficient cells, it was observed that UPR was triggered with PERK, IRE1 and eIF2 being activated, with a devastating effect on cellular function (Knee et al., 2003). Both calnexin and calreticulin contain the ERSE in their promoter. ATF6 is the transcription factor that activates this stress element, resulting in the expression of calnexin, as seen in cells infected with RSV (Bitko and Barik, 2001) and calreticulin, as demonstrated in thapsigargin or tunicamycin (an inhibitor of glycosylation) treated HeLa cells (Llewellyn and Roderick, 1998).

IRE1 recruits TRAF2 (TNF receptor associated factor-2) and stimulates the stress-activated JNK (c-Jun amino-terminal kinase) pathway (Urano et al., 2000) (Figure 1- 8). Activation of this pathway requires formation of a trimeric complex between IRE1, TRAF2 and ASK1 (apoptosis signaling kinase 1), resulting in the activation of ASK1 (Matsukawa et al., 2004). Active ASK1 triggers the JNK pathway, leading to cell death (Matsukawa et al., 2004). An interaction between TRAF2 and caspase 12 is observed (Figure 1- 8) with TRAF2 promoting the clustering of caspase 12 and releasing caspase 12 upon ER stress, presumably by sequestering IRE1 (Yoneda et al., 2001). This mechanism may be a prerequisite for caspase 12 activation (Yoneda et al., 2001). These interactions may connect extenuating ER stress and apoptosis. Activation of these three ER transmembrane proteins, IRE1, ATF6 and PERK, is responsible for the downregulation of protein synthesis, resulting in a reduced influx of nascent protein into the ER, upregulation of ER chaperones, preparing the ER to handle increased levels of unfolded proteins, as well as upregulating proteins involved in the ERAD, responsible for degradation of the misfolded proteins.

ER and Apoptosis

Cellular regulation of apoptosis (pre-programmed cell death) is of critical importance for the prevention of cellular destruction. Apoptosis is a necessary process utilized by an organism to remove redundant or damaged cells, an important function during development (Meier et al., 2000) and tissue homeostasis (Danial and Korsmeyer, 2004). Apoptosis is critical as a line of defense against foreign pathogens (Siegel et al., 2003) and defective cells (Norbury and Zhivotovsky, 2004). Therefore, any disruption in the apoptotic pathway plays a fundamental role in the pathogenesis of human disease, including gene suppression, activation, or mutation (Thatte and Dahanukar, 1997). Uncontrolled activation of apoptosis can lead to Alzheimer's and Parkinson's disease (Mattson, 2000), while an inhibition in apoptosis can lead to cancer and autoimmune disease (Green and Evan, 2002). Death inducing signals can be intrinsic, such as ER stress, or extrinsic, with specific receptors on the cell surface, culminating in the activation of caspases, responsible for cellular degradation (Breckenridge et al., 2003a; Danial and Korsmeyer, 2004; Ferrari et al., 2002; Green and Evan, 2002; Hajnoczky et al., 2003; Siegel et al., 2003; Strasser et al., 2000).

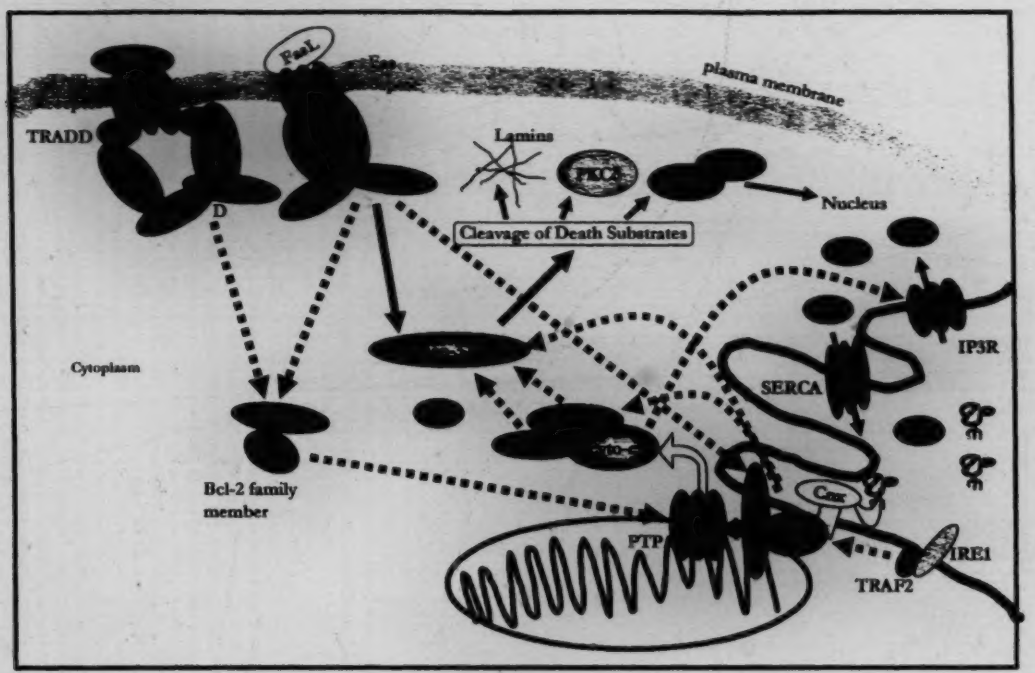

Figure 1- 9

Figure legend on the next page.

Figure 1- 9 — The apoptotic cascade.

Apoptosis can be signaled through two different but interconnected pathways, the extrinsic (receptor-mediated) pathway and the intrinsic (ER stress) pathway. The extrinsic pathway utilizes caspase 8-dependent cleavage of caspase 3 as well as facilitating the involvement of the mitochondria via caspase 8-dependent cleavage of Bap31 and recruitment of Bcl-2 family members to the mitochondria, resulting in the release of cytochrome *c* and subsequent formation of a caspase 9 complex, leading to the apoptotic cascade. The intrinsic pathway involves caspase 12, resulting in direct activation of caspase 9 and recruits the mitochondria, potentially via caspase 12-dependent cleavage of Bap31, facilitating an amplified caspase cascade. Solid black arrow indicates receptor-mediated pathway while broken black arrows indicate pathways with recruitment of mitochondra. Broken gray arrows indicate ER stress induced apoptotic pathway. TNF, tumour necrosis factor; TRADD, TNF receptor associated death domain; FasL, Fas ligand; FADD, Fas ligand receptor associated death domain; Casp-8, caspase 8; PKC, protein kinase c; iCAD, inhibitor of CAD; CAD, caspase activated DNase; Apaf-1, apoptotic protease activating factor-1; cyto *c*, cytochrome *c*; PTP, permeability transition pore; Cnx, calnexin; SERCA, Sarco/endoplasmic reticulum Ca^{2+}-ATPase; IP_3R, inositol triphosphate receptor; IRE1, inositol requiring element 1; TRAF2, TNF receptor associated factor 2.

Caspases form a large family of cysteine-dependent aspartate-specific proteases containing a highly conserved pentapeptide active site, QACRG and are involved in all aspects of apoptosis. The caspase family can be divided into two distinct groups, the initiator caspases, including caspase 2, 8, 9, 10 and 12, that contain a longer pro-domain and cleave and activate other caspases, and the effector caspases, such as caspase 3, 6 and 7 that have a short pro-domain and directly cleave cellular components to cause cellular destruction (Creagh et al., 2003; Denault and Salvesen, 2002; Earnshaw et al., 1999; Nicholson and Thornberry, 1997; Saraste and Pulkki, 2000; Slee et al., 1999; Thornberry and Lazebnik, 1998; Wang, 2000).

The extrinsic apoptotic pathway involves a Death Receptor, such as the TNFR (tumor necrosis factor receptor) or the FasR (Fas ligand receptor), located at the plasma membrane and activated by specific ligands and expressly recruit caspase 8 upon activation (Ashkenazi, 2002) (Figure 1- 9). This process is triggered by binding of the ligand to the receptor, resulting in trimerization and autoactivation of the receptor (Naismith and Sprang, 1998) and recruitment of adaptor proteins, such as TRADD (TNF receptor associated death domain) or FADD (Fas associated death domain). These complexes recruit caspase 8 via an interaction with the DED (death effector domain), with the whole complex termed DISC (death initiator signaling complex) (Sartorius et al., 2001). Formation of this complex results in proximity-induced dimerization (Boatright and Salvesen, 2003; Donepudi et al., 2003) and activation of caspase 8 that signals the caspase cascade (Denault and Salvesen, 2002; Earnshaw et al., 1999; Kam and Ferch, 2000; Sartorius et al., 2001) (Figure 1- 9). Once effector caspases (caspase 3, 6 and 7) are cleaved and activated by an initiator caspase, they directly act on cellular components such as the cytoskeleton (Earnshaw et al., 1999; Ferraro et al., 2003; Kluck et al., 1997; Liu et al., 1996; Yang et al., 1997), membrane proteins (Remillard and Yuan, 2004) and other cellular proteins such as DNA repair enzymes, gelsolin and PKCδ (Nicholson and Thornberry, 1997; Slee et al., 1999; Thornberry and Lazebnik, 1998) (Figure 1- 9). The effector caspases also activate other proteins such as CAD (caspase activated DNase) by cleaving its inhibitor, iCAD, with CAD targeting to the nucleus and involved in the degradation of DNA (Enari et al., 1998; Sakahira et al., 1998) (Figure 1- 9). Caspase 3 is also responsible for cleaving several membrane localized transporters, including the IP_3R in the ER membrane, resulting in IP_3-independent Ca^{2+} release and

signaling of apoptosis (Hirota et al., 1999) and cleavage of PMCA, rendering the transporter unable to regulate the cytoplasmic Ca^{2+} concentration (Chami et al., 2003). NaK-ATPase is also cleaved by caspase 3, resulting in loss of intracellular ion regulation and resultant volume shrinkage (Dussmann et al., 2003; Mann et al., 2001).

The intrinsic pathway, stimulated by metabolic pressure or ER stress, usually involves the mitochondria, Bcl-2 family members and the initiator caspase 9 (Figure 1-9). Bcl-2 proteins have both pro- and anti-apoptotic functions, are both membrane bound and soluble and localize to several locations within the cell, including the cytoplasm (Schinzel et al., 2004), the mitochondria (Schinzel et al., 2004) and the ER (Annis et al., 2004; Zong et al., 2003). A number of Bcl-2 family members target to the mitochondria, including Bax (Wang, 2001), which interacts with the VDAC (voltage-dependent anion channel) (Marzo et al., 1998), or with the PTP (permeability transition pore) (Brini et al., 2000; Gross et al., 1999). This interaction leads to the extrusion of a small amount of cytochrome *c*, which binds and promotes Ca^{2+} release via the IP_3R in the ER membrane. This localized Ca^{2+} increase adjacent to the mitochondria triggers a much larger portion of cytochrome *c* to be released from all mitochondria (Boehning et al., 2003). Cytochrome *c* is responsible for the proximity-induced activation of caspase 9 (Katoh et al., 2004), in conjunction with a cytoplasmic factor, Apaf-1 (apoptotic protease activating factor-1) to form an apoptosome (Salvesen and Renatus, 2002) (Figure 1- 9).

Protracted ER stress is also responsible for stimulation and activation of the apoptotic cascade via the ER localized caspase 12. Caspase 12 is ubiquitously expressed and is synthesized as an inactive proenzyme consisting of a regulatory prodomain and two catalytic subunits (Nakagawa and Yuan, 2000). Activation of caspase 12 is limited to conditions that stimulate ER stress (Nakagawa et al., 2000). The caspase 12-deficient mouse model is partially resistant to apoptosis induced by ER stress but is sensitive to other apoptotic stimulation (Nakagawa et al., 2000). Active caspase 12 has the potential to directly cleave and activate caspase 9 without cytochrome *c* or Apaf-1. Active caspase 9 then can directly cleave caspase 3, setting into motion the destruction machinery (Morishima et al., 2002; Rao et al., 2002) (Figure 1- 9). TRAF2-caspase 12 complex (Yoneda et al., 2001), leads to proximity-induced dimerization and activation of caspase 12 (Shi, 2004), with TRAF2 also interacting with IRE1, a member of UPR (Urano et al., 2000), triggering activation of the JNK pathway (Urano et al., 2000; Yoneda et al., 2001)

(Figure 1- 8 and 1-9). This may represent a direct connection between accumulation of misfolded protein, resulting in ER stress and the apoptotic pathway. Another link between ER stress and apoptosis may be via Bap31, a pro-apoptotic membrane protein localized to the ER (Figure 1- 9). Bap31 (a B-cell receptor associated protein–31) is a 28-kDa integral membrane protein containing a cytoplasmic domain that associates with caspase 8, Bcl-XL and Bcl-2 (Ng et al., 1997). Caspase 8 is responsible for cleaving Bap31, producing a p20 N-terminal transmembrane portion of Bap31 which is retained in the ER membrane to induce apoptosis via an interaction with Drp1 (dynamin related protein 1) (Breckenridge et al., 2003b). Recent evidence determined that overexpression of this p20 fragment caused a significant release of Ca^{2+} from the ER, potentially via the transporter A4 (Wang et al., 2003), with associated Ca^{2+} uptake into the mitochondria, leading to caspase 8 induced cytochrome *c* release (Ng et al., 1997). The link between misfolded protein and Bap31 may involve calnexin (Figure 1- 9).

Apoptosis and Ca^{2+}

Recent evidence has identified a vital executioner role for Ca^{2+} during the apoptotic process (Breckenridge et al., 2003a; Distelhorst and Roderick, 2003; Rizzuto et al., 2004). Modification of cytoplasmic Ca^{2+} levels is observed during genetic stress in human lung carcinoma A549 cells (Amuthan et al., 2002), betulinic acid treatment of MDCK (Madin-Darby Canine Kidney Epithelial) cells (Chou et al., 2000) and thapsigargin treatment of mouse lymphoma cells (Distelhorst and McCormick, 1996). High ER Ca^{2+} levels regulate apoptosis (Brini et al., 2000; Jayaraman and Marks, 1997; Ma et al., 1999). In contrast, low levels of ER Ca^{2+} result in ER stress, Ca^{2+} toxicity and cellular death (Kobrinsky and Kirchberger, 2001).

The ER has been identified to associate with mitochondria by establishing transient mitochondria-associated-membranes (MAMs), mediating the transfer of nascent glycosphingolipids (Ardail et al., 2003; Vance, 1990), but most recently, Ca^{2+} transfer between the two organelles appears to be an intrinsic part of the apoptotic cascade (Rizzuto et al., 2003; Szabadkai and Rizzuto, 2004; Szabadkai et al., 2003). Drp1 (dynamin related protein 1) has been identified to localize to punctate vesicles between the ER and the mitochondria and is hypothesized to regulate dynamic interaction between the two organelles (Pitts et al., 1999). The family of dynamins are large GTPases

with mechanochemical properties that are observed to constrict and tubulate membranes (Yoon et al., 2001). Drp1 has been established to be intrinsically involved in mitochondrial fission (Chen and Chan, 2005; De Vos et al., 2005) with an antagonistic effect on the mitochondrial PTP, sensitizing cells to disruption in permeability during apoptosis (Kong et al., 2005). This potential membrane interaction may play an important role during a number of the ER-dependent functions, such as Ca^{2+} signaling, protein synthesis and apoptosis (Rizzuto et al., 2004). Upon local increases in Ca^{2+}, mitochondria accumulate Ca^{2+}, affecting the respiratory chain (McClintock et al., 2002), the ATP synthase (Shchepina et al., 2002), as well as releasing cytochrome *c* (Darios et al., 2003). This Ca^{2+} transfer might be mediated via Bcl-2 family members, both at the ER membrane and at the mitochondrial membrane. It has been postulated that Ca^{2+} may even transfer directly between the two organelles (Darios et al., 2003). Specifically, the pro-apoptotic Bcl-2 protein Bid, once localized to the mitochondrial membrane, may be involved in the transfer of Ca^{2+} from the ER to the mitochondria (Csordas et al., 2002). Mobilization of ER Ca^{2+} stores rather than cytoplasmic Ca^{2+} (Diaz-Horta et al., 2002), in conjunction with accumulation of Ca^{2+} by the mitochondria, appears to activate the apoptotic cascade (Breckenridge et al., 2003a) and dictate the fate of a cell (Rizzuto et al., 2004). Calreticulin-deficient cells with decreased ER luminal Ca^{2+} are resultantly less sensitive to apoptotic stimulation (Nakamura et al., 2000), while HeLa cells, mouse embryonic fibroblasts (Nakamura et al., 2000), human embryonic kidney cells (Arnaudeau et al., 2002) and rat cardiomyocytes (Kageyama et al., 2002), all overexpressing calreticulin, had an increased sensitivity to apoptosis. Alterations in calreticulin protein levels have a drastic effect on the cellular response to apoptosis, via the availability of Ca^{2+} for release. It appears that calreticulin, via its Ca^{2+} binding capabilities, regulates the amount of Ca^{2+} available for release from the ER lumen.

As the ER luminal Ca^{2+} level plays an important role in the activation and sustentation of apoptosis, resultantly, there are many apoptosis related factors that are Ca^{2+}-dependent, including presentation of phosphatidylserine (PS) in the outer leaflet of the membrane and the cysteine protease, calpain. The Ca^{2+}-dependent factor involved in apoptosis, the "eat me" phosphatidylserine signal, is projected by a cell undergoing apoptosis (Draper et al., 2004). Appearance of PS on the cell surface involves three enzymes, a Ca^{2+}-dependent scramblase, responsible for randomly moving lipids between

the two leaflets of the plasma membrane, an ATP-dependent aminophospholipid translocase that transfers PS from the outer to the inner leaflet and a third unidentified enzyme, specifically responsible for depositing PS to the outer leaflet (Balasubramanian and Schroit, 2003). The presentation of phosphatidylserine recruits a Ca^{2+}- and caspase-dependent adaptor protein, annexin we that is rapidly upregulated upon apoptotic stimulation (Arur et al., 2003).

An additional Ca^{2+}-dependent cytoplasmic factor, the cysteine protease calpain is active during normal cellular mechanisms, including cell cycle (Choi et al., 1997; Pariat et al., 1997) and cellular remodeling (Potter et al., 1998). Activation of calpain is dependent on an increase in cytoplasmic Ca^{2+} (Nath et al., 1996) and takes place secondary to caspase activation during the apoptotic cascade (Hajnoczky et al., 2003; Wood and Newcomb, 1999). Proteolysis mediated by calpain does not take place at a specific amino acid residue, unlike caspases. Calpain activation by Ca^{2+} has been seen under a number of different conditions (Wang, 2000), including ER stress (Nakagawa and Yuan, 2000). Potentially one of the most interesting substrates of calpain is the endogenous inhibitor of calcineurin, CAIN/Cabin1 (calcineurin binding protein 1) (Lai et al., 1998; Lai et al., 2000; Sun et al., 1998). Calpain-mediated cleavage of CAIN/Cabin1 generates a p32 (32-kDa) product that allows dissociation of calcineurin, resulting in calcineurin-dependent activation of transcription factors such as MEF2 (myocyte enhancer factor 2) and NFAT (nuclear factor of activated T-cells) (Kim et al., 2002).

In summary, ER Ca^{2+} release, in conjunction with Ca^{2+}-dependent enzymes and Ca^{2+} buffering proteins, may be partially responsible for the apoptotic signal (Chou et al., 2000; Distelhorst and McCormick, 1996; Hajnoczky et al., 2003; Mattson and Chan, 2003; Rizzuto et al., 2004). Both calcineurin (Asai et al., 1999), a Ca^{2+}-dependent phosphatase, and calreticulin (Nakamura et al., 2000), a Ca^{2+} buffering protein, are implicated in cellular response to apoptosis.

RESEARCH OBJECTIVE

The Objective for my PhD Thesis was to investigate at the molecular level, the structure and function of calreticulin and calnexin, with a special emphasis on their chaperone function and role in the regulation of cellular sensitivity to apoptosis.

Considering that the importance of the ER in a variety of processes, including the synthesis, post-translational modification and folding of membrane-associated, secreted and integral membrane proteins as well as being centrally involved in the maintenance of intracellular Ca^{2+} homeostasis, examination of the function of calreticulin and calnexin in the ER is a fundamental objective of this thesis. Calreticulin is necessary during intracellular signaling and essential throughout development, in particular during cardiogenesis (Mesaeli et al., 1999), ER Ca^{2+} homeostasis, protein folding (Nakamura et al., 2001a) and apoptosis (Arnaudeau et al., 2002; Nakamura et al., 2000). Calnexin, a close homolog of calreticulin, may also be implicated in these processes. The role of calnexin in quality control may ultimately be responsible for maintaining cellular viability, specifically in relation to apoptosis.

RESEARCH HYPOTHESIS

Considering the function that both calreticulin and calnexin perform during quality control as well as in the regulation of cellular sensitivity to apoptosis; my hypothesis is that specific attributes of calreticulin and calnexin may provide the necessary structure and function required to modulate protein folding and may be involved in the modulation of apoptosis. We propose to address two main questions: (i) what molecules interact with calreticulin and calnexin and what amino acids of calreticulin and calnexin are responsible for protein folding and quality control (ii) and specifically, are calnexin protein interactions accountable for affecting cellular sensitivity to apoptosis?

Chapter Two — Materials and Methods

Chemicals and Materials

Ac-DEVD-AFC, ampicillin, ANS, APMSF, aprotinin, arabinose, ATP-Mg^{2+}, benzamidine, β-mercaptoethanol, bombesin, bradykinin, BSA, $CaCl_2$, carbachol, CHAPS, chloroform, coomassie blue, CS, DEPC, digitonin, DMF, DMSO, DNase I, DTT, E-64, EDTA, EGTA, ethidium bromide, FluroTag-FITC Conjugation Kit, glucose, glutaraldehyde, guanidine hydrochloride, Hepes, imidazole, ionomycin, IPTG, kanamycin, KCl, leupeptin, mannitol, $MgCl_2$, $MgSO_4$, MDH, NaCl, $Na_3Citrate.2H_2O$, paraformaldehyde, PEG 8000, pepstatin, phosphoramidone, PIPES, phenol, PMSF, poly L-lysine, Ponceau-S, propylene oxide, proteinase K, RNase A, saponin, sodium cacodylate, sodium deoxycholate, sucrose, sulfinpyrazone, thapsigargin, TLCK, TPCK, Tris-HCl, trypsin, tunicamycin, Tween-20, X-galactosidase and $ZnCl_2$ were from Sigma-Aldrich, Oakville, Ontario. Skim milk powder was from COSTCO, Ottawa, Ontario. The caspase inhibitors, Z-DEVD-FMK (caspase 3 inhibitor II) and Z-IETD-FMK (caspase 8 inhibitor II) were from BioVision Inc, Mountain View, California. SDS-PAGE reagents, Triton X-100, Chelex and molecular weight markers were from BioRad Inc, Hercules, California. Molecular markers used were myosin (200,000 Da), phosphorylase b (97,400 Da), bovine serum albumin (66,000 Da), ovalbumin (46,000 Da), carbonic anhydrase (30,000 Da) and lysozyme (14,300 Da). The Random Prime-It II kit was from Stratagene, La Jolla, California. Odyssey Blocking Buffer for Western immunoblotting was from Licor Biosciences Inc, Lincoln, Nebraska. Annexin V-FITC Cell Death Detection Kit was obtained from BD Biosciences, San Jose, California. The *In situ* TUNEL Cell Death Detection Kit and the Caspase 3 Activity Assay were from Roche Diagnostics, Laval, Quebec. Cascade Blue Acetyl Azide, Fura 2-AM, Vinol 205S, anti-rabbit FITC, anti-rabbit Texas Red, anti-rabbit Alexa 546, anti-rabbit Alexa 488, anti-rat Alexa 488 and anti-goat Alexa-488 secondary antibodies were from Invitrogen Life Technologies, Burlington, Ontario. Goat anti-rabbit horseradish peroxidase, rabbit anti-goat horseradish peroxidase and rabbit anti-rat horseradish peroxidase were purchased from Jackson Immunochemicals, Westgrove, Pennsylvania. EGGstract IgY purification system was from Promega, Madison, Wisconsin. Effectene Transfection Reagent, DNA Purification Columns and Ni^{2+}-NTA agarose beads were from Qiagen, Mississauga, Ontario. CM5 sensor chips, Amine Coupling Kit and the BIA Evaluation Analysis Program were from BIAcore Inc, Piscataway, New Jersey. DMEM, αMEM,

GMEM, FCS, penicillin/streptomycin, 0.05% Trypsin-EDTA solution, glutamine, sodium pyruvate, 1 X non-essential amino acids, Geneticin, Zeocin, *Pfx* DNA polymerase, M-MLV Reverse Transcriptase Kit, restriction enzymes, pBAD/glIII A and pCDNA3.1/Zeo plasmids were obtained from Invitrogen Life Technologies, Burlington, Ontario. Sephadex G-25M, Q-Sepharose, Heparin-Sepharose and ECL chemiluminescent detection system were purchased from GE Healthcare Bio-Sciences, Baie d'Urfe, Quebec. Protein A-Sepharose and rabbit anti-HA was purchased from Roche Diagnostics, Laval, Quebec. Centrifugal Filter Devices were purchased from Millipore, Bedford, Massachusetts. Osmium tetroxide was obtained from Polyscience, Warrington, Pennsylvania. Anti-Bcl-2 and anti-Bax antibodies were from Upstate Cell Signaling Solutions, Charlottesville, Virginia. Rat anti-caspase 12 antibodies were kindly provided by Dr. D.Y. Juang, Department of Cell Biology, Harvard Medical School, Boston. Rabbit anti-caspase 3 and anti-caspase 8 were from Dr. Don Nicholson, Merck Frost Therapeutic Centre for Research, Pt. Claire, Quebec and from Dr. R.C. Bleackley, Department of Biochemistry, University of Alberta, Edmonton, Alberta. Goat anti-calreticulin, rabbit anti-calnexin, rabbit anti-PDI and rabbit anti-ERp57 were generated by our laboratory (Baksh et al., 1995a; Corbett et al., 2000; Knoblach et al., 2003). Rabbit anti-BiP, rabbit anti-GRP94 and rabbit anti-Bcl-2 were purchased from Stressgen Inc., Victoria, British Columbia. Affinity purified rabbit anti-Bap31 antibody #2453 was generously provided by Dr. G. Shore, Department of Biochemistry, McGill University, Montreal, Quebec. Anti-cytochrome *c*, Anti-IP_3R and anti-PARP antibodies were from BD Biosciences, Mississauga, Ontario. Rabbit anti-bradykinin receptor antibody was kindly provided by Dr. W. Muller-Esterl, Institute for Biochemistry, University Hospital, Frankfurt, Germany. Mouse anti-SV40 was from Santa Cruz Biotechnology, Santa Cruz, California. Rabbit anti-BiP/GRP78 and rabbit anti-SERCA2 were kindly provided by L. M. Hendershot, Department of Medical Biochemistry and Genetics, Texas A&M University, College Station, Texas and K. P. Campbell, Howard Hughes Medical Institute, University of Iowa, Iowa City, Iowa, respectively. Radiolabeled $^{45}Ca^{2+}$ and ^{32}P-αATP was from GE Healthcare Bio-Sciences, Baie d'Urfe, Quebec. All other chemicals were from Sigma-Aldrich unless otherwise noted. All chemicals were of the highest grade available.

Isolation and Generation of Calreticulin and Calnexin-Deficient Mouse Embryonic Fibroblasts

Wild-type (K41) and calreticulin-deficient (K42) mouse embryonic fibroblasts used in these studies were derived from day 10 mouse embryos (Mesaeli et al., 1999) while wild-type and calnexin-deficient mouse embryonic fibroblasts were derived from day 12 mouse embryos. Whole embryos were washed with PBS (137 mM NaCl, 2.7 mM KCl, 4.3 mM $Na_2HPO_4 \cdot H_2O$, 1.4 mM KH_2PO_4, pH 7.3) and minced using scalpel blades. Cells were dissociated from the minced tissue by incubating in 0.05% Trypsin-EDTA solution at 37°C for ten minutes with agitation. The cellular suspension was centrifuged at 2000 x g (Eppendorf centrifuge 5702, Brinkmann, Mississauga, Ontario) for one minute to remove large debris and the supernatant containing dissociated fibroblasts was diluted with DMEM supplemented with 10% FCS, placed in one well of a 6-well tissue culture plate and incubated for two days at 37°C in a 5% CO_2 tissue culture incubator. Immortalized fibroblast cultures were generated by stably transfecting the cells with pSV7 plasmid containing cDNA encoding the SV40 T-antigen (Conzen and Cole, 1995) using Effectine Reagent as recommended by the manufacturer. 10 μg of DNA was mixed with Effectine Reagent and added to 10 cm plate containing primary fibroblasts at 50% confluency. Stably transfected cells were selected by reducing the serum concentration from 10% to 5% with transformants being isolated on the basis of rapid colony formation after two-three weeks of growth in low serum in DMEM. Colonies were selected by manual trypsinization and transferred to a well each in a 96-well plate. Cells were maintained in DMEM containing 10% FCS and 1% penicillin/streptomycin in a 5% CO_2 incubator. Upon reaching confluency, cells were trypsinized and transferred to a 24-well plate and grown until confluent, then transferred to 10 cm dishes. Positive fibroblast cultures were tested by Western blot analysis for SV40 expression using anti-SV40 antibodies at dilution of 1:300. All cell lines generated in this study are listed in Table 2- 1.

Cell Culture

Wild-type and calreticulin-deficient (Nakamura et al., 2001b) or calnexin-deficient mouse embryonic fibroblasts used in this study were grown at 37°C in a 5% CO_2 environment in DMEM containing 10% FCS. Transfections were carried out using

Effectene transfection reagent as recommended by the manufacturer and stable transfected cell lines were selected with 350 μg/ml Zeocin. *crt*$^{-/-}$ cells were transfected with pcDNA3.1/Zeo expression vectors containing cDNA encoding either wild-type or mutant calreticulin. The following cell lines expressing wild-type calreticulin (*crt*$^{-/-}$-wt) or specific histidine mutants (*crt*$^{-/-}$-His25Ala, *crt*$^{-/-}$-His82Ala, *crt*$^{-/-}$-His128Ala and *crt*$^{-/-}$-His153Ala) were generated. The following cell lines expressing wild-type calreticulin (*crt*$^{-/-}$-wt) or specific mutants (*crt*$^{-/-}$-Cys88Ala, *crt*$^{-/-}$-Cys120Ala, *crt*$^{-/-}$-Glu238Arg, *crt*$^{-/-}$-Glu239Arg, *crt*$^{-/-}$-Asp241Arg, *crt*$^{-/-}$-Glu243Arg, *crt*$^{-/-}$-Trp244Ala and *crt*$^{-/-}$-Trp302Ala) were also generated. The human CEM and NKR T-lymphoblastoid leukemia cell lines, generously provided by Dr. T. Elliott, University of Southampton, Southampton, Hampshire, were maintained at 37°C in DMEM supplemented with 10% FCS and 1% penicillin/streptomycin. The human leukemic cell line, CEM and a natural killer-resistant variant of CEM, termed NKR, immunoselected from an unmutagenized CEM population was deficient in calnexin as identified by 2D-electrophoresis. Cells lines are listed in Table 2- 1.

Flow Cytometry of Antibody Labeled Wild-type and Calreticulin-Deficient Mouse Embryonic Fibroblasts

For flow cytometry, cells were suspended in a solution containing 1 mM EDTA, 150 mM NaCl, 50 mM Tris, pH 7.3, washed, incubated with PBS containing 2% FCS and labeled with rabbit anti-bradykinin receptor antibodies at a 1:10 dilution for twenty minutes at 4°C. Secondary antibody was anti–rabbit FITC conjugated antibody at a 1:50 dilution. FACS analysis was performed using a FACScan Instrument (BD Biosciences Inc, San Jose, California). Analysis of labeled cells was determined using the program CellQuest (BD Biosciences Inc., San Jose, California). Results are presented as the relative mean fluorescence intensity of the population labeled with primary and secondary antibodies minus that obtained with secondary antibody alone.

Western Blot Analysis of Cell Lysates

Adherent wild-type and calreticulin or calnexin-deficient fibroblasts were grown to confluency on 10 cm dishes. Cells were lysed with 300 μL ice-cold Modified RIPA buffer (50 mM Tris, pH 7.5, 150 mM NaCl, 1 mM EGTA, 1 mM EDTA, 1% Triton X-

100, 0.5% sodium deoxycholate, 0.1% SDS) containing protease inhibitors: 0.5 mM PMSF, 0.5 mM benzamidine, 0.05 μg/mL aprotinin, 0.025 μg/mL phosphoramidone, 0.05 μg/mL TLCK, 0.1 μg/mL TPCK, 0.05 μg/mL APMSF, 0.05 μg/mL E-64, 0.025 μg/mL leupeptin and 0.01 μg/mL pepstatin (Milner et al., 1992a). Cells were scraped into microfuge tubes, incubated on ice for thirty minutes and lysates clarified by centrifuging at 14,000 rpm (Eppendorf 5415C microfuge, F-45-18-11 rotor, Brinkmann, Mississauga, Ontario) for five minutes. Supernatants were transferred to clean microfuge tubes and protein concentration determined. The human CEM and NKR T-lymphoblastoid leukemia cell lines were maintained at 37°C in DMEM supplemented with 10% FCS and 1% penicillin/streptomycin. Cells at a density of 2 X 10^6 cells/mL, were harvested by centrifugation at 100 x g for five minutes (Eppendorf centrifuge 5702, Brinkmann, Mississauga, Ontario), washed two times with PBS and solubilized with ice-cold Modified RIPA containing 50 mM Tris pH 7.5, 150 mM NaCl, 1 mM EDTA, 1 mM EGTA, 1% Triton X-100, 0.5% sodium deoxycholate, 0.1% SDS and the following mixture of protease inhibitors: 0.5 mM PMSF, 0.5 mM benzamidine, 0.05 μg/mL aprotinin, 0.025 μg/mL phosphoramidone, 0.05 μg/mL TLCK, 0.1 μg/mL TPCK, 0.05 μg/mL APMSF, 0.05 μg/mL E-64, 0.025 μg/mL leupeptin, 0.01 μg/mL pepstatin (Milner et al., 1992a). Lysates were incubated on ice for thirty minutes, scraped with a rubber policeman and centrifuged at 11,000 x g (Eppendorf 5415C microfuge and F-45-18-11 rotor, Brinkmann, Mississauga, Ontario) for twenty minutes to pellet insoluble matter. Supernatants were transferred to a clean microfuge tube and protein analysis was performed. Samples were then diluted to appropriate concentration in SDS-PAGE sample buffer (10% SDS, 10 mM DTT, 20% glycerol, 200 mM Tris-HCl pH 6.8, 0.05% bromophenol blue) and the indicated amounts of total protein were loaded onto gels and separated by SDS-PAGE (7.5, 10 and 12.5% acrylamide) (Laemmli, 1970). After gel electrophoresis, the gels were electrophoretically transferred to nitrocellulose membrane using a semi-dry transfer apparatus (Hoefer Inc., San Francisco, California) (Towbin et al., 1979). After transfer, nitrocellulose membranes were stained with Ponceau S and Western blot analysis of calreticulin-deficient mouse embryonic fibroblasts and calnexin-deficient lymphocytes was carried out using standard methods (Guo et al., 2003; Martin et al., 2006; Zuppini et al., 2002). Briefly, the membranes were blocked in 5% skim milk

powder dissolved in PBS for thirty minutes at room temperature with shaking. The blocked membranes were incubated with primary antibody diluted in 5% milk powder in PBS for one hour. After incubation with the primary antibody, the membranes were washed twice for five minutes each in 0.05% Tween-20 in PBS followed by one five minute wash in PBS alone. The membranes were then incubated with the appropriate horseradish peroxidase-conjugated secondary antibody diluted 1:10,000 in 5% milk powder in PBS for one hour. The wash steps were repeated as above. Detection of the bound antibodies was done using ECL chemiluminescent detection system. X-ray film (FUJIfilm, Mississauga, Ontario) was placed on the covered membrane for various time points and developed using a Kodak X-OMAT 200 Processor (Eastman Kodak Company, Rochester, New York). For quantification, X-ray films were scanned and saved as jpeg files. Quantitative immunoblotting was carried out and analyzed as previously described (Mery et al., 1996; Nakamura et al., 2000; Van Delden et al., 1992). Briefly, films of immunoreactive protein bands were scanned using a Hewlett Packard Scanjet 5550c (Hewlett Packard, Palo Alto, California) and the slope of the correlation between the amount of protein loaded on the SDS-PAGE gel and the optical density of the protein band was determined. The slopes were compared to determine changes in the level of protein in different cell lines or after thapsigargin treatment (Zuppini et al., 2002). Western blot analysis of wild-type and calnexin-deficient mouse embryonic fibroblasts was performed using the Odyssey system (Licor Biosciences Inc, Lincoln, Nebraska). Briefly, membranes were washed with PBS for several minutes to remove the Ponceau S stain and then blocked in Odyssey Blocking Buffer (Licor Biosciences Inc, Lincoln, Nebraska) (diluted 1:1 with PBS) for one hour at room temperature with gentle shaking. Primary antibody was diluted in Odyssey Blocking Buffer (diluted 1:1 with PBS) with the addition of 0.1% Tween-20 and incubated with the blot for one hour at room temperature with gentle shaking. Membranes were washed four times for five minutes each at room temperature in PBS with 0.1% Tween-20 by gentle shaking, using a generous amount of buffer. The blot was incubated in secondary antibody in the dark for one hour at room temperature with gentle shaking. Membranes were washed four times for five minutes in PBS with 0.1% Tween-20 by gentle shaking and then a final wash with PBS. Blots were visualized using the Odyssey Instrument (Licor Biosciences Inc, Lincoln, Nebraska) which utilizes a laser to scan at two different wavelengths, 700

nm and 800 nm. Files were saved as jpegs with cropping and editing carried out in Adobe Photoshop CS (Adobe, San Jose, California) and Microsoft PowerPoint 2002 (Adobe, San Jose, California). Quantification was done using Image J (The National Institute of Health, Bethesda, Maryland). Loading was normalized using single band coomassie staining, as all other loading controls observed (actin, tubulin and GAPDH) were affected by thapsigargin drug treatment. Normalization was calculated by assigning the untreated wild-type a fold induction of one and all other samples were subsequently compared to wild-type. Experiments were done independently and a minimum of four times. Statistics were performed using one-way Anova testing. P-values were a maximum of 0.05 and a minimum of 0.0001. All statistics were calculated using Origin 7.0 software (OriginLab, Northampton, Massachusetts). Dilutions of individual antibodies used for Western blots are listed in Table 2- 3.

Plasmids and Site-directed Mutagenesis of Calreticulin and Calnexin

For *E. coli* expression of calreticulin or S-Cnx, wild-type full-length rabbit calreticulin cDNA or wild-type, truncated calnexin cDNA was amplified. S-Cnx corresponds to the luminal portion of the protein containing the N- and P-domains without the transmembrane segment and the cytoplasmic tail. cDNA was cloned into *NcoI* and *XbaI* restriction enzyme sites of plasmid pBAD/glIII A, to generate pBAD-HisCrt or pBAD-HisCnx. To express calreticulin in eukaryotic cells, the rabbit calreticulin cDNA was amplified and cloned into *EcoRI* and *XbaI* of pcDNA3.1/Zeo. For easy detection of the recombinant protein, a HA [redacted]s engineered to the C-terminus of calreticulin, followed by the KDEL ER retention/retrieval signal to generate pcDNA-CRT-HA. Plasmids containing mutant calreticulin were transfected into wild-type and calreticulin-deficient mouse embryonic fibroblasts, using Effectine Reagent as recommended by the manufacturer. Site specific mutagenesis was carried out using a megaprimer polymerase chain reaction technique (Ho et al., 1989; Sarkar and Sommer, 1990) using Gene Amp PCR system 9700 thermal cycler (Perkin Elmer, Wellesley, Massachusetts) and *Pfx* DNA polymerase. For biochemical and biophysical studies, calreticulin or calnexin mutant proteins were expressed in *E. coli*. To generate the *E. coli* calreticulin expression vector, cDNA encoding calreticulin (*PstI-NotI* restriction DNA fragment of pcDNA-CRT-HA plasmids) was cloned into *PstI-NotI* restriction sites of

pBAD-CRT plasmid. The following histidine to alanine, or histidine deletion mutants were generated: H25A, H82A, H128A, H153A and H25Del, H82Del, H128Del and H153Del deletion mutants. Identical results were obtained whether histidine to alanine or histidine deletion mutations were used. Wild-type calreticulin and H25A, H82A, H128A, H153A mutants are designated as CRT-WT and CRT-His25Ala, CRT-His82Ala, CRT-His128Ala and CRT-His153Ala, respectively. As well, the following site specific mutants of calreticulin were also generated: C88A, C120A, E238R, E239R, D241R, E243R, W244A and W302A. Wild-type calreticulin and C88A, C120A, E238R, E239R, D241R, E243R, W244A, W302A mutants are designated as CRT-WT and CRT-Cys88Ala, CRT-Cys120Ala, CRT-Glu238Arg, CRT-Glu239Arg, CRT-Asp241Arg, CRT-Glu243Arg, CRT-Trp244Ala and CRT-Trp302Ala, respectively. For expression of calnexin, cDNA encoding the soluble luminal domain of calnexin (*PstI-NotI* restriction DNA fragment of pcDNA-Cnx-HA plasmid) was cloned into *PstI-NotI* restriction sites of pBAD-Cnx plasmid. The following mutants were generated: E351R and W428A and designated as Cnx-Glu351Arg and Cnx-Trp428Ala. Plasmids used in this study are listed in Table 2- 2.

Generation and Purification of Recombinant Proteins

Mouse calreticulin and calnexin proteins were expressed in Top10F' *E. coli* cells, while human ERp57 protein was expressed in DH5α *E.coli* cells. Briefly, both calreticulin and calnexin *E. coli* cultures were grown to the mid-log phase followed by the induction of the expression of recombinant proteins with arabinose (final concentration of 0.002%) for four hours. Cells were centrifuged at 3,300 x g for ten minutes (Beckman Centrifuge Model # J2-21M, Beckman, Fullerton, California) and the pellet was re-suspended in a buffer containing 50 mM Tris, pH 8.0, 300 mM NaCl and 10% glucose. The re-suspended *E. coli* pellet was lysed two times using a French Press (Spectronic Instruments Inc., Rochester, New York), set at 1000 p.s.i. followed by centrifugation at 12,000 x g (Beckman Centrifuge Model J2-21M, JA-17 rotor, Beckman, Fullerton, California) for twenty minutes. Supernatant containing the His-tagged proteins were purified by one-step Ni-NTA agarose affinity chromatography using native conditions (Guo et al., 2003; Martin et al., 2006). Briefly, samples of *E. coli* lysates were mixed with

the Ni-NTA agarose beads equilibrated with buffer containing 50 mM Tris, pH 8.0 and 300 mM NaCl, applied onto column, washed and eluted with a buffer containing 50 mM Tris, pH 8.0, 300 mM NaCl and 20 mM imidazole. Over 90% of the protein was purified to homogeneity by one-step Ni-NTA agarose column chromatography. Human ERp57 was cloned into the pET9 vector and protein was isolated from DH5α *E. coli* (Studier et al., 1990). The construct encoded the protein without a signal sequence (residue 25-505) (Koivunen et al., 1996) but with an additional alanine residue at the N-terminus. Briefly, cultures were grown with 30 μg/ml kanamycin until an OD_{600} of 0.8 was reached. The *E. coli* culture was induced with 1 mM IPTG for 4.5 hours and cells harvested by centrifugation at 3,600 x g for ten minutes (Beckman Centrifuge Model # J2-21M, JA-17 rotor, Beckman, Fullerton, California). Cell pellet was resuspended in 50 mM Tris-HCl pH 8, with protease inhibitors: 0.5 mM PMSF, 0.5 mM benzamidine, 0.05 μg/mL aprotinin, 0.025 μg/mL phosphoramidone, 0.05 μg/mL TLCK, 0.1 μg/mL TPCK, 0.05 μg/mL APMSF, 0.05 μg/mL E-64, 0.025 μg/mL leupeptin, 0.01 μg/mL pepstatin (Milner et al., 1992a) and frozen. The frozen lysate was thawed and 100 μg/ml of DNase we and 10 mM $MgCl_2$ was added. Cell lysate was incubated at room temperature for twenty minutes and sonicated at 100 watts three times for forty-five seconds (Ultrasonic Power Inc., Freeport, Illinois). The suspension was centrifuged at 22,000 x g for thirty minutes at 4°C (Beckman Centrifuge Model J2-21M, JA17 rotor, Beckman Coulter, Fullerton, California). The soluble cell lysate with inhibitors was loaded onto a heparin-sepharose column equilibrated with 10 mM Tris-HCl, pH 7.4. Proteins were eluted stepwise with 200 and 600 mM NaCl in the same buffer. The 600 mM NaCl fraction was dialyzed against 10 mM Tris-HCl, pH 7.4 and ERp57 was further purified on a Q-Sepharose column eluted with a gradient of 0-400 mM NaCl in the same buffer (Corbett et al., 1999; Zapun et al., 1998). Recombinant proteins were concentrated by centrifugation using an Amicon Ultra-4 30,000 MWCO (Molecular Weight Cut-Off) Centrifugal Filter Device (Millipore, Bedford, Massachusetts) and proteins were dissolved in a buffer containing 10 mM Tris, pH 7.0 and 1 mM EDTA. Plasmids used in this study are listed in Table 2- 2.

Cascade Blue Covalent Labeling of Purified Wild-type Calnexin Protein

Purified S-Cnx was labeled with Cascade Blue acetyl azide (Whitaker et al., 1991) by adaptation to a FluroTag FITC Conjugation Kit procedure as recommended by the manufacturer. Briefly, CB (1.11 mg/ml) was dissolved in 100 mM carbonate/bicarbonate buffer, pH 9.0. 600 μg of purified calnexin in 100 mM sodium carbonate/bicarbonate buffer, pH 9.0, was used for labeling. The dye was added drop wise to the protein mixture with constant stirring. The reaction vial was incubated in the dark for two hours at room temperature with gentle stirring. Labelled protein was separated from free dye using a Sephadex G-25M column (3.5 mL) previously equilibrated with PBS. The reaction mixture was applied and fractions (0.25 mL each) were eluted with PBS. The fluorescence of each fraction was determined at the excitation wavelength 385 nm and the emission wavelength 430 nm using a PTI spectrofluorometer system C43/2000 (Photon Technology International Inc, Birmingham, New Jersey). Fractions containing labelled protein were pooled and used directly for protein interaction studies. 2 μL of the pooled sample was used for analysis with the subsequent addition of 400 μM EGTA, 2 mM Ca^{2+}, 500 μM Zn^{2+} or 1 mM ATP and the fluorescence of CB-Cnx was monitored at the excitation wavelength of 385 nm and the emission wavelength of 430 nm using a PTI spectrofluorometer system C43/2000 (Photon Technology International Inc, Birmingham, New Jersey).

Protein Aggregation Assay of Calreticulin and Calnexin Wild-type and Mutant Proteins

The protein aggregation assay was carried out in a mixture containing 1 μM of MDH mixed with various amounts of soluble wild-type and mutant protein at room temperature (Guo et al., 2003; Martin et al., 2006). Samples were incubated at 44^{0}C in 50 mM sodium phosphate, pH 7.5 (total volume, 1.2 mL) and monitored for light scattering for two hours. The denatured MDH was suspended in a buffer containing 10 mM Tris-HCl, pH 7.0, 150 mM NaCl, 5 mM $CaCl_2$ followed by the addition of wild-type or mutant protein (0.25 μM) (Guo et al., 2003; Martin et al., 2006). IgY was isolated from chicken egg yolk according to the protocol of the EGGstract IgY purification system and was dialyzed overnight against denaturing buffer containing 100 mM Tris, pH 7.0, 6

M guanidinum hydrochloride and 40 mM DTT. The denatured IgY protein (0.25 μM) was suspended in a buffer containing 10 mM Tris-HCl, pH 7.0, 150 mM NaCl, 5 mM $CaCl_2$ (Guo et al., 2003; Martin et al., 2006) followed by addition of wild-type or mutant protein (0.25 μM). Protein aggregation was induced by increasing sample temperature to 44^0C. Light scattering was measured using a PTI spectrofluorometer system C43/2000 (Photon Technology International Inc, Birmingham, New Jersey) equipped with a temperature-controlled cell holder, with the excitation and emission wavelengths set to 320 nm and 360 nm, respectively (Guo et al., 2003; Martin et al., 2006).

Intrinsic Fluorescence Assay of Calreticulin and Calnexin Wild-type and Mutant Proteins

Intrinsic fluorescence measurements were performed at 25°C using a PTI spectrofluorometer system C43/2000 (Photon Technology International Inc, Birmingham, New Jersey) as described (Guo et al., 2003; Martin et al., 2006). 3 μM of wild-type or mutant proteins were used for fluorescence measurements in buffer containing 10 mM MOPS, pH 7.1, 3 mM $MgCl_2$ and 150 mM KCl (Khanna et al., 1986). The excitation wavelength was set to 286 nm and scanning emission wavelengths were monitored from 295 nm to 450 nm. The effects of a range of concentrations of Zn^{2+}, Ca^{2+} and ATP on the intrinsic fluorescence of the proteins were evaluated at a midpoint wavelength of 334 nm.

Proteolytic Digestion of Calreticulin and Calnexin Wild-type and Mutant Proteins

10 μg of purified wild-type or mutant protein expressed in *E. coli* was incubated with trypsin at 1:100 (trypsin/protein; w/w); with a final trypsin concentration of 10 μg/mL (Corbett et al., 2000) in the absence or presence of 2 mM Ca^{2+}, 1 mM Zn^{2+} or 1 mM ATP-Mg^{2+}, with samples taken at 0.5, 1, 2, 5, 10 and 20 minute time points. The time course samples were separated on SDS-PAGE (10% acrylamide) and stained with Coomassie Blue (Guo et al., 2003).

CD Analysis of Calreticulin and Calnexin Wild-type and Mutant Proteins

Using a protein concentration of 300 μg/mL, CD analysis was performed at 25°C using a Jasco J720 spectropolarimeter (Jasco Inc., Easton, MD) (Corbett et al.,

2000) interfaced to an Epson Equity 386/25 and controlled by Jasco software (Corbett et al., 1999). The thermostabled cell holder was maintained at 25°C with a Lauda RMS circulatory water bath (Lauda, Westbury, New York). Each sample was scanned 8 times with water used as the control. The voltage multiplier was kept between 600 and 700 V to prevent distortion of the CD spectrum. Protein concentration was determined using a Beckman DU650 UV-Visible spectrophotometer (Beckman, Fullerton, California). Molar ellipticities were calculated from the equation: $[\theta] = mdeg * (MW/(mrw*c*L))$, with θ mean residue ellipticity units as $mdeg.cm^2.dmol^{-1}$, mdeg as the experimental result, multiplied by the factor 904.4361635 as calculated by the MW (molecular weight of 57,522.14 for calnexin, 47994.52 for calreticulin) divided by the mrw (mean residue weight of calreticulin = 416, calnexin = 505) multiplied by c (concentration of 0.3 mg/mL) multiplied by L (path length of 0.5 mm). The CD spectra were analyzed for secondary structure elements by the Contin ridge regression analysis program of Provencher and Glöckner (Provencher and Glöckner, 1981).

Surface Plasmon Resonance Analysis of Calreticulin and Calnexin Wild-type and Mutant Proteins

The Biacore Inc. SPR biosensor monitors biomolecular interactions by detecting changes in total mass in the aqueous layer at the surface of a sensor chip with the measurement of variation in the critical angle needed to produce total internal refraction. The change in critical angle is directly proportional to the amount of interacting protein and is expressed as resonance units (RU). The shift in RU is plotted against time and is displayed as a sensogram. The Biacore 3000 SPR biosensor, CM5 sensor chips, Amine Coupling Kit and the BIAevaluation 3.2 analysis program were all from Biacore Inc., Piscataway, New Jersey. The sensor chip was activated, coupled and blocked using the Amine Coupling Kit from Biacore. Specifically, two lanes on a CM5 chip were activated using a 1:1 mixture of N-hydroxysuccinimide/N-ethyl-N'-(3-dimethylaminopropyl)-carbodiimide hydrochloride for seven minutes at a flow rate of 5 µL per minute, total injection of 35 µL. One µM purified protein, termed ligand (calreticulin, calnexin or mutant proteins), was immobilized on the second lane in 10 mM sodium acetate buffer at pH 4 with a flow rate of 5 µL per minute until lane was well coupled, approximately 2000 RU's, roughly 7 µL total injection. The control lane and remaining sites in the

coupled lane were then blocked with 1 M ethanolamine at pH 8.5 for seven minutes with a flow rate of 5 μL per minute, total injection of 35 μL. The experiments were performed at 20°C using freshly filtered Running Buffer (20 mM Tris, pH 7, 135 mM KCl, 2 mM $CaCl_2$, 0.05% Tween-20 and the following mixture of protease inhibitors: 0.5 mM PMSF, 0.5 mM benzamidine, 0.05 μg/mL aprotinin, 0.025 μg/mL phosphoramidone, 0.05 μg/mL TLCK, 0.1 μg/mL TPCK, 0.05 μg/mL APMSF, 0.05 μg/mL E-64, 0.025 μg/mL leupeptin and 0.01 μg/mL pepstatin (Milner et al., 1992a), at a flow rate of 30 μL per minute to minimize mass transfer effects. Protein to be analyzed (either ERp57 or ATP), termed analyte, was diluted in flow buffer and was centrifuged at 11,000 x g (Eppendorf 5415C microfuge and F-45-18-11 rotor, Brinkmann, Mississauga, Ontario) for ten minutes to pellet insoluble debris followed by dilution in a titration curve of 5,000 nM to 5 nM (representative curves are shown at a concentration of 5,000 nM), with a three minute injection time, total volume of 90 μL, followed by a fifteen minute dissociation time and regenerated using Regeneration Buffer (Running Buffer containing 800 mM KCl) followed by a two minute stabilization time. The analyte was simultaneously passed over the blank flow cell and this baseline was subtracted from the experimental flow cell. The analyte was not found to interact with the blank flow cell; however, this control eliminated any alterations caused by subtle differences in solvent. The maximum relative response value for each injection was calculated using BiaEvaluation 3.2 kinetic assay result wizard (Biacore Inc., Piscataway, New Jersey). All curves were fitted using the Drifting Baseline (1:1 langmuir binding).

Analysis of Ca^{2+} Binding to Recombinant Proteins

Ca^{2+} binding was estimated by equilibrium dialysis. Buffer used for dialysis was 10 mM Mops, pH 7.1, 150 mM KCl and 100 μM EGTA. 800 μg of protein was placed into a dialysis bag (Millipore, Bedford, Massachusetts) with a molecular weight cut off of 10-13-kDa. Radiolabeled ^{45}Ca was diluted as a serial titration of 1 nM to 5 mM of free Ca^{2+} (adjusted for the EGTA concentration (Portzehl et al., 1964) (entropy.brneurosci.org/egta.html). Sample bags containing protein were incubated in $^{45}Ca^{2+}$ serial dilution solutions at 4°C for forty eight hours on a rocking platform (Perkin Elmer, Wellesley, Massachusetts). Aliquots were taken from inside and outside the bag

for scintillation analysis followed by calculation of the radiolabled Ca^{2+} bound to the protein as well as determination of the protein concentration.

Measurements of Intracellular Ca^{2+} Concentration

Measurement of intrinsic Ca^{2+} concentration were performed as described (Mery et al., 1996). Cells were plated at 3 X 10^6 cells/10 cm plate for twenty four hours. Media was removed and 4 mL of fresh, 37°C DMEM supplemented with 10% FCS was added to a dish. Fura 2-AM was added to a final concentration of 2 μM and the dish was incubated for forty five minutes. Media was removed and cells were washed with PBS followed by addition of fresh, 37°C media and incubated for fifteen minutes in 37°C incubator. Media was removed and cells were washed with PBS. Cells were trypsinized for several minutes in 37°C incubator and combined with fresh, 37°C DMEM supplemented with 10% FCS. Cells were centrifuged at 100 x g (Eppendorf centrifuge 5702, Brinkmann, Mississauga, Ontario) for two minutes, supernatant was removed and cells were re-suspended in 37°C Ca^{2+}-Buffer (143 mM NaCl, 6 mM KCl, 1 mM $MgSO_4$, 20 mM Hepes, pH 7.4, 0.1% glucose, 1 mM $CaCl_2$, all solutions made in Chelex water (40g Chelex/L, mix 1 hour and filter), using 1 N NaOH to pH. Sulfinpyrazone was added to 1.01 mg /10 mL Buffer (aliquot ~100 mg dry sulfinpyrazone in microfuge tube and add DMSO to 1 mg/μL, then add 5 μL to 50 mL of buffer)) by pipeting. Cells were counted, centrifuged at 100 x g (Eppendorf Centrifuge 5702, Brinkmann, Mississauga, Ontario) for two minutes and re-suspended by gentle pipeting in 37°C Ca^{2+}-Free Buffer at 1 X 10^6 cells/mL (143 mM NaCl, 6 mM KCl, 1 mM $MgSO_4$, 20 mM Hepes, pH 7.4, 0.1% glucose, all solutions made in Chelex water (40g Chelex/L, mix 1 hour and filter), using 1 N NaOH to pH. Sulfinpyrazone was added to 1.01 mg/10 mL buffer (aliquot ~100 mg dry sulfinpyrazone in microfuge tube and add DMSO to 1 mg/μL, then add 5 μL to 50 mL of buffer)). Measurements were performed on a PTI spectrofluorometer system C43/2000 equipped with a temperature-controlled cuvet holder set at 37°C. A ratio of 340/380 nm exitation was used and an emission of 510 nm was detected using FELIX software (Photon Technology International Inc., Birmingham, New Jersey). For the suspension cell lines, CEM and NKR T-lymphoblast cells (2 x 10^7/mL) were loaded with the fluorescent Ca^{2+} indicator Fura 2-AM (2 μM), taking precautions to avoid dye sequestration (Mery et al., 1996) to obtain the measurement of cytoplasmic Ca^{2+}

concentration ($[Ca^{2+}]_c$). A quartz cuvet was filled with 1 mL of cell suspension (fibroblasts: 1 X 10^6 cells/mL, lymphoblasts: 2 x 10^7/mL) diluted in the Ca^{2+}-Free Buffer. At one minute, 2 mM EGTA was added to chelate any Ca^{2+} present in solution. At approximately two minutes, a final concentration of 600 nM bradykinin, 100 μM ATP, 100 μM carbachol, or 100 nM bombesin, was added to measure IP_3-mediated-Ca^{2+} release. As well, 300 nM thapsigargin, 2 μM ionomycin, or 2 μM ionomycin with 300 nM thapsigargin was added to measure the Ca^{2+} capacity of the ER. Measurement of store-operated Ca^{2+} influx was determined by the addition of 2 mM external $CaCl_2$. Maximum fluorescence value was obtained by the addition of 7.5 μM ionomycin and 4 mM $CaCl_2$ and a minimum value obtained with the addition of 32 mM EGTA, 24 mM Tris-HCl pH 8 and 0.4% Triton X-100. Data was analyzed using Excel software (Microsoft, Redmond, Washington) with the calculation: $[Ca^{2+}]c=K_d(R-Rmin)/(Rmax-R)$. R = Fluorescence Intensity at 340 nm divided by fluorescence intensity at 380nm. K_d = 224 (at 37°C for Fura-2). K_d = 440 (at 37°C for Fura-2/AM in our Ca^{2+} free buffer) The 360 nm scaling factor was 1. The benefit of 380 nm is a better signal to noise ratio. The 380 nm scaling factor means equation is multiplied by (F380max/F380min). $[Ca^{2+}]$ is calculated in nM.

Generation of the Calnexin-Deficient Mouse

The ES cell line, KST286 was purchased from the Gene Trap Resource at http://baygenomics.ucsf.edu. BayGenomics used gene trapping to generate the calnexin gene disrupted stem cells. A portion of DNA consisting of the β-galactosidase reporter gene with the neomycin resistance gene was inserted randomly into genomic DNA (Baygenomics, San Francisco, California). The insertion of the artificial DNA into the genome disrupts the RNA splicing machinery, resulting in the prevention of protein translation. This insertion can be determined using the activity of the artificial reporter gene and the activity of the disrupted gene in mouse tissue can be identified.

The calnexin gene is located on chromosome 11 at site qB1.3 with the accession number NM_007597. The ES cell line, KST286, transfected with the gene trap vector pGT1TMpfs (BayGenomics, University of San Francisco, San Francisco, California) containing the first 7 exons of the calnexin gene with the β-galactosidase-neomycin was

inserted at 721 basepairs at the end of exon 7, disrupting the calnexin gene with β-galactosidase and neomycin. The BayGenomics ES cell line was generated from 129P2 (formerly 129/Ola) ES cell lines, predominantly the E14Tg2A.4 subclone (feeder cell independent (Nichols et al., 1990)). Parental cell lines (CGR8 and E14Tg2A) were established from delayed blastocysts on gelatinized tissue culture dishes in ES cell medium containing LIF (leukemia inhibitory factor - necessary for the maintenance of undifferentiated embryonic stem cells) (Nichols et al., 1990). Sub-lines were isolated by plating cells at a single-cell density, picking and expanding single colonies and testing several clones for germ-line competence.

Purchased ES cell lines were thawed and passaged for six days in ES cell medium (GMEM, 2 mM glutamine, 1 mM sodium pyruvate, 1 X non-essential amino acids, 10% FCS, 1:1000 dilution β-mercaptoethanol and 1000 U LIF in the absence of neomycin. On the day of injection, the medium was changed several hours before harvesting the cells. A confluent 25 cm^2 flask was trypsinized for four minutes and diluted into nine mL of cold ES cell medium without LIF, pelleted and resuspended in 0.8 mL of ES cell medium (without LIF) in a sterile 1.5 mL screw-top microcentrifuge tube. Before they were added to the injection chamber, cells were kept on ice (for up to several hours) to prevent clumping. Blastocysts were flushed from pregnant C57BL/6 females and collected into a CO_2-independent medium containing 10% FCS. Blastocysts were expanded for one to two hours in ES cell medium in a 37°C/5% CO_2 incubator, transferred to a hanging drop chamber and cooled to 4°C. ES cells were added to the hanging drops and the blastocysts are injected with enough cells (20 or more) to fill the blastocoele. Injected blastocysts were then transferred to pseudo pregnant recipient females (10-15 blastocysts/uterine horn). Typically, injection of ten blastocysts will yield an average of twice male chimeras with germline mosaicism. These ES cells were microinjected into 3.5-d-old C57BL/6J blastocysts to generate chimeric mice. Chimeric males were analyzed for germline transmission by mating with C57BL/6J females and the progeny were analyzed by PCR analysis, β-galactosidase staining and Southern blot analysis (see below). Deficient mice were generated in the HSLAS facility at the University of Alberta with the assistance of Dr. P. Dickie.

Isolation and Purification of DNA

A portion of the embryo was harvested and resuspended in cell lysing buffer (10 mM Tris-HCl pH 8.0, 150 mM NaCl, 10 mM EDTA, 0.5% SDS) containing 0.2 mg/mL proteinase K. Sample was incubated at 50°C for sixteen hours. Lysates were centrifuged at 19,000 x g (Eppendorf 5415C microfuge and F-45-18-11 rotor, Brinkmann, Mississauga, Ontario) for five minutes. Supernatant was removed to a clean microfuge tube and 250 µL of phenol and 250 µL of chloroform were added followed by vigorous shaking. Sample was centrifuged at 19,000 x g for five minutes (Eppendorf 5415C microfuge and F-45-18-11 rotor, Brinkmann, Mississauga, Ontario) with the top layer containing the DNA transferred to a clean microfuge tube. DNA was precipitated by the addition of 500 µL of isopropanol with mixing. DNA was pelleted by centrifugation at 14,000 rpm for fifteen minutes at room temperature. DNA pellet was washed with 70% ethanol by centrifugation at 14,000 rpm for ten minutes at room temperature. Pellet was air dried for ten minutes and resuspended in 100 µL of sterile water containing 10 µg/mL RNase A and incubated at 50°C for one hour. Concentration was measured using UV/Visible spectrophotometer at absorbance 260 nm.

PCR Analysis of Wild-type and Calnexin-Deficient Mouse Embryos

DNA harvested from embryo was used for PCR with neomycin specific primers: neo-F1K (5'-TATTCGGCTATGACTGGGCACAA-3') and neo-R1K (5'-AGCAATATCACGGGTAGCCAACG-3') giving a 631 base pair fragment (Turksen, 2004). Primers used in this study are listed in Table 2- 4.

X-Galactosidase Staining and Western Blot Analysis of Wild-type and Calnexin-Deficient Mouse Embryos

To check genotype, β-galactosidase staining followed by Western blot analysis was used. Briefly, 167 µL of 20 mg/mL X-galactosidase solubilized in DMF was added to 10 mL of Z-buffer (60 mM Na_2HPO_4, 40 mM NaH_2PO_4, 10 mM KCl and 1 mM $MgSO_4$, pH 7.0). Protein was purified from embryos using Trizol Reagent. Briefly, embryos were resuspended in 500 µL of Trizol Reagent and homogenized using a microfuge homogenizer. Samples were incubated at room temperature for five minutes

followed by the addition of 100 µL of chloroform and mixed with vigorous shaking. The sample was incubated at room temperature for two minutes and centrifuged at 11,000 x g (Eppendorf 5415C microfuge and F-45-18-11 rotor, Brinkmann, Mississauga, Ontario) for fifteen minutes at 4°C. The aqueous phase was used for isolation of RNA. The organic phase was transferred to a clean microfuge tube and protein was precipitated with 0.4 mL of isopropanol. Samples were incubated at room temperature for ten minutes and centrifuged at 11,000 x g (Eppendorf 5415C microfuge and F-45-18-11 rotor, Brinkmann, Mississauga, Ontario) for ten minutes at 4°C. The protein pellet was washed three times for twenty minutes at room temperature with 2 mL of 0.3 M guanidine hydrochloride in 95% ethanol. After the final wash, the pellet was washed with 95% ethanol and centrifuged at 11,000 x g (Eppendorf 5415C microfuge and F-45-18-11 rotor, Brinkmann, Mississauga, Ontario) for five minutes at 4°C. The pellet was dried thoroughly and dissolved in 1% SDS by pipetting and incubation at 50°C for ten minutes. Insoluble matter was pelleted at 11,000 rpm for ten minutes at 4°C. Soluble protein was transferred to clean microfuge tube. 5 µL of protein solution was dotted on filter paper and incubated with 3.5 mL of Z-buffer + X-galactosidase, sixteen hours at 37°C. Blue signal indicated heterozygote or homozygote knockout while no stain indicated wild-type. Further identification of homozygote embryo was done by Western blot analysis using rabbit anti-calnexin antibody at a dilution of 1:500.

Southern Blot Analysis of Wild-type and Calnexin-Deficient Embryos

Genomic DNA was purified from mouse tails using Trizol Reagent as described above. *EcoRI*-digested genomic DNA was used for Southern blot detection of the calnexin gene. The 150 base pair probe used for the Southern blot analysis was generated by PCR using the primers: Kcnx150F (5′-GATCAGTTCCACGACAAGACC-3′) and Kcnx150R (5′-CAGATCTGCATCTGGCCTCT-3′). Genomic DNA was run on a 0.8% agarose/TAE gel and transferred to nylon membrane (company) overnight using a buffer composed of 20 X SSC (3 M NaCl, 0.3 M Na_3citrate.$2H_2O$, pH 7.0, 0.02% DEPC treated DDH_2O). Using the Prime-it II Kit from Stratagene, 50 µg of DNA, 10 µL of Random 9mer Primer and 23 µL DEPC treated water were boiled for five minutes and put on ice. 10 µL of dATP buffer, 5 µL of radiolabeled ^{32}P-αATP and 1 µL of the

Klenow fragment of DNA polymerase we enzyme were incubated at 37°C for ten minutes. The probe was purified using a Sephadex G25 column (3.5 mL), diluted in hybridization buffer (2 X SSC) and heated to 95°C for five minutes to denature. Probe was added to generous amount of hybridization buffer (2 X SSC) and incubated overnight at 60°C with rotation (Hybaid Micro-4, Thermo Electron Corporation, Waltham, Massachusetts). The nylon membrane was washed twice with 2 X SSC with 0.5% SDS for fifteen minutes, followed by a single wash with 2 X SSC with 50% formamide. Nylon membrane was wrapped in kitchen wrap and overlaid with film. The product from Southern blot gave a size of approximately 5,000 base pair if disrupting insert was present while product was 8,000 base pair if there was no insert.

Purification of RNA

Trizol Reagent was used for the isolation of total RNA. Briefly, the cell culture, both floating and adherent were resuspended in 1 mL of Trizol Reagent and mixed thoroughly. Sample was incubated for five minutes at room temperature to allow complete dissociation of nucleoprotein complexes. 0.2 mL of chloroform was added per mL of Trizol Reagent and the sample was shaken vigorously for fifteen seconds and incubated at room temperature for two minutes. Sample was centrifuged at 11,000 x g (Eppendorf 5415C microfuge and F-45-18-11 rotor, Brinkmann, Mississauga, Ontario) for fifteen minutes at 4°C. Phase separation occurs with the top phase containing RNA transferred to clean microfuge tube. RNA was precipitated by adding 0.5 mL isopropanol/mL Trizol. Sample was incubated at room temperature for ten minutes followed by centrifugation at 11,000 rpm for ten minutes at 4°C. The RNA pellet was washed with 75% ethanol by centrifugation at 11,000 rpm for five minutes at 4°C. The RNA pellet was briefly dried and resuspended in thirty µL of sterile water.

RT-PCR Analysis

RT-PCR first strand cDNA synthesis was carried out using M-MLV Reverse Transcriptase Kit. One µg of RNA was added to a nuclease-free microcentrifuge tube with 1 µL oligo $(dT)_{12-18}$ (stock concentration 500 mg/ml), 1 µL of 10 mM dNTP mix (10 mM each: dATP, dGTP, dCTP, dTTP) and sterile water, bringing volume up to 12

μL. The tube was heated to 65°C for five minutes and chilled on ice, followed by a brief pulse in microcentrifuge (Eppendorf 5415C microfuge and F-45-18-11 rotor, Brinkmann, Mississauga, Ontario). 4 μL of 5x First Strand Buffer, 2 μL of 0.1 M DTT and 1 μL of RNaseOut (if <50 ng total RNA) was added and tube was mixed gently and incubated for two minutes at 37°C. Finally, 1 μL of M-MLV Reverse Transcriptase was added and tube mixed gently and incubated at 42°C for thirty minutes. Tube was heat-inactivated for ten minutes at 94°C. Using only 10% of the first strand reaction (2 μL from above), 5 μL of 10 X PCR Buffer, 1 μL of 10 mM dNTP (as above), 1 μL gene specific forward primer (25 mM stock), 1 μL gene specific reverse primer (25 mM stock), 2 μL cDNA from above reaction, 38 μL sterile H_2O and 1 μL *Taq* polymerase. The PCR program was set as: 94°C for five minutes (94°C for one minute, 60°C for one minute and 72°C for one minute) x thirty-five cycles, followed by 72°C for five minutes. 10 μL of PCR product was combined with DNA loading buffer (6 mM EDTA, 300 mM NaOH, 18% Ficoll in water, 0.15% Bromocresol Green, 0.25% Xylene Cyanol), run on 3% agarose gel and visualized with ethidium bromide. The following oligodeoxynucleotides were used for PCR-driven amplification of calreticulin cDNA fragments: 5'-GATAAAGGGTTGCAGACAAGC-3' - and 5'-CCCAGACTTGACCTGCC-3'. Levels of calreticulin mRNA were normalized by comparison with levels of actin mRNA. Actin mRNA was amplified using the following primers: 5'-GACGAGGCCCAGAGCAAGAG-3' and 5'-CCAGACAGCACTGTGTTGGC-3'. Primers used in this study are listed in Table 2- 4.

Apoptosis and Caspase Assays

For detection and quantification of apoptosis in T-lymphoblasts, we used the TUNEL Cell Death Detection Kit-fluorescein. To induce apoptosis, cells (2 x 10^7 cells/mL) were treated with 1 μM thapsigargin for sixteen hours at 37°C. Cells were then washed in PBS containing 2% FCS and subjected to TUNEL assay, as recommended by the manufacturer. Briefly, cells were harvested by trypsinization and centrifuged at 100 x g (Eppendorf Centrifuge 5702, Brinkman, Mississauga, Ontario) for two minutes. Cell pellet was resuspended in PBS containing 2% FCS at 2 X 10^7 cells/mL and 100 μL of

cells were combined with 4% PFA. Cells were pelleted and washed with PBS containing 2% FCS and resuspended in permeabilization buffer (0.1% Triton X-100 in 0.1% sodium citrate, pH 7.4), incubated on ice for two minutes, centrifuged for two minutes at 100 x g (Eppendorf Centrifuge 5702, Brinkman, Mississauga, Ontario) and resuspended in 20 µL of TUNEL reaction mixture (19 µL of TUNEL label and 1 µL of TUNEL enzyme). Sample was incubated at 37°C for two hours, followed by the addition of 180 µL of PBS containing 2% FCS, centrifuged for two minutes at 100 x g and resuspended in 200 µL of PBS containing 2% FCS. DNA fragmentation was detected by flow cytometry. In each experiment, a negative control received the label solution without the terminal transferase. Prior to the TUNEL reaction, DNA strand breaks in positive controls were induced by treating cells with one µg of DNase I/mL for ten minutes at room temperature, in a buffer containing 50 mM Tris pH 7.5, 1 mM $MgCl_2$ and one mg/mL BSA. Caspase 3 activity was measured in microtiter plates using the Caspase 3 Activity Assay as described by the manufacturer. Cytosolic extracts were prepared as described (Bossy-Wetzel et al., 1998). Briefly, cells were collected by centrifugation at 200 rpm for five minutes at 4°C. The cells were then washed twice with ice-cold PBS, pH 7.4, followed by centrifugation at 200 rpm for five minutes. The pellet was resuspended in 600 µL of extraction buffer, containing 220 mM mannitol, 68 mM sucrose, 50 mM PIPES-KOH, pH 7.4, 50 mM KCl, 5 mM EGTA, 2 mM $MgCl_2$, 1 mM DTT and protease inhibitors; 0.5 mM PMSF, 0.5 mM benzamidine, 0.05 µg/mL aprotinin, 0.025 µg/mL phosphoramidone, 0.05 µg/mL TLCK, 0.1 µg/mL TPCK, 0.05 µg/mL APMSF, 0.05 µg/mL E-64, 0.025 µg/mL leupeptin and 0.01 µg/mL pepstatin (Milner et al., 1992a). After thirty minutes incubation on ice, cells were homogenized with a glass dounce and a B pestle (40 strokes). Cell homogenates were spun at 14,000 rpm for fifteen minutes and supernatants were removed and stored at –70°C. Cleavage of Ac-DEVD-AFC by the cytoplasmic proteins (140 µg) was monitored fluorometrically, at a γmax of 485 nm, using a C43/2000 fluorometer. Cells were also treated with 20 µM Z-DEVD-FMK (caspase 3 inhibitor II) and 20 µM Z-IETD-FMK (caspase 8 inhibitor II) for sixteen hours at 37°C in the presence or absence of 1 µM thapsigargin. Cytochrome *c* release was assessed using specific anti-cytochrome *c*

antibodies at a dilution of 1:250 (Bossy-Wetzel et al., 1998). The Annexin V-FITC cell death detection kit was used for the detection and quantification of apoptosis in fibroblasts. To induce apoptosis, cells were treated with 1 μM thapsigargin for sixteen hours at 37°C. Cells were collected from the media by centrifugation at 1,200 rpm for three minutes and the attached cells collected by tissue culture trypsinization and combined with media collected cells. Cells were then washed with PBS, diluted to 1 X 10^6 cells/mL and subjected to Annexin V/PI assay, as recommended by the manufacturer. Annexin V-FITC detects phosphatidylserine appearance on the cell surface as an indication of apoptosis and the FITC fluorescence can be detected by flow cytometry. PI is a standard flow cytometric viability probe and is used to distinguish viable from nonviable cells. A portion of cells (1 X 10^5) was combined with 5 μL of Annexin V-FITC and 10 μL of PI. Cells were gently vortexed and incubated at room temperature for fifteen minutes in the dark. 400 μL of Binding Buffer was added and analyzed by flow cytometry. Control reactions of Annexin V, PI and no label were completed. FACS analysis was performed using a FACScan Instrument (BD Biosciences Inc, San Jose, California). Analysis of labelled cells was determined using the program CellQuest (BD Biosciences Inc. San Jose, California).

Indirect Immunofluorescence and Electron Microscopy

Cells were grown on 25 mm circular coverslips in DMEM supplemented with 10% FCS and 1% penicillin-streptomycin to approximately 50% confluency. Coverslips were removed and washed with PBS, then fixed with 4% paraformaldehyde in PBS for fifteen minutes. Primary antibody was diluted in 0.1% saponin, 2% milk powder in PBS and incubated on the coverslip for one hour. Coverslips were washed three times with 0.1% saponin in PBS. The secondary antibody was diluted in 0.1% saponin, 2% milk powder in PBS and incubated on the coverslip for one hour. Coverslips were rinsed three times in PBS and mounted using Vinol 205S and examined with a Bio-Rad Laboratories confocal fluorescence microscope model MRC-600 (BioRad Inc., Hercules, California) equipped with a krypton/argon laser set at wavelength 488 or for co-localization studies, images were collected using the Cellular Imaging Facility (Department of Oncology, Cross Cancer Institute, University of Alberta, Edmonton).

Images were collected with a Zeiss (Carl Zeiss, Jena, Germany) Confocal Laser Scanning Microscope (LSM 510, software version LSM 3.2) mounted on a Zeiss Axiovert M100 inverted microscope fitted with a 63X (N.A. 1.40) oil immersion lens for CEM T-cells and with a 40X Plan-Neofluar lens (N.A. 1.3) for MEFs. The instrument is equipped with four lasers (with six laser lines) and four PMT detectors. The 488nm laser line (from 25mW argon laser) and 543nm laser line (from 1mW HeNe laser) were used to visualize Alexa-488 and Alexa-546 used in the experiments. A band-pass filter 505-530 was used to collect emission from Alexa-488 and a long-pass filter (560nm) was used to collect signal from Alexa-546. To avoid cross-talking of the fluorophores, the sequential scanning mode of the instrument was used to collect images from double labeled samples. Three-dimensional image z-stacks were collected with a pixel dimension of 1024 μm (x) X 1024 μm (y) with a step size of 0.3 μm (z). The images were processed with Imaris (Bitplane, Zurich, Switzerland) to analyze degree of co-localization. A standard threshold of 10% of maximal signal was used. The colocalization coefficient was calculated using the Imaris software and was between 0.5 and 0.6 for all images. For confocal immunofluorescence analysis of CEM cells, cells were pelleted onto poly L-lysine coated 25 mm glass coverslips using a Shandon-Elliot cytospin (Shandon-Elliot, London, England) at setting 50 for two minutes. Coverslips were then fixed in ice-cold methanol for five minutes at 20°C and permeabilized in buffer containing 0.1% Triton X-100, 100 mM PIPES, pH 6.9, 1 mM EGTA and 4% (w/v) polyethylene glycol 8000, for ten minutes at room temperature. Cells were washed three times over ten minutes in PBS before and after permeabilization. Coverslips were blocked in the above buffer with the addition of 2% milk powder for thirty minutes. Primary antibody was diluted in the above buffer with the addition of 2% milk powder and coverslips were incubated for one hour. Secondary antibodies were diluted in the above buffer with the addition of 2% milk powder and coverslips were incubated for one hour. Coverslips were washed four times with PBS, fixed with Vinol 205S and examined with a Bio-Rad Laboratories confocal fluorescence microscope model MRC-600 equipped with a krypton/argon laser. For electron microscopy of wild type and calnexin-deficient cells, cells were harvested at confluency and fixed for 1.5 hours at room temperature in 2.5% glutaraldehyde in 0.1 M sodium cacodylate buffer, pH 6.9. Samples were post fixed in 1% osmium tetroxide (Polyscience, Warrington, PA) in 0.1 M sodium cacodylate buffer,

pH 7.0 for 1.5 hours and dehydrated in ethanol and propylene oxide. Cells were then embedded in Araldite epoxy resin (SPI Supplies, West Chester, Pennsylvania) and sections were analyzed with a Hitachi S-2500 Scanning Electron Microscope (Dr. Ming Chen, Chemistry, U of A). Dilutions of individual antibodies used for immunocytochemistry are listed in Table 2- 5.

Drug Treatment of Cells

Human leukemic T-cells termed CEM (parental line) and NKR (calnexin-deficient) were cultured in αMEM supplemented with 10% FCS and 1% penicillin/streptomycin. ER stress was induced with 1 μM thapsigargin for sixteen hours (Zuppini et al., 2002). Caspase inhibitors were used as follows: 20 μM caspase 3 inhibitor (z-DEVD-fmk) and 20 μM caspase 8 inhibitor (z-IETD-fmk) in the presence or absence of 1 μM thapsigargin for sixteen hours at 37°C. CEM cells treated with thapsigargin were harvested by centrifugation and resuspended in 300 μL of ice-cold Modified RIPA containing 50 mM Tris pH 7.5, 150 mM NaCl, 1 mM EDTA, 1 mM EGTA, 1% Triton X-100, 0.5% sodium deoxycholate, 0.1% SDS, 0.5 mM benzamidine, 0.5 mM PMSF and 1:2,000 dilution of the following mixture of protease inhibitors: 0.5 mM PMSF, 0.5 mM benzamidine, 0.05 μg/mL aprotinin, 0.025 μg/mL phosphoramidone, 0.05 μg/mL TLCK, 0.1 μg/mL TPCK, 0.05 μg/mL APMSF, 0.05 μg/mL E-64, 0.025 μg/mL leupeptin, 0.01 μg/mL pepstatin, (Milner et al., 1992a). Fibroblasts were harvested by separately collecting floating cells from the media by centrifugation at 1,200 rpm for three minutes as well as collecting cells harvested by scraping with a rubber policeman. Floating and adherent cells were combined and resuspended in 300 μL of ice-cold Modified RIPA containing 50 mM Tris pH 7.5, 150 mM NaCl, 1 mM EDTA, 1 mM EGTA, 1% Triton X-100, 0.5% sodium deoxycholate, 0.1% SDS, 0.5 mM benzamidine, 0.5 mM PMSF and 1:2,000 dilution of the following mixture of protease inhibitors: 0.5 mM PMSF, 0.5 mM benzamidine, 0.05 μg/mL aprotinin, 0.025 μg/mL phosphoramidone, 0.05 μg/mL TLCK, 0.1 μg/mL TPCK, 0.05 μg/mL APMSF, 0.05 μg/mL E-64, 0.025 μg/mL leupeptin, 0.01 μg/mL pepstatin, (Milner et al., 1992a). The cellular lysates were incubated on ice for thirty minutes and centrifuged at 11,000 x g (Eppendorf 5415C microfuge and F-45-18-11 rotor, Brinkmann, Mississauga, Ontario)

to pellet insoluble material. Supernatants were transferred to a new microfuge tube and protein determination was done on the cellular lysates. This was followed by SDS-PAGE (10% acrylamide) and Western blot analysis.

Immunoprecipitation

Immunoprecipitation assays followed by Western blot analysis were carried out as described (Zuppini et al., 2002). Briefly, 500 µL of Lysis buffer (2% CHAPS in 50 mM Hepes, pH 7.4 and 200 mM NaCl) was used to lyse pelleted cells (CEM and NKR) or added to each 10 cm plate (wild-type and calnexin-deficient mouse embryonic fibroblasts) and cells were scraped using a rubber policeman. Lysis buffer was prepared containing protease inhibitors: 0.5 mM PMSF, 0.5 mM benzamidine, 0.05 µg/mL aprotinin, 0.025 µg/mL phosphoramidone, 0.05 µg/mL TLCK, 0.1 µg/mL TPCK, 0.05 µg/mL APMSF, 0.05 µg/mL E-64, 0.025 µg/mL leupeptin, 0.01 µg/mL pepstatin, (Milner et al., 1992a). Lysed cells were transferred to a microfuge tube and centrifugation in an Eppendorf 5415C microfuge with a F-45-18-11 rotor (Brinkmann, Mississauga, Ontario) at 14,000 rpm for ten minutes at 4°C. Supernatants were transferred to new microfuge tubes and lysates were pre-cleared by adding 60 µL of a 10% Protein A-Sepharose slurry (in 50 mM Hepes, pH 7.4 and 200 mM NaCl) and rotated at ten rpm and 4°C for thirty minutes. Immunoprecipitation was performed by adding both the appropriate antibody and 100 µL of a 10% Protein A-sepharose slurry and microfuge tubes were rotated for four hours to overnight. Beads were pelleted by briefly centrifuging for ten seconds at 14,000 rpm (Eppendorf 5415C microfuge and F-45-18-11 rotor, Brinkmann, Mississauga, Ontario) and then washed three times with 200 µL of 1% Chaps/50 mM Hepes, pH 7.4 and 200 mM NaCl and once with 50 mM Hepes, pH 7.4 and 200 mM NaCl. Beads were resuspended in 30 µL SDS-PAGE sample buffer (10% SDS, 10 mM DTT, 20% glycerol, 200 mM Tris-HCl pH 6.8 and 0.05% bromophenol blue), boiled for three minutes and centrifuged at 19,000 x g (Eppendorf 5415C microfuge and F-45-18-11 rotor, Brinkmann, Mississauga, Ontario) for one minute to pellet beads. Proteins in the supernatants were separated on SDS-PAGE (10% acrylamide), transferred to nitrocellulose membrane and used for Western blot analysis.

Determination of Protein Concentration

Protein concentration was determined using a Beckman System 6300 amino acid analyzer (Beckman, Fullerton, California) or by using Bio-Rad protein assay reagent with BSA as a standard (Bradford, 1976; Guo et al., 2003; Martin et al., 2006).

Table 2- 1 — Cell lines generated.

K41	wild-type	
K42	*crt*$^{-/-}$	
K42 cells expressing calreticulin mutants:		
Wild-type	*crt*$^{-/-}$-wt	
His25Ala mutant	*crt*$^{-/-}$-His25Ala	*crt*$^{-/-}$-H^{25}
His82Ala mutant	*crt*$^{-/-}$-His82Ala	*crt*$^{-/-}$-H^{82}
His128Ala mutant	*crt*$^{-/-}$-His128Ala	*crt*$^{-/-}$-H^{128}
His153Ala mutant	*crt*$^{-/-}$-His153Ala	*crt*$^{-/-}$-H^{153}
Cys88Ala mutant	*crt*$^{-/-}$-Cys88Ala	*crt*$^{-/-}$-C^{88}
Cys120Ala mutant	*crt*$^{-/-}$-Cys120Ala	*crt*$^{-/-}$-C^{120}
Glu238Arg mutant	*crt*$^{-/-}$-Glu238Arg	*crt*$^{-/-}$-E^{238}
Glu239Arg mutant	*crt*$^{-/-}$-Glu239Arg	*crt*$^{-/-}$-E^{239}
Asp241Arg mutant	*crt*$^{-/-}$-Asp241Arg	*crt*$^{-/-}$-D^{241}
Glu243Arg mutant	*crt*$^{-/-}$-Glu243Arg	*crt*$^{-/-}$-E^{243}
Trp244Ala mutant	*crt*$^{-/-}$-Trp244Ala	*crt*$^{-/-}$-W^{244}
Trp302Ala mutant	*crt*$^{-/-}$-Trp302Ala	*crt*$^{-/-}$-W^{302}

CEM	wild-type human jurkat T-lymphoblastoid leukemia cell lines.
NKR	calnexin-deficient human jurkat T-lymphoblastoid leukemia cell lines.
8WT	wild-type mouse embryonic fibroblasts.
9KO	calnexin-deficient mouse embryonic fibroblasts.

Table 2- 2 — Plasmid DNA used in this study.	
Plasmid Name	**Description**
pcDNA3.1/Zeo	Contains Zeocin resistance gene
pcDNA-Crt-HA	pcDNA3.1/Zeo with Crt wild-type cDNA with HA tag
pBAD/glIII A	Plasmid for *E. coli* expression
pSV7	Plasmid for immortalization, contains SV40 promoter
pBAD-HisCrt	pBAD/glIII A containing Crt cDNA with His tag
pBAD-HisCnx	pBAD/glIII A containing S-Cnx cDNA with His tag
Plasmids for transfection:	
pcDNA-Crt-HA	Plasmid expressing wild-type Crt with HA tag
pcDNA-H25A	Plasmid expressing H25A mutant Crt with HA tag
pcDNA-H82A	Plasmid expressing H82A mutant Crt with HA tag
pcDNA-H128A	Plasmid expressing H128A mutant Crt with HA tag
pcDNA-H153A	Plasmid expressing H153A mutant Crt with HA tag
pcDNA-H25Del	Plasmid expressing H25Del mutant Crt with HA tag
pcDNA-H82Del	Plasmid expressing H82Del mutant Crt with HA tag
pcDNA-H128Del	Plasmid expressing H128Del mutant Crt with HA tag
pcDNA-H153Del	Plasmid expressing H153Del mutant Crt with HA tag
pcDNA-C88A	Plasmid expressing C88A mutant Crt with HA tag
pcDNA-C120A	Plasmid expressing C120A mutant Crt with HA tag
pcDNA-E238R	Plasmid expressing E238R mutant Crt with HA tag
pcDNA-E239R	Plasmid expressing E239R mutant Crt with HA tag
pcDNA-D241R	Plasmid expressing D241R mutant Crt with HA tag
pcDNA-E243R	Plasmid expressing E243R mutant Crt with HA tag
pcDNA-W244A	Plasmid expressing W244A mutant Crt with HA tag
pcDNA-W302A	Plasmid expressing W302A mutant Crt with HA tag
Plasmids for calreticulin protein purification:	
pBAD-CRT-wt	Plasmid expressing wild-type Crt with His tag
pBAD-CRT-His25Ala	Plasmid expressing H25A mutant Crt with His tag
pBAD-CRT-His82Ala	Plasmid expressing H82A mutant Crt with His tag
pBAD-CRT-His128Ala	Plasmid expressing H128A mutant Crt with His tag
pBAD-CRT-His153Ala	Plasmid expressing H153A mutant Crt with His tag
pBAD-CRT-Cys88Ala	Plasmid expressing C88A mutant Crt with His tag
pBAD-CRT-Cys120Ala	Plasmid expressing C120A mutant Crt with His tag
pBAD-CRT-Glu238Arg	Plasmid expressing E238R mutant Crt with His tag
pBAD-CRT-Glu239Arg	Plasmid expressing E239R mutant Crt with His tag
pBAD-CRT-Asp241Arg	Plasmid expressing D241R mutant Crt with His tag
pBAD-CRT-Glu243Arg	Plasmid expressing E243R mutant Crt with His tag
pBAD-CRT-Trp244Ala	Plasmid expressing W244A mutant Crt with His tag
pBAD-CRT-Trp302Ala	Plasmid expressing W302A mutant Crt with His tag
Plasmids for calnexin protein purification:	
pBAD-Cnx-Glu351Arg	Plasmid expressing E351R mutant S-Cnx with His tag
pBAD-Cnx-Trp428Ala	Plasmid expressing W428A mutant S-Cnx with His tag

Table 2- 3 — Antibodies used in this study.

Antibody Name	Dilution for Western Blot	Dilution for Immunolocalization	Source
Rat anti-caspase 12	1:20	1:20 or 1:2	Dr. J.Y. Juang
Goat anti-calreticulin	1:500	1:70	Generated in our lab
Rabbit anti-calnexin	1:500	1:100 or 1:800	Generated in our lab
Rabbit anti-caspase 8	1:2000	-	Dr. D. Nicholson
Rabbit anti-caspase 3	1:1000	-	Dr. D. Nicholson
Rabbit anti-ERp57	1:1000	-	Generated in our lab
Rabbit anti-Bap31	1:8000	1:200	Dr. G. Shore
Rabbit anti-GRP94	1:1000	-	Stressgen Inc.
Rabbit anti-BiP	1:1000	-	Stressgen Inc. Dr. L. Hendershot
Rabbit anti-PDI	1:1000	-	Generated in our lab
Rabbit anti-Bcl-2	1:200	-	Stressgen Inc. or Upstate Cell Signaling Solutions
Rabbit anti-HA	1:300	-	Roche Diagnostics
Rabbit anti-IP_3R	1:1000	-	BD Biosciences
Rabbit anti-SERCA2	1:1000	-	Dr. L. Hendershot
Rabbit anti-Bax	1:1000	-	Upstate Cell Signaling Solutions
Rabbit anti-BK Receptor	1:10 (FACS)	-	Dr. W. Muller-Esterl
Mouse anti-SV40	1:300	-	Santa Cruz
Rabbit anti-cytochrome *c*	1:250	-	BD Biosciences
Rabbit anti-PARP	1:2000	-	BD Biosciences

Table 2- 4 — Primers used in this study.

Neomycin specific primers for identification of embryos:
Neomycin Forward neo-F1K (5′-TATTCGGCTATGACTGGGCACAA-3′)
Neomycin Reverse neo-R1K (5′-AGCAATATCACGGGTAGCCAACG-3′)
Calnexin specific primers for Southern blot analysis:
Calnexin Forward Kcnx150F (5′-GATCAGTTCCACGACAAGACC-3′)
Calnexin Reverse Kcnx150R (5′-CAGATCTGCATCTGGCCTCT-3′)
Calreticulin specific primers used for PCR-driven amplification of calreticulin cDNA fragments:
Calreticulin Forward (5′-GATAAAGGGTTGCAGACAAGC-3′)
Calreticulin Reverse (5′-CCCAGACTTGACCTGCC-3′)
Actin specific primers used for semi-quantitative PCR:
Actin Forward (5′-GACGAGGCCCAGAGCAAGAG-3′)
Actin Reverse (5′-CCAGACAGCACTGTGTTGGC-3′)

Chapter Three — Mutational Analysis of Calreticulin

Versions of this chapter have been previously published:

1. Lei Guo, Jody Groenendyk, Sylvia Papp, Monika Dabrowska, Barbara Knoblach, Cyril Kay, J. M. Robert Parker, Michal Opas and Marek Michalak. **Identification of an N-domain Histidine Essential for Chaperone Function in Calreticulin.** J. Biol. Chem., Vol. 278, Issue 50, 50645-50653, December 12, 2003.

2. Virginie Martin, Jody Groenendyk, Simone Steiner, Lei Guo, Monika Dabrowska, J.M. Robert Parker, Werner Müller-Esterl, Michal Opas and Marek Michalak. **Identification by Mutational Analysis of Amino Acid Residues Essential in the Chaperone Function of Calreticulin.** The Journal of Biological Chemistry vol. 281, no. 4, pp. 2338–2346, January 27, 2006.

Introduction

Calreticulin is a luminal chaperone Ca^{2+} buffering protein (Johnson et al., 2001) and is involved in numerous processes that are necessary for cellular Ca^{2+} homeostasis and intracellular Ca^{2+} signaling, most notably providing the Ca^{2+} necessary for the function and activity of the phosphatase, calcineurin (Groenendyk et al., 2004; Guo et al., 2002; Lynch et al., 2005; Lynch and Michalak, 2003; Michalak et al., 2002b). It is composed of three different domains, a globular N-domain, a P-domain and a C-domain. The N-domain contains the polypeptide and carbohydrate binding sites (Kapoor et al., 2004; Saito et al., 1999), the histidines involved in the interaction with Zn^{2+} (Baksh et al., 1995b), a potential ATP binding site (Corbett et al., 2000) and a disulfide linkage (Andrin et al., 2000). The P-domain is composed of a flexible, extended, finger-like region that interacts with ERp57 (Oliver et al., 1999) in a chaperone-dependent manner (Ellgaard et al., 2002; Frickel et al., 2002) and in conjunction with the N-domain, may form a functional protein-folding unit (Nakamura et al., 2001b). The C-domain contains a stretch of acidic amino acids that provide the high capacity Ca^{2+} binding sites (Baksh and Michalak, 1991). Calreticulin deficiency is embryonic lethal and cells derived from calreticulin-deficient embryos have impaired Ca^{2+} handling ability as well as compromised protein folding and quality control (Knee et al., 2003; Mesaeli et al., 1999; Nakamura et al., 2001b) indicating the importance of these two functions of calreticulin. Generation of calreticulin-deficient cells has provided a convenient system to test the site-directed mutational analysis of calreticulin.

In this part of my study, we generated several mutants of calreticulin, followed by examination of their chaperone activity, specifically bradykinin-mediated Ca^{2+} release and aggregation assays. The secondary and tertiary structure of calreticulin and the mutant proteins are investigated using intrinsic fluorescence, CD analysis and trypsin digestion. Calreticulin-deficient cells exhibit negligible bradykinin-dependent Ca^{2+} release, but expression of wild-type protein as well as Glu238Arg, Glu239Arg, Asp241Arg and Glu243Arg mutants rescue this Ca^{2+} release. The cysteine mutants (Cys88Ala and Cys120Ala) only partially rescue Ca^{2+} release and both the tryptophan mutants (Trp244Ala and Trp302Ala) were unable to rescue bradykinin-dependent Ca^{2+} release. We identify the amino acids involved in the interaction between calreticulin and ERp57. Of the four histidine residues located in the N-domain of calreticulin, only one, His153

is essential for calreticulin function as well as significantly affecting the structure of calreticulin. Conformational change in the structure of calreticulin induced by mutation of a single amino acid residue has negative consequences for chaperone function, demonstrating that mutations in chaperones may play a significant role in protein folding disorders.

Results

Expression of Mutants in Calreticulin-Deficient Cells

Several domains have been identified in calreticulin by 3D structural modeling (Michalak et al., 2002b). The N-terminal globular domain of the protein contains a carbohydrate (lectin) binding site (Schrag et al., 2001), conserved histidine and tryptophan residues and a disulphide bridge (Andrin et al., 2000). The central, proline-rich P-domain of calreticulin forms an extended arm and binds ERp57 (Ellgaard et al., 2002). The N-domain of calreticulin contains four conserved histidine residues involved in Zn^{2+} binding (Baksh et al., 1995b). Previous studies have determined that Zn^{2+} binding to calreticulin results in significant conformational modifications which promotes the interaction of calreticulin with substrate (Baksh et al., 1995a; Baksh et al., 1995b; Corbett et al., 2000; Khanna et al., 1986; Li et al., 2001b; Saito et al., 1999). To assess the role of the N-domain histidines in calreticulin function, we mutate His25Ala, His82Ala, His128Ala and His153Ala and generate a series of plasmids containing cDNA encoding these single site mutations, designated as CRT-His25Ala, CRT-His82Ala, CRT-His128Ala and CRT-His153Ala, respectively. Several other conserved residues contained within the N-domain of calreticulin are also targeted for mutation; two cysteine residues that form a disulfide bridge in the globular N-domain (Cys88Ala and Cys120Ala) and a tryptophan found in the globular N-domain, Trp302Ala. The P-domain, involved in an interaction with ERp57, contains an acidic region located at the tip of the arm. We target these residues for mutation, specifically Glu238Arg, Glu239Arg, Asp241Arg, Glu243Arg and Trp244Ala. These mutations are also incorporated into a series of plasmids containing cDNA, designated as CRT-Cys88Ala, CRT-Cys120Ala, CRT-Trp302Ala, CRT-Glu238Arg, CRT-Glu239Arg, CRT-Asp241Arg, CRT-Glu243Arg and CRT-Trp244Ala .

Calreticulin-deficient cells are stably transfected with these expression vectors to create cell lines expressing wild-type calreticulin (*crt*$^{-/-}$-wt), the specific histidine mutants *crt*$^{-/-}$-His25Ala, *crt*$^{-/-}$-His82Ala, *crt*$^{-/-}$-His128Ala and *crt*$^{-/-}$-His153Ala, or the other specific mutations, *crt*$^{-/-}$-Cys88Ala, *crt*$^{-/-}$-Cys120Ala, *crt*$^{-/-}$-Glu238Arg, *crt*$^{-/-}$-Glu239Arg, *crt*$^{-/-}$-Asp241Arg, *crt*$^{-/-}$-Glu243Arg, *crt*$^{-/-}$-Trp244Ala and *crt*$^{-/-}$-Trp302Ala. For easy identification of recombinant proteins, the HA epitope is introduced at the C-terminal. Previous studies in our laboratory showed that a C-terminal HA epitope does not affect calreticulin function (Arnaudeau et al., 2002; Gao et al., 2002; Nakamura et al., 2001b). Western blot analysis demonstrates that all of the transfected cells express recombinant calreticulin (Figure 3- 1 and Figure 3- 2). A notably lower level of expression of recombinant protein is consistently observed in cells expressing the His25Ala and His128Ala mutants (Figure 3- 1A) and although several different stably transfected cell lines are generated; we are unable to obtain cells with a higher level of expression. Next we carried out immunofluorescence analysis of the cell lines to examine if the recombinant calreticulin is localized to the ER. All the histidine mutant cell lines (*crt*$^{-/-}$-wt, *crt*$^{-/-}$-His25Ala, *crt*$^{-/-}$-His82Ala, *crt*$^{-/-}$-His128Ala and *crt*$^{-/-}$-His153Ala) express recombinant calreticulin with the protein localizing to an ER-like network (Figure 3- 1). Immunofluorescence analysis also confirms that the other site specific mutants (*crt*$^{-/-}$-Cys88Ala, *crt*$^{-/-}$-Cys120Ala, *crt*$^{-/-}$-Glu238Arg, *crt*$^{-/-}$-Glu239Arg, *crt*$^{-/-}$-Asp241Arg, *crt*$^{-/-}$-Glu243Arg, *crt*$^{-/-}$-Trp244Ala and *crt*$^{-/-}$-Trp302Ala) also localize normally (Figure 3- 2).

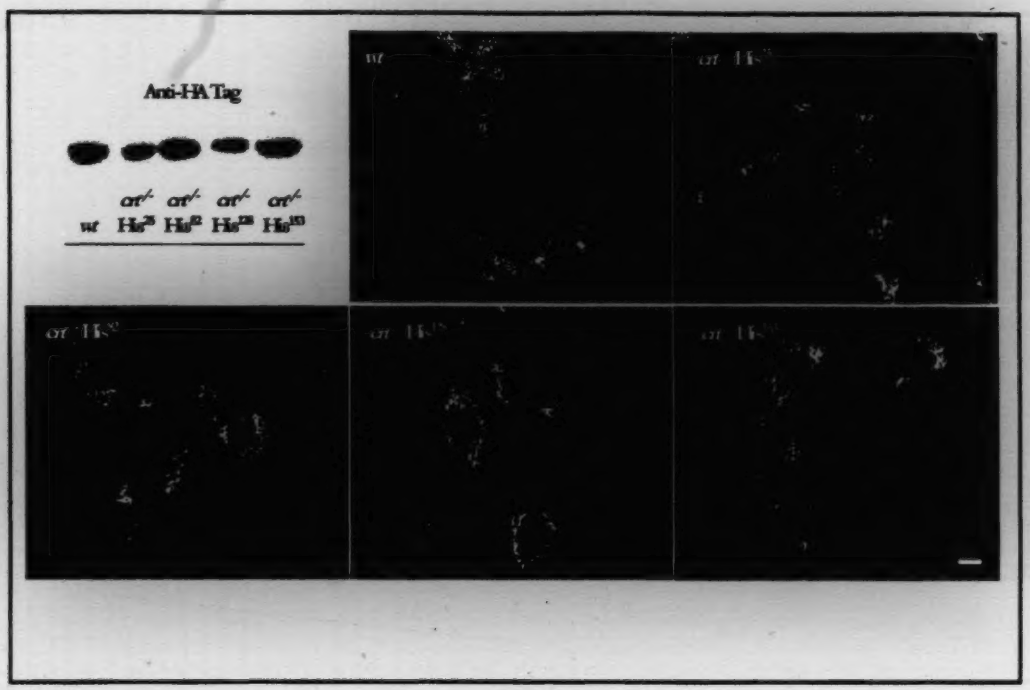

Figure 3- 1

Figure 3- 1 — Expression of histidine mutants in calreticulin-deficient mouse embryonic fibroblasts.

Western blot analysis and immunostaining of calreticulin in mouse embryonic fibroblasts (MEFs). Proteins from calreticulin-deficient cells expressing different calreticulin histidine mutants were solubilized using RIPA buffer, separated by SDS-PAGE (10% acrylamide), transferred to nitrocellulose membrane and probed with rabbit anti-hemagglutinin (anti-HA Tag) antibodies. Specific lanes represent (from left to right) *wt*, *crt*$^{-/-}$ cells expressing wild-type calreticulin; *crt*$^{-/-}$ His^{25}, cells expressing His25Ala mutant; *crt*$^{-/-}$ His^{82}, cells expressing His82Ala mutant; *crt*$^{-/-}$ His^{128} cells expressing His128Ala mutant and *crt* $^{-/-}$ His^{153} cells expressing His153Ala mutant. Calreticulin-deficient cells expressing different mutants were immunostained with anti-calreticulin antibodies. Scale bar=10 μm. These experiments were performed in collaboration with Dr. L. Guo.

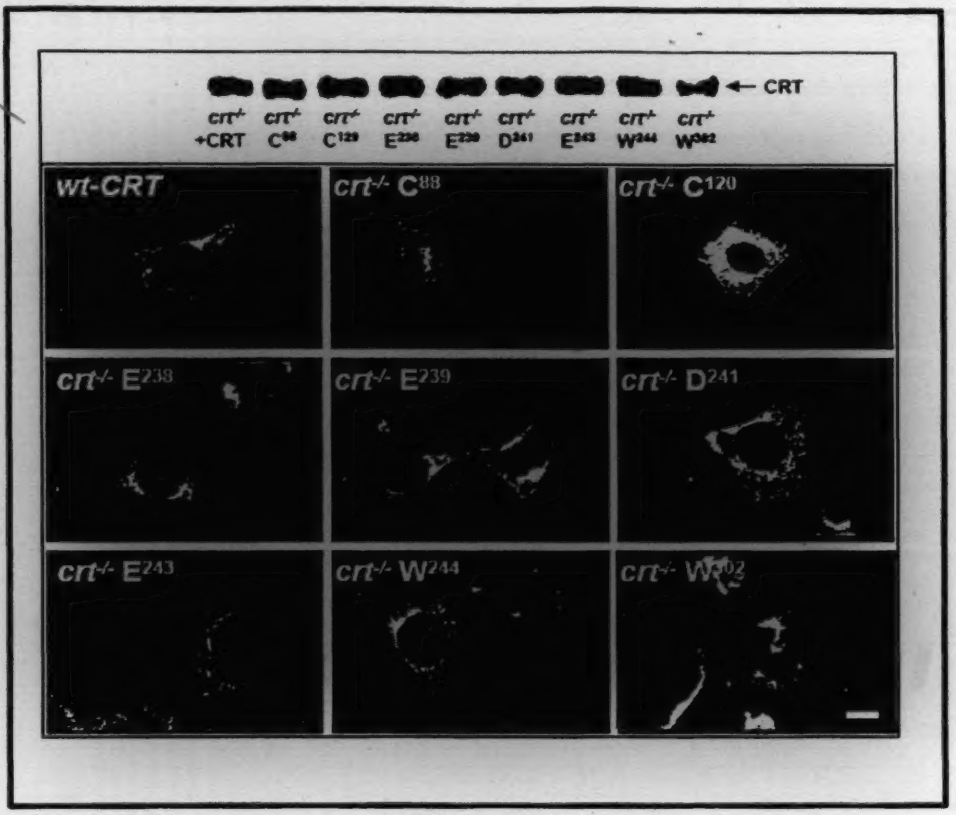

Figure 3- 2

Figure 3- 2 — Expression of calreticulin mutants in calreticulin-deficient mouse embryonic fibroblasts.

Western blot analysis and immunostaining of calreticulin in MEFs. *Upper panel*, proteins from calreticulin-deficient cells expressing different calreticulin mutants were lysed, separated by SDS-PAGE (10% acrylamide), transferred to nitrocellulose membrane and probed with rabbit anti-hemagglutinin (anti-HA tag) antibody. *Lower panel*, calreticulin-deficient cells expressing Glu238Arg, $crt^{-/-}$ E^{238}; Glu239Arg, $crt^{-/-}$ E^{239}; Asp241Arg, $crt^{-/-}$ D^{241}; Glu243Arg, $crt^{-/-}$ E^{243}; Trp244Ala, $crt^{-/-}$ W^{244}; Trp302Ala, $crt^{-/-}$ W^{302} were probed with anti-calreticulin antibody. Scale bar=10 μm. These experiments were performed in collaboration with Dr. V. Martin.

Bradykinin-Induced Ca^{2+} Release in Cells Expressing Calreticulin Mutants

Calreticulin-deficient cells have inhibited bradykinin-dependent Ca^{2+} release which is restored by expression of full length recombinant calreticulin (Figure 3- 3 and Figure 3- 4A) (Nakamura et al., 2001b). In the absence of calreticulin, the bradykinin receptor is unable to bind bradykinin to generate $InsP_3$-dependent signals because it is not folded properly, but with calreticulin present, it is folded correctly and is able to bind bradykinin (Nakamura et al., 2001b). Consequently, measurement of bradykinin-dependent Ca^{2+} release from the ER makes an excellent model system to study the function of calreticulin and calreticulin mutants in *crt*$^{-/-}$ cells. We took advantage of this, using the recovery of bradykinin-dependent Ca^{2+} release from the ER, in *crt*$^{-/-}$ cells, as a model system in which to compare the function of calreticulin and the various mutants we have generated. We perform these experiments with the Ca^{2+}-sensitive fluorescent dye Fura-2-AM. Figure 3- 3 and Figure 3- 4A show that, as expected, bradykinin causes a rapid and transient increase in the cytoplasmic Ca^{2+} concentration in wild-type cells but not in *crt*$^{-/-}$ cells (Nakamura et al., 2001b). Also, expression of recombinant calreticulin in *crt*$^{-/-}$ cells restores bradykinin-dependent Ca^{2+} release (Figure 3- 3 and Figure 3- 4A *crt*$^{-/-}$ +CRT). Bradykinin-induced Ca^{2+} release is then measured in the *crt*$^{-/-}$-His25Ala, *crt*$^{-/-}$-His82Ala, *crt*$^{-/-}$-His128Ala and *crt*$^{-/-}$-His153Ala cell lines. Expression of the His25Ala, His82Ala and His128Ala mutants fully restore bradykinin-dependent Ca^{2+} release (Figure 3- 3), whereas expression of the His153Ala mutant does not. This demonstrates that His153 must play an essential role in the structure and chaperone function of calreticulin.

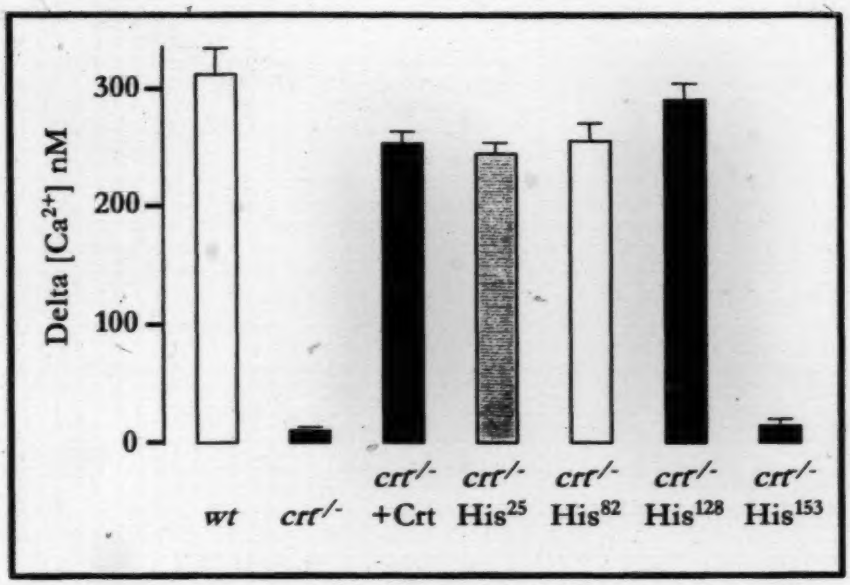

Figure 3- 3

Figure 3- 3 — Bradykinin-induced Ca^{2+} release in cells expressing calreticulin mutants.

Cells expressing different calreticulin mutants were loaded with the fluorescent Ca^{2+} indicator Fura 2-AM and stimulated with 200 nM bradykinin (Nakamura et al., 2001b). *wt*, wild-type cells; *crt*$^{-/-}$, calreticulin-deficient cells; *crt*$^{-/-}$+Crt, calreticulin-deficient cells expressing wild-type calreticulin; *crt*$^{-/-}$-His^{25}, cells expressing His25Ala mutant; *crt*$^{-/-}$-His^{82}, cells expressing His82Ala mutant; *crt*$^{-/-}$-His^{128} cells expressing His128Ala mutant and *crt*$^{-/-}$-His^{153} cells expressing His153Ala mutant. The amount of Ca^{2+} released by bradykinin is shown. Data are mean ± S.E. *(n=3)*.

Next, we measure bradykinin-dependent Ca^{2+} release in calreticulin-deficient cells (*crt*$^{-/-}$) expressing the other calreticulin mutants. In *crt*$^{-/-}$ cells expressing recombinant calreticulin with mutations at the tip of extended arm of the P-domain, bradykinin-dependent Ca^{2+} release is partially recovered (Figure 3- 4A). Specifically, expression of the mutants Glu238Arg, Glu239Arg, Asp241Arg and Glu243Arg restore bradykinin-dependent Ca^{2+} release to 55%, 75%, 73% and 78% of the control, respectively (Figure 3- 4A). In contrast, expression of the Trp302Ala calreticulin mutant does not restore bradykinin-dependent Ca^{2+} release, while expression of Trp244Ala mutant restores only ~10% of the activity (Figure 3- 4A). Yet, Trp244Ala and Trp302Ala calreticulin mutants have no effect on Ca^{2+} capacity of the ER stores (Figure 3- 4B). The expression of SERCA and $InsP_3$ receptors (Figure 3- 4C) is not altered in *crt*$^{-/-}$ cells expressing the Trp244Ala and Trp302Ala mutants. Furthermore, flow cytometry analysis reveales that the cell surface localization of the bradykinin receptor is not affected by the expression of Trp244Ala and Trp302Ala calreticulin mutants (Figure 3- 4D). We conclude that Trp244 and Trp302 residues play an essential role in the function of calreticulin concerning the folding of the bradykinin receptor.

I also investigate the functional consequence of mutating the cysteine residues involved in formation of the disulphide-bridge in the N-domain of calreticulin (Cys88Ala and Cys120Ala). Figure 3- 4A shows that bradykinin-dependent Ca^{2+} release is increased by only 38% and 40%, compared with the control, in cells expressing the Cys88Ala and Cys120Ala mutants, respectively. These data demonstrate that the cysteine residues are critical in determining the ability of calreticulin to function properly as a chaperone.

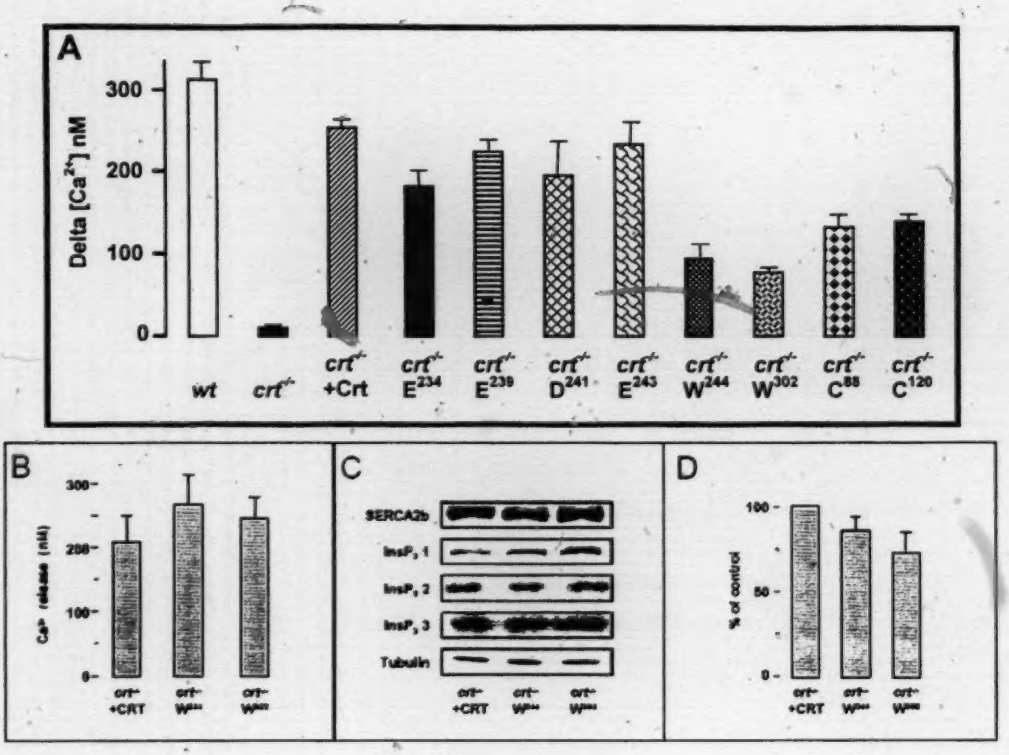
A
Delta [Ca2+] nM
300
200
100
0
wt
crt-/-
crt-/- +Crt
crt-/- E234
crt-/- E239
crt-/- D241
crt-/- E243
crt-/- W244
crt-/- W302
crt-/- C88
crt-/- C120
B
C
SERCA2b
InsP3 1
InsP3 2
InsP3 3
Tubulin
D
% of control
100
50
0

Figure 3- 4

Figure 3- 4 — Bradykinin-induced Ca^{2+} release in cells expressing calreticulin mutants.

A, cells expressing different calreticulin mutants were loaded with the fluorescent Ca^{2+} indicator Fura 2-AM and stimulated with 200 nM bradykinin (Nakamura et al., 2001b). *wt*, wild-type cells; *crt*$^{-/-}$, calreticulin-deficient cells; *crt*$^{-/-}$*+CRT*, calreticulin-deficient cells expressing wild-type calreticulin; *crt*$^{-/-}$-E^{238}, cells expressing Glu238Arg mutant; *crt*$^{-/-}$-E^{239}, cells expressing Glu239Arg mutant; *crt*$^{-/-}$-D^{241}, cells expressing Asp241Arg mutant; *crt*$^{-/-}$-E^{243}, cells expressing Glu243Arg mutant; *crt*$^{-/-}$-W^{244}, cells expressing Trp244Ala mutant; *crt*$^{-/-}$-W^{302}, cells expressing Trp302Ala mutant; *crt*$^{-/-}$-C^{88}, cells expressing Cys88Ala mutant; *crt*$^{-/-}$-C^{120}, cells expressing Cys120Ala mutant. The amount of Ca^{2+} release by bradykinin is shown. *B*, thapsigargin-releasable Ca^{2+} in calreticulin-deficient cells expressing wild-type calreticulin (*crt*$^{-/-}$*+CRT*), in cells expressing the Trp244Ala mutant (*crt*$^{-/-}$-W^{244}) and in cells expressing the Trp302Ala mutant (*crt*$^{-/-}$-W^{302}). Data are mean ±S.E. (*n*=3). *C*, SERCA2b and $InsP_3$ receptors expression in calreticulin-deficient cells. Western blot analysis was carried out. *crt*$^{-/-}$*+CRT*, calreticulin-deficient cells expressing wild-type calreticulin; *crt*$^{-/-}$-W^{244}, cells expressing Trp244Ala mutant; *crt*$^{-/-}$-W^{302}, cells expressing Trp302Ala mutant. Anti-tubulin antibodies were used as a loading control. *D*, bradykinin receptor expression on cell surface in calreticulin-deficient cells expressing wild-type calreticulin (*crt*$^{-/-}$*+CRT*), in cells expressing Trp244Ala mutant (*crt*$^{-/-}$-W^{244}) and in cells expressing Trp302Ala mutant (*crt*$^{-/-}$-W^{302}). Results are presented as a percentage of control (calreticulin-deficient cells expressing wild-type calreticulin). Data are mean ±S.E. *(n=3)*. Panels *A, B* and *C* were generated in collaboration with Dr. V. Martin.

Effect of Calreticulin Mutants on Thermal Aggregation of MDH and IgY

In order to examine the role of His153, Cys88, Cys120, Trp244 and Trp302 in the chaperone activity of calreticulin, we exploited an *in vitro* assay (Saito et al., 1999) measuring thermal aggregation. These assays utilize malate dehydrogenase (MDH) and IgY (Saito et al., 1999). MDH is a cytoplasmic protein that lacks N-linked oligosaccharides while IgY contains 27% monoglucosylated oligosaccharides and by treating with DTT and guanidine-HCl, is reduced and denatured. Once denatured, MDH and IgY are susceptible to heat-induced aggregation at 44°C, as measured by light scattering and have been widely used as model substrates in aggregation and refolding assays with other molecular chaperones (Lee et al., 1997; Manna et al., 2001; Veinger et al., 1998). For example, full-length recombinant calreticulin effectively prevents MDH or IgY thermal-induced aggregation *in vitro* (Saito et al., 1999).

To further investigate the role of these specific residues in calreticulin function, we examined the effectiveness of the mutants in preventing thermal aggregation of MDH and IgY, *in vitro*. In order to do this, we expressed the recombinant proteins in *E. coli* and purified them. Figure 3- 5 and Figure 3- 7A show that one-step purification of the recombinant proteins on a Ni^{2+}-column was sufficient. As previously reported, when MDH is heated to 44°C it begins to form insoluble aggregates that can be detected by light scattering (Figure 3- 5 and Figure. 3-7A) (Lee et al., 1997; Manna et al., 2001; Saito et al., 1999; Veinger et al., 1998). As expected, aggregation was reduced in the presence of different concentrations of wild-type calreticulin (Saito et al., 1999). The His82Ala mutant prevented aggregation of MDH similar to wild-type protein (Figure 3- 5B). In addition, the Cys88Ala, Cys120Ala, Glu238Arg, Glu239Arg, Asp241Arg and Glu243Arg calreticulin mutants all prevented heat-induced aggregation of MDH and to an extent similar to that observed for the wild-type protein (data not shown). However, addition of the His153Ala calreticulin mutant to 0.1 μM (calreticulin/MDH=0.1:1) or 0.2 μM (calreticulin/MDH=0.2:1), did not prevent MDH aggregation (Figure 3- 5B and Figure 3- 7A). As well, the Trp302Ala and Trp244Ala calreticulin mutants were also not effective in preventing heat-induced aggregation of MDH (Figure 3- 7A), suggesting that these residues are critical in the ability of calreticulin to prevent MDH aggregation. Next we tested the effectiveness of calreticulin mutants in preventing aggregation of a glycosylated substrate, IgY. The majority of the effects of calreticulin on IgY aggregation

are mediated by calreticulin-carbohydrate interactions (Saito et al., 1999). As expected, full-length calreticulin (0.25 μM) effectively prevented aggregation of chemically denatured IgY (0.25 μM) (Figure 3- 6 and Figure 3- 7B). The His25Ala, His82Ala and His128Ala mutants (0.25 μM) were also effective in preventing aggregation of IgY (0.25 μM) (data not shown). However, in keeping with the results of the MDH-refolding experiments (Figure 3- 5B and Figure 3- 7A), the His153Ala mutant (0.25 μM) (Figure 3- 6), the Trp302Ala and the Trp244Ala mutants (0.25 μM) (Figure 3- 7B) did not prevent aggregation of IgY (0.25 μM) (Figure 3- 6 and Figure 3- 7B).

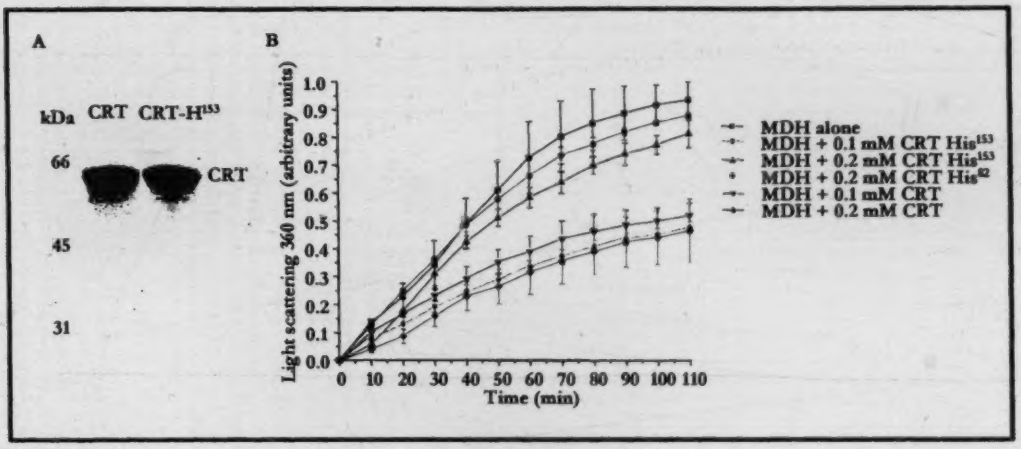

Figure 3- 5

Figure 3- 5 — Effects of calreticulin mutants on thermal aggregation of MDH, a non-glycosylated substrate.

A, SDS-PAGE (10% acrylamide) of recombinant wild-type (CRT) and His153Ala (CRT *His153Ala*) mutant of calreticulin used for aggregation studies are shown in *B. B,* 1 μM MDH was incubated in the presence or absence of wild-type calreticulin or calreticulin His82Ala or His153Ala mutant (0.25 μM) as indicated. Proteins were pre-incubated at room temperature followed by monitoring aggregation at 44°C at 360 nm (Saito et al., 1999). Data are mean ±S.E. *(n=4).*

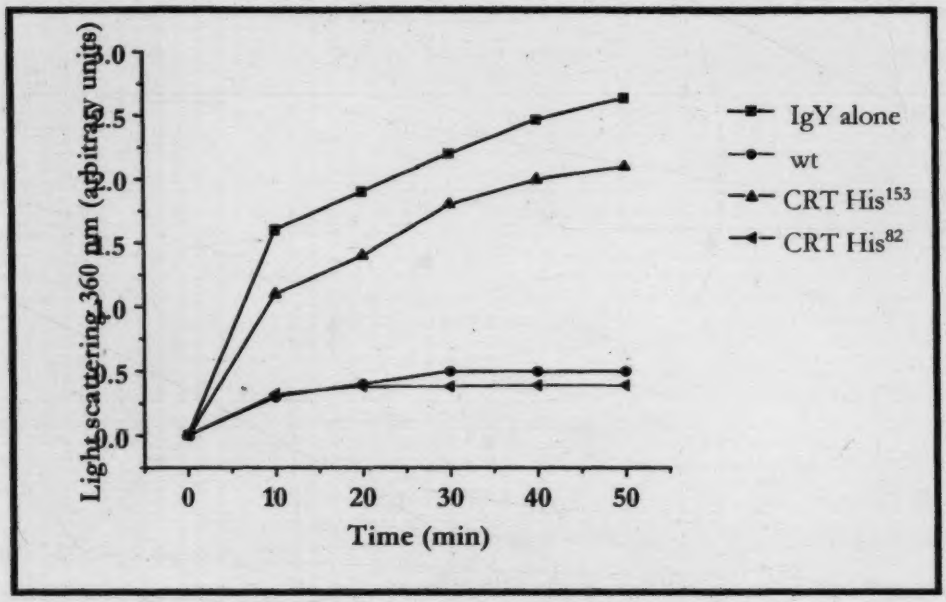

Figure 3- 6

Figure 3- 6 — Effects of calreticulin on thermal aggregation of IgY, a glycosylated substrate.

Effect of calreticulin and calreticulin on the thermal aggregation of IgY (0.25 μM) was monitored at 44°C by measuring light scattering at 360 nm. Wild-type (*wt*), His153Ala (*CRT His153*) and His82Ala (*CRT His82*) mutants of calreticulin (0.25 μM) were tested as indicated. Data are mean ±S.E. *(n=4)*.

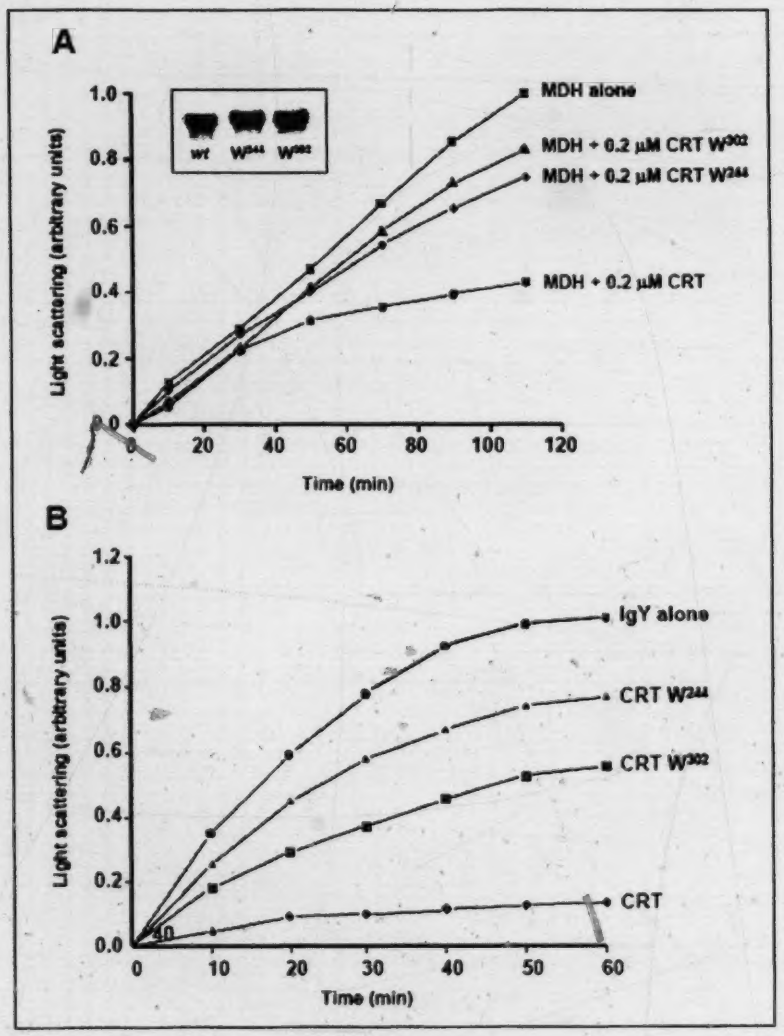

Figure 3- 7

Figure 3- 7 — Effects of Trp302Ala and Trp244Ala calreticulin mutants on thermal aggregation of MDH and IgY.

1 μM MDH *(A)* or 0.25 μM IgY *(B)* was incubated in the presence or absence of wild-type calreticulin or calreticulin mutants (0.2 μM) as indicated, followed by monitoring aggregation at 360 nm. *Box*, SDS-PAGE (10% acrylamide) of recombinant wild-type *(wt)* and Trp244Ala *(CRT W^{244})* and Trp302Ala *(CRT W^{302})* mutants of calreticulin used for aggregation and conformational change studies is shown.

Structural Analysis of Calreticulin Mutants

Molecular modeling of the structure of calreticulin, based on the known crystal structure of calnexin (Schrag et al., 2001), demonstrates that His153 is located in a "pocket" close to a putative carbohydrate/substrate binding site (see Figure 3- 18). This region is involved in Zn^{2+} binding to calreticulin (Baksh et al., 1995b) and so mutation of this His153 residue may trigger Zn^{2+}-dependent conformational changes in the protein, affecting its interactions with substrates (Saito et al., 1999). Disruption of the disulfide linkage (Cys88Ala and Cys120Ala), site specific mutation of Trp302Ala and mutations at the tip of the P-domain may also potentially disrupt the tertiary structure of the protein. To test these hypotheses, we carried out intrinsic fluorescence, CD analysis and limited proteolysis of wild-type and mutant protein. First, we measure the intrinsic fluorescence of recombinant calreticulin and the calreticulin mutants. The intrinsic fluorescence emission of a protein is affected by the movement of charged groups and by hydrophobic changes in the microenvironment, particularly those resulting from movement of tryptophan residues into the solvent. Thus, the emission scan provides information on changes in tertiary structures. If the protein is excited at 286 nm, where absorption is predominantly by tryptophan, the emission maximum at 334 nm represents the contribution of tryptophan. Fluorescence emission spectra are measured for wild-type calreticulin and for calreticulin mutants at varying Zn^{2+} concentrations (Figure 3- 8A-D and Figure 3- 9A-C). Figure 3- 8A demonstrates that in the absence of Zn^{2+} both wild-type calreticulin and the His153Ala mutant have an emission maximum wavelength of 334 nm. However, the basal intrinsic fluorescence intensity (λ334) of wild-type calreticulin is over 30% higher than that observed for the His153Ala mutant (Figure 3- 8A and B). This indicates that the mutant protein has less tryptophan exposed to the solvent. In the presence of increasing concentrations of Zn^{2+}, there is a significant increase in the intensity of fluorescence from wild-type calreticulin (Figure 3- 8A and D, Figure 3- 9A), indicating Zn^{2+}-dependent conformational changes in the protein. In contrast, the His153Ala calreticulin mutant shows only minor changes in intrinsic fluorescence as a function of increasing Zn^{2+} concentration (Figure 3- 8B and C). Fluorescence emission spectra for the calreticulin mutants Cys88Ala, Cys120Ala, Glu238Arg, Glu239Arg, Asp241Arg, Glu243Arg and Trp302Ala are indistinguishable from the spectrum observed for the wild-type protein (data not shown), indicating that

mutation of these residues in calreticulin does not significantly affect the conformation of the protein. On the contrary, the mutant Trp244Ala shows greater changes in intrinsic fluorescence at lower Zn^{2+} concentrations than does wild-type calreticulin (Figure 3- 9B), the maximal change being observed at 0.25 mM Zn^{2+}. The effect of Zn^{2+} on the specific conformation of calreticulin is enhanced in the absence of the Trp244Ala mutation (Figure 3- 9C). This indicates that the effect of Zn^{2+} on the structure and conformation of calreticulin is compromised with the mutation of His153 or Trp 244. Ca^{2+}-dependent changes in intrinsic fluorescence were also measured for all mutants. There is no significant difference in the Ca^{2+}-dependent intrinsic fluorescence observed in wild-type calreticulin, in the mutants, Trp244Ala (Figure 3- 9D and E), His153Ala (Figure 3- 8E and F) and in the mutants Cys88Ala, Cys120Ala, Glu238Arg, Glu239Arg, Asp241Arg, Glu243Arg, Trp302Ala (data not shown).

ANS has been used extensively to monitor hydrophobic sites on the surface of proteins (Matulis et al., 1999; Matulis and Lovrien, 1998). The fluorescence emission intensity of ANS increases and undergoes a spectral blue shift when placed in a hydrophobic environment. Both wild-type and the His153Ala mutant calreticulin induced a blue shift of the ANS emission spectrum from 498 mm to 473 nm (Figure 3- 10), with the addition of Zn^{2+} inducing a further blue shift from 473 nm to 468 nm (Figure 3- 10). At 468 nm, addition of wild-type calreticulin induced a 4.5-fold increase in ANS fluorescent intensity compared with 3-fold for the His153Ala mutant calreticulin (Figure 3- 10). The addition of Zn^{2+} further enhanced ANS fluorescent intensity, up to 7-fold for wild-type calreticulin compared with only 4.5-fold for His153Ala mutant (Figure 3- 10). This indicates that the His153Ala calreticulin mutant has a tighter conformation with less hydrophobic surface exposed than wild-type calreticulin.

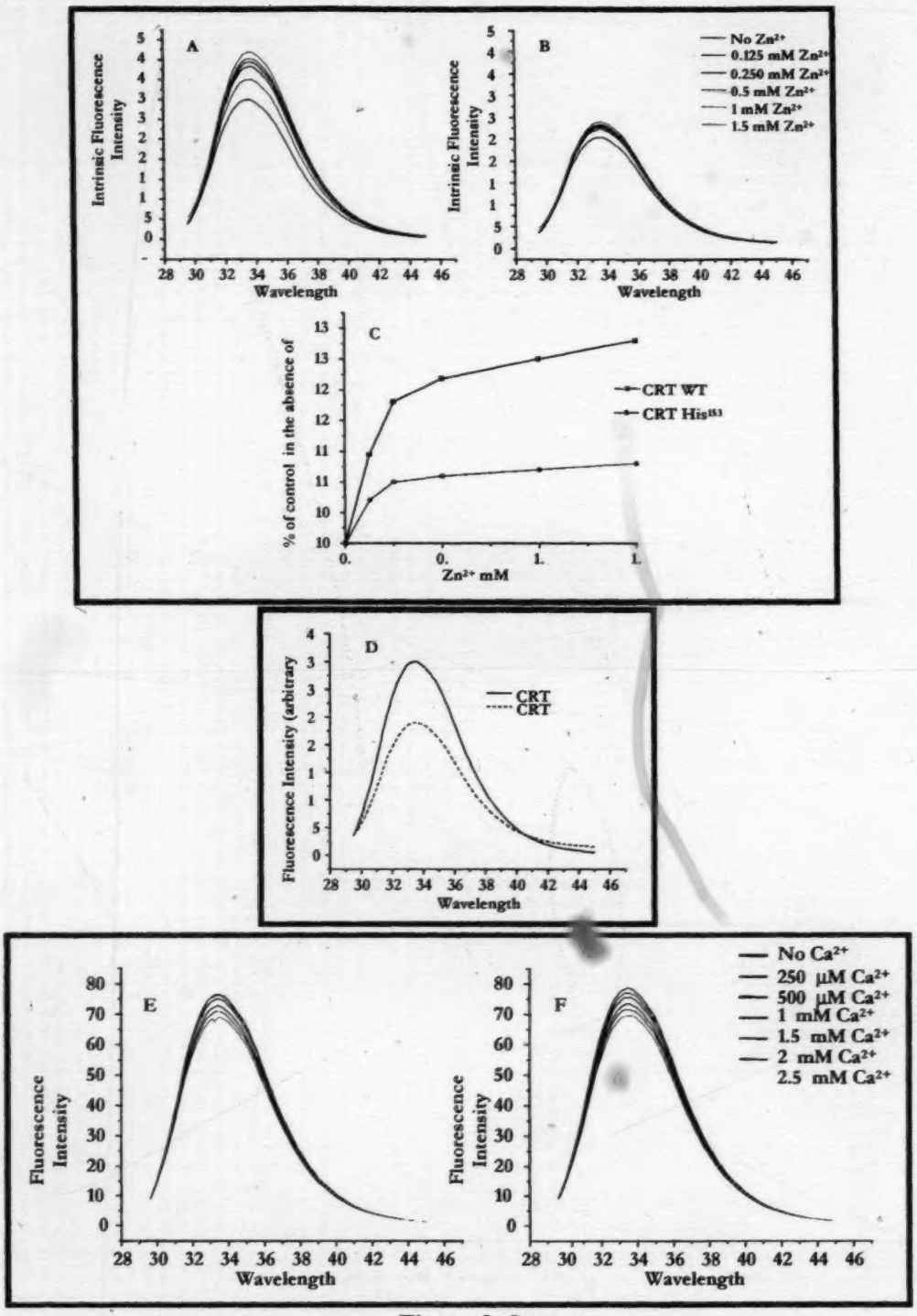
A
B
C
D
E
F
Intrinsic Fluorescence Intensity
Wavelength
No Zn2+
0.125 mM Zn2+
0.250 mM Zn2+
0.5 mM Zn2+
1 mM Zn2+
1.5 mM Zn2+
% of control in the absence of
Zn2+ mM
CRT WT
CRT His153
Fluorescence Intensity (arbitrary
CRT
CRT
Fluorescence Intensity
No Ca2+
250 µM Ca2+
500 µM Ca2+
1 mM Ca2+
1.5 mM Ca2+
2 mM Ca2+
2.5 mM Ca2+

Figure 3- 8

Figure 3- 8 — Conformational changes in His153Ala mutant.

Intrinsic tryptophan fluorescence emission spectra analysis of wild-type calreticulin *(CRT wt)* and the His153Ala *(CRT His153)* mutant. Intrinsic fluorescence analysis was carried out in the absence and presence of increasing concentration of Zn^{2+}. *A*, wild-type calreticulin; *B*, His153Ala mutant. Kinetics of Zn^{2+}-dependent changes in intrinsic fluorescence of wild-type and His153Ala mutant of calreticulin are shown in *C*. *D*, wild-type calreticulin and His153Ala mutants demonstrate a significant difference in global intrinsic fluorescence. Ca^{2+}-dependent changes in intrinsic fluorescence of wild-type calreticulin *(E)* or His153Ala mutant *(F)*. The excitation wavelength was set to 286 nm and the range of emission wavelength was set to 295-450 mm.

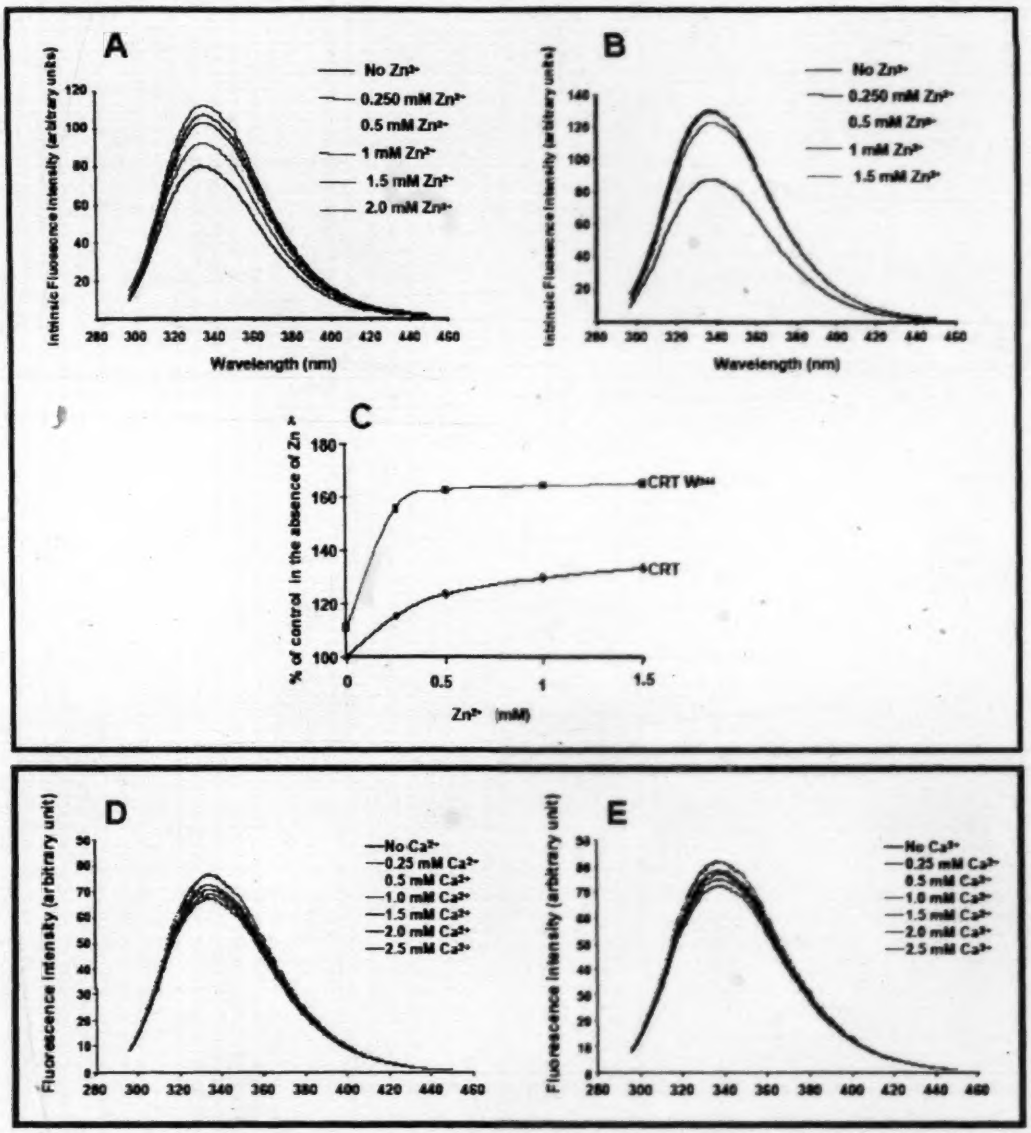

Figure 3- 9

Figure 3- 9 — Conformational change in Trp244Ala calreticulin mutant.

Intrinsic tryptophan fluorescence emission spectra analysis of wild-type calreticulin *(A)* and Trp244Ala mutant *(B)* was carried out in the absence and presence of increasing concentrations of Zn^{2+}. Zn^{2+}-dependent changes in intrinsic fluorescence of wild-type and Trp244Ala mutant of calreticulin are shown in *C*. Ca^{2+}-dependent changes in intrinsic fluorescence of wild-type calreticulin *(D)* and Trp244Ala *(E)* mutant. The excitation wavelength was set at 286 nm and the range of emission wavelength was set to 295–450 nm.

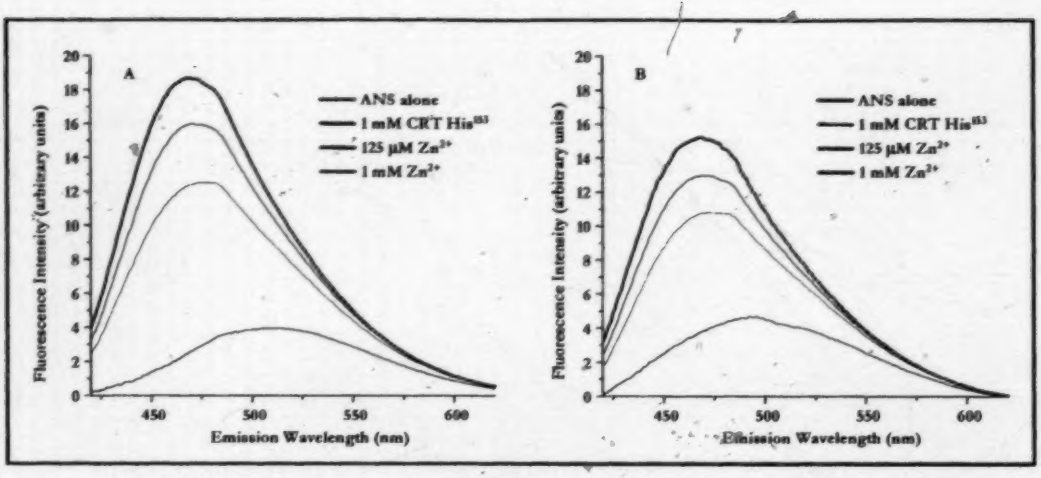

Figure 3- 10

Figure 3- 10 — Conformational changes in His153Ala revealed by ANS fluorescence.

ANS binding to calreticulin and His153Ala mutant. ANS fluorescence was measured in the absence or presence of increasing concentration of Zn^{2+} as indicated.

To determine whether the observed differences in fluorescence behavior (Figure 3- 8 and 3-9) reflect conformational differences between the wild-type and mutant proteins, we carried out CD analysis of the purified proteins. Figure 3- 11 shows that the CD spectra of calreticulin and the His153Ala mutant are very similar in shape. The Contin version program for calculating secondary structural elements (Table 3- 1) estimates the α-helical content for both proteins as 12-14%. In contrast, the combined β-sheet and β-turn content for the two proteins differs significantly, at 58% for wild-type calreticulin and 73% for the His153Ala mutant. This general increase in β-sheet-β-turn in the mutant protein supports the findings of our fluorescence experiments and indicates that mutation of His153Ala has a significant effect on the structure of calreticulin. Both proteins undergo a conformational change upon addition of Zn^{2+} with a reduction in the amount of α-helix (Table 3- 1, Figure 3- 11). The addition of Zn^{2+} to wild-type calreticulin results in fewer β-sheet structures and an increase in β-turn and unordered structures (Table 3- 1). In contrast, addition of Zn^{2+} to the His153Ala mutant calreticulin results in reduced β-sheet-β-turn content and a significant increase in unordered structures (Table 3- 1). We also perform CD spectra of wild-type calreticulin and the Cys88Ala, Cys120Ala, Trp244Ala and Trp302Ala mutants, demonstrating very little difference in shape (Figure 3- 12). Trp244Ala and Trp302Ala mutants exhibit slight increases in β-sheet-β-turn whereas Cys80 and Cys120Ala show a slight decrease in β-sheet-β-turn (Figure 3- 12). These minor changes in the conformation of Cys88Ala, Cys120Ala, Trp244Ala and Trp302Ala mutations may contribute, in part, to a disruption of the chaperone function.

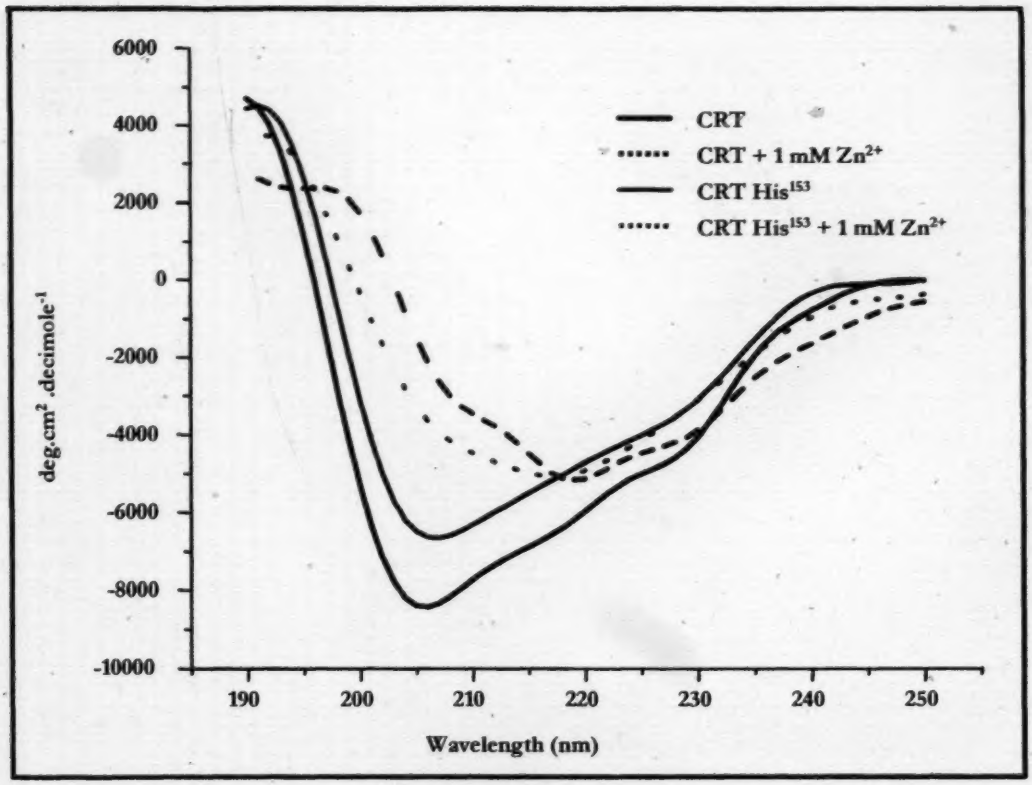

Figure 3- 11

Figure 3- 11 — CD analysis of calreticulin and His153Ala calreticulin mutant.

CD spectra of purified calreticulin *(black line)* and His153Ala *(red line)*. The data are plotted as molar ellepticity versus wavelength for the proteins in the absence *(solid line)* and presence of Zn^{2+} *(broken line)*. Data kindly provided by Dr. Kay's laboratory.

Table 3- 1 — Provencher-Glochner secondary structural analysis

Provencher-Glochner secondary structural analysis of wild-type calreticulin and calreticulin His153Ala mutant in the absence and presence of Zn^{2+}

	α-helix	β-sheet	β-turn	unordered	scale factor
WT CRT	0.14	0.40	0.18 (both 0.58)	0.27	1.0
WT CRT 1 mM Zn^{2+}	0.08	0.29	0.24 (both 0.53)	0.39	1.0
CRT His153Ala	0.12	0.50	0.23 (both 0.73)	0.15	0.999
CRT His153Ala 1 mM Zn^{2+}	0.09	0.46	0.19 (both 0.65)	0.27	0.998

Measurements were carried out in the presence of a buffer containing 10 mM Tris, pH 7.4 and 1 mM EDTA. Numbers indicate amount compared to 1.0.

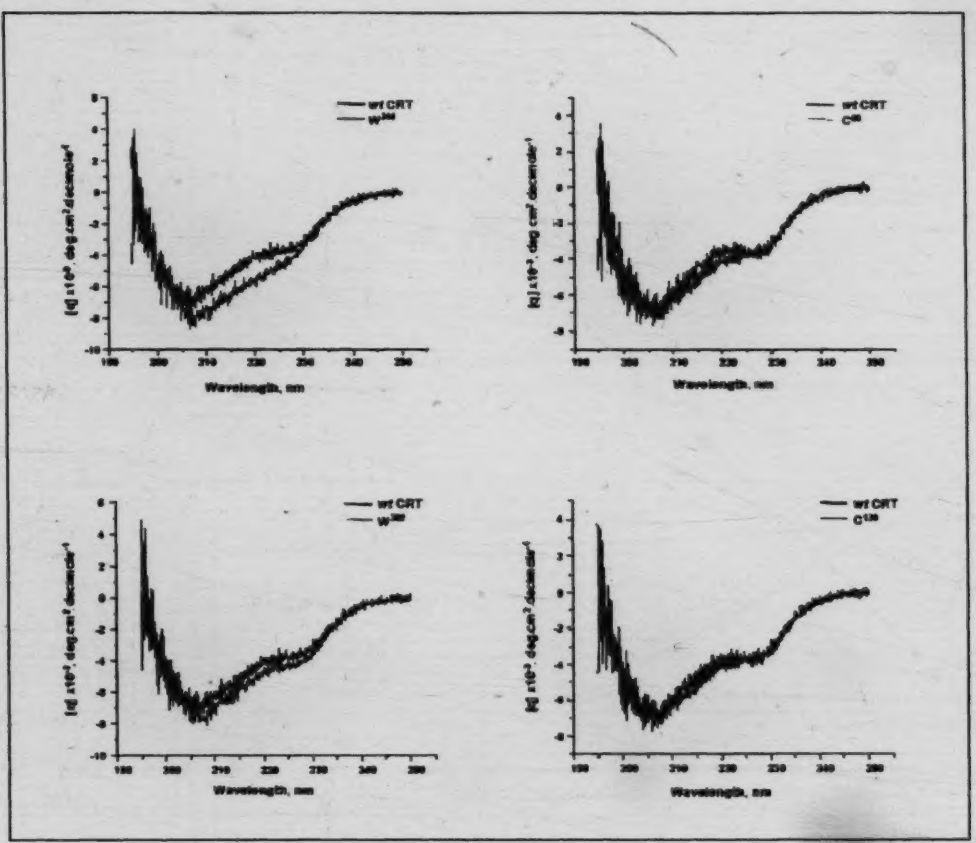

Figure 3- 12

Figure 3- 12 — CD analysis of calreticulin and calreticulin mutants.

CD spectra of purified wild-type calreticulin (*wtCRT*) and calreticulin mutants (Trp244Ala, W^{244}; Trp302Ala, W^{302}; Cys88Ala, C^{88}; and Cys120Ala, C^{120}). The data are plotted as molar ellipticity *versus* wavelength.

Finally, we investigate conformational differences between calreticulin and calreticulin mutants using limited proteolysis. It has been shown previously that the resistance of recombinant calreticulin to trypsin is an excellent measure of its folding (Corbett et al., 2000). Here we examine the effect of the mutants; His153Ala, Glu239Arg, Glu243Arg, Trp244Ala and Trp302Ala, on the trypsin resistance of calreticulin. Purified proteins are treated with trypsin (trypsin:calreticulin=1:100) for up to twenty minutes and analyzed by SDS-PAGE (10% acrylamide). Figure 3- 13 and Figure 3- 14A show that a significant proportion of wild-type calreticulin is resistant to trypsin digestion for up to ten minutes. In contrast, the His153Ala calreticulin mutant full length protein is completely degraded and undetectable after five minutes of treatment with the trypsin (Figure 3- 13). This increased susceptibility to proteolysis further verifies that mutation of His153Ala in calreticulin leads to significant alteration of its structure. In agreement with our earlier observations (Corbett et al., 2000), in the presence of 2 mM Ca^{2+}, wild-type calreticulin is relatively resistant to trypsin digestion (trypsin/calreticulin = 1:100) (Figure 3- 14A). Mutation of Glu239Arg at the tip of the extended arm of the P-domain of calreticulin (Figure 3- 14B) and of Trp302Ala in the carbohydrate binding region (Figure 3- 14C), have no effect on the sensitivity of the protein to trypsin digestion, in the presence of Ca^{2+}. Both mutants are relatively resistant to digestion, similar to the wild-type protein. In contrast, the Ca^{2+}-dependent trypsin resistance of calreticulin is lost when the residues Glu243Arg and Trp244Ala are mutated (Figure 3- 14D and E). Calreticulin binds Ca^{2+} at high affinity/low capacity and low affinity/high capacity sites (Baksh and Michalak, 1991) and it is possible that changes in Ca^{2+} binding to the protein could alter its sensitivity to trypsin. Therefore, we measured Ca^{2+} binding to calreticulin and the calreticulin mutants. Ca^{2+} binding to the high affinity and to the high capacity Ca^{2+} binding sites in calreticulin is not affected in the calreticulin mutants used in the present studies (Table 3- 2). We conclude that the increased susceptibility to Ca^{2+}-dependent proteolysis seen in the mutants Glu243Arg and Trp244Ala indicates that mutation of these amino acid residues leads to significant alteration in the structure of calreticulin.

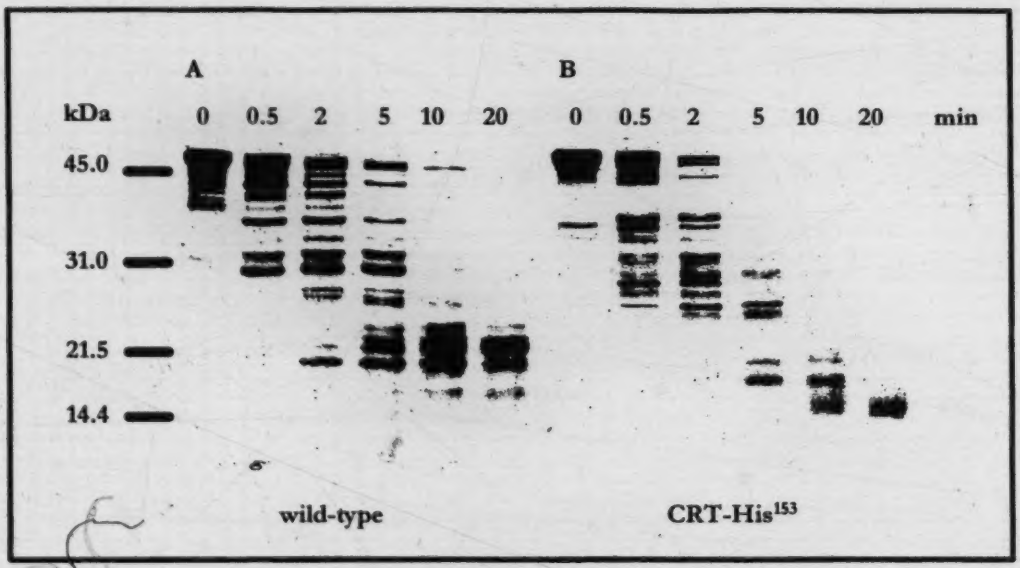

Figure 3- 13

Figure 3- 13 — Trypsin digestion of calreticulin and His153Ala mutant.

Calreticulin *(A)* and His153Ala *(B)* calreticulin mutant were expressed in *E. coli* and the purified proteins were incubated with trypsin at 1:100 (trypsin/protein; w/w) at 37°C. Aliquots were taken at the time points indicated and the proteins were separated on a SDS-PAGE (10% acrylamide) and stained with Coomassie Blue.

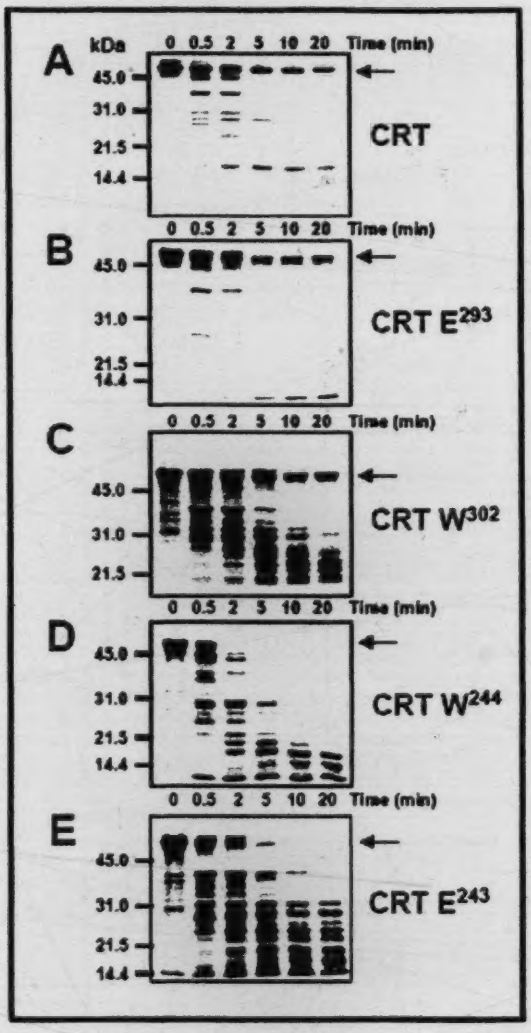

Figure 3- 14

Figure 3- 14 — Trypsin digestion of calreticulin and calreticulin mutants.

Calreticulin and calreticulin mutants were expressed in *E. coli* and the purified proteins were incubated with trypsin at 1:100 (trypsin/protein; w/w) at 37°C. Aliquots were taken at the time points indicated and the proteins were separated on SDS-PAGE (10% acrylamide) and stained with Coomassie Blue. Protein designated as CRT E239, Glu239Arg; CRT W302, Trp302Ala; CRT W244, Trp244Ala; CRT E243, Glu243Arg. The arrows indicate the location of calreticulin. *CRT*, calreticulin.

Table 3- 2 — Ca^{2+} binding to recombinant calreticulin

Ca^{2+} binding to recombinant calreticulin was measured by equilibrium dialysis (Baksh and Michalak, 1991).

Protein	mol of Ca^{2+}/mol of protein	K_d (mM)	mol of Ca^{2+}/mol of protein	K_d (μM)
Wild-type CRT	22.0	2.0	1.0	6.0
CRT-Glu238Arg	20.0	1.7	0.9	6.5
CRT-Glu239Arg	19.0	2.1	1.1	7.0
CRT-Asp241Arg	20.0	1.9	1.1	7.5
CRT-Glu243Arg	21.5	1.8	1.0	6.5
CRT-Cys88Ala	19.0	1.9	1.0	6.0
CRT-Cys120Ala	18.5	1.9	1.0	7.0
CRT-Trp244Ala	22.0	2.0	1.1	7.5
CRT-Glu302Arg	19.0	2.2	1.0	7.0

Association of ERp57 with Calreticulin

Calreticulin associates with ERp57, a thiol-disulfide oxidoreductase and a close homolog of protein disulfide isomerase (Molinari and Helenius, 1999; Oliver et al., 1999; Pollock et al., 2004). ERp57 binds to the tip of the hairpin-like P-domain of calreticulin (Ellgaard et al., 2002; Frickel et al., 2002) and promotes disulfide bond formation in glycoprotein substrates (Oliver et al., 1997; Zapun et al., 1998). Several of the calreticulin residues mutated in this study (Glu238Arg, Glu239Arg, Asp241Arg, Glu243Arg, Trp244Ala) are within the region believed to contain the ERp57 binding site (Ellgaard et al., 2002; Frickel et al., 2002; Leach et al., 2002). We made a number of attempts to show ERp57-calreticulin interactions using GST-pull down experiments. Unfortunately, these experiments were difficult to control and reproduce because a significant amount of both calreticulin and ERp57 bound nonspecifically to the affinity beads. Therefore, we tested whether any of these residues are involved in promoting the ERp57-calreticulin association. To do this we employed surface plasmon resonance (SPR) analysis. Recombinant calreticulin and the calreticulin mutants were immobilized to a BIAcore sensor chip and the binding of recombinant ERp57 in the flow buffer was measured. As shown in Figure 3- 15, binding of ERp57 to calreticulin was detected. Mutation of the residue Glu238Arg in calreticulin, located at the tip of the P-domain, had no significant effect on ERp57 binding to the immobilized protein (Figure 3- 15). In contrast, the mutants Glu239Arg and Glu243Arg showed significantly reduced binding of ERp57 and the mutants Asp241Arg and Trp244Ala did not bind ERp57 at all (Figure 3- 15). Interestingly, mutation of the Trp302 residue, which is localized in the N-terminal carbohydrate binding site away from the P-domain of calreticulin, significantly enhanced binding of ERp57 to the protein (Figure 3- 15).

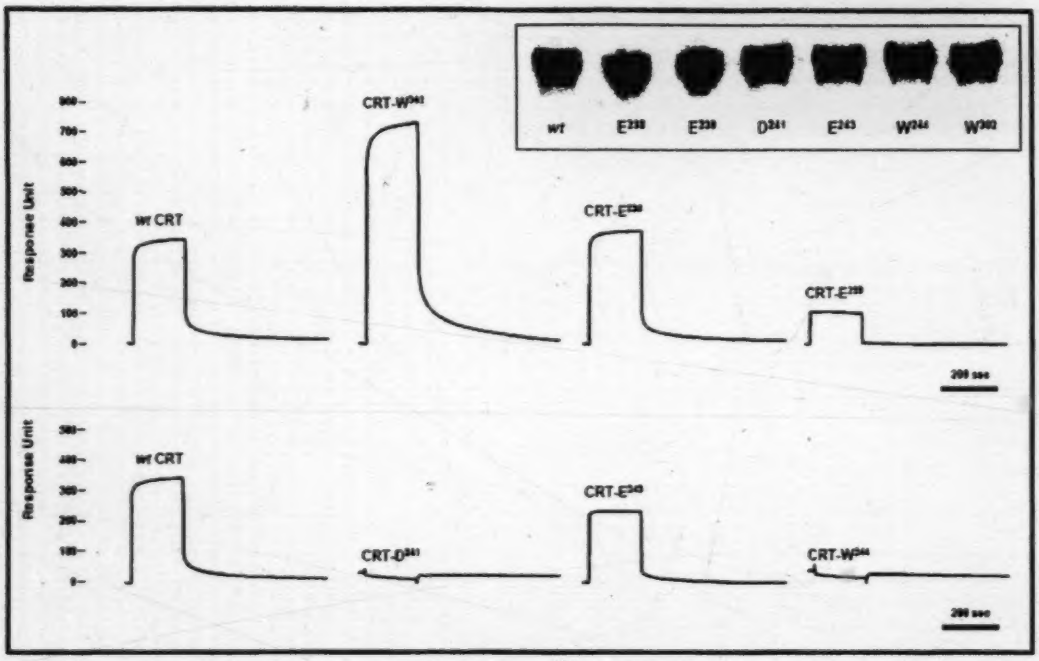

Figure 3- 15

Figure 3- 15 — Surface plasmon resonance analysis of interactions between ERp57 and calreticulin.

Recombinant ERp57 was injected over immobilized calreticulin *(CRT)* or calreticulin mutants. Results were monitored with real-time sensorgram. SDS-PAGE (10% acrylamide) of recombinant wild-type *(wt)* and calreticulin mutants is shown.

As many chaperones are regulated by ATP binding or hydrolysis (Bukau and Horwich, 1998; Mayer and Bukau, 2005; Veinger et al., 1998), we tested the ability of calreticulin to bind ATP. Calreticulin interaction with ATP has been previously reported but the site of nucleotide binding has not been determined (Nigam et al., 1994). Specifically, the ability of calreticulin to suppress the aggregation of *in vitro* substrates was enhanced by the addition of ATP (Saito et al., 1999). Calreticulin contains a putative hydrophobic nucleotide binding site, ^{131}MFGPD^{135} located on the surface of the N-terminal globular domain in close proximity to the carbohydrate/substrate binding domain and may potentially form a cleft that comprises part of the ATP binding region. Calreticulin bound ATP-Mg^{2+} (Figure 3- 16). ATP-Na^{+}, ADP, CTP and NAD also bound in a similar manner, but AMP, GTP, TTP or AMP-PNP (non-hydrolysable isoform) did not bind (Figure 3- 16). As well, specific mutants of calreticulin appeared to influence the ATP-Mg^{2+} interaction (Figure 3- 18). When EGTA was present, there was significant reduction in binding (results not shown), implying that a specific conformation of the protein supplied by divalent cations may be necessary to promote ATP binding to the protein. We conclude that ATP binding to calreticulin appears to be conformation-dependent.

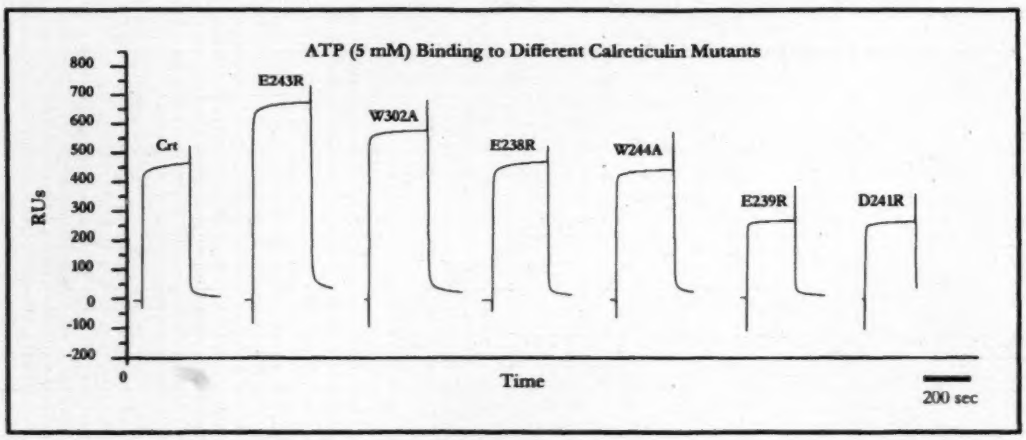

Figure 3- 16

Figure 3- 16 — Surface plasmon resonance analysis of the interaction of ATP with calreticulin and mutants.

SPR analysis was carried out in the presence of 5 mM ATP-Mg^{2+} and injected over the chip with the covalently coupled protein (CRT, E243R, Glu243Arg; W302A, Trp302Ala; E238R, Glu238Arg; W244A, Trp244Ala; E239R, Glu239Arg; and D241R, Asp241Arg), with results monitored by a real-time sensorgram.

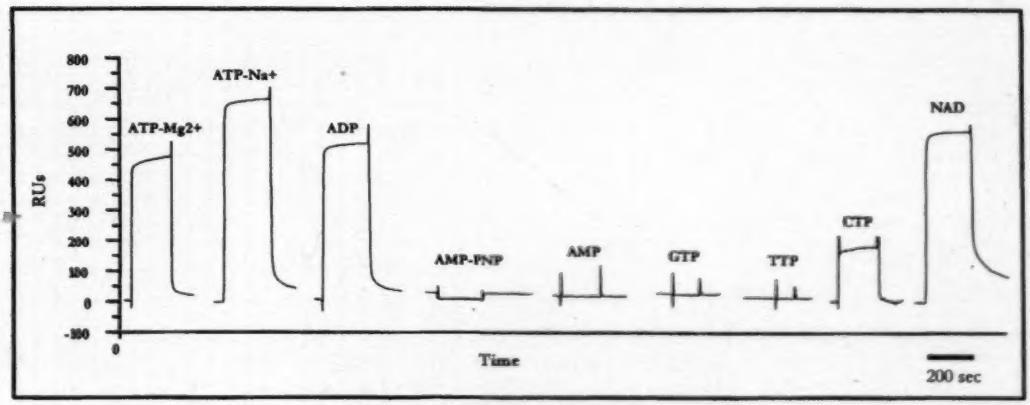

Figure 3- 17

Figure 3- 17 — SPR analysis of the interaction of wild-type calreticulin protein with various nucleotides.

Calreticulin was covalently coupled to the chip followed by the injection of 5 mM ATP or ATP-related molecules, with a real-time sensorgram monitoring results.

Discussion

In this study, we reconstitute the ER of calreticulin-deficient cells with calreticulin mutants and then perform functional analysis, *in vivo*. This was followed by *in vitro* investigation of the structure of various purified, recombinant calreticulin mutants, to assess the effect of specific mutations on the structure and function of the protein.

We initially focus on the N-terminal histidine residues of calreticulin because of their known role in Zn^{2+} binding and most importantly, because Zn^{2+}-dependent conformational changes are critical for calreticulin-substrate interactions (Saito et al., 1999). Remarkably, mutation of just one histidine residue (His153Ala) abolishes calreticulin function as measured by its inability to rescue the *crt*$^{-/-}$ phenotype. Calreticulin-deficient cells have impaired bradykinin-dependent Ca^{2+} release (Nakamura et al., 2001b). In these cells, bradykinin does not bind to the cell surface bradykinin receptor, likely because the receptor is incorrectly folded (Nakamura et al., 2001b). Bradykinin-dependent Ca^{2+} release from the ER is rescued by transfection with wild-type calreticulin (Nakamura et al., 2001b) and mutants His25Ala, His82Ala, or His128Ala. In contrast, bradykinin-induced Ca^{2+} release in *crt*$^{-/-}$ cells is not rescued by transfection with the His153Ala mutant. Studies on the activity of purified recombinant calreticulin and the calreticulin mutants show that wild-type calreticulin and the His25Ala, His82Ala and His128Ala mutants all prevent *in vitro* thermal aggregation of MDH and IgY, whereas the His153Ala mutant does not. We conclude that His153 is essential for the chaperone function of calreticulin.

We also focus on amino acid residues located in the carbohydrate binding pocket of calreticulin, on the disulphide bridge in the N-domain and on several residues at the tip of the extended arm of the P-domain. We report identification of two tryptophan residues that appear to be critical for chaperone function of calreticulin; Trp302 located in the carbohydrate binding pocket and Trp244 found at the tip of the extended arm of the P-domain. Furthermore, we identify four other amino acid residues (Glu239Arg, Asp241Arg, Glu243Arg and Trp244Ala) at the tip of the extended arm of the P-domain of calreticulin that are important in the binding interaction between ERp57 and calreticulin, with Asp241Arg and Trp244Ala abolishing the interaction with ERp57 and Glu239Arg and Glu243Arg significantly reducing the interaction. We further identify Trp302 as directly responsible for the specific interaction of the P-domain with ERp57,

enhancing the interaction of ERp57 with calreticulin. We also find that mutation of the cysteine residues (Cys88Ala and Cys120Ala) that form the disulphide bridge also disrupts calreticulin chaperone function by approximately 60%.

To investigate the molecular mechanism behind the loss of chaperone activity in the mutants, we use intrinsic fluorescence measurements, CD analysis and limited proteolysis. These studies enable us to determine whether the mutations affect the biophysical properties of calreticulin. The reduced intrinsic fluorescence of the His153Ala mutant indicates that some local conformational changes may have occurred in the mutant calreticulin. Importantly, Zn^{2+}-dependent conformational changes, a signature of calreticulin behavior (Khanna et al., 1986), are also compromised in the His153Ala mutant. This agrees with our previous observation that the N-domain histidine residues are involved in Zn^{2+} binding to calreticulin (Baksh et al., 1995b). The ANS fluorescence analysis indicates that the His153Ala mutant has a significantly lower surface hydrophobicity than wild-type calreticulin. Finally, our CD analysis reveals that the His153Ala mutant differs significantly from wild-type calreticulin in β-sheet-β-turn content and the limited proteolysis studies indicates that the His153Ala mutant is more susceptible to trypsin digestion that the wild-type protein. The His153Ala mutation results in local changes in the conformation of calreticulin, with severe effects on its ability to function as a molecular chaperone. We have modeled the 3D structure of calreticulin (Michalak et al., 2002b) based on crystallographic data available for calnexin (Schrag et al., 2001) and NMR data available for the P-domain of calreticulin (Ellgaard et al., 2001a). This model provides an excellent framework for interpretation of our results and for determining the role of the His153Ala-containing region (loop) in protein folding (Figure 3- 18). The crystal structure of calnexin reveals that it consists of a globular β-sandwich domain and an elongated P-domain, forming an extended arm containing the repeat motifs (Schrag et al., 2001). The central, P-domain of calreticulin also forms an elongated arm-like structure (Ellgaard et al., 2001a). The extended arm is curved, creating an opening which likely forms a substrate binding site, as well as the carbohydrate-binding site (Ellgaard et al., 2001a). Our 3D model of the N-terminal globular domain and proline-rich, central P-domain (Figure 3- 18) of calreticulin demonstrates that the N-terminal domain is predicted to form a globular β-sheet

structure (Michalak et al., 2002b). Together with the extended P-domain they form a functional folding unit in calreticulin (Michalak et al., 2002b; Nakamura et al., 2001b).

Importantly, the model of the structure of calreticulin helps to visualize the location of the N-terminal histidine residues investigated in this study (Figure 3- 18). His25, His82, and His128 are all found on the outer surface of the globular N-domain of the protein, away from the extended arm structure of the P-domain (Figure 3- 18). These residues appear to be located away from the substrate binding region in calreticulin and, therefore, their mutation or deletion has no effect on the function of calreticulin as a molecular chaperone. In contrast, His153 (Figure 3- 18) is found on the top of a loop which is part of a short β-strand located at the interface between the globular N-domain and the "extended arm" P-domain (Figure 3- 18). The loop containing His153 is predicted to be flexible with some lateral mobility towards the extend arm of the P-domain. This flexibility may significantly influence the shape of the substrate (carbohydrate) binding pocket (Figure 3- 18).

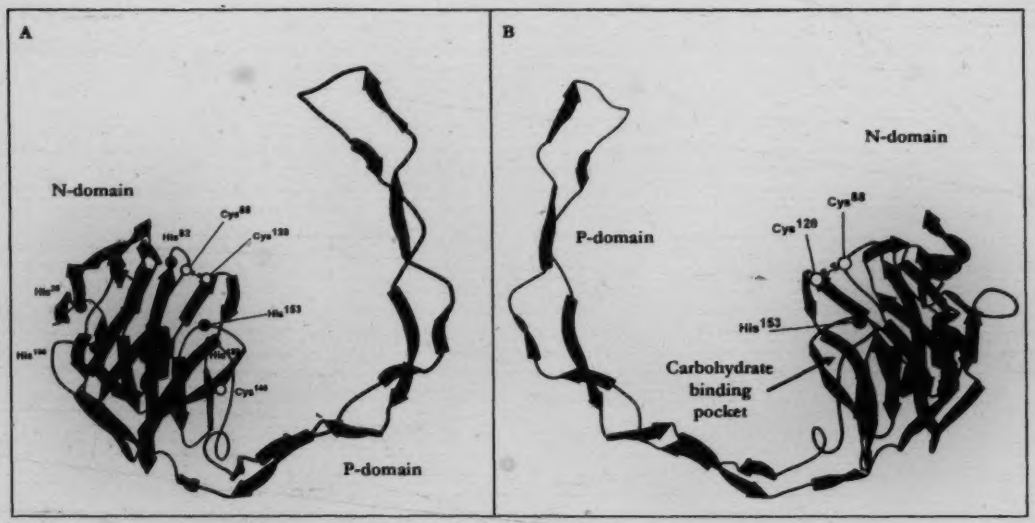

Figure 3- 18

Figure 3- 18 — Putative 3D model of calreticulin.

The N- and P-domain of calreticulin are modeled based on the NMR studies of the P-domain of calreticulin (Ellgaard et al., 2001b) and crystallographic studies of calnexin (1JHN) (Schrag et al., 2001). The alignment was started with residue Glu1 of calreticulin and Ser67 of calnexin. The globular N-domain is shown in green and the extended arm of the P-domain is represented in red. Yellow balls represent the cysteine (Cys88Ala–Cys120Ala), which form a C–C bridge in calreticulin. Red balls indicate location of histidine residues in the N-domain of calreticulin. Location of a putative carbohydrate binding pocket is indicated. *B*, represents a 180° rotation of a model shown in *A*.

Calreticulin and calnexin bind their glycoprotein substrates primarily via monoglucosylated glycans ($Glc_1Man_9GlcNAc_2$). The 3D structure of the luminal domain of calnexin shows a binding site for the terminal glucose moiety of the carbohydrate within the globular N-domain of the protein (Schrag et al., 2001). Molecular modeling of calreticulin, based on calnexin structure, indicates that these proteins may have a similar carbohydrate binding pocket (Michalak et al., 2002b). Structural and modeling analyses indicate that the glucose binding pocket in both proteins contains a centrally located tryptophan residue and several charged amino acid residues (Michalak et al., 2002b; Schrag et al., 2001). Recent, *in vitro* mutational analysis of calreticulin indicates that the residues Tyr109, Met131, Asp135 and Asp317 localized in the putative carbohydrate binding site are involved in binding of $Glc_1Man_9GlcNAc_2$ sugar moiety (Kapoor et al., 2004). Asp135 and Tyr109 are likely the most important contributors towards polar interactions between the sugar and calreticulin (Kapoor et al., 2004). Here we show that the centrally located Trp302 residue in calreticulin is essential for the chaperone function of the protein *in vivo*, likely because of a critical role in carbohydrate binding. Mutation of Trp302Ala may produce important structural changes in the sugar binding site and/or in the N-terminal domain, which lead to the loss of calreticulin chaperone function. This is supported by our observation that the Trp302Ala mutant failed to prevent thermal aggregation of MDH. The Trp302 residue may form a hydrogen bond with the Man_3 of the sugar moiety (Kapoor et al., 2004). Interestingly, although calreticulin forms functional complexes with ERp57 via its P-domain (Ellgaard et al., 2002; Frickel et al., 2002; Leach et al., 2002), the Trp302Ala calreticulin mutant exhibited greatly increased binding of ERp57. This indicates that a single amino acid mutation in the globular N-domain of calreticulin affects the structure and function of the distant P-domain.

Calreticulin and calnexin are lectin-like chaperones with a similar specificity for monoglucosylated carbohydrates. However, there are a number of protein substrates which are unique to either calreticulin or calnexin (Michalak et al., 1999) and it is not obvious what determines this substrate specificity. It is possible that the histidine residues in the N-domains of the two proteins play a role, since there are 9 histidine residues in the N-terminal globular domain of calnexin (Schrag et al., 2001; Wada et al., 1991) and only 2 of these are conserved in calreticulin. The conserved residues are His128, which had no effect on calreticulin function in this study and His153 (His237 in

calnexin). Although the His153 is conserved in calnexin, the amino acid sequences that flank this critical residue differ in the two proteins. For example, upstream of His273 in calnexin there are ten amino acid residues which form a short α-helix not found in calreticulin (Schrag et al., 2001). The loop containing His273/His153Ala is therefore significantly longer in calnexin than in calreticulin and may have different mobility. It is thus conceivable that the "loop" which contains the His153 residue may contribute to determination of substrate specificity of calreticulin.

The P-domain of calreticulin forms an unusual extended arm-like structure where the C- and N-terminus of the P-domain are in close proximity (Ellgaard et al., 2001b). The structure is stabilized by three short antiparallel β-sheets. Three small hydrophobic clusters containing two tryptophan rings, including Trp244, provide additional stability (Ellgaard et al., 2001a). In this study, mutation of Trp244Ala resulted in one of the most severe effects on calreticulin function. The Trp244Ala mutant of calreticulin was unable to restore bradykinin-dependent Ca^{2+} release in calreticulin-deficient cells, it did not prevent thermally-induced aggregation of MDH and it did not bind ERp57. Biophysical studies of this mutant of calreticulin suggested that conformational changes might be responsible for the loss of chaperone activity and lost ability to form a complex with ERp57. Figure 3- 19 shows that Trp244 plays a critical role in determining the structure of the tip of the extended arm in the P-domain of calreticulin (Ellgaard et al., 2001b). The indole rings of residues Trp244 and Trp236 provide essential stability for the P-domain and the region involved in binding of ERp57 (Figure 3- 19A). The mutant Trp244Ala has a disturbed structure in this region, likely creating an unstable cavity (Figure 3- 19B and D). This, in turn, must have a significant effect on ability of the substrate (carbohydrate) to bind to the globular N-domain of calreticulin.

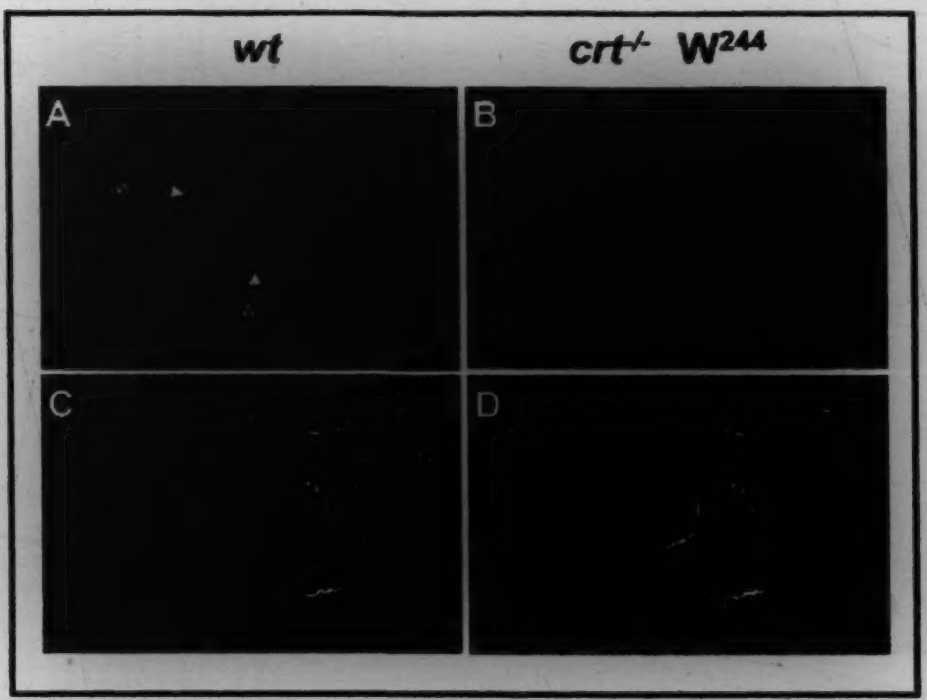

Figure 3- 19

Figure 3- 19 — Three-dimensional structure of the tip of the P-domain of calreticulin.

The structure of the tip of the P-domain of calreticulin is based on NMR studies (Ellgaard et al., 2001b). *A* and *C*, wild-type calreticulin; *B* and *D*, Trp244Ala calreticulin mutant. The location of the pair of interactive tryptophan residues Trp244 *(yellow)* and Trp236 *(green)* is indicated. *C* and *D*, a stereo view of the electron density around the Trp244Ala, indicating a cavity *(D)* in the P-domain with the mutated Trp244Ala.

NMR and biochemical analyses of the P-domain of calreticulin indicate that the tip of the extended arm binds ERp57 (Ellgaard et al., 2002; Frickel et al., 2002; Leach et al., 2002). NMR studies revealed that ERp57 may bind to a region of calreticulin encompassing residues 225-251 (Frickel et al., 2002). We investigated several amino acid residues at the tip of the P-domain to determine their role in ERp57-calreticulin interactions (for the location of specific residues see Figure 3- 20). Mutation of Glu238Arg did not effect ERp57 binding to calreticulin, whereas the mutants Asp241Arg and Trp244Ala did not bind any measurable ERp57 and the mutants Glu239Arg and Glu243Arg demonstrated significantly reduced binding of ERp57. We conclude that the negatively charged residues Glu239, Asp241 and Glu243 and the residue Trp244, are essential for formation of the ERp57-calreticulin complex (Figure 3-20). The residues Glu239, Asp241 and Glu243 are located on the concave side of the tip of the P-domain and they likely provide electrostatic forces critical in formation of the complex with ERp57. It is unlikely that Trp244 is directly involved in ERp57-calreticulin interactions, but rather it seems to play a role in maintaining the structural stability of the tip of the P-domain. It was surprising to find that even though the mutants Glu239Arg, Asp241Arg and Glu243Arg did not bind ERp57 efficiently, they were able to partially restore bradykinin-dependent Ca^{2+} release in $crt^{-/-}$ cells, suggesting that ERp57 binding to calreticulin may not be critical for its chaperone function, specifically related to the bradykinin receptor. Glutathione S-transferase (GST) pull down analysis with the P-domain of calnexin indicates that ERp57, as well as binding to calreticulin, also binds to the P-domain of calnexin (Leach et al., 2002). Interestingly, NMR analysis showed that certain single amino acid mutations on the tip of the P-domain of calnexin had no significant effect on ERp57 binding; however double mutants abolished this interaction (Pollock et al., 2004). In calnexin, the residues Asp342, Asp344, Asp346, Asp348, Glu350 and Glu352 are all involved, with the residues Asp344 and Glu352 being the most important (Pollock et al., 2004). This is in agreement with our data which implicate Glu243 (in calnexin Glu351) and Glu239 (in calnexin Asp343) as critical residues for ERp57 binding to calreticulin. Results indicate that clusters of negatively charges residues at the tip of the P-domain, in both calreticulin and calnexin, must play an important role in promoting and stabilizing association with ERp57.

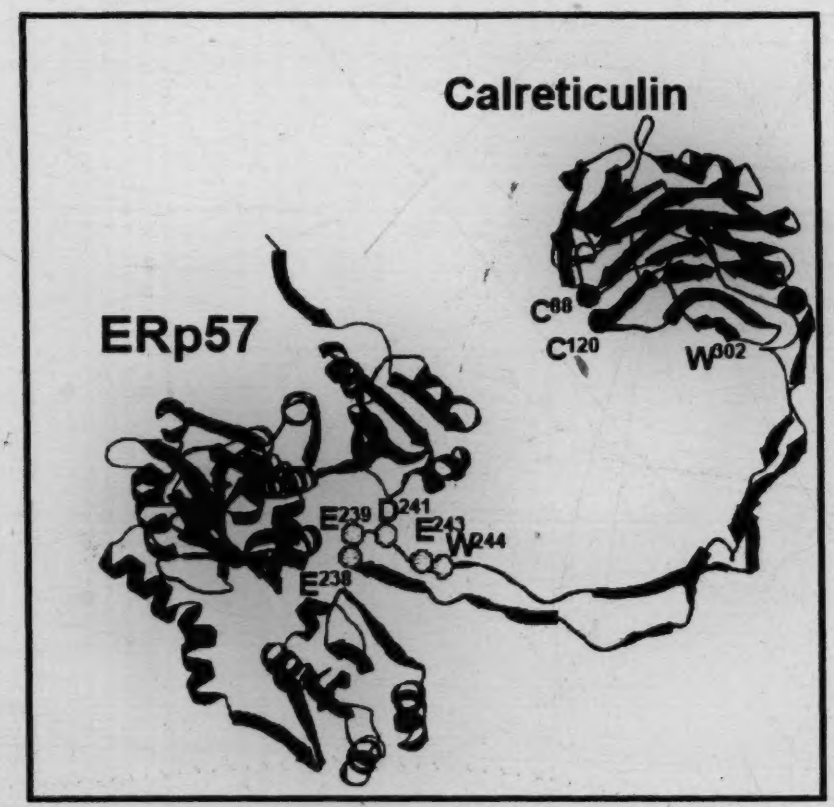

Figure 3- 20

Figure 3- 20 — Model of interaction of ERp57 and calreticulin and the location of the mutated amino acid residues.

ERp57 contains three domains connected by two loops that may be bent to form a pocket. An arginine-rich pocket of the ERp57 structure formed by the domains may slide over the tip of the P-domain (in *red*) of calreticulin to form structural and functional complexes. The location of Glu238 (E238), Glu239 (E239), Asp241 (D241), Glu243 (E243) and Trp244 (W244) at the tip of the P-domain, Trp302 (W302) in the carbohydrate binding pocket and Cys88 (C88) and Cys120 (C120) at the surface of the N-domain to form the disulfide bond are indicated by yellow, orange and green balls, respectively. The N and P-domain of calreticulin are modeled based on the NMR studies of the P-domain of calreticulin (Ellgaard et al., 2001b) and crystallographic studies of calnexin (Schrag et al., 2001).

As many of the processes occurring in the lumen of the ER are energy expensive, the concentration of ATP is of paramount importance. Several functions within the ER demand the presence of ATP, including phosphorylation (Chen et al., 1996; Csermely et al., 1995) and protein degradation (Hirschberg et al., 1998). In addition, ATP is required by a number of molecular chaperones for correct folding of substrates as well as an important structural molecule within the tertiary conformation of a number of these chaperones (Corbett et al., 2000; Dorner and Kaufman, 1994; Fink, 1999; Grenert et al., 1999). Several chaperones, including BiP/GRP78 and PDI utilize hydrolysis of ATP to release the folded protein (Guthapfel et al., 1996; Wei et al., 1995), while GRP94 does not need ATP for the interaction with substrate, but ATP hydrolysis is necessary for the folding process (Grenert et al., 1999). Two other chaperones, calnexin and calreticulin presumably utilize ATP to regulate conformational changes (Dierks et al., 1996; Saito et al., 1999). Calreticulin was first identified to utilize ATP when it was bound selectively to a denatured protein column and specifically eluted with ATP (Nigam et al., 1994). The N-domain of calreticulin was identified to have only had weak ATPase activity, but that addition of 1-3 mM ATP enhanced the chaperone function of calreticulin (Saito et al., 1999). ATP rendered calreticulin more resistant to protease digestion and enhances the aggregation suppression activity of calreticulin and calnexin *in vitro* (Corbett et al., 2000; Ihara et al., 1999; Ou et al., 1995; Saito et al., 1999). ER luminal conditions appear to be critical for proper protein folding and quality control, with any disruption in these conditions leading to ER stress and potentially apoptosis.

The ER lumen contains ATP which is required to support correct folding, as well as formation of disulfide bonds (Braakman et al., 1992; Dorner and Kaufman, 1994; Dorner et al., 1990). As well, an ATP transporter has also been identified in the ER (Beminsone and Hirschberg, 1998; Clairmont et al., 1992). As suggested previously (Nigam et al., 1994; Saito et al., 1999), both ATP and Zn^{2+} bind to calreticulin and modify the conformation of the protein and therefore the function. While there is no obvious ATP binding region, Corbett et al. (Corbett et al., 2000) observes that addition of ATP during trypsin digestion results in protection of the C-terminus of calreticulin, implying involvement of the C-terminus in ATP binding (Corbett et al., 2000). They also determine that calreticulin binds ATP using an ATP-agarose affinity column but does not hydrolyze ATP (Corbett et al., 2000). In this study, we attempted to further clarify

the binding site of ATP. Using SPR analysis, we observed a robust interaction of ATP-Mg^{2+} with calreticulin. To elucidate this interaction, we monitored the binding of ATP-Mg^{2+} with the calreticulin mutants covalently immobilized to the chip. The site specific mutations did not appear to affect the interaction of ATP with calreticulin to any great degree. To further understand the interaction between ATP and calreticulin, we used various nucleotides similar to ATP, to observe any effect on the binding. Both ATP-Na^{+}, ADP and NAD bound in a similar manner to ATP-Mg^{2+}, but interestingly, AMP, AMP-PNP (non-hydrolysable isoform), TTP and GTP did not interact with calreticulin, while CTP had about half the interaction as ATP-Mg^{2+}. It appears that the only similarity between CTP and ATP is with the nucleotides having two hydrogen molecules located in the same place, available for hydrogen-bonding. It seems that there is also a requirement for at least two phosphate groups present in the nucleotide for binding to calreticulin to take place. Elucidation of the specific site for nucleotide binding will take further study.

In conclusion, a number of cell biological, molecular and biophysical studies are used to identify functionally important regions and amino acid residues in calreticulin. It appears that specific factors found in the ER, including Ca^{2+}, Zn^{2+} and ATP perform an important task as stabilizers of the tertiary structure of calreticulin and therefore directly regulate the function of the protein. Specific amino acids potentially involved in the coordination of these factors, located directly in (Trp302) or near (His153) the carbohydrate pocket are critical for the chaperone function of the protein. Further, modification of a residue(s) in the carbohydrate binding region may have a profound effect on the structural and functional properties (mobility and stability) of the P-domain, as documented by increased ERp57 binding by the calreticulin mutant Trp302Ala. Conversely, specific amino acid residues located in the P-domain (Trp244) may influence the function of the lectin-like N-domain of calreticulin. The data presented here provides ample evidence that modification of these single site amino acids in calreticulin drastically affect the secondary and tertiary structure of this protein, resulting in loss of function. Finally, our data here indicates that the interaction between ERp57 and calreticulin and presumably with calnexin may not be a prerequisite for folding of all substrates. In summary, our work indicates that a single amino acid mutation in calreticulin, an ER luminal chaperone, significantly affects protein folding.

Chapter Four — Mutational Analysis of Calnexin

Introduction

Calnexin is a 90-kDa, lectin-like ER membrane protein (Bergeron et al., 1994) that binds Ca^{2+} with high affinity (Ellgaard and Helenius, 2003; Michalak et al., 2002b; Tjoelker et al., 1994), ATP (Ou et al., 1995), monoglucosylated carbohydrates (Bergeron et al., 1994; Ware et al., 1995) and non-glycosylated proteins (Ellgaard and Frickel, 2003; Johnson et al., 2001), in conjunction with calreticulin and ERp57. Calnexin contains three functional and structural domains. The N-domain contains a Ca^{2+} binding site, the majority of the glycoprotein binding site as well as a Zn^{2+}-dependent ERp57 binding site (Leach et al., 2002; Tjoelker et al., 1994). The P-domain of calnexin is rich in proline residues, contains a Ca^{2+} binding site (Tjoelker et al., 1994) and in conjunction with the N-domain, is important for chaperone activity (Leach et al., 2002). The C-domain contains a transmembrane alpha helix and a negatively charged cytoplasmic tail that binds Ca^{2+} with moderate affinity (Tjoelker et al., 1994). X-ray crystallography has identified the N-terminus as a globular Ca^{2+} binding domain, in addition, once the crystal was soaked with glucose, exhibited an interaction with this glucose moiety (Schrag et al., 2001). Structural and modeling analyses indicate that the glucose binding pocket in calnexin contains a centrally located tryptophan residue and several charged amino acid residues (Michalak et al., 2002b; Schrag et al., 2001). Using NMR, the primary ERp57 binding site on calnexin was narrowed down to a small peptide derived from the tip of the P-domain (Pollock et al., 2004), as well, a secondary Zn^{2+}-dependent ERp57 binding site was identified in the N-domain using pulldown studies (Leach et al., 2002).

In this part of my study, we carried out structural and functional characterization of purified soluble calnexin (S-Cnx, containing the N- and P-domains of the protein). To identify structural regions important in calnexin function, we generated several calnexin mutants and examined their role in calnexin function. Two mutations are conserved, tryptophan 428 in calnexin, similar to essential tryptophan 302 in calreticulin, potentially involved in the interaction with substrate (Michalak et al., 2002b; Schrag et al., 2001) and glutamate 351 in calnexin, similar to glutamate 243 in calreticulin, which was identified to have a significant influence on the interaction with ERp57 (Martin et al., 2006). These two amino acid residues in calnexin were specifically targeted for mutation; tryptophan 428, located in the globular N-domain substrate binding pocket and glutamate 351,

found at the tip of the P-domain, followed by structural and functional analysis. Both mutations modified protein structure and function to different degrees.

Results

Cascade Blue Analysis of S-Cnx

Previous experiments indicated that Zn^{2+}, ATP and Ca^{2+} all bind or affect the structure or function of S-Cnx (Leach et al., 2002; Ou et al., 1995). We demonstrated this using CB covalent linkage to S-Cnx (Figure 4- 1). S-Cnx is composed of the majority of the protein, excluding the transmembrane domain and the cytoplasmic C-terminus. Cascade Blue acetyl azide reacts with aliphatic amines in proteins to yield stable carboxamides, is highly fluorescent and resists quenching upon protein conjugation (Corbett et al., 1999). The dye is sensitive to the exposure of the hydrophilic or hydrophobic environments in a protein. This measurement can be used to monitor conformational changes in proteins resulting in exposure of the conjugated CB to protein microenvironments of a different polarity (Corbett et al., 1999). Interestingly, CB-S-Cnx had a significant decrease in fluorescence upon addition of 500 μM Zn^{2+}, but a slight increase with the addition of 1 mM ATP. Addition of 2 mM Ca^{2+} resulted in an increase of fluorescence. This indicated to us that Zn^{2+} appears to have the largest effect on the overall hydrophobicity of S-Cnx, as suggested by the decrease in CB fluorescence. Of note, the addition of 400 μM EGTA at the start of the experiment resulted in CB-S-Cnx not responding to the addition of Zn^{2+}, Ca^{2+} or ATP, implying that chelation of Ca^{2+} from CB-S-Cnx resulted in a conformation that did not respond to the addition of Zn^{2+}, Ca^{2+} or ATP. Addition of EGTA at the end of the experiment resulted in recovery of lost fluorescence of CB-S-Cnx, resulting from the addition of Zn^{2+}. CB fluorescence analysis indicates that S-Cnx interacts with Zn^{2+}, Ca^{2+} and ATP.

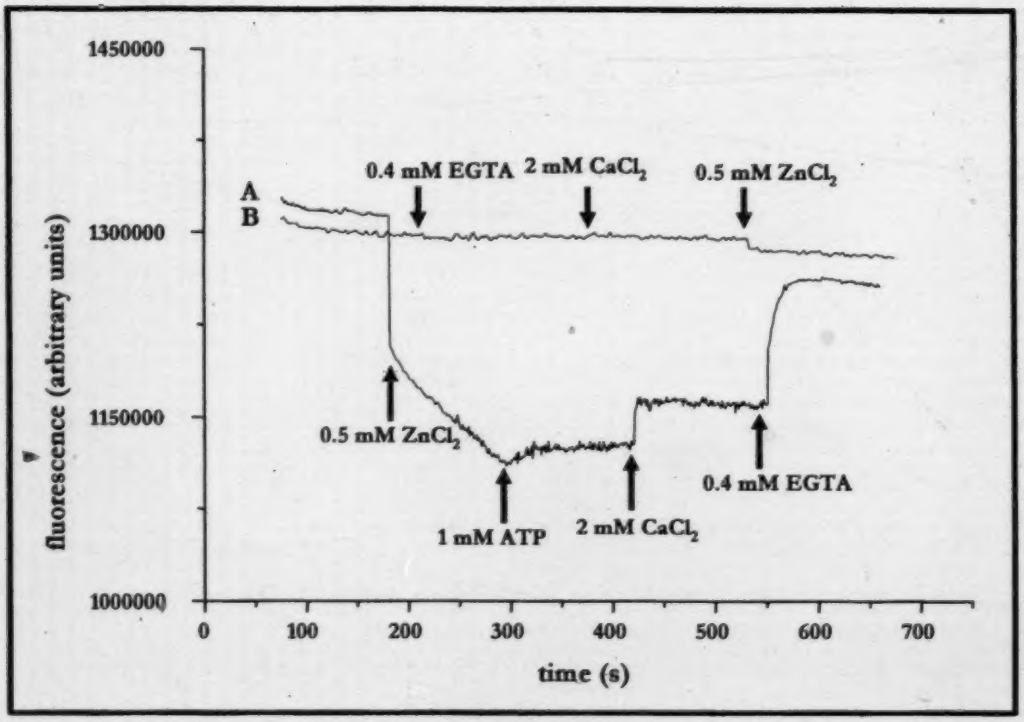

Figure 4- 1

Figure 4- 1 Cascade blue analysis of structural changes in purified calnexin protein.

A. Effects of 500 μM $ZnCl_2$, 1 mM ATP, 2 mM $CaCl_2$ and 400 μM EGTA on the fluorescence intensity of CB-S-Cnx, as well *(B)* the addition of 400 μM EGTA before addition of $CaCl_2$ or $ZnCl_2$, abolishing any decrease in fluorescence. Results are representative of three or more independent experiments. Arrowheads depict the time of addition.

CD Analysis of Purified S-Cnx

CD analysis of purified S-Cnx protein in the absence or presence of Ca^{2+}, Zn^{2+} and ATP revealed that the protein contains minor amounts of α-helix (located in the globular domain) and a more significant proportion of β-sheet (mainly contained in the N- and P-domains) (Schrag et al., 2001). As this technique was used successfully for our experiments with calreticulin, we attempted to identify any modification in secondary structure. We determined that there were slight changes in α-helix and β-sheet secondary structures with the addition of Ca^{2+}, Zn^{2+} and ATP (Table 4- 1). Addition of Ca^{2+} resulted in a minor loss in the percentage of β-turn and an increase in the random coil structure of S-Cnx, but little change in α-helix, indicating there may be potential Ca^{2+}-dependent changes in the globular domain. The addition of Zn^{2+} resulted in a larger decrease in α-helix and β-sheet secondary structure, also suggesting that there are Zn^{2+}-dependent changes in the globular and P-domains. In contrast, the addition of ATP resulted in an increase in α-helix and β-sheet structure and less random coil, indicating that ATP is interacting with S-Cnx, resulting in more secondary structure. It appears that Ca^{2+}, Zn^{2+} and ATP interact with S-Cnx but without generating severe modifications in secondary structure. CD analysis was then performed on the soluble mutant proteins generated from an *E. coli* expression system and revealed that the mutations resulted in no significant changes in the secondary structure of calnexin (Figure 4- 2).

Table 4- 1 — CD analysis of S-Cnx.

	α helix	β sheet	β turn	Random	Scale
S-Cnx	0.20 (.008)	0.22 (.009)	0.19 (.010)	0.39 (.013)	1.001
+ 2 mM Ca^{2+}	0.19 (.010)	0.22 (.011)	0.15 (.013)	0.43 (.018)	1.000
+ 1 mM Zn^{2+}	0.16 (.010)	0.19 (.010)	0.21 (.013)	0.43 (.015)	1.000
+ 1 mM ATP	0.22 (.007)	0.25 (.009)	0.17 (.010)	0.36 (.013)	1.001

Table 4- 1 — CD analysis of purified S-Cnx protein.

Measurements were carried out in the presence of a buffer containing 25 mM Pipes, pH 6.8, 100 mM NaCl, 1 mM dithiothreitol, 1 mM EGTA. The Zn^{2+} and Ca^{2+} concentrations given are the free amount in the solution. Results are an average of eight runs. SE indicated in brackets.

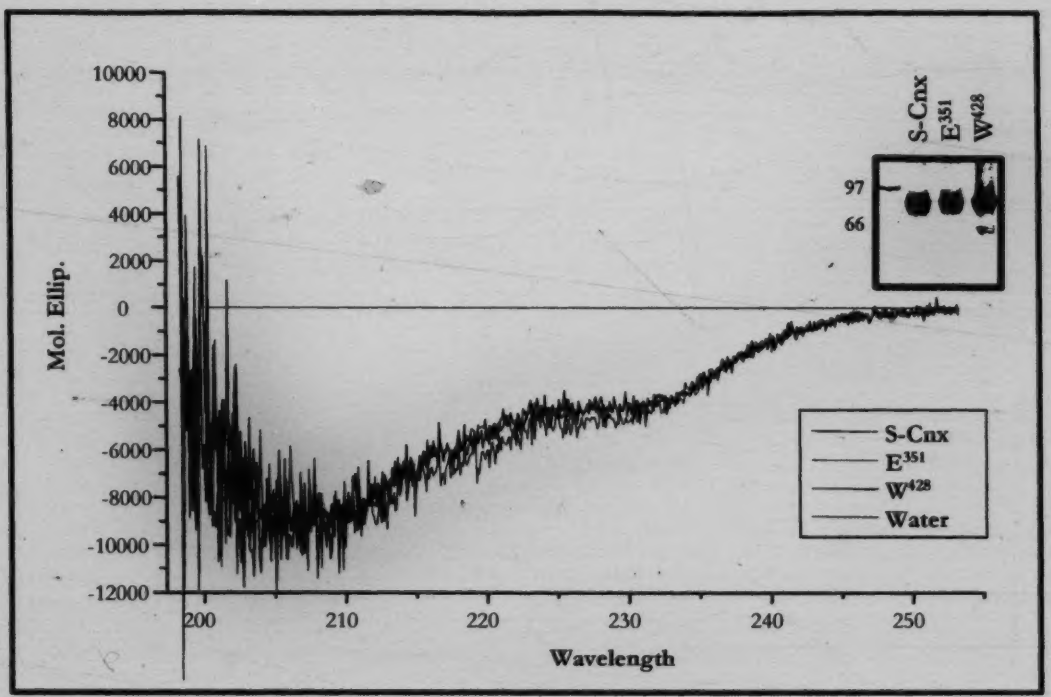

Figure 4- 2

Figure 4- 2 — CD analysis of purified wild-type and mutant S-Cnx protein.

Insert, SDS-PAGE (10% acrylamide) of purified S-Cnx and S-Cnx mutants Glu351Arg, E^{351} and Trp428Ala, W^{428}. 300 µg/ml protein diluted in water. Results are an average of eight runs.

Limited Trypsin Digestion of S-Cnx and Mutants

Previous experiments with calreticulin mutants identified specific amino acid residues that were responsible for modifying the trypsin accessible portions of the protein (Corbett et al., 2000). We used a similar technique to determine the effect of site specific mutations on S-Cnx and the accessibility of trypsin to the protein. S-Cnx and S-Cnx mutant proteins containing the Glu351Arg and Trp428Ala mutations were incubated with trypsin followed by SDS-PAGE (10% acrylamide) analysis (Figure 4- 3). Wild-type S-Cnx was partially resistant to trypsin as observed by a portion of the full length protein being present at the twenty minute time point. This protection was further enhanced in the presence of Ca^{2+} but the protection was completely lost with Zn^{2+} or ATP, implying that both Zn^{2+} and ATP binding result in wild-type S-Cnx becoming more accessible to trypsin digestion, while Ca^{2+} binding results in the protein having less accessibility. One of the two site specific mutations, the Trp428Ala mutation, resulted in the loss of protection of the protein from trypsin in the absence of Ca^{2+}, Zn^{2+} or ATP, but only in the presence of Ca^{2+} was this protection recovered. This implied that the tryptophan mutation results in conformational changes that expose more trypsin accessible sites but that addition of Ca^{2+} once again resulted in the protein being protected (Figure 4- 3). Potentially, Ca^{2+} binding to the protein can overcome the loss in structure that results from the mutation of the tryptophan. The other mutation, Glu351Arg, did not result in any significant changes in trypsin accessibility as compared to wild-type. It appears that Ca^{2+}, Zn^{2+} and ATP all interact with S-Cnx and modify the trypsin susceptibility of the protein.

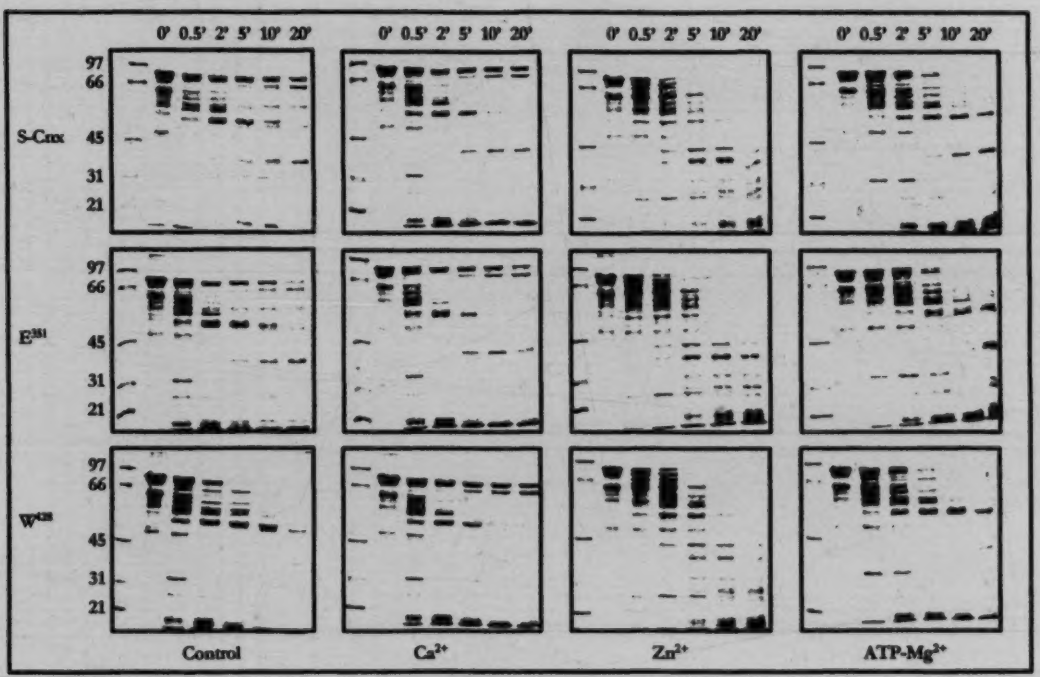

Figure 4- 3

Figure 4- 3 — Trypsin digestion of purified wild-type and mutant calnexin protein.

Purified S-Cnx and mutant proteins Glu351Arg (E^{351}) and Trp428Ala (W^{428}) were incubated with trypsin (1:100; trypsin/protein; w/w) at 37°C in the presence of 2 mM Ca^{2+}, 1 mM Zn^{2+} or 1 mM ATP-Mg^{2+}, with samples taken at 0.5, 1, 2, 5, 10 and 20 minute time points. Digestion was stopped at time points indicated and the proteins were separated by SDS-PAGE (10% acrylamide), followed by staining with Coomassie Blue. The positions of Bio-Rad molecular weight marker proteins are indicated.

Intrinsic Fluorescence of S-Cnx and Mutants

Fluorescence emission spectra were measured for wild-type S-Cnx and for mutants at varying concentrations of Ca^{2+}, Zn^{2+} and ATP. Figure 4- 4 demonstrated that S-Cnx had an emission maximum at 334 nm and established that increasing amounts of Ca^{2+} and ATP resulted in a decrease in intrinsic fluorescence at a wavelength of 334 nm, signifying an interaction between the purified protein and these molecules, indicative of ATP and Ca^{2+}-dependent conformational changes in the protein. Addition of Zn^{2+} did not affect the fluorescence emission spectra for the S-Cnx mutant Glu351Arg, but there was a considerable change in overall fluorescence with the Trp428Ala mutant. This was interesting as S-Cnx is identified to have a Zn^{2+}-dependent ERp57 binding site in the N-domain (Leach et al., 2002). Fluorescence emission spectra for the calnexin mutants, Glu351Arg and Trp428Ala had similar slopes to the wild-type protein, indicating that mutation of these residues in S-Cnx did not significantly affect the conformation of the protein.

The Ability of S-Cnx to Prevent Aggregation

To test for chaperone function of S-Cnx or S-Cnx mutants *in vitro*, the proteins were incubated with either IgY or MDH and light scattering was measured. Wild-type S-Cnx (0.25 μM) efficiently prevented the aggregation of both IgY (0.25 μM) and MDH (1 μM) (Figure 4- 5). As expected, both the Glu351Arg and Trp428Ala mutants (0.25 μM) were unable to prevent the aggregation of IgY to the same extent as wild-type S-Cnx, but both still retained partial chaperone activity. In contrast, both the mutants enhanced the aggregation of MDH. As MDH is not glycosylated and as calnexin has been linked to chaperoning glycosylated proteins, this result may identify calnexin as specifically chaperoning glycosylated substrates versus non-glycosylated substrates. Aggregation assays indicate that S-Cnx has an intrinsic ability to prevent aggregation of glycosylated substrates that is partially lost upon the mutation of Glu351 and Trp428.

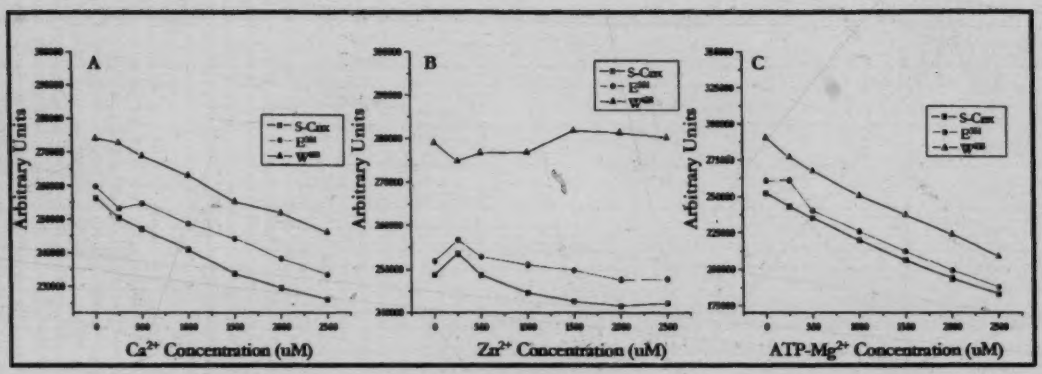

Figure 4- 4

Figure 4- 4 — Intrinsic fluorescence of purified soluble wild-type and mutant calnexin protein.

Intrinsic tryptophan fluorescence emission analysis of wild-type S-Cnx, Glu351Arg (E^{351}) and Trp428Ala (W^{428}) mutants was carried out in the absence and presence of increasing concentrations of Zn^{2+}, Ca^{2+} and ATP. Ca^{2+}-dependent changes in intrinsic fluorescence of wild-type, Glu351Arg and Trp428Ala mutants of S-Cnx are shown in *A*. Zn^{2+}-dependent changes in intrinsic fluorescence of wild-type, Glu351Arg and Trp428Ala mutants of S-Cnx are shown in *B*. ATP-dependent changes in intrinsic fluorescence of wild-type, Glu351Arg and Trp428Ala mutants of S-Cnx are shown in *C*. The excitation wavelength was set at 286 nm and the emission wavelength was set to scan from 295–450 nm with a maximum emission wavelength of 334 as demonstrated.

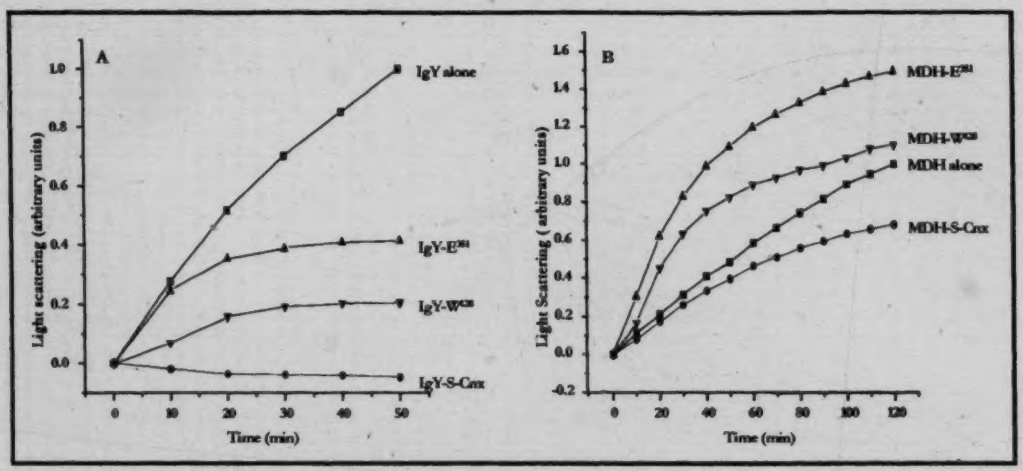

Figure 4- 5

Figure 4- 5 — Aggregation assay using purified soluble wild-type and mutant calnexin protein.

A, Effect of S-Cnx and mutants Glu351Arg (E^{351}) and Trp428Ala (W^{428}) (0.25 μM) on the thermal aggregation of IgY (1 μM) was monitored at 44°C by measuring light scattering at 360 nm. *B*, MDH (0.25 μM) was incubated in the presence or absence of wild-type S-Cnx or calnexin Glu351Arg and Trp428Ala mutants (0.25 μM) as indicated. Proteins were pre-incubated at room temperature followed by monitoring aggregation at 44°C at 360 nm. Data are mean ±S.E.; n=4.

Protein Interaction of S-Cnx and Mutants with ERp57

ERp57 binding to S-Cnx and S-Cnx mutants was monitored by SPR. Purified S-Cnx or Glu351Arg and Trp428Ala mutant proteins were covalently linked to the chip and termed the ligand, with ERp57 as the analyte in solution flowed over the linked protein. An increase in mass was observed with wild-type protein and ERp57, indicating an interaction between the two (Figure 4- 6). This interaction was amplified slightly upon mutation of Glu351Arg but significantly increased (2.5 fold) with the mutation of Trp428. This indicates that the Glu351Arg mutation does not significantly affect the interaction of S-Cnx with ERp57 as expected. In contrast, the corresponding conserved residue in calreticulin (Glu243Arg), modifies the interaction with ERp57 (Martin et al., 2006). This suggests that calreticulin and calnexin may interact with ERp57 in different manners. Similar to calreticulin (Martin et al., 2006), the Trp428Ala mutation enhanced the interaction of ERp57 with calnexin. This indicated that mutation of this tryptophan which is contained in the globular domain could affect interaction of the P-domain with ERp57, potentially because of a shifting in the tertiary structure of the globular domain. On the other hand, this mutation may also result in conformational changes which expose another ERp57 binding site, such as the Zn^{2+}-dependent site located in the globular domain (Leach et al., 2002), or strengthen the primary site found in the P-domain (Figure 4- 7). Universal changes in the globular N-domain may affect the interaction of the P-domain of S-Cnx with ERp57 or enhance the binding of the globular domain to ERp57.

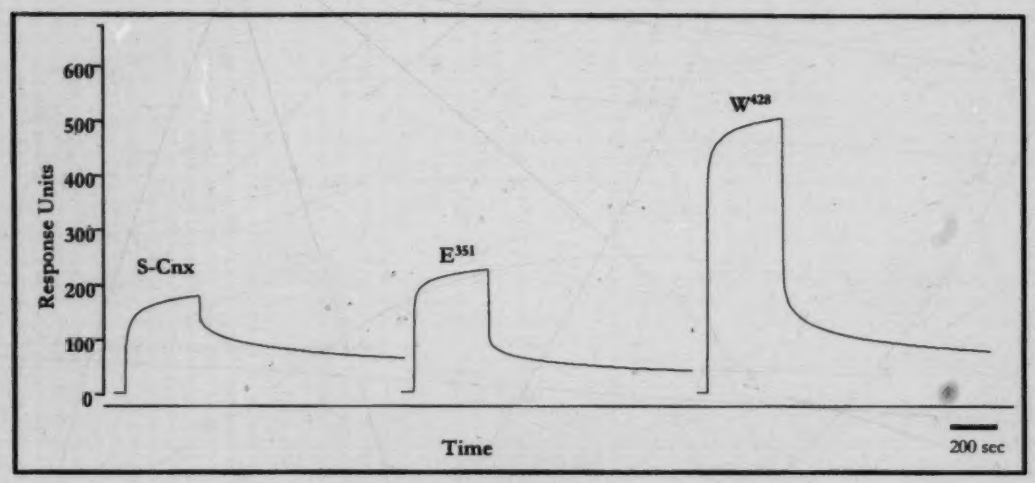

Figure 4- 6

Figure 4- 6 — SPR analysis of the interaction between S-Cnx and ERp57.

Recombinant ERp57 was injected over immobilized S-Cnx or calnexin mutants Glu351Arg and Trp428Ala (E^{351} and W^{428}), with coupling recorded with a real time sensorgram.

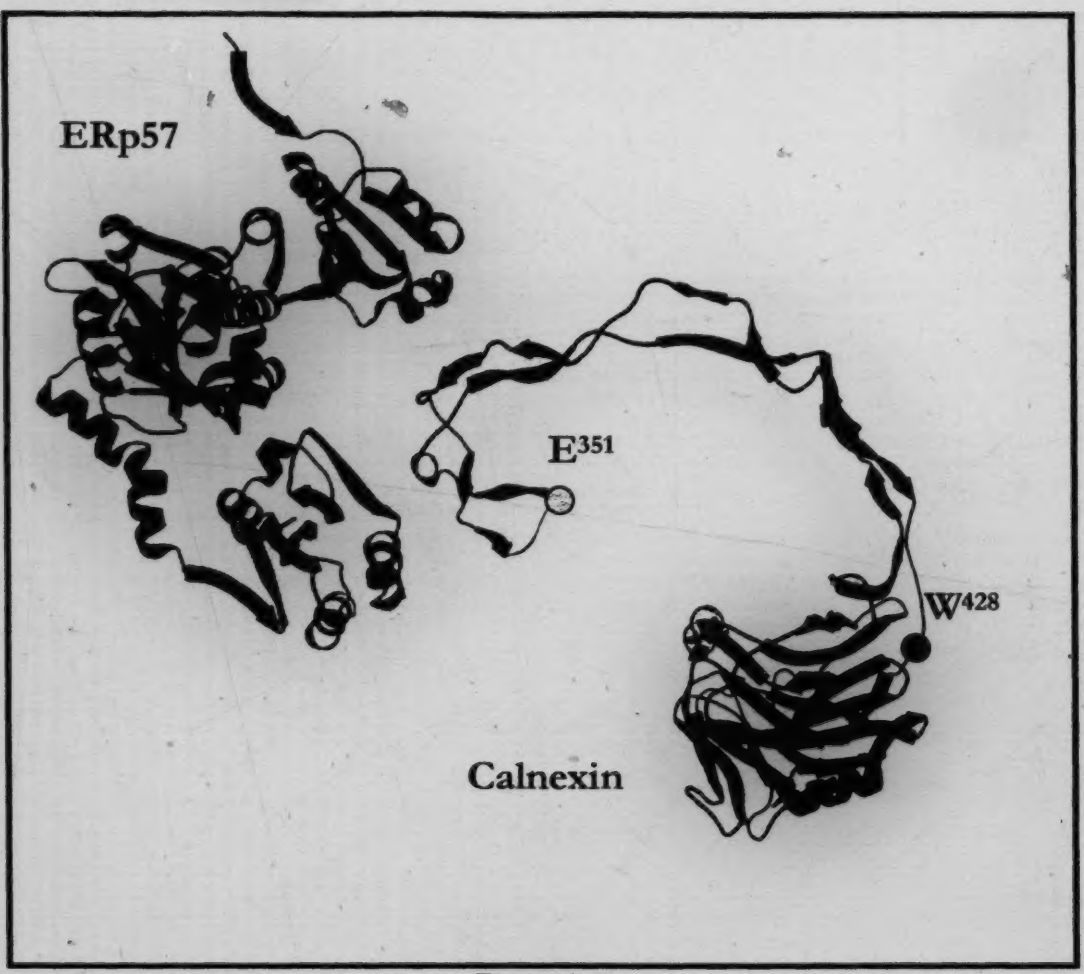

Figure 4- 7

Figure 4- 7 — Model of calnexin and ERp57.

Crystal structure of calnexin (1JHN) modeled with ERp57, demonstrating where the two proteins may interact. The two calnexin mutations are depicted in blue for Glu351Arg (E^{351}) and green for Trp428Ala (W^{428}).

Interaction of Calnexin and Mutants with ATP

ATP binding to calnexin has been previously reported (Ou et al., 1995) but the nucleotide binding site has not been identified. In this study we have set out to characterize the ATP binding site in calnexin using SPR analysis. As expected, calnexin bound ATP-Mg^{2+} (Figure 4- 8). Interestingly, ATP-Na^{+}, ADP, CTP and NAD also bound in a similar manner, but AMP, GTP, TTP or AMP-PNP (non-hydrolysable isoform) did not bind. When EDTA/EGTA were present, there was a significant decrease in binding (results not shown), implying that a specific conformation of the protein supplied by divalent cations may be necessary to promote ATP binding to the proteins. We conclude that ATP binding to calnexin appears to be conformation dependent. SPR technique was utilized to identify if mutation of Glu351Arg and Trp428Ala affect the capacity of calnexin to bind ATP-Mg^{2+}. Calnexin was previously identified to bind ATP without hydrolysis (Ou et al., 1995), leading to a significant conformational change. Our results demonstrated that wild-type S-Cnx showed a significant interaction with ATP-Mg^{2+} which was enhanced upon the mutation of Glu351Arg and further enhanced with the mutation of Trp428Ala (Figure 4- 8). If this was a charge-based interaction, one would see a loss in mass rather than an increase, leading us to speculate that these two mutations have global effects on the structure of the whole protein, leading to enhancement of binding with ATP-Mg^{2+}, either by new sites being exposed, or by a tighter interaction of the primary site with ATP-Mg^{2+}.

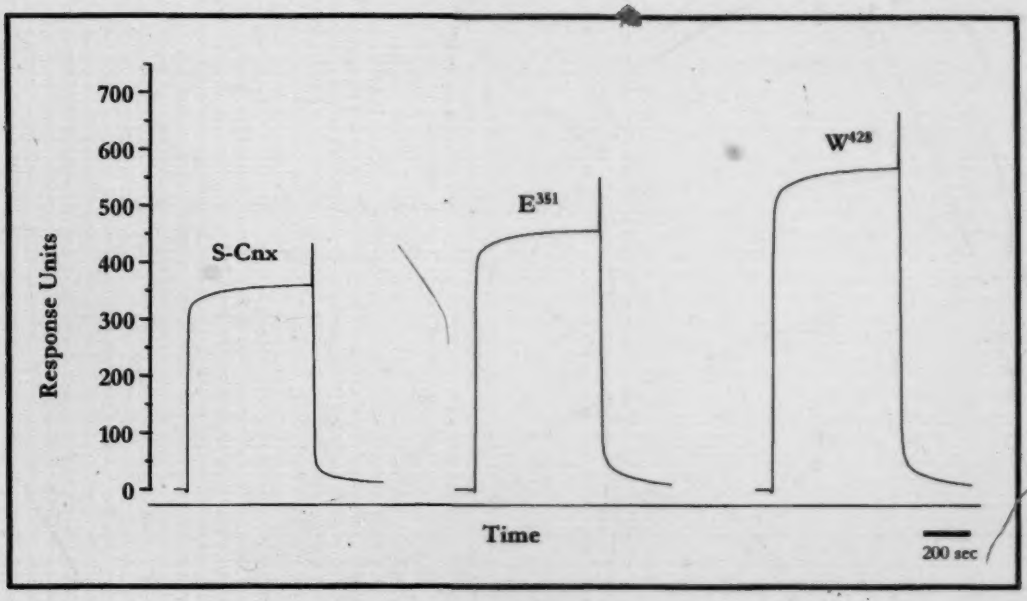

Figure 4- 8

Figure 4- 8 — SPR Analysis of the interaction of calnexin with ATP-Mg^{2+}.

Five mM ATP-Mg^{2+} was injected over immobilized S-Cnx or calnexin mutants Glu351Arg and Trp428Ala (E^{351} and W^{428}).

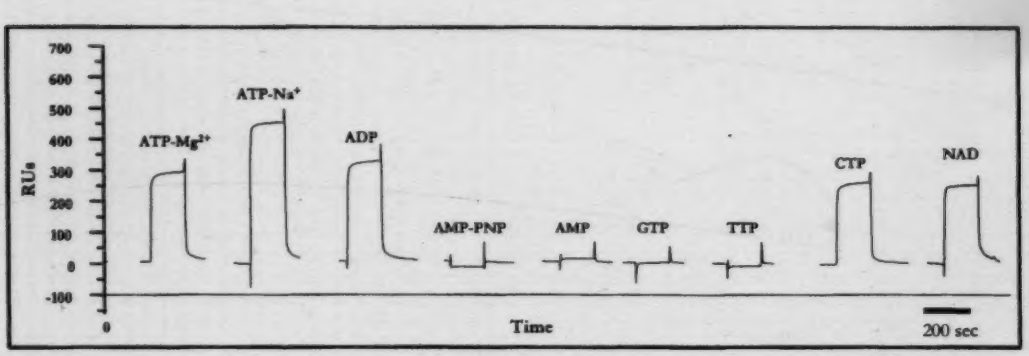

Figure 4- 9

Figure 4- 9 — SPR Analysis of ATP binding to calnexin.

Five mM of ATP-Mg^{2+}, ATP-Na^{+}, ADP, AMP, AMP-PNP, GTP, TTP, CTP or NAD was injected over immobilized S-Cnx.

Discussion

Protein folding is one of the most essential biological processes with several factors within the ER necessary for proper folding, including Ca^{2+}, Zn^{2+}, molecular chaperones and ATP. Ca^{2+} is essential for proper Ca^{2+} signaling as well as directly regulating protein folding within the ER (Berridge et al., 2003; Webb and Miller, 2003). Molecular chaperones are necessary for modulating the proper folding of nascent proteins and preventing aggregation (Ma and Hendershot, 2004). Several functions associated with the ER demand the presence of ATP, including phosphorylation (Chen et al., 1996; Csermely et al., 1995) and protein degradation (Hirschberg et al., 1998). In addition, ATP is required by a number of molecular chaperones for correct folding of substrates as well as an important structural molecule within the tertiary conformation of a number of these chaperones (Corbett et al., 2000; Dorner and Kaufman, 1994; Fink, 1999; Grenert et al., 1999). However, there is limited information on the molecular processes involved in protein folding, as well as how these processes occur *in vivo*.

We identified the importance of Ca^{2+}, Zn^{2+} and ATP on the conformation of calnexin. Previous research identifies that calnexin has a Zn^{2+}-dependent ERp57 binding site (Leach et al., 2002), a Ca^{2+} binding site (Ellgaard and Frickel, 2003; Michalak et al., 2002b; Tjoelker et al., 1994) and also binds ATP (Ou et al., 1995). Use of CB covalent linkage indicated global changes in hydrophobicity of the protein as a result of molecular exchange (Corbett et al., 1999). The assay verified the importance of these molecules on the tertiary structure of calnexin, with Zn^{2+} resulting in the largest changes in the hydrophobicity of calnexin. Interestingly, Ca^{2+} also appeared to play a large role as the addition of EGTA prior to the addition of other molecules abolished the global changes completely. This implied that Ca^{2+} bound to a high affinity site of calnexin during purification severely affected the interaction of the protein with the other molecules if it was chelated with EGTA. ATP did not have a significant effect on the hydrophobicity of CB-calnexin.

CD analysis on the purified soluble protein further confirmed that Ca^{2+}, Zn^{2+} and ATP bound to S-Cnx and modified its conformation. This may have a significant impact on the chaperone function of calnexin. Zn^{2+} and ATP interact with purified S-Cnx, leading to increase sensitivity to trypsin, potentially demonstrating an unfolding of the protein or a loss of tertiary structure. The Glu351Arg mutation did not affect the

trypsin digestion pattern as compared to wild-type. Interestingly, the Trp428Ala mutation significantly affected the tryptic pattern, with a complete loss of any protected full length protein, even when there were no external molecules present. This suggested that the Trp428Ala mutation resulted in the soluble protein having more trypsin accessible sites present which implied a less compact conformation. When Ca^{2+} was present, the Trp428Ala mutant protein was protected, similar to wild-type protein. It appeared that binding of Ca^{2+} to S-Cnx led to a tighter conformation with less trypsin accessible sites, independent of the Trp428Ala mutation. Zn^{2+} may result in a change in conformation to a specific domain of the protein, agreeing with the CB and CD analysis. Results indicate that calnexin interacts with Ca^{2+}, Zn^{2+} and ATP. Further studies were performed directly observing the intrinsic fluorescence of S-Cnx and the two calnexin mutants, Glu351Arg and Trp428. The two mutations did not significantly affect these interactions. The inability of Zn^{2+} to change the intrinsic fluorescence appeared to be in direct contrast to the CB, CD and trypsin analysis. Potentially, the binding of Zn^{2+} to the purified protein does not involve significant changes in tryptophan exposure to solvent.

As calnexin is a chaperone of glycosylated proteins, we wanted to identify whether the two mutations, Glu351Arg and Trp428Ala, affected the chaperone function of the protein. Wild-type S-Cnx prevented the aggregation of IgY efficiently, with both mutations resulted in the protein being significantly unable to prevent aggregation. This result suggested that both the Glu351Arg mutation and the Trp428Ala mutation affected the chaperone function of calnexin, presumably as a result of conformational changes leading to inability of the protein to interact with glycosylated substrate (IgY) and other molecules, such as Ca^{2+}, Zn^{2+}, ATP, or substrate. S-Cnx was able to prevent the aggregation of MDH with both mutations resulted in enhanced aggregation of MDH.

The ERp57 binding site has been mapped to the P-domain of calnexin (Leach et al., 2002), further narrowed down to a specific sequence identified by NMR (Pollock et al., 2004). SPR analysis on purified wild-type S-Cnx and mutant proteins indicated that both the Glu351Arg and Trp428Ala mutations do not lead to a loss of the interaction with ERp57 and that the Trp428Ala mutation resulted in an increase in the interaction. This enhancement in binding may be a result of exposure of several more ERp57 binding sites, such as the Zn^{2+}-dependent ERp57 binding site found in the N-domain (Leach et al., 2002). This was similar in manner to calreticulin, with the conserved

Trp302Ala mutation having enhanced binding to ERp57. Further work needs to be carried out to identify the specific amino acids that may lead to complete loss of ERp57 binding to calnexin, similar to that described for calreticulin (Martin et al., 2006).

The ER lumen also contains ATP which is required to support correct folding, as well as formation of disulfide bonds in many proteins (Braakman et al., 1992; Dorner and Kaufman, 1994; Dorner et al., 1990). ATP within the lumen of the ER is essential for the function of several chaperones, such as BiP/GRP78 and PDI which utilize the hydrolysis of ATP to release the folded protein (Guthapfel et al., 1996; Wei et al., 1995). Calnexin and calreticulin may utilize ATP to regulate conformational changes (Dierks et al., 1996; Saito et al., 1999), enhancing the aggregation suppression activity *in vitro* (Corbett et al., 2000; Ihara et al., 1999; Ou et al., 1995; Saito et al., 1999). While there are no obvious classical ATP binding regions in calreticulin or calnexin, Corbett et al. (Corbett et al., 2000) observes that addition of ATP during trypsin digestion of calreticulin results in protection of the C-domain, implying involvement of this region in ATP binding (Corbett et al., 2000). They also determine that calreticulin binds ATP using an ATP-agarose affinity column, but do not observe hydrolysis of ATP (Corbett et al., 2000). Calnexin contains a putative hydrophobic nucleotide binding site (Walker B: ddddD; d = hydrophobic residue) (de Wet et al., 2001), ^{190}MFGPD^{194} specifically. Calnexin and calreticulin do not contain the classical Walker A and B sites that constitute a nucleotide binding site, but modeling of this hydrophobic region places it on the surface of the N-terminal globular domain, in close proximity to the carbohydrate/substrate binding site and may potentially form a cleft that is part of the structure of the ATP binding region. SPR analysis revealed that calnexin does bind ATP and that both mutations (Glu351Arg and Trp428) enhance it. Glu351Arg and Trp428Ala mutations may expose more ATP binding sites as a result of conformational changes. Interestingly, ATP-Na^+, ADP, CTP and NAD also bound in a similar manner, but AMP, GTP, TTP or AMP-PNP (non-hydrolysable isoform) did not bind. When EDTA/EGTA was present, there was a significant decrease in nucleotide interaction with calnexin, implying that a specific conformation of the protein supplied by divalent cations may be necessary to promote ATP binding to the proteins. One thing that ATP, ADP, CTP and NAD have in common is a similarly located amine moiety, potentially involved in hydrogen bonding, which may explain the interaction with S-Cnx. It also

seems that there needs to be at least two phosphate groups present in the nucleotide for binding to calnexin to take place, also suggesting conformational requirements. Calnexin binds ATP in a conformationally-dependent manner.

Therefore, similar in manner to calreticulin, conformation change that results from molecular interaction of S-Cnx with Ca^{2+}, Zn^{2+}, ATP, or ERp57, directly affect the chaperone function of the protein. Site specific mutation of two residues, Glu351Arg and Trp428Ala, indicated that modification of these residues resulted in conformational change that led to a partial loss of chaperone activity, demonstrating an importance for molecular interactions responsible for the appropriate structural conformation of calnexin.

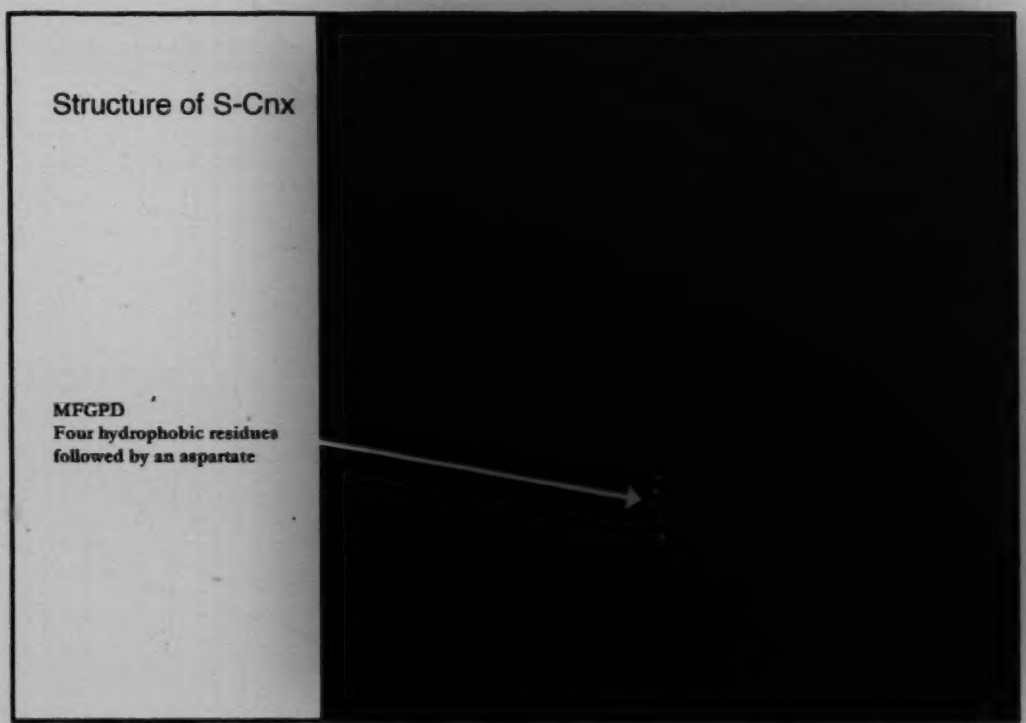

Figure 4- 10

Figure 4- 10 — Modeling of the crystal structure of S-Cnx and the putative ATP binding site.

Utilizing the program Chimera (University of California, San Francisco, California) the hydrophobic sequence 'MFGPD' was modeled onto the X-ray crystal structure of calnexin (1JHN).

Chapter Five — Calnexin and Apoptosis

Versions of this chapter have been previously published:

1. Anna Zuppini, Jody Groenendyk, Lori A. Cormack, Gordon Shore, Michal Opas, R. Chris Bleackley and Marek Michalak. **Calnexin Deficiency and Endoplasmic Reticulum Stress-Induced Apoptosis.** Biochemistry, 41 (8), 2850 -2858, 2002.

2. Jody Groenendyk, Anna Zuppini, Gordon Shore, Michal Opas, R. Chris Bleackley and Marek Michalak. **Caspase 12 in Calnexin-deficient Cells.** Submitted 2006.

Introduction

The ER plays a critical role in many cellular functions and recently has been implicated to play an important role during apoptotic signaling (Breckenridge et al., 2003a; Rao et al., 2004). However, the pathways that lead from ER stress to cellular destruction and apoptosis are not well understood. It is well known that caspases, a family of cysteine proteases, play a vital role during apoptosis (Demaurex and Distelhorst, 2003) with the activation of caspases triggering a cascade of proteolysis of specific substrates. This targeted protein cleavage leads to activation of nuclease activity, alterations in DNA repair processes and modifications in membrane dynamics (Shi, 2002; Widlak and Garrard, 2005). Caspase 12 is ubiquitously expressed in all cells and localized to the ER membrane and like other caspases, is synthesized as an inactive proenzyme consisting of a regulatory prodomain and two catalytic subunits (Nakagawa and Yuan, 2000; Rao et al., 2001). Caspase 12 is activated by conditions that elicit ER stress, such as disturbances in protein folding or disruption of intracellular Ca^{2+} stores (Demaurex and Distelhorst, 2003; Nakagawa and Yuan, 2000). Bap31 is another ER protein involved in apoptosis (Ng et al., 1997). Bap31 is a polytopic, integral protein of the ER membrane, is cleaved in its cytoplasmic domain upon an apoptotic signal by caspase 8, generating a proapoptotic p20 membrane fragment (Ng et al., 1997). The membrane localized p20 fragment strongly sensitizes mitochondria to caspase 8-induced cytochrome *c* release, thereby recruiting the mitochondria in the apoptotic cascade from the ER, an indication of cross talk occurring between these two organelles (Breckenridge et al., 2003b; Nguyen et al., 2000).

In this part of my studies, we utilize calnexin-deficient human T-lymphocyte cells (Scott and Dawson, 1995) and calnexin-deficient mouse embryonic fibroblasts (MEFs) to analyze the cascade of events occurring during programmed cell death induced by ER stress, as well as examining the role of calnexin during ER stress-induced apoptosis. We discover that calnexin forms a complex with Bap31, a 28-kDa integral membrane protein containing a cytoplasmic domain that associates with caspase 8, Bcl-XL and Bcl-2 (Ng et al., 1997). We also revealed that caspase 12 interacts with Bap31 and calnexin, indicating that a three way complex of calnexin-Bap31-caspase 12 might play an important role during apoptotic pathways initiated via the ER membrane.

Results

Previous studies have identified a human cell line that is deficient in calnexin (Scott and Dawson, 1995). Initially, the natural killer resistant (CEM-NK_R) cells were generated from a human T lymphoblastoid cell line, CEM, which was subjected to immunoselection by co-culturing with peripheral blood mononuclear cells, identifying resistance to natural killer (NK) cell-mediated lysis. The CEM-NK_R cells have a disruption in their expression of cell surface NK target antigens (Howell et al., 1985), mediated by MHC class I molecules. Analysis and comparison of the two dimensional proteome of the two cell lines, CEM and CEM-NK_R, identifies a significant difference in calnexin expression, with expression completely lost in the CEM-NK_R cells.

Identification of a Caspase 12-like Protein in Human Leukemic T-cells

Western blot analysis using anti-rat caspase 12 antibodies (Figure 5- 5A) reveales that both control (CEM) and calnexin-deficient human leukemic T-cells (NKR) contain a caspase 12-like protein, similar to that seen in A549 human lung carcinoma cells (Bitko and Barik, 2001). It was recently determined in the majority of humans that caspase 12 contains a TGA stop codon at amino acid position 125 that results in the synthesis of a truncated protein product, while in approximately 20% of the African American populace, this polymorphism is not present and the sequence encodes a full length caspase 12 proenzyme (Fischer et al., 2002; Saleh et al., 2004). Attempts at identifying this caspase 12-like protein by immunoprecipitation followed by mass spectroscopy analysis resulted in the tentative detection of a CARD 8 protein. CARD proteins contain a caspase recruitment domain domain (CARD), similar to initiator caspases (Figure 5- 1). CARD is a homotypic protein interaction module composed of a bundle of six α-helices. CARD is associated in sequence and structure to the death domain and the death effector domain, which work in similar pathways and show parallel interaction properties. The CARD domain usually associates with other CARD-containing proteins, forming either dimers or trimers. CARD domains can be found alone, or in combination with other domains. CARD-containing proteins are involved in apoptosis through their regulation of caspases that contain CARDs in their N-terminal pro-domains, including human caspases 1, 2, 9, 11 and 12 (Hofmann et al., 1997). Potentially, CARD8 may be interacting with caspase 12 and involved in the regulation of this caspase. Unfortunately,

we were unable to unequivocally identify caspase 12. In contrast to humans, full length caspase 12 is expressed in mice and therefore, in an attempt to further elucidate the relationship between caspase 12 and calnexin, we generated calnexin-deficient MEFs, isolated from calnexin-deficient mouse embryos. Calnexin-deficient mice were produced by random disruption of the calnexin gene using a β-galactosidase reporter and neomycin resistance gene DNA sequence. Embryonic stem cells were transfected and the resultant blastocyst was injected into a surrogate mouse mother. Heterozygote offspring were bred to generate a homozygote calnexin-deficient mouse. Subsequent Southern blot analysis determined that calnexin transcription was indeed disrupted and no protein product was generated (Figure 5- 2).

Caspase 12 Amino Acid Sequence - Mouse

```
        10         20         30         40         50         60
MAARRTHERD PIYKIKGLAK DMLDGVFDDL VEKNVLNGDE LLKIGESASF ILNKAENLVE
        70         80         90        100        110        120
NFLEKTDMAG KIFAGHIANS QEQLSLQFSN DEDDGPQKIC TPSSPSESKR KVEDDEMEVN
       130        140        150        160        170        180
AGLAHESHLM LTAPHGLQSS EVQDTLKLCP RDQFCKIKTE RAKEIYPVME KEGRTRLALI
       190        200        210        220        230        240
ICNKKFDYLF DRDNADTDIL NMQELLENLG YSVVLKENLT AQEMETELMQ FAGRPEHQSS
       250        260        270        280        290        300
DSTFLVFMSH GILEGICGVK HRNKKPDVLH DDTIFKIFNN SNCRSLRNKP KILIMQACRG
       310        320        330        340        350        360
RYNGTIWVST NKGIATADTD EERVLSCKWN NSITKAHVET DFIAFKSSTP HNISWKVGKT
       370        380        390        400        410
GSLFISKLID CFKKYCWCYH LEEIFRKVQH SFEVPGELTQ MPTIERVSMT RYFYLFPGN
```

CARD8 Amino Acid Sequence - Human

```
        10         20         30         40         50         60
MMRQRQSHYC SVLFLSVNYL GGTFPGDICS EENQIVSSYA SKVCFEIEED YKNRQFLGPE
        70         80         90        100        110        120
GNVDVELIDK STNRYSVWFP TAGWYLWSAT GLGFLVRDEV TVTIAFGSWS QHLALDLQHH
       130        140        150        160        170        180
EQWLVGGPLF DVTAEPEEAV AEIHLPHFIS LQGEVDVSWF LVAHFKNEGM VLEHPARVEP
       190        200        210        220        230        240
FYAVLESPSF SLMGILLRIA SGTRLSIPIT SNTLIYYHPH PEDIKFHLYL VPSDALLTKA
       250        260        270        280        290        300
IDDEEDRFHG VRLQTSPPME PLNFGSSYIV SNSANLKVMP KELKLSYRSP GEIQHFSKFY
       310        320        330        340        350        360
AGQMKEPIQL EITEKRHGTL VWDTEVKPVD LQLVAASAPP PFSGAAFVKE NHRQLQARMG
       370        380        390        400        410        420
DLKGVLDDLQ DNEVLTENEK ELVEQEKTRQ SKNEALLSMV EKKGDLALDV LFRSISERDP
       430
YLVSYLRQQN L
```

Figure 5- 1

Figure 5- 1 — MS/MS analysis of caspase 12 antibody immunoprecipitation.

Tentative identification of a CARD8 protein that was immunoprecipitated with the anti-rat caspase 12 antibody. Peptide extracts were analyzed on a Bruker REFLEX III (Bremen/Leipzig, Germany) time of flight mass spectrometer using MALDI in positive ion mode. Obtained peptide maps were used for database searching to identify proteins. Furthermore, for each sample, 1-2 selected peptides were fragmented using MALDI MS/MS analysis done on a PE Sciex API-QSTAR pulsar (MDS-Sciex, Toronto, Ontario, Canada). The obtained partial sequence information for each peptide was used to either confirm the previously obtained results from the peptide map search. The peptide fragment identified a protein named CARD8. The peptide identity was 1109.40 — DPYPVSYLR. CARD regions of both proteins are highlighted in red. Potentially, the two proteins could be interacting via their CARD domains.

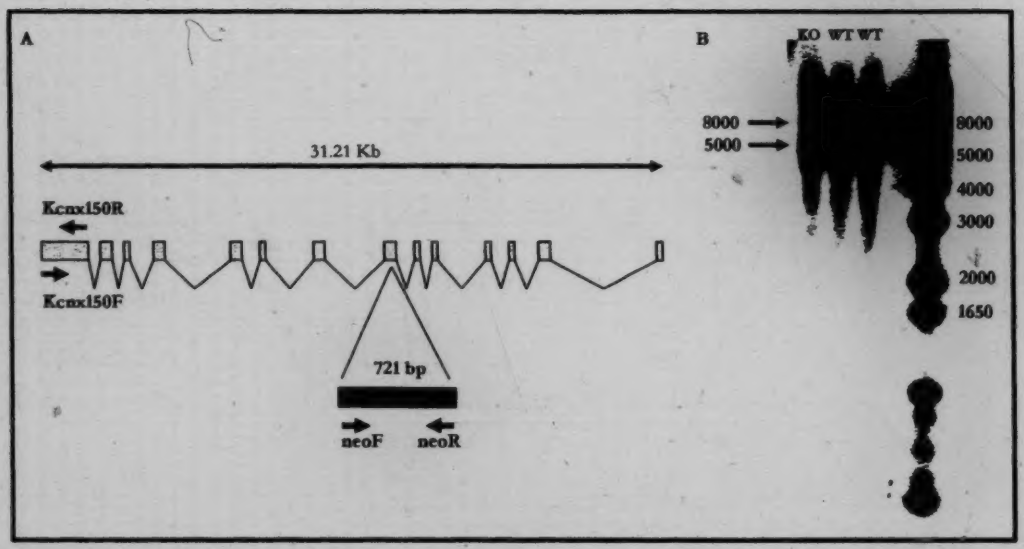

Figure 5- 2

Figure 5- 2 — Construct used to generate calnexin-deficient mouse and identification by Southern blot analysis.

An ES cell line (KST286) obtained from BayGenomics was used to generate a calnexin-deficient mouse. *(A).* The β-galactosidase/neomycin reporter plasmid was inserted in exon 7 at basepair 721, resulting in a disrupted gene product. A complete calnexin protein product was not generated. *(B).* Southern blot analysis using a 150 basepair probe generated by PCR with specific primers, Kcnx150F and Kcnx150R, recognized successful insertion of the reporter plasmid. An 8,000 basepair product identified full length calnexin gene while a 5,000 basepair product determined insertion of the reporter plasmid leading to a truncated gene product. KO, calnexin-deficient mouse; WT, wild-type mouse; β-gal, β-galactosidase; neoF, neomycin forward primer; neoR, neomycin reverse primer; Kcnx150R, calnexin reverse primer; Kcnx150F, calnexin forward primer (see primer list under "Materials and Methods").

ER Stress Response in Calnexin-Deficient Cells — CEM and NKR

We use NKR (calnexin-deficient) cells and their CEM parental cell line to investigate ER function when calnexin was absent. Figure 5- 3A shows that the NKR cells do not express calnexin, as expected. However, these cells express significantly higher levels of calreticulin (50% increase) compared with the parental CEM cell line (Figure 5- 3 B). The NKR cells also express more BiP/GRP78 (60% increase) and SERCA2 (50% increase) (Figure 5- 3C and E) proteins. No significant difference in the expression of ERp57 protein is observed (Figure 5- 3D).

Since an increased level in BiP/GRP78 protein expression is associated with ER stress (Kozutsumi et al., 1988), we investigate whether the calnexin deficiency affects thapsigargin-induced ER stress. Figure 5- 3C shows that, in both cell lines, thapsigargin increases the level of expression of BiP/GRP78 [1.9±0.1-fold (mean±SE); n=3]. The incubation of cells with thapsigargin also results in a slightly increased level of expression of ERp57 and SERCA2 [1.2±0.1-fold (mean±SE); n=3] (Figure 5- 3D and E). However, thapsigargin treatment of both the CEM and calnexin-deficient (NKR) cells results in significantly reduced levels of calreticulin (Figure 5- 3B). This is a surprising result because it is well-documented that thapsigargin treatment induces high-level expression of the calreticulin protein and mRNA in several cell lines (Llewellyn et al., 1996; Nguyen et al., 1996; Waser et al., 1997). At present, there is no explanation for why thapsigargin treatment results in decreased levels of calreticulin in these cells, but as the calnexin-deficient MEFs do not have a similar effect with calreticulin; it may be a cell-specific phenomenon.

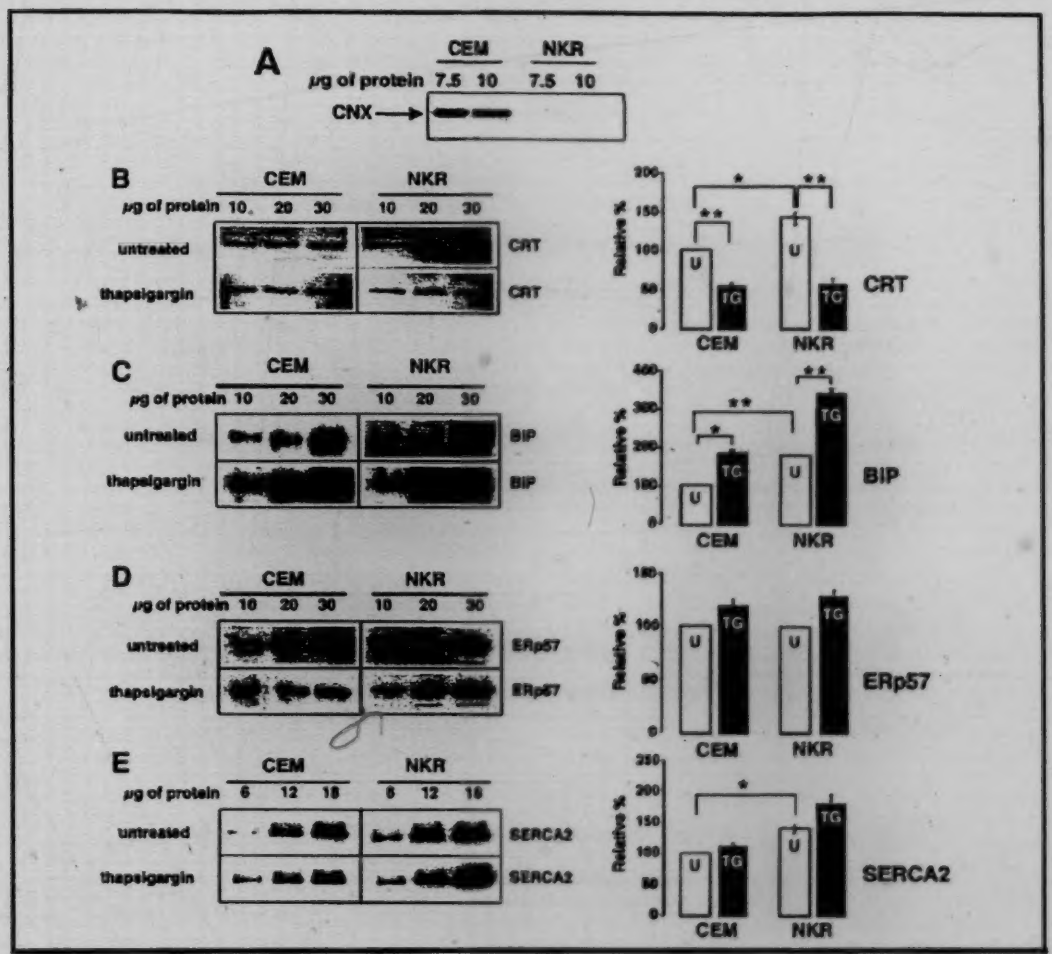

Figure 5- 3

Figure 5- 3 — Expression of ER-associated proteins in CEM and NKR cells.

CEM and NKR cells are harvested and lysed with RIPA buffer. Protein extracts are separated via SDS-PAGE (10% acrylamide), transferred onto nitrocellulose membranes and probed with anti-calnexin *(A)*, anti-calreticulin *(B)*, anti-BiP/GRP78 *(C)*, anti-ERp57 *(D)* and anti-SERCA2 *(E)* antibodies. Quantitative analysis is carried out by densitometry scanning of immunoreactive protein bands. Empty bars, untreated cells; black bars, cells treated with 1 µM thapsigargin for sixteen hours at 37°C. The 100% value corresponds to untreated CEM cells. Data are means ±SD of three independent experiments. CEM, parental cell line; NKR, calnexin-deficient cell line; CNX, calnexin; CRT, calreticulin. Statistically significant at $p < 0.001$ (two asterisks) and $p < 0.005$ (one asterisk). Experiments performed in collaboration with Dr. A. Zuppini.

ER Stress Response in Calnexin-Deficient Cells — MEFs

The calnexin-deficient MEFs as expected, did not express any calnexin (Figure 5-4. In contrast to NKR (see Figure 5- 3), the expression of ER resident proteins in calnexin-deficient MEFs demonstrated no significant differences in expression of calreticulin, Grp94 or PDI (Fig. 5-4B-D). However, calnexin-deficient MEFs contained approximately 60% more BiP/GRP78 (Fig. 5-4E), suggestive of ER stress in the absence of calnexin. Interestingly, there was an approximately 70% decrease in ERp57 protein expression in calnexin-deficient MEFs (Figure 5- 4F). Next we investigated whether the calnexin-deficiency affected thapsigargin-induced ER stress and apoptosis. Figure 5- 4E shows that in wild-type and calnexin-deficient MEFs, thapsigargin induced the expression of BiP/GRP78 protein. The incubation of calnexin-deficient cells with thapsigargin also resulted in a slightly decreased expression of Grp94 and ERp57 (Figs. 5-4D and E).

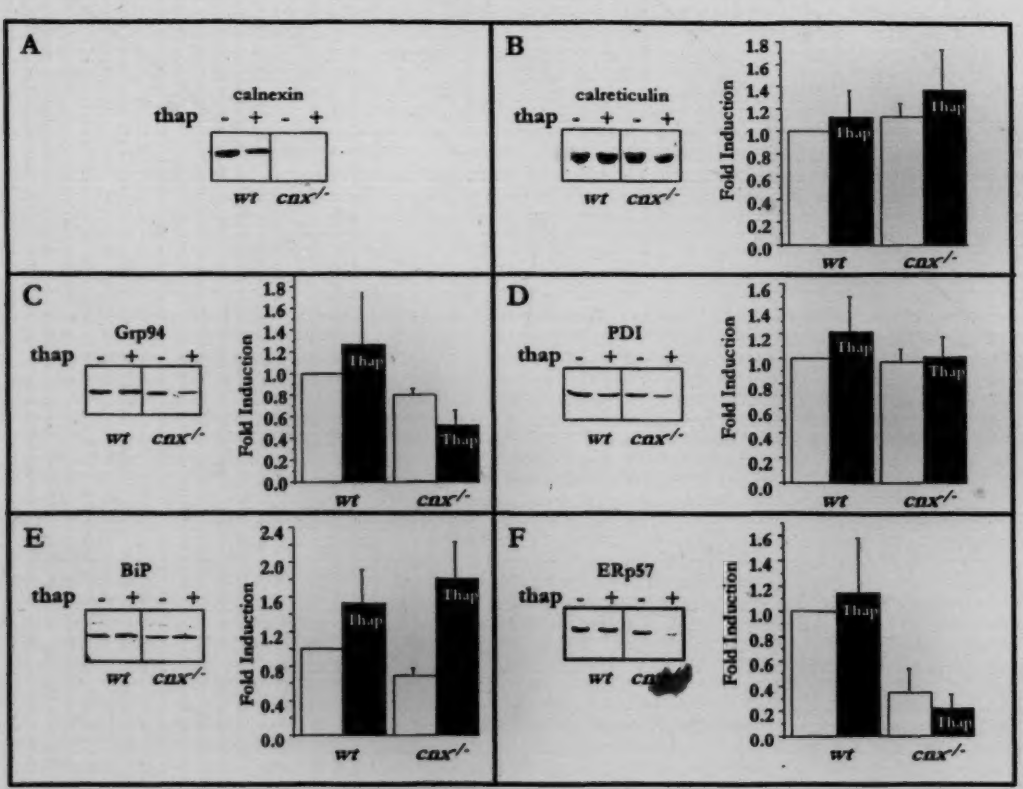

Figure 5- 4

Figure 5- 4 — Expression of ER proteins in calnexin-deficient MEFs.

Protein extracts were separated by SDS-PAGE (10% acrylamide), transferred onto nitrocellulose membrane and probed with anti-calnexin *(A)*, anti-calreticulin *(B)*, anti-Grp94 *(C)*, anti-PDI *(D)*, anti-BiP/GRP78 *(E)* and anti-ERp57 *(F)* antibodies. Histograms represent the quantitative analysis of immunoreactive protein bands. Data are mean ±SE of three or more independent experiments. *wt*, wild-type MEFs; *cnx*$^{-/-}$, calnexin-deficient MEFs; empty bars, untreated cells; black bars labeled Thap, cells treated with 1 μM thapsigargin for sixteen hours at 37°C. The 1-fold values correspond to untreated wild-type cells. Results are statistically significant at a p-value of 0.063 for BiP/GRP78 expression and a p-value of 0.05 for ERp57 expression (one-way Anova testing).

Expression of Apoptotic Proteins in Calnexin-Deficient Cells after ER Stress-Induced Apoptosis — CEM and NKR

The calnexin-deficient human T-cells (NKR) have increased expression of caspase 12 antibody immunoreactive protein bound (referred throughout as caspase 12-like protein) [1.9±0.06-fold increase (mean±SE); n=3] compared with the parental cell line (CEM) (Figure 5- 5A). To investigate the role of caspase 12-like protein in ER stress-induced apoptosis, we use thapsigargin. Continuous exposure to thapsigargin (sixteen hours) results in processing of this caspase 12-like protein (Figure 5- 5 A). Specifically, in both cell lines (CEM and NKR), the amount of caspase 12-like protein in the treated cells is reduced, relative to the amount in untreated cells [2.5±0.06-fold in CEM and 1.5±0.05-fold in NKR (mean±SE); n=3] (Figure 5- 5A). Thapsigargin treatment also causes activation of caspase 3, as visualized by the processing of a 32-kDa proenzyme (Figure 5- 5 B). Specifically, we found a 1.6±0.09-fold (mean±SE; n=3) reduction of the level of caspase 3 in the thapsigargin-treated cells (Figure 5- 5B).

Another member of the caspase family, caspase 8, cleaves the ER membrane apoptotic protein Bap31 (Rudner et al., 2001). Caspase 8 is synthesized as two isoforms (54- and 52-kDa, respectively) which are processed to form two heterodimers known as p18 and p10 (Scaffidi et al., 1997). Here we compare the processing of caspase 8, in response to thapsigargin treatment, in the control (CEM) and calnexin-deficient (NKR) human leukemic T-cell lines. Treatment with thapsigargin induces processing of caspase 8 only in the control CEM cell line [protein levels were 2.2±0.02-fold lower in treated than in untreated cells (mean±SE); n=3] (Figure 5- 5C) and there was negligible processing of caspase 8 in the calnexin-deficient T-cells (Figure 5- 5C).

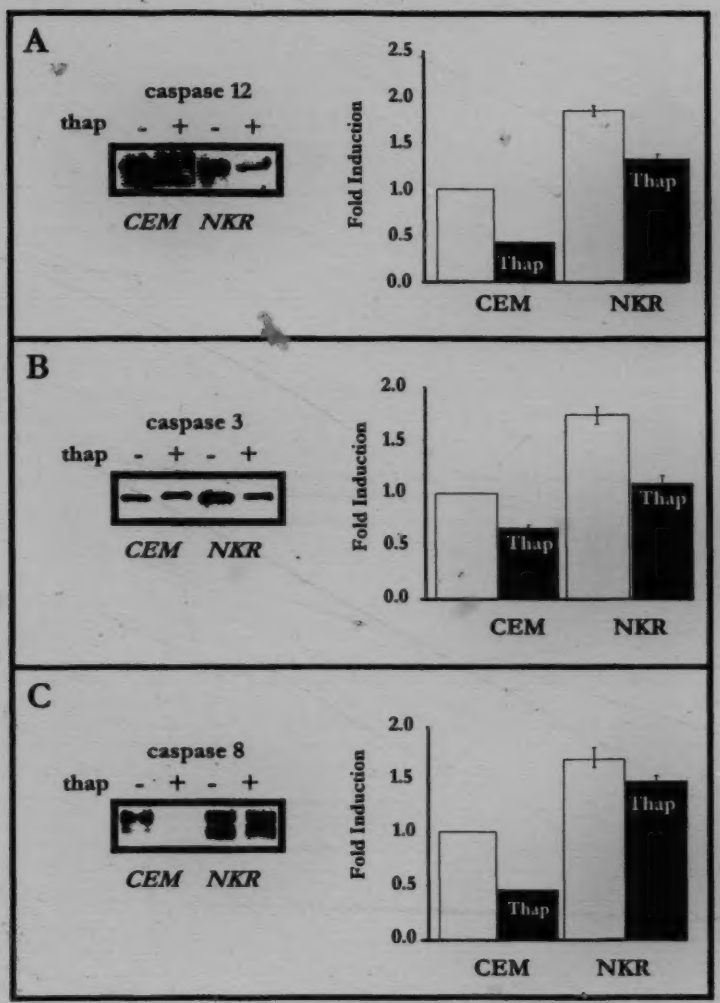

Figure 5- 5

Figure 5- 5 — Expression of caspase family proteins in CEM and NKR cell lines.

Protein extracts were separated by SDS-PAGE (10% acrylamide), transferred onto nitrocellulose membrane and probed with anti-caspase 12 *(A)*, anti-caspase 3 *(B)* and anti-caspase 8 *(C)* antibodies. The doublet demonstrated in *(C)* is specific to the anti-caspase 8 antibody. Histograms represent the quantitative analysis of immunoreactive protein bands. Data are mean ±SD of three independent experiments. CEM, parental cell line; NKR, calnexin-deficient cell line; empty bars, untreated cells; black bars labeled Thap, cells treated with 1 μM thapsigargin for sixteen hours at 37°C. The 1-fold values correspond to untreated CEM cells. Experiments performed in collaboration with Dr. A. Zuppini.

Several members of the Bcl-2 family of proteins are localized to the ER (Zhu et al., 1996) and intrinsically involved in apoptosis (Schinzel et al., 2004). Bcl-2 is an antiapoptotic protein, whereas Bax is a proapoptotic protein; importantly, in leukemic cell lines, the Bax:Bcl-2 ratio is critical in determining whether cells will resist drug-induced apoptosis (Salomons et al., 1997), specifically correlating with sensitivity to dexamethasone treatment in cancer patients. We find a significantly greater level of expression of Bcl-2 in the CEM cells than in the calnexin-deficient (NKR) cells (Figure 5- 6A). In contrast, the level of expression of Bax is greater in the calnexin-deficient cells (Figure 5- 6B). Following treatment with thapsigargin and the induction of ER stress, the expression of Bcl-2 and Bax is upregulated in CEM cells, by 1.5±0.1-fold (mean±SE; n=3) and 1.4±0.1-fold (mean±SE; n=3), respectively (Figure 5- 6A and B). In contrast, the expression of Bcl-2 and Bax is downregulated in the calnexin-deficient NKR cells (Figure 5- 6A and B). Although Bcl-2 and Bax are expressed at different levels in the CEM and the calnexin-deficient NKR cells, in both cell types the relative ratio of Bax to Bcl-2 is unaffected by treatment with thapsigargin (Figure 5- 6C).

Expression of Apoptotic Proteins in Calnexin-Deficient Cells after ER Stress-Induced Apoptosis — MEFs

Western blot analysis with anti-rat caspase 12 antibodies demonstrated that both wild-type and calnexin-deficient MEFs expressed the caspase 12 protein (Figure 5- 7A). Caspase 12 expression was slightly reduced in calnexin-deficient MEFs (Figure 5- 7A) with the protein undergoing specific cleavage in the presence of thapsigargin, indicating that a deficiency in calnexin did not interfere with thapsigargin-dependent activation of caspase 12. Caspase 3 expression is also significantly downregulated (approximately 50%) in the calnexin-deficient MEFs, but similar to caspase 12, deficiency in calnexin does not appear to notably affect cleavage of caspase 3 (Figure 5- 7B). As well, direct observation of Bcl-2 protein expression (Figure 5- 7C) demonstrated a significant down regulation in calnexin-deficient MEFs (approximately 40%), indicating that calnexin-deficient MEFs, similar to NKR cells, have modified their apoptotic program.

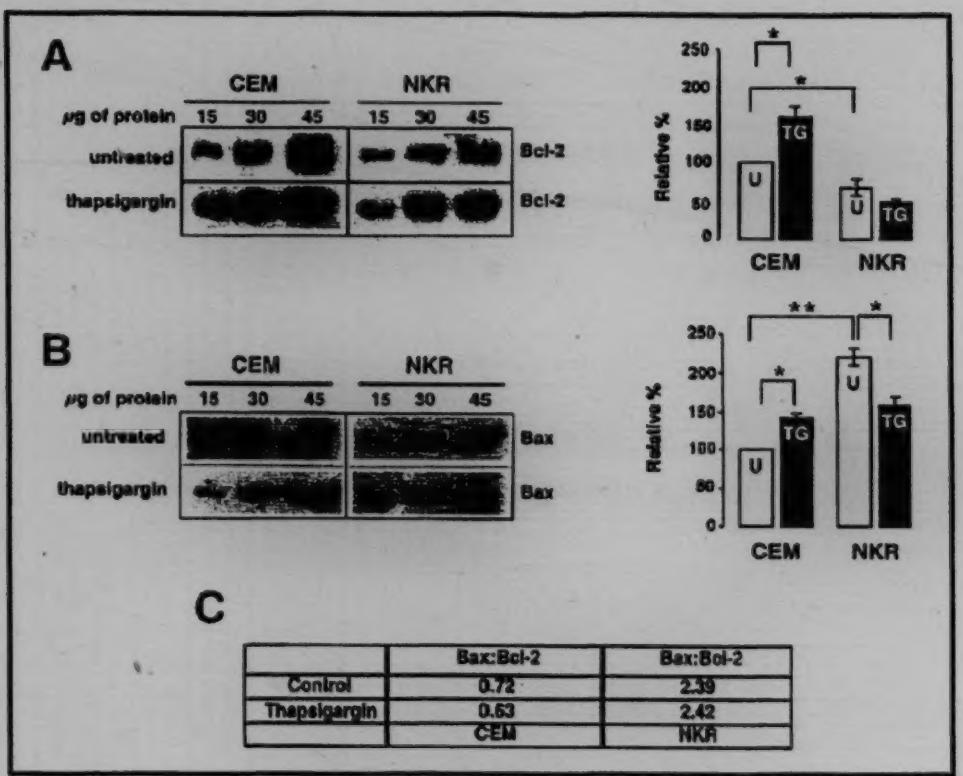

Figure 5- 6

Figure 5- 6 — Bax and Bcl-2 in calnexin-deficient cells.

Cells were lysed and proteins separated by SDS-PAGE (10% acrylamide) followed by western blot analysis. Protein blots were probed with anti-Bax *(A)* or anti-Bcl-2 *(B)* antibodies. Quantitative analysis was carried out by densitometry scanning of immunoreactive protein bands and the results are shown on the right: (empty bars) untreated cells (U) and (black bars) thapsigargin-treated cells (TG). The 100% value corresponds to untreated CEM cells. Data are means ±SD of three independent experiments. Panel *C* shows relative Bax:Bcl-2 ratio in CEM and NKR cells. CEM, parental cell line; NKR, calnexin-deficient cells. Statistically significant at $p < 0.001$ (two asterisks) and $p < 0.005$ (one asterisk). Experiments performed in collaboration with Dr. A. Zuppini.

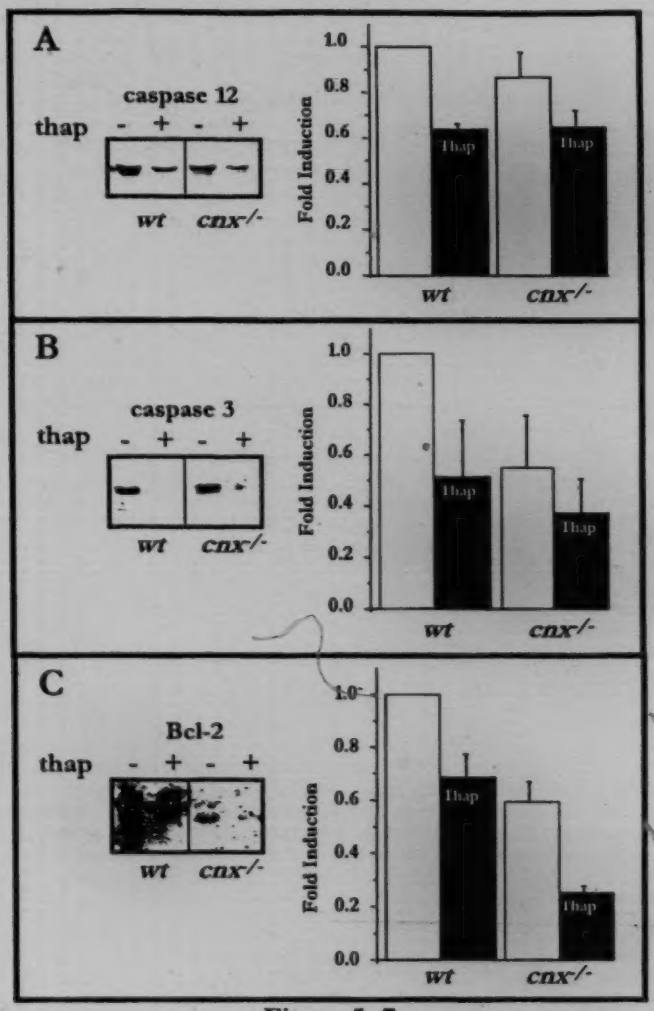

Figure 5- 7

Figure 5- 7 — Expression of apoptotic proteins in calnexin-deficient cells.

Protein extracts were separated by SDS-PAGE (10% acrylamide), transferred onto nitrocellulose membrane and probed with anti-caspase 12 *(A)*, anti-caspase 3 *(B)* and anti-Bcl-2 *(C)* antibodies. Histograms represent the quantitative analysis of immunoreactive protein bands. Data are mean ±SE of three or more independent experiments. *wt*, wild-type MEFs; *cnx*$^{-/-}$, calnexin-deficient MEFs; empty bars, untreated cells; black bars labeled Thap, cells treated with 1 μM thapsigargin for sixteen hours at 37°C. The 1-fold values correspond to untreated wild-type cells. Results are statistically significant at a p-value of 0.0001 for Bcl-2 expression, a p-value of 0.12 for caspase 3 and a p-value of 0.007 for caspase 12 expression (one-way Anova testing).

ER Stress-Induced Apoptosis in Calnexin-Deficient Cells

To examine the events that link ER stress to apoptosis, we monitored cytochrome *c* release, caspase activity, PARP cleavage and DNA fragmentation in wild-type (CEM) and calnexin-deficient (NKR) cells after treatment with thapsigargin. The release of cytochrome *c* from mitochondria is a key event in apoptosis (Goldstein et al., 2000). We assess the release of cytochrome *c* by cell fractionation and western blot analysis. Figure 5- 8A demonstrates thapsigargin-induced release of cytochrome *c* in CEM and NKR cells. Neither the CEM nor the NKR cells contain detectable cytoplasmic cytochrome *c* (Figure 5- 8, lanes 1 and 3). After treatment with thapsigargin, the release and accumulation of cytochrome *c* are similar in CEM and NKR cells (Figure 5- 8, lanes 2 and 4). In both cell lines, treatment with thapsigargin activates caspase 3, as estimated on the basis of the rate of cleavage of the fluorometric substrate DEVD-AFC (Figure 5- 8B). In the CEM cells, the activity is increased [2.0±0.2-fold (mean±SE); n=3] and in the calnexin-deficient (NKR) cells, it is increased [4.0±0.6-fold (mean±SE); n=3] (Figure 5- 8B). However, PARP cleavage is similar in both CEM and NKR cells (Figure 5- 8C). Lastly, we analyze DNA fragmentation using a TUNEL assay. Thapsigargin treatment of CEM cells results in a 7.4±0.2-fold (mean±SE; n=3) increase in TUNEL positive cells, whereas treatment of calnexin-deficient (NKR) cells results in a 1.8±0.3-fold (mean±SE; n=3) increase (Figure 5- 8D). These results demonstrate that the calnexin-deficient cells (NKR) are more resistant than the parental cell line (CEM) to apoptosis induced by ER stress. In line with these results, calnexin-deficient MEFs are significantly resistance to thapsigargin-induced apoptosis (approx. 6 fold) as measured by Annexin V binding to the cell surface (Figure 5- 9).

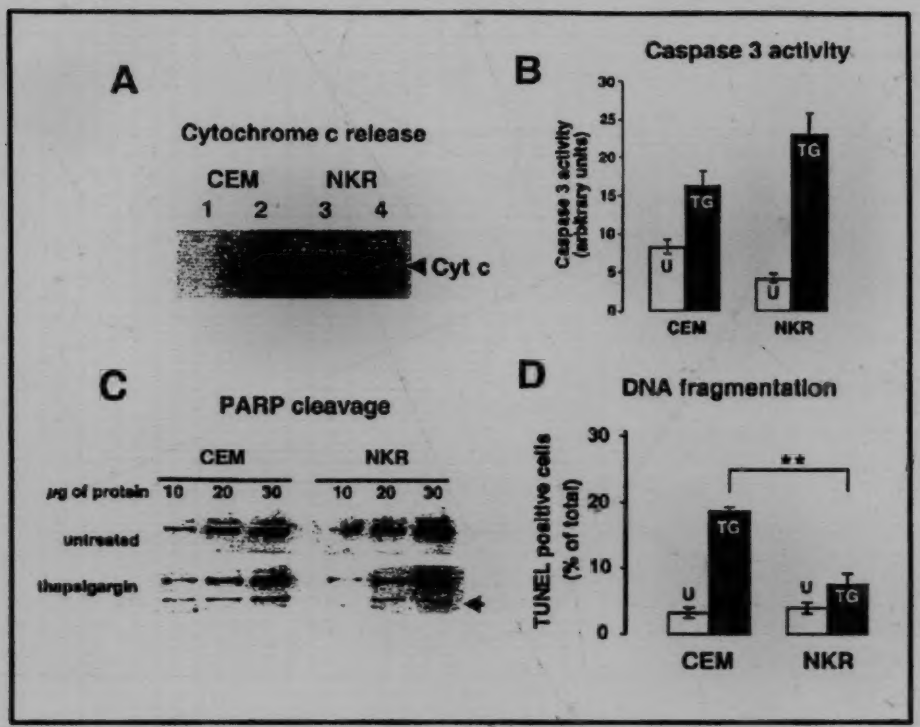

Figure 5- 8

Figure 5- 8 — ER stress-induced apoptosis in calnexin-deficient cells.

Cytochrome *c* release *(A)*, caspase 3 activity *(B)*, PARP cleavage *(C) and* DNA fragmentation *(D)* were assessed in CEM and calnexin-deficient (NKR) cells. *(A)* Cytochrome *c* accumulation in the cytoplasm was assessed by western blot analysis: lanes 1 and 3, cytoplasmic extract from untreated cells; lanes 2 and 4, cytoplasmic extracts from cells incubated with 1 μM thapsigargin. *(B)* The caspase 3 activity in control and thapsigargin-treated cells was measured using the fluorimetric substrate Ac-DEVD-AFC. Results are means ±SD of three independent experiments. *(C)* The PARP cleavage was identified by western blot analysis (arrow) in control (untreated) and thapsigargin-treated cells. *(D)* DNA fragmentation was monitored by a TUNEL assay in control, untreated (-) and thapsigargin-treated (+) cell populations. Empty bars, untreated cells; black bars, cells treated with 1 μm thapsigargin for sixteen hours. Results are means ±SD of three independent experiments. Statistically significant at $p < 0.001$ (two asterisks) and $p < 0.005$ (one asterisk). Experiments were performed in collaboration with Dr. A. Zuppini.

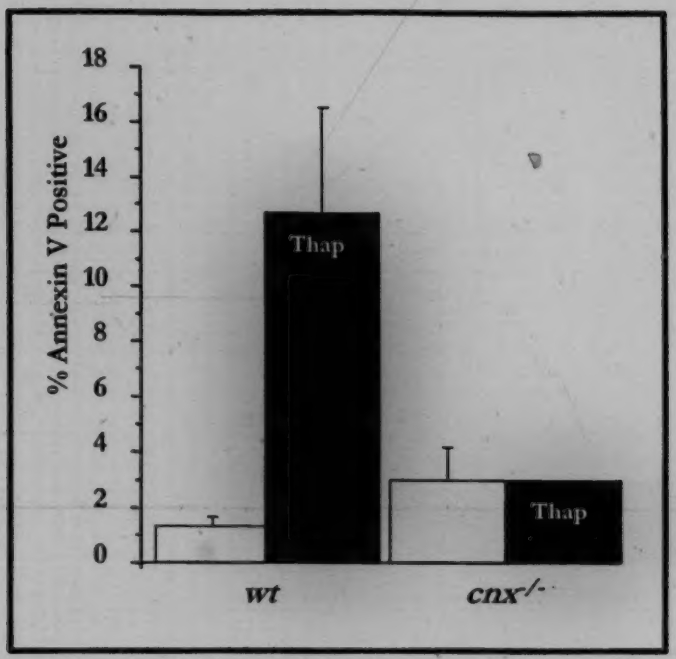

Figure 5- 9

Figure 5- 9 — Percent apoptosis as measured by Annexin V and PI - FACS analysis.

Both Annexin V and PI staining was observed and labeling was determined using a FACScan instrument (BD Bioscience Inc. San Jose, California). Data are mean ±SE of three or more independent experiments. Results are statistically significant at a p-value of 0.02 (one-way Anova testing). Empty bar indicates untreated cells; black bar indicates 1 μm thapsigargin treated cells for sixteen hours.

ER Ca^{2+} Homeostasis in Calnexin-Deficient Cells

We observe that both CEM and NKR cells expressed Bap31, SERCA2 and calreticulin, with these proteins localized in a similar manner to an ER-like network, as well as in the nuclear envelope (Figure 5- 10A, B). As expected, there is no expression of calnexin in the NKR cells (Figure 5- 10B). Morphologically, in electron micrographs, the ER appears intact in both CEM and NKR (Figure 5- 10C), with typical nuclear, ER and mitochondrial morphology. Similarly, observation of the wild-type and calnexin-deficient MEFs by EM also demonstrates no significant changes in ER morphology (Figure 5-11). Importantly, thapsigargin treatment of CEM and calnexin-deficient (NKR) cells has no effect on the intracellular localization of Bap31, SERCA and calreticulin (Figure 5-10). Our results demonstrated that calnexin deficiency and ER stress (thapsigargin treatment) do not affect the localization of ER proteins (integral membrane proteins, Bap31 and SERCA and luminal protein calreticulin) in the CEM and NKR cells. Calnexin deficiency and ER stress also do not affect the morphology of the ER.

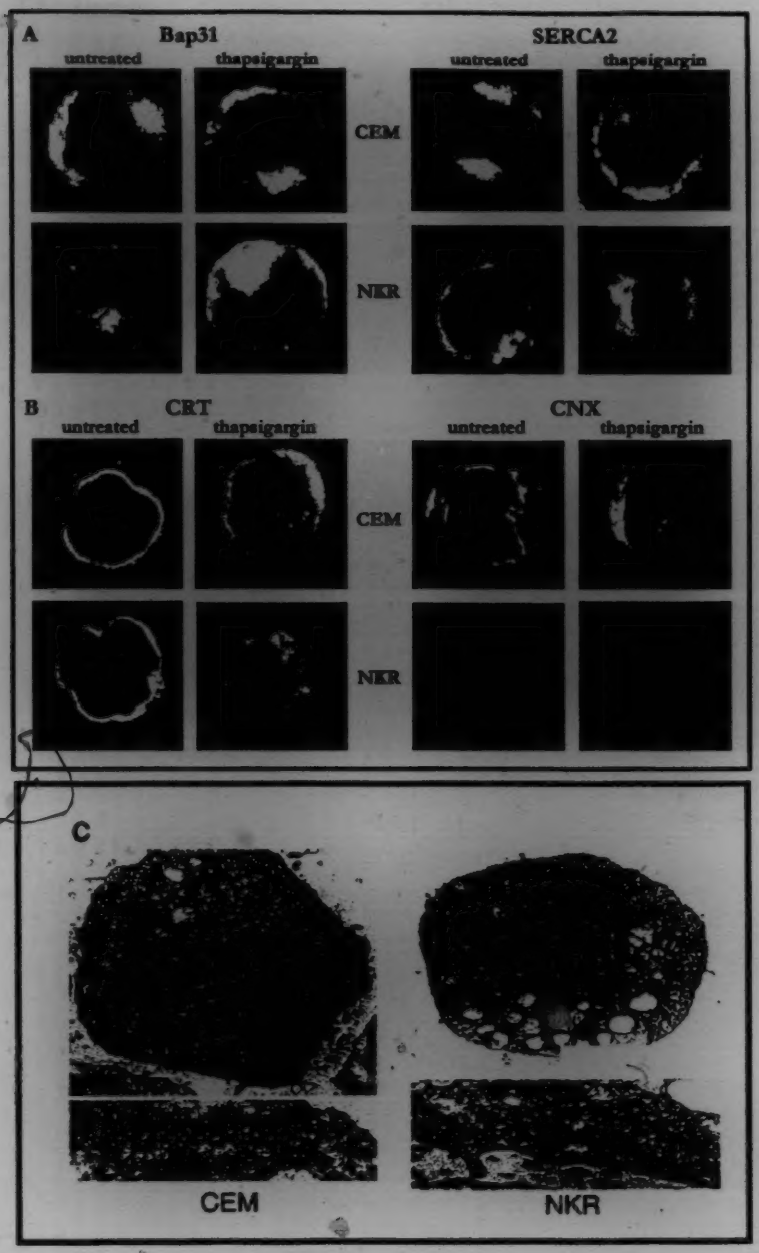
A
Bap31
untreated
thapsigargin
SERCA2
untreated
thapsigargin
CEM
NKR
B
CRT
untreated
thapsigargin
CNX
untreated
thapsigargin
CEM
NKR
C
CEM
NKR

Figure 5- 10

Figure 5- 10 — Immunofluorescence and electron microscope analysis of calnexin-deficient NKR cells.

Immunolocalization of Bap31 and SERCA2 *(A) and* calreticulin and calnexin *(B)* in CEM (wild-type) and NKR (calnexin-deficient) cells. Cells were also treated with 1 μM thapsigargin for sixteen hours followed by immunostaining with specific antibodies. In all cell lines, Bap31, SERCA2, calreticulin (CRT) and calnexin (CNX) were localized to the ER-like network. Calnexin-deficient NKR cells do not contain calnexin and therefore did not stain with anti-calnexin antibodies *(B). (C)* Electron microscopy of wild-type (CEM) and calnexin-deficient (NKR) cells.

Figure 5- 11

Figure 5- 11 — Electron microscopy of wild-type and calnexin-deficient MEFs.

Arrows indicate the location of ER membranes. No significant difference in ER was observed between wild-type (WT) and calnexin-deficient fibroblasts ($Cnx^{-/-}$).

Ca^{2+} Homeostasis in the Absence of Calnexin

Changes in Ca^{2+} concentration in the cytoplasm and in the lumen of the ER affect apoptosis (Rizzuto et al., 2003). Calnexin, an integral ER membrane protein, might affect Ca^{2+} uptake and release from the ER in several ways, including direct regulation of the SERCA Ca^{2+} pump (Roderick et al., 2000; Vangheluwe et al., 2005). These actions could either affect apoptotic processes or lead to changes in the expression of proteins involved in apoptosis (Foyouzi-Youssefi et al., 2000; Nakamura et al., 2000; Pinton et al., 2000). In the following experiments, we investigate whether calnexin deficiency affects the ER Ca^{2+} capacity, or cytoplasmic Ca^{2+} concentrations in NKR cells. The CEM cells contain 9.5±2.6 pmol of $Ca^{2+}/10^6$ cells (mean ±SE; n=3) and the calnexin-deficient NKR cells contain 11.3±1.2 pmol of $Ca^{2+}/10^6$ cells (mean ±SE; n=3) (Figure 5- 12). Thus, the absence of calnexin does not affect the Ca^{2+} storage capacity of the ER in the NKR cells. Next, we use a Ca^{2+}-sensitive fluorescent dye, Fura 2-AM, to investigate the effects of calnexin deficiency on cytoplasmic Ca^{2+} concentrations ($[Ca^{2+}]_{cyt}$). Basal $[Ca^{2+}]_{cyt}$ values in control (CEM) and calnexin-deficient (NKR) cells are similar [34.9±3.7 nM (mean±SD); n=3]. When cells were treated with thapsigargin, the peak and duration of the $[Ca^{2+}]_c$ elevations are comparable (Figure 5- 13A). We compare agonist-induced Ca^{2+} release in the CEM and calnexin-deficient NKR cells. In preliminary experiments, we test the effect of 100 nM carbachol, 100 μM ATP and 50 nM bombesin on Ca^{2+} release. Of these agonists, only carbachol results in Ca^{2+} release from both CEM and NKR cells (Figure 5- 13B) and therefore it is used in subsequent experiments. Carbachol, a muscarinic agonist, induces Ca^{2+} release from the ER via an $InsP_3$-dependent pathway (Felder et al., 1992). Carbachol induces a rapid and transient increase in the $[Ca^{2+}]_{cyt}$ in both CEM and NKR cell lines (Figure 5- 1 3B). Similarly, increases in $[Ca^{2+}]_{cyt}$ are observed when both cell types are stimulated with ionomycin [204±21 nM (mean±SE); n=3], or ionomycin and thapsigargin [212.3±35 nM (mean±SE); n=3]. In all cases, the peak and the duration of the elevations in $[Ca^{2+}]_{cyt}$ are comparable in CEM and calnexin-deficient NKR cells. Results demonstrate that calnexin deficiency affects neither the storage capacity of the ER nor thapsigargin- and $InsP_3$-dependent Ca^{2+} release from the ER in NKR cells.

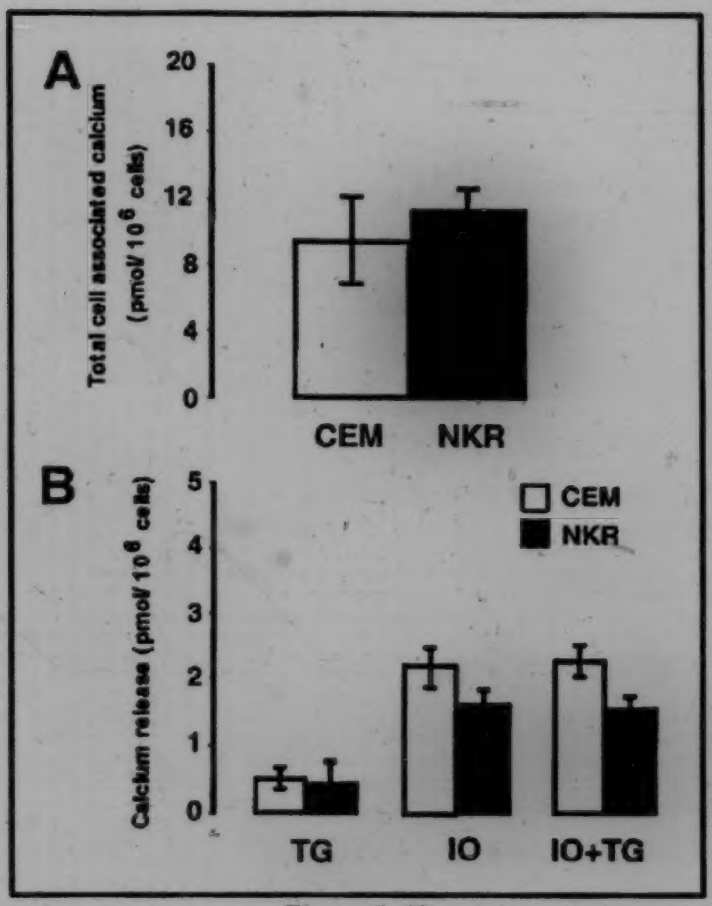

Figure 5- 12

Figure 5- 12 — Total ER Ca^{2+} content of calnexin-deficient NKR cells.

Total cellular Ca^{2+} content was determined using equilibrium incubation with $^{45}Ca^{2+}$ followed by addition of thapsigargin (estimates the Ca^{2+} pool in thapsigargin-sensitive Ca^{2+} stores) or ionomycin (estimates the Ca^{2+} pool in thapsigargin-insensitive Ca^{2+} stores). The Ca^{2+} content was measured in wild-type (CEM) and calnexin-deficient (NKR) cells. TG, thapsigargin; IO, ionomycin. Results are means ±SD of three independent experiments. Experiments performed in collaboration with Dr. A. Zuppini.

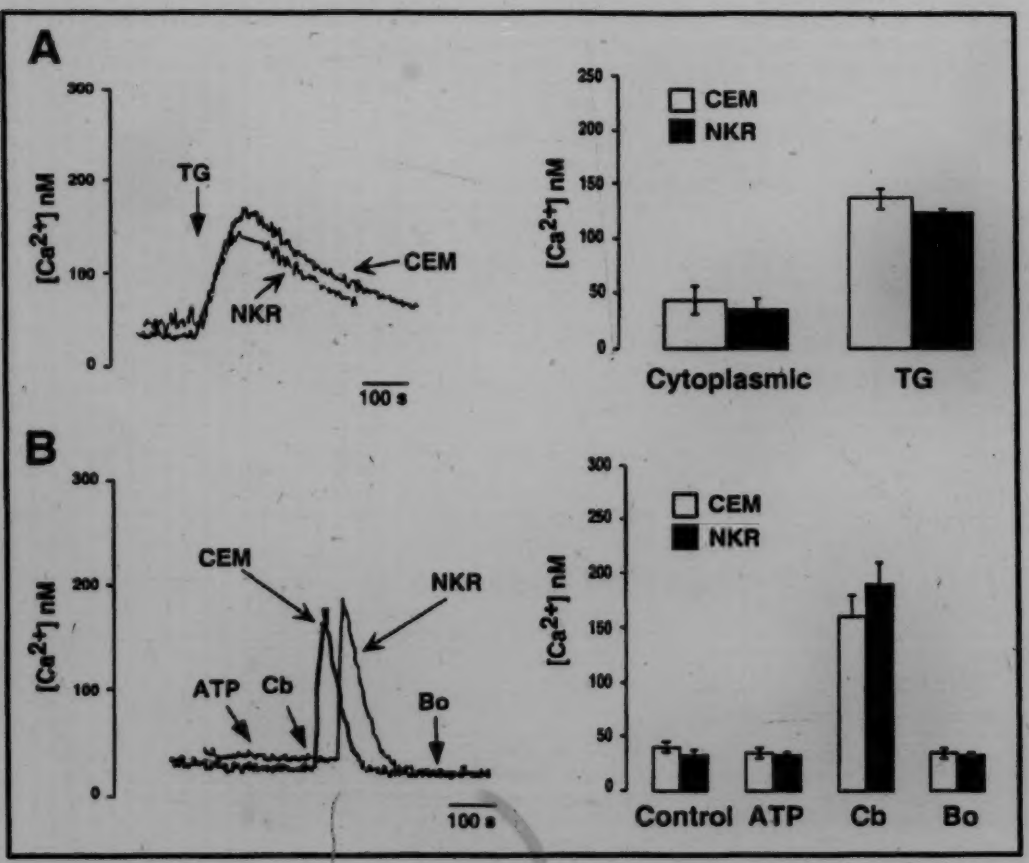

Figure 5- 13

Figure 5- 13 — Agonist-induced Ca^{2+} release in calnexin-deficient NKR cells.

Cells were loaded with the fluorescent Ca^{2+} indicator, Fura 2-AM and stimulated with thapsigargin (TG) *(A)* or 100 μM ATP and 100 μM carbachol (Cb) or 100 nM bombesin (Bo) *(B)*. CEM, wild-type cells; NKR, calnexin-deficient cells. Panel *A* shows typical traces showing thapsigargin (TG) stimulation of cells in a Ca^{2+}-free medium. *(B)* There was no Ca^{2+} released by ATP or bombesin, but a significant Ca^{2+} release with the addition of carbochol. There was no significant difference in carbachol-induced Ca^{2+} release in the cell lines that were investigated. Data are means ±SE (n=3). Experiments performed in collaboration with Dr. A. Zuppini.

The Effects of Caspase Inhibitors on Ca^{2+} Signaling in Human Leukemic T-cells

The peak and duration of the elevation in $[Ca^{2+}]_{cyt}$ are similar in CEM and NKR cells after thapsigargin treatment, indicating that they have the same ER storage capacity. Here, we use Fura 2-AM to determine whether caspase inhibitors have any effect on intracellular Ca^{2+} homeostasis in the human leukemic T-cell lines investigated. Figure 5-14 shows that in cells treated for sixteen hours with z-IETD-fmk, a caspase 8 inhibitor and z-DEVD-fmk, a caspase 3 inhibitor, thapsigargin induces an immediate increase in $[Ca^{2+}]_{cyt}$ which is followed by a sustained elevation of $[Ca^{2+}]_{cyt}$. Following treatment with the caspase 8 inhibitor (z-IETD-fmk), the elevation in $[Ca^{2+}]_{cyt}$ is higher and faster in the calnexin-deficient cells (NKR) than in the control cells (CEM) (Figure 5- 14A). In contrast, the elevation in $[Ca^{2+}]_{cyt}$ in the two cell lines is indistinguishable following treatment with the caspase 3 inhibitor (z-DEVD-fmk) (Figure 5- 14C). In previous experiments, we use carbachol to elicit $InsP_3$-dependent Ca^{2+} release from the ER in the control (CEM) and calnexin-deficient (NKR) cells. In the presence of z-IETD-fmk (the caspase 8 inhibitor), carbachol treatment causes a rapid release of Ca^{2+} in both cell types, with increased $[Ca^{2+}]_{cyt}$ (Figure 5- 14B). In the presence of z-DEVD-fmk (the caspase 3 inhibitor), carbachol again induces a rapid increase in the $[Ca^{2+}]_{cyt}$ in both cell types. However, the return to basal levels of $[Ca^{2+}]_{cyt}$ (recovery time) that results from removal of Ca^{2+} from the cytoplasm is significantly longer in calnexin-deficient (NKR) cells (Figure 5- 14D), indicating an impaired function of normal Ca^{2+} removal systems, which include SERCA and/or the plasma membrane Ca^{2+}-ATPase.

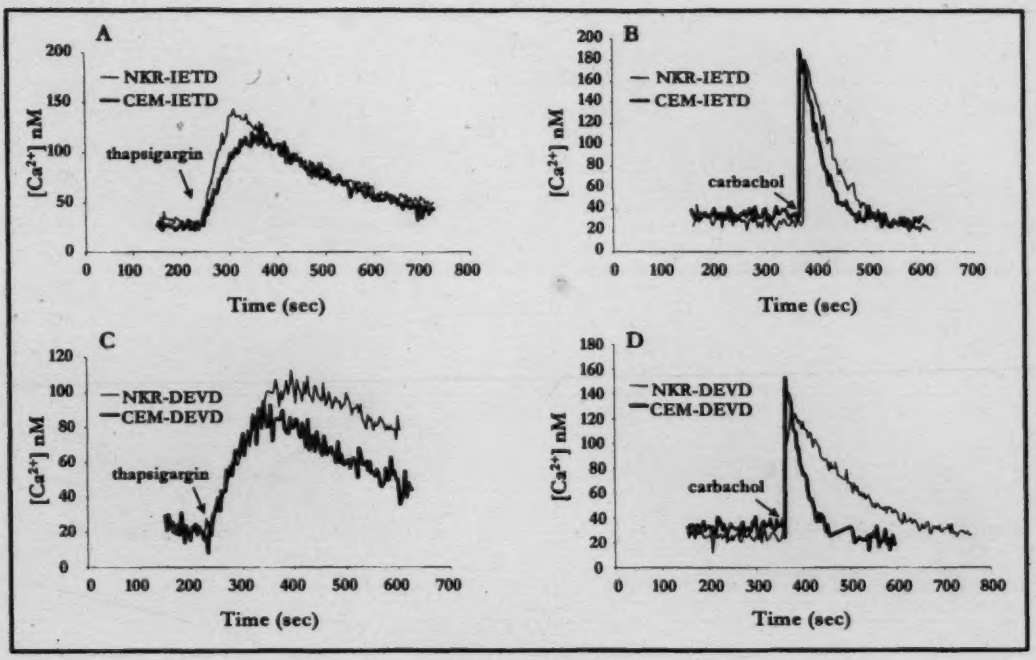

Figure 5- 14

Figure 5- 14 — Ca^{2+} release induced by thapsigargin and carbachol in calnexin-deficient cells incubated with caspase inhibitors.

After sixteen hours treatment with either 20 μM caspase 8 inhibitor z-IETD-fmk, or 20 μM caspase 3 inhibitor z-DEVD-fmk, cells were loaded with the fluorescent Ca^{2+} dye, Fura 2-AM and stimulated with 100 nM thapsigargin *(A,C)* or 100 μM carbachol *(B,D)* in a Ca^{2+}-free medium. Panels *A* and *C* show typical traces induced by thapsigargin in a Ca^{2+}-free medium. A significant Ca^{2+} release was obtained by addition of carbachol in both cell lines treated with the different inhibitors *(B,D)*. Experiments performed in collaboration with Dr. A. Zuppini.

Bap31 in Calnexin-Deficient Cells

Bap31 is an integral membrane protein of the ER that is involved in apoptotic pathways (Ng et al., 1997; Ng and Shore, 1998). Activation of apoptosis results in the cleavage of Bap31 by caspase 8, generating a 20-kDa, p20 proteolytic fragment (Ng and Shore, 1998). Using western blot analysis, we determine that the calnexin-deficient NKR cells express almost 3-fold more Bap31 than the parental CEM cell line (Figure 5- 15). Treatment of CEM cells with thapsigargin induces apoptosis and cleavage of Bap31 to produce the p20 fragment (Figure 5- 15). Most significantly, in the absence of calnexin there is no significant cleavage of Bap31 (Figure 5- 15).

Bap31 also was significantly affected in the calnexin-deficient MEFs (Figure 5-16), with resistant to cleavage in calnexin-deficient MEFs treated with thapsigargin. In contrast, in wild-type MEFs, thapsigargin treatment resulted in significant cleavage of Bap31, with generation of the resultant p20 fragment (Figure 5- 16). Therefore we conclude that calnexin influences the cleavage of Bap31 into the p20 fragment, followed by subsequent activation of the apoptotic pathway.

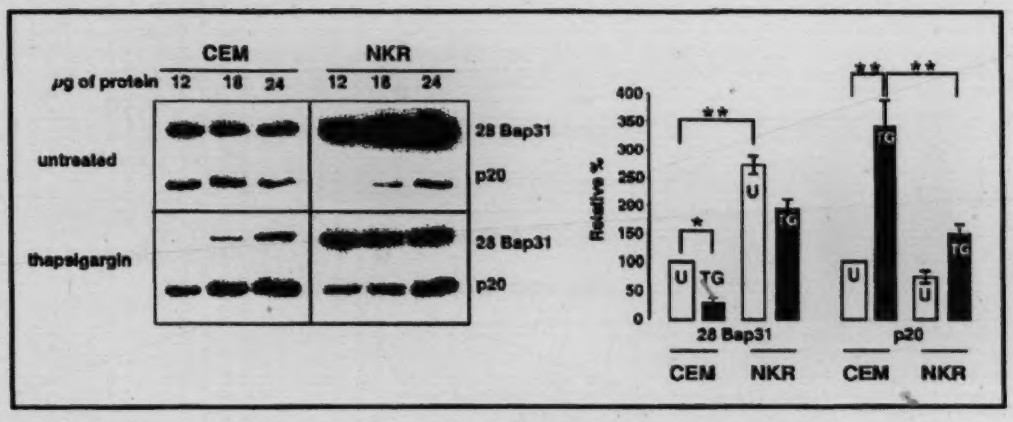

Figure 5- 15

Figure 5- 15 — Expression of Bap31 in CEM and NKR cells.

CEM and NKR cells were harvested and lysed with RIPA buffer. Protein extracts were separated via SDS-PAGE (10% acrylamide), transferred onto nitrocellulose membranes and probed with anti-Bap31 antibody. Quantitative analysis was carried out independently for Bap31 (28 Bap31) and its proteolytic fragment, p20, by densitometry scanning of immunoreactive protein bands: (empty bars) untreated cells (U) and (black bars) thapsigargin-treated cells (TG). Cells were treated with 1 µM thapsigargin for sixteen hours at 37°C. The 100% value corresponds to untreated CEM cells. Data are means ±SD of three independent experiments. CEM, parental cell line; NKR, calnexin-deficient cell line. Statistically significant at $p < 0.001$ (two asterisks) and $p < 0.005$ (one asterisk). Experiments performed in collaboration with Dr. A. Zuppini.

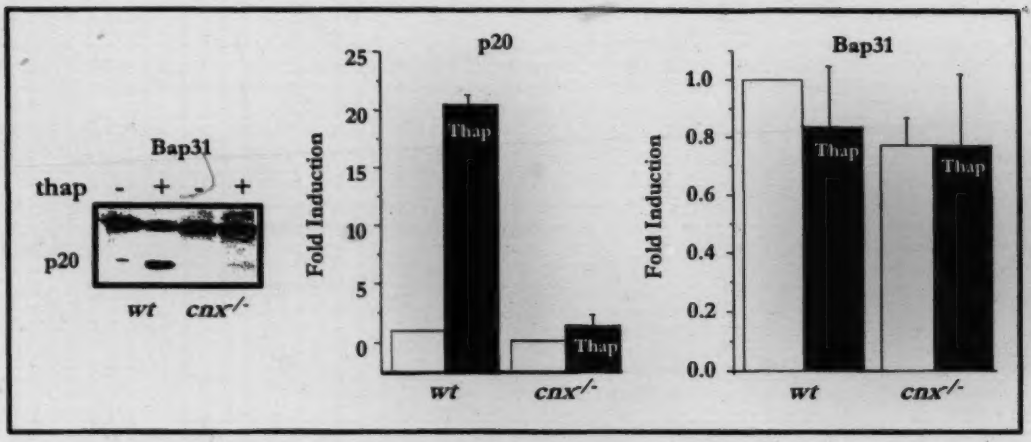

Figure 5- 16

Figure 5- 16 — Expression of Bap31 and generation of the p20 fragment.

Protein extracts were separated by SDS-PAGE (10% acrylamide), transferred onto nitrocellulose membrane and probed with anti-Bap31 antibody. Histograms represent the quantitative analysis of immunoreactive protein bands. Data are mean ±SE of four or more independent experiments. *wt*, wild-type mouse embryonic cell line; *cnx*$^{-/-}$, calnexin-deficient mouse embryonic cell line; white bars, untreated cells; black bars labeled Thap, cells treated with 1 μM thapsigargin for sixteen hours at 37°C. The 1-fold values correspond to untreated wild-type cells. Statistically significant at a p-value of 0.0005 for p20 fragment generation (one-way Anova testing).

The Effect of Caspase Inhibitors on Bap31 Cleavage in Human Leukemic T-cells

Human Bap31 binds caspase 8 proenzyme (Ng and Shore, 1998) and is cleaved upon activation of caspase cascades in HeLa cells, with this cleavage being affected by caspase inhibitors (Maatta et al., 2000). We therefore sought to verify the identity of the caspase that may be responsible for the caspase-dependent cleavage of Bap31 occurring during ER stress-induced apoptosis in the presence (CEM cells), or absence (NKR cells) of calnexin. Cells are incubated with 1 μM thapsigargin in the presence or absence of the caspase 8 inhibitor z-IETD-fmk (20 μM) and the caspase 3 inhibitor z-DEVD-fmk (20 μM). This is followed by western blot analysis to measure Bap31 cleavage. The caspase 8 inhibitor, z-IETD-fmk, prevents considerable Bap31 cleavage in the wild-type cell line and completely prevents any cleavage of Bap31 in the calnexin-deficient cell line (Figure 5- 17). In conjunction, the caspase 3 inhibitor, z-DEVD-fmk also prevents significant cleavage of Bap31 to the p20 fragment. In contrast to the caspase 8 inhibitor, the caspase 3 inhibitor, z-DEVD-fmk, does not abolish Bap31 cleavage in the calnexin-deficient cells (Figure 5- 17). Previous studies with HeLa cells and photodynamic therapy have shown that the caspase 3 inhibitor z-DEVD-fmk blocks cleavage of both caspase 8 and Bap31, suggesting that the processing of these two molecules occurs downstream of caspase 3 activation (Granville et al., 1998). We observe a similar hierarchy of activation in the CEM parental cell line during thapsigargin-induced apoptosis. However, it appears that the calnexin-deficient cells have altered regulation in the apoptotic pathways activated by thapsigargin treatment.

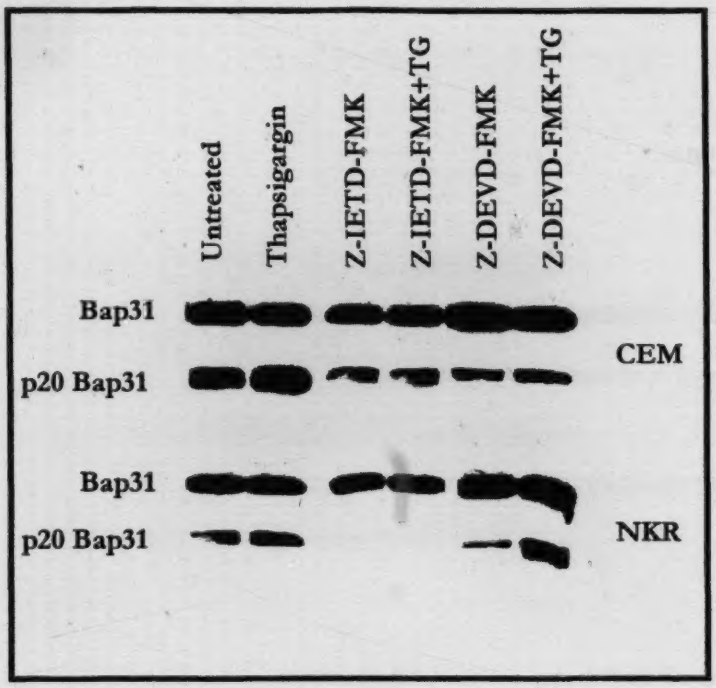

Figure 5- 17

Figure 5- 17 — Expression of Bap31 and generation of the p20 fragment.

Protein extracts were separated by SDS-PAGE (10% acrylamide), transferred onto nitrocellulose membrane and probed with anti-Bap31 antibody. Cells were treated with either 20 μM caspase 8 inhibitor z-IETD-fmk or 20 μM caspase 3 inhibitor z-DEVD-fmk for sixteen hours at 37°C, in the presence or absence of 1 μM thapsigargin. No inhibitors were present in either the untreated or the 1 μM thapsigargin-treated cells. CEM, parental cell line; NKR, calnexin-deficient cell line. Experiments performed in collaboration with Dr. A. Zuppini.

Interaction between Bap31, Caspase 12 and Calnexin

Next, we investigate whether calnexin and Bap31 may form functional protein complexes. To test this we carry out immunoprecipitation experiments. We incubate cellular proteins with anti-Bap31 antibodies, followed with western blot analysis using anti-calnexin antibodies. Figure 5- 18 shows that anti-Bap31 antibodies were able to immunoprecipitate a protein complex in CEM cells, containing immunoreactive calnexin, indicating that calnexin and Bap31 form a complex in the ER. As expected, no calnexin is found in Bap31 immunoprecipitates derived from the NKR calnexin-deficient cells (Figure 5- 18). Western blot analysis reveals that the immunoprecipitated calnexin-Bap31 complex does not contain any calreticulin, ERp57, or Bcl-2 (data not shown). Total cell lysates from CEM (control) and NKR (calnexin-deficient) human leukemic T-cells was incubated with anti-caspase 12 antibody, followed by western blot analysis of immunoprecipitated proteins with anti-Bap31 antibody. Figure 5- 19 showed that a 28-kDa protein band was detected in the western blot analysis by the anti-Bap31 antibody, indicating that the caspase 12-like protein immunoprecipitation retrieved Bap31, suggesting that they form a complex in the ER in the CEM and NKR human leukemic T-cell lines. The interaction between Bap31 and caspase 12 was also observed in the absence of calnexin in the NKR cells (Figure 5- 19). To test if caspase 12 formed a complex with Bap31 in MEFs, we carried out additional immunoprecipitation experiments, utilizing wild-type calnexin-deficient MEFs, with 3T3 cells as a fibroblast control. Anti-Bap31 was able to precipitate a full length Bap31 product (Figure 5- 20A), as well as a product that was recognized by the anti-caspase 12 antibody (Figure 5- 20B) and the anti-calnexin antibody (similar to CEM - Figure 5- 20C). Bap31 interacted with caspase 12 in MEFs, in the presence and absence of calnexin. We concluded that the caspase 12-like protein in humans and caspase 12 in mice both form protein complexes with Bap31.

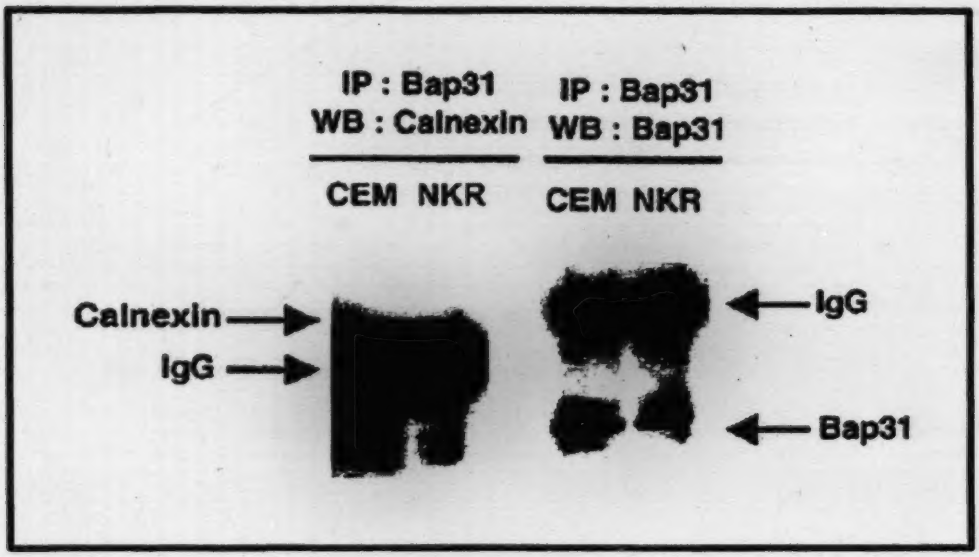

Figure 5- 18

Figure 5- 18 — Bap31 and calnexin complex.

Cellular extracts were immunoprecipitated with anti-Bap31 antibodies, followed by SDS-PAGE (10% acrylamide), transfered to nitrocellulose membrane and Western blot analysis with either anti-calnexin (left) or anti-Bap31 (right) antibodies. Experiments performed in collaboration with Dr. A. Zuppini.

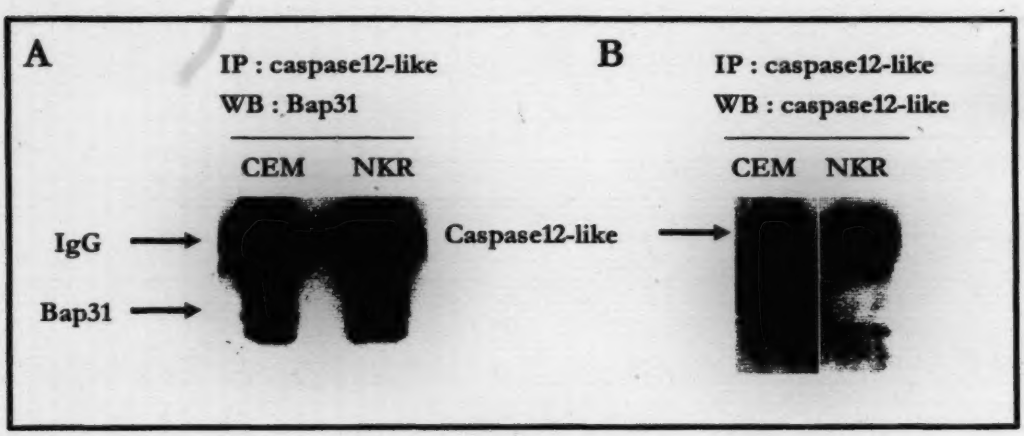

Figure 5- 19

Figure 5- 19 — Caspase 12-like protein and Bap31 form a complex in CEM cells.

Protein extracts were incubated with anti-caspase 12 antibodies, separated by SDS-PAGE (10% acrylamide) and transferred onto nitrocellulose membrane. Western blot analysis was done either with anti-Bap31 *(A)* or anti-caspase 12 *(B)* antibodies. IP, immunoprecipitation; WB, western blot; CEM, wild-type lymphoblasts; NKR, calnexin-deficient lymphoblasts.

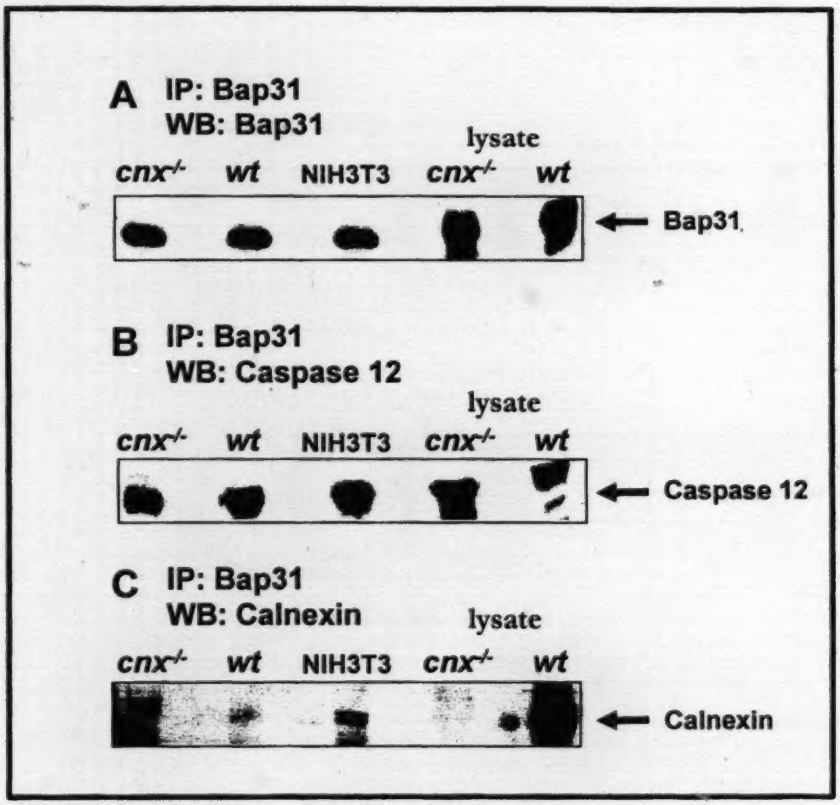

Figure 5- 20

Figure 5- 20 — Caspase 12, Bap31 and calnexin form a complex in MEFs.

Protein extracts were incubated with anti-caspase 12 antibodies, separated by SDS-PAGE (10% acrylamide) and transferred onto nitrocellulose membrane. Western blot analysis was done either with anti-Bap31 *(A)*, anti-caspase 12 *(B)* or anti-calnexin *(C)* antibodies. IP, immunoprecipitation; WB, western blot. Results are representative of three or more independent experiments.

Intracellular Localization of Caspase 12, Calnexin and Bap31 in Wild-type CEM and MEFs

Immunostaining with anti-calnexin antibody reveals a reticulated staining pattern corresponding to the ER in CEM lymphoblasts (Figure 5- 21). An anti-caspase 12 antibody shows a similar dotted staining of CEM cells (Figure 5- 21). Quantitative analysis of merged images indicates that approximately 30% of caspase 12-like protein and calnexin staining overlapped, indicating that they co-localized to the ER (Figure 5-21, merged image).

Indirect immunocytochemistry of MEFs indicated that the majority of calnexin (Figure 5- 22A-red), caspase 12 (Figure 5- 22A-green) and Bap31 (Figure 5- 22B-red) colocalized to the same compartment. Figure 5- 22A and B show that approximately 67.1% (± 1.6%) of caspase 12 positive staining (Figure 5- 22A-green) co-localized with calnexin (Figure 5- 22A-red) and approximately 81.3% (± 3.3%) of caspase 12 positive staining (Figure 5- 22B-green) co-localized with Bap31 (Figure 5- 22B-red). This further supports our observation that caspase 12, Bap31 and calnexin form complexes in the ER.

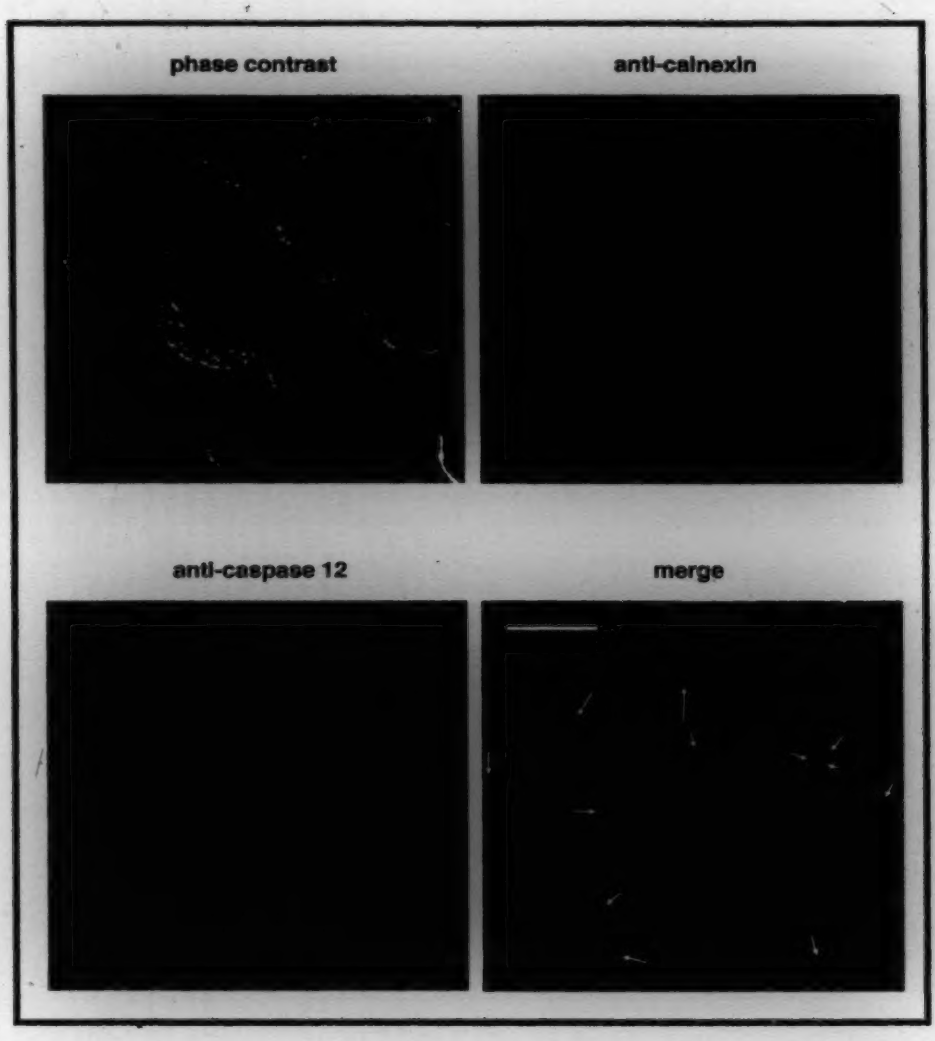

Figure 5- 21

Figure 5- 21 — Immunofluorescence analysis of CEM cells.

Immunolocalization of calnexin (red) and caspase 12-like protein (green). Merged image (bottom right panel) shows that that approximately 30% of anti-caspase 12-like protein positive staining co-localized with calnexin (arrows). Experiments were carried out by Ms. Christine Frantz.

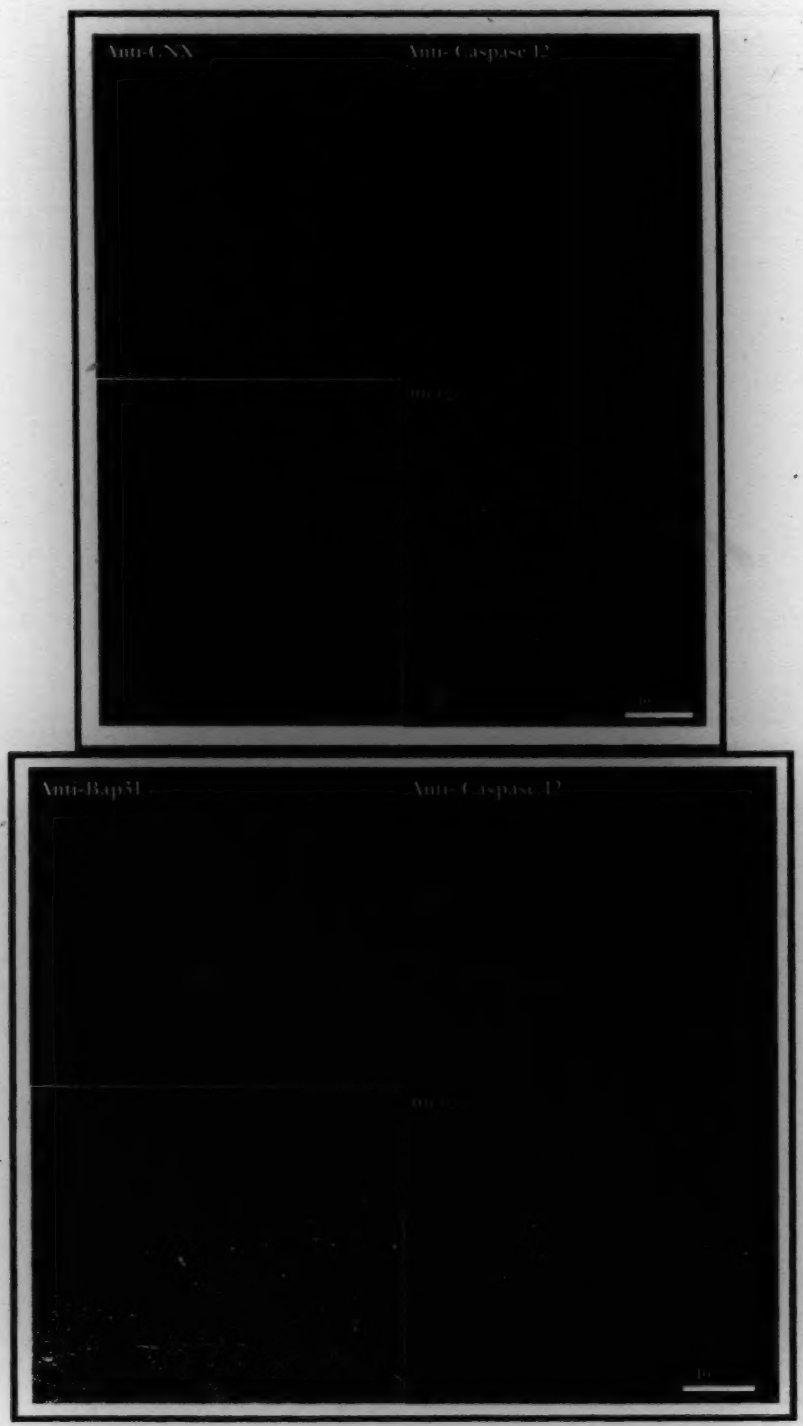

Figure 5- 22

Figure 5- 22 — Coimmunolocalization of calnexin, caspase 12 and Bap31.

Confocal microscopy indicates that these proteins colocalize to the ER in MEFs. Fixed and permeabilized cells were incubated with anti-calnexin (red) and anti-caspase 12 (green). The merged image indicated 67.1% (±1.6%) colocalization of caspase 12 positive staining with calnexin positive staining *(A)*. As well, fixed and permeabilized cells were incubated with anti-Bap31 (red) and anti-caspase 12 (green), with the merged image indicating 81.32% (±3.3%) colocalization of caspase 12 positive staining with Bap31 positive staining *(B)*. The merged image indicates colocalization as designated in white. Data are mean ±SE of three or more independent experiments. The colocalization coefficient value was 0.5565 for caspase 12 and calnexin and 0.5495 for caspase 12 and Bap31.

Discussion

In this study, we investigate a role for calnexin, caspase 12 and Bap31 during ER stress-induced apoptosis. We utilize a calnexin-deficient, leukemic T-cell line (Malyguine et al., 1998; Scott and Dawson, 1995) as well as calnexin-deficient MEFs. Apoptosis assays demonstrate that calnexin-deficient cells were relatively resistant to apoptosis induced by ER stress. We also determine that the cleavage of Bap31 resulting from ER stress, is significantly inhibited in calnexin-deficient cells. While the extent of Bap31 cleavage is reduced, the cleavage of caspase 3 and 8 are unchanged by thapsigargin treatment. Therefore the reduction in the level of Bap31 cleavage may be responsible for the observed resistance of the calnexin-deficient cells to apoptosis induced by ER stress.

In this study we also identified a caspase 12-like protein in human leukemic cell lines CEM (wild-type) and NKR (calnexin-deficient). Analysis of the human genome reveals that the caspase 12 gene contains an internal stop codon, indicating that caspase 12 may not be expressed in the majority of the human population (Fischer et al., 2002; Saleh et al., 2004). However, human T-cells contain a caspase 12-like protein localized to the ER, as demonstrated by immunoreactivity of an anti-caspase 12 antibody against a band in cell lysates. The size of this band corresponds to the molecular weight of caspase 12 and behaves similar in manner to the protein identified in MEFs. In order to determine whether the protein identified in the human cell line is the same as mouse caspase 12, we generated calnexin-deficient and wild-type mouse embryonic fibroblasts (MEFs). We demonstrated by monitoring the processing of caspase 12, that this protein was involved in apoptosis induced by specific ER stress in both human T-cells and mouse cells. Most importantly, we established that caspase 12 formed a complex with Bap31, an ER integral membrane protein which is involved in apoptosis, as well as with calnexin, an ER integral membrane chaperone.

Changes in the expression of calreticulin, an ER luminal homologue of calnexin, affect cell sensitivity to thapsigargin-induced apoptosis (Nakamura et al., 2000). Calreticulin-deficient cells are significantly resistant to apoptosis, with this resistance accompanied by a decrease in the level of release of cytochrome *c* from the mitochondria and by low levels of caspase 3 activity (Nakamura et al., 2000). These results indicate that the ER and the lumen of the ER are intrinsically involved in the release of cytochrome *c* from mitochondria and in the increased caspase activity that occurs during apoptosis.

This suggests "communication" between the ER and mitochondria, which likely involves Ca^{2+} playing an important role in determining cell sensitivity to apoptosis. However, in the leukemic T-cell lines used in the present study, we find that ER-dependent Ca^{2+} homeostasis is not affected in calnexin-deficient cells, indicating that calnexin does not play a role in Ca^{2+} storage in the ER. Despite this, the calnexin-deficient cells are relatively resistant to apoptosis induced by ER stress. This indicates that the role of calnexin deficiency in apoptosis is unlikely to be mediated by Ca^{2+}, allowing the suggestion that luminal and integral membrane proteins of the ER may act with different mechanisms during apoptosis. Interestingly, a deficiency in calnexin along with the addition of caspase inhibitors appeared to disrupt the recovery from high cytoplasmic Ca^{2+} levels. Calnexin as a chaperone may affect the function of SERCA or the IP_3R or both. The chaperone function of calnexin may also play a critical role during intracellular Ca^{2+} signaling via the localization and function of plasma membrane transporters. This regulation of intracellular Ca^{2+} levels may be lost under conditions of calnexin deficiency and caspase inhibition.

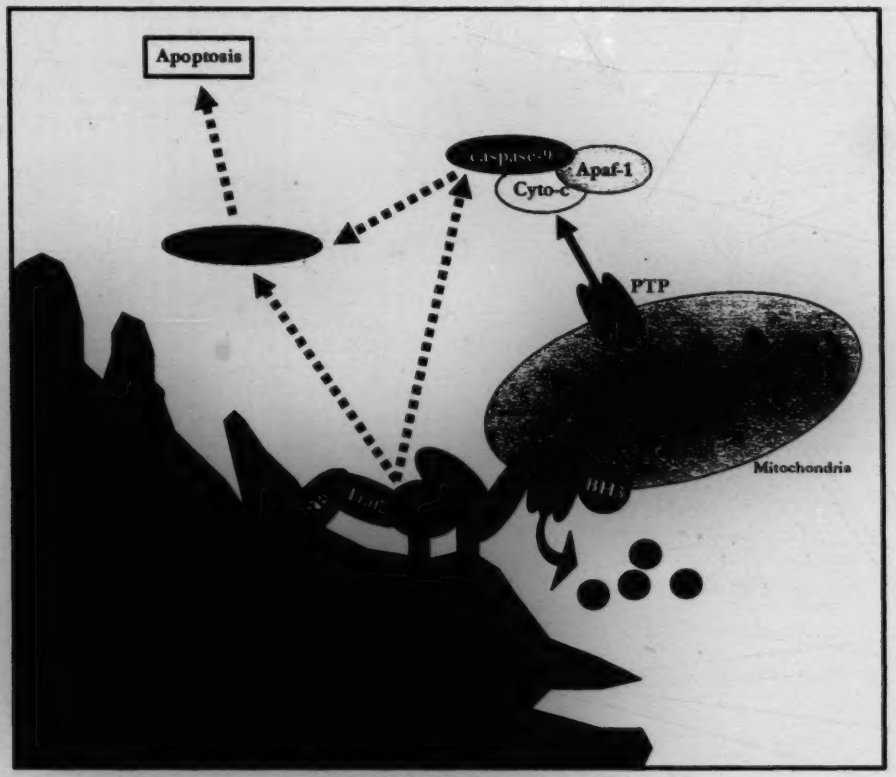

Figure 5- 23

Figure 5- 23 — Model of the regulation of ER stress induced apoptosis.

Caspase 12, Bap31 and calnexin form complexes that may be stimulated under conditions inducing ER stress. This may provide a link between ER stress and apoptosis. PTP, permeability transition pore; Apaf-1, apoptosis protease associated factor-1; Cyto-c, cytochrome *c*; Drp1, dynamin related protein-1; IRE1, inositol response element 1; TRAF2, TNF-receptor associated factor 2; BH3, BH3 domain containing protein.

In the absence of calnexin, there is a disruption in the transduction of the apoptosis signal. Interestingly, even though thapsigargin-induced cell death is significantly reduced in calnexin-deficient cells, the activation of caspase 12 and caspase 3 is not altered. A previous study on apoptosis induced by photodynamic therapy, suggests that processing of caspase 8 and Bap31 might occur downstream of caspase 3 activation (Granville et al., 1998). However, we find that caspase 8 is not activated in calnexin-deficient human leukemic T-cells (NKR). Despite these changes, thapsigargin treatment induces mitochondrial apoptotic pathways (with the consequent release of cytochrome *c* from the mitochondria) in both CEM and calnexin-deficient NKR cell lines. We have demonstrated an interaction between Bap31, calnexin and caspase 12 (Figure 5- 23). One important finding of this work was the identification of caspase 12-Bap31-calnexin complexes localized to the ER membrane. Together, these data suggested that the Bap31 complex (Ng and Shore, 1998) might also include calnexin and caspase 12, assisting in the functioning of the signaling complex that triggers apoptosis in response to ER stress. Caspase 12, Bap31 and calnexin may also form a novel complex, specifically activated under conditions of ER stress, which will require additional investigation. These findings support the hypothesis that calnexin plays a role in modulating cell sensitivity to apoptosis induced by ER stress, in conjunction with caspase 12 and Bap31. The complex comprising caspase 12, Bap31 and calnexin must be important in the apoptotic cascade stimulated by ER stress in two ways: first, in the perception of the signal, with the consequent activation of caspase 12; and second, in the cleavage of Bap31, followed by generation of the apoptotic p20 fragment and stimulation of the mitochondrial pathway (Figure 5- 23). The human leukemic T-cells as well as the MEFs were able to perceive the signal that results from thapsigargin treatment and to initiate the programmed cell death cascade, in particular activating the mitochondrial pathway. However, calnexin-deficiency apparently affected this apoptotic cascade by blocking the cleavage of Bap31. Calnexin may be a link which allows activation of caspase 8 or 12 and the consequent cleavage of Bap31 to produce the apoptosis inducer fragment p20. One Bap31-interacting membrane protein, the putative ion channel protein of the endoplasmic reticulum, A4, was identified as a constitutive binding partner of Bap31 in human cells (Wang et al., 2003) and may be involved in signaling Ca^{2+} release from the ER and subsequent uptake into the mitochondria. It

appears that ER luminal factors are able to manage the chaperones responsible for protein folding and transcriptional cascades, as well as directly regulating proteins involved in apoptosis (Berridge, 2002; Breckenridge et al., 2003a). Our results are consistent with the view that calnexin, Bap31 and caspase 12 may form functional complexes which play an important role during ER stress-induced apoptosis (Figure 5-23). In conclusion, we demonstrate that calnexin may not be essential during initiation of ER stress, but that the protein plays an important role in later events involving ER stress-induced Bap31 cleavage and DNA fragmentation. These findings further support that apoptosis may depend on both the presence of external apoptosis-activating signals and internal factors represented by the ER and other intracellular organelles.

Chapter Six — Structural and Functional Analysis of Calreticulin and Calnexin

Versions of this chapter have been previously published:

1. Anna Zuppini, Jody Groenendyk, Lori A. Cormack, Gordon Shore, Michal Opas, R. Chris Bleackley and Marek Michalak. **Calnexin Deficiency and Endoplasmic Reticulum Stress-Induced Apoptosis.** Biochemistry, 41 (8), 2850 -2858, 2002.

2. Lei Guo, Jody Groenendyk, Sylvia Papp, Monika Dabrowska, Barbara Knoblach, Cyril Kay, J. M. Robert Parker, Michal Opas and Marek Michalak. **Identification of an N-domain Histidine Essential for Chaperone Function in Calreticulin.** J. Biol. Chem., Vol. 278, Issue 50, 50645-50653, December 12, 2003.

3. Virginie Martin, Jody Groenendyk, Simone Steiner, Lei Guo, Monika Dabrowska, J.M. Robert Parker, Werner Müller-Esterl, Michal Opas and Marek Michalak. **Identification by Mutational Analysis of Amino Acid Residues Essential in the Chaperone Function of Calreticulin.** The Journal of Biological Chemistry vol. 281, no. 4, pp. 2338–2346, January 27, 2006.

4. Jody Groenendyk, Anna Zuppini, Gordon Shore, Michal Opas, R. Chris Bleackley and Marek Michalak. **Caspase 12 in Calnexin-deficient Cells.** Submitted 2006.

The ER performs a valuable function in being the major storage organelle for intracellular Ca^{2+} (micro to millimolar range), therefore involved in the management of many cellular processes. Perhaps an equally important role of the ER includes the synthesis, folding and post-translational modification of membrane associated, secreted and integral membrane proteins (Baumann and Walz, 2001; Sitia and Braakman, 2003), many of these proteins being glycosylated. These tasks are performed in the lumen of the ER in conjunction with Ca^{2+}-dependent chaperones responsible for the appropriate folding of nascent glycoproteins and the prevention of improperly folded proteins (Molinari and Helenius, 2000). The ER folding program is termed quality control and is comprised of several proteins, including calreticulin and calnexin (Bedard et al., 2005; Groenendyk and Michalak, 2005).

We manipulate the ER luminal environment to further understand what it does. In this study, site specific mutations of calreticulin and calnexin were observed with resultant effects on their chaperone function as well as protein interactions necessary for chaperone function and apoptosis. We identified a role for specific residues of calreticulin and calnexin and ER luminal conditions that are necessary for protein folding, as well as protein interactions involved in apoptosis.

Identification of a critical histidine residue in calreticulin, His153, involved in the coordination of Zn^{2+} in the N-domain of calreticulin, is observed to be essential for the function of calreticulin. Mutation of this amino acid abolishes the chaperone function of calreticulin as observed *in vivo* and *in vitro*. The His153Ala mutation result in local changes in the conformation of calreticulin and this severely affects its ability to function as a molecular chaperone. Identification of two essential tryptophan residues, Trp244, located at the tip of the P-domain and Trp302, located at the base of the P-domain close to the oligosaccharide binding pocket of the globular N-domain, are observed both *in vivo* and *in vitro* to be necessary for the chaperone function of calreticulin. Mutation of Trp302Ala results in significant modification to the secondary structure in the oligosaccharide binding domain of calreticulin, abolishing the chaperone function of calreticulin. Mutation of Trp244Ala results in the most severe effect on calreticulin function with a disturbance of the tertiary structure at the tip of the P-domain, translating to a disruption of the chaperone function of the globular N-domain. Two amino acids important for calnexin function, Glu351 and Trp428, were observed to

directly regulate the structure of calnexin. Mutation of Glu351Arg and Trp428Ala disrupted calnexin chaperone function *in vitro* as well as disrupted the tertiary structure of calnexin.

Identification of calreticulin and calnexin amino acids involved in the interaction with ERp57 were also determined, with mutation of the calreticulin residues Asp241Arg and Trp244Ala not binding ERp57 and calreticulin residues Glu239Arg and Glu243Arg demonstrating significantly reduced ERp57 binding. These amino acid residues in calreticulin are all localized to the tip of the P-domain, presumably where ERp57 binding occurs. A similarly located conserved residue in calnexin, Glu351Arg (conserved with calreticulin Glu243Arg) did not demonstrate the same disturbance in ERp57 binding, implying these two proteins may interact with ERp57 in slightly different manners. Interestingly, mutation of another amino acid in calreticulin, Trp302Ala, also affects ERp57 binding, with this residue located in the globular N-domain. Mutation of Trp302Ala results in significantly enhanced ERp57 binding as a result of either stabilization of the P-domain, with the ability to bind more ERp57, or exposing another ERp57 binding site located at a different location. Mutation of this conserved residue in calnexin, Trp428Ala, also demonstrated enhanced ERp57 binding, presumably as a result of structural changes in the conformation of the protein. Identification of factors in the ER necessary for the proper conformation of calreticulin and calnexin were recognized, including Zn^{2+}, Ca^{2+} and ATP. Utilizing these site directed mutants of both calreticulin and calnexin, Zn^{2+} was determined to play an important role as a structural molecule in the N-domain. Ca^{2+} was determined to perform a task as an enhancer of stability in calreticulin and calnexin. Calreticulin and calnexin were observed to bind ATP using the sensitive technique, SPR analysis.

As a specific conformation is necessary for chaperone function, this conformation may also be a direct regulator of ER stress-induced apoptosis. Calnexin-deficient human T-lymphoblast and calnexin-deficient MEFs were determined to have abolished Bap31 cleavage as well as resistance to apoptosis. Identification of the involvement of caspase 12 in ER stress-induced apoptosis, with formation of a three way complex between calnexin, Bap31 and caspase 12, may be involved in the proper transmission of ER stress inducing apoptosis, specifically recruiting the mitochondria.

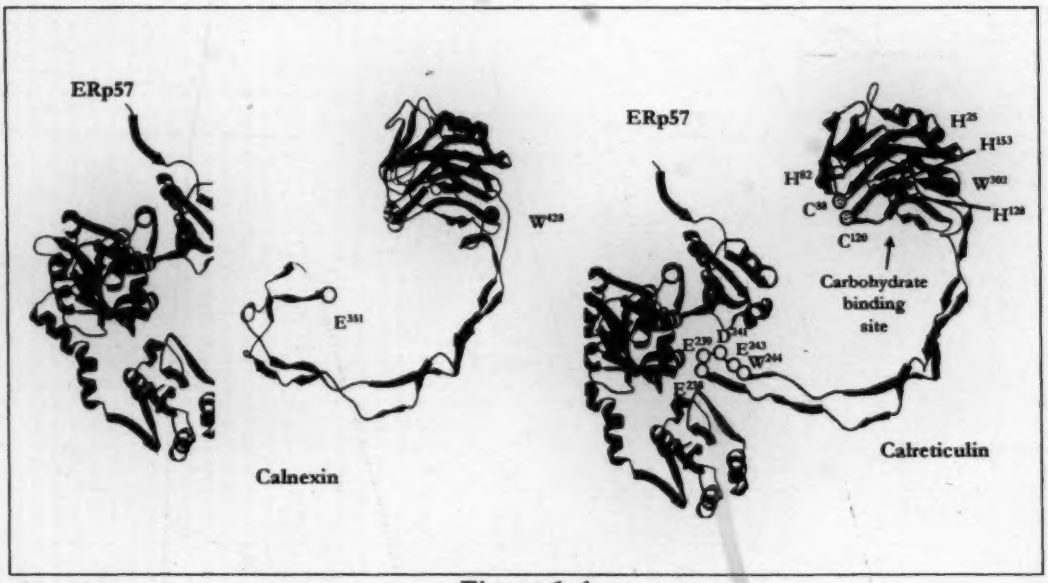

Figure 6- 1

Figure 6- 1 — Model of the interaction between ERp57 and calreticulin or calnexin with the location of the mutated amino acid residues.

ERp57 may be made of three domains connected by two loops. The loops may be bent to form a pocket surrounded by two site domains. An arginine-rich pocket of the ERp57 structure formed by three domains may slide over the tip of the P-domain (in *red*) of calreticulin or calnexin to form a structural and functional complex. The locations of Glu238, Glu239, Asp241, Glu243 and Trp244 at the tip of the P-domain, Trp302 in the carbohydrate putative pocket and Cys88 and Cys120 at the surface of the N-domain to form the disulfide bond are indicated by yellow, green and blue balls, respectively. The Glu351Arg and Trp428Ala mutations of calnexin are demonstrated with blue and green balls respectively. The N and P-domain of calreticulin are modeled based on the NMR studies of the P-domain of calreticulin (Ellgaard et al., 2001b) and crystallographic studies of calnexin (Schrag et al., 2001).

3D Model of Calreticulin and Calnexin

Recent modeling studies of the 3D structure of calreticulin (Michalak et al., 2002b), based on crystallographic data available for calnexin (Schrag et al., 2001) and NMR data available for the P-domain of calreticulin (Ellgaard et al., 2001b), suggest a strong structural homology between calreticulin and calnexin (Figure 6- 1). This information provides the framework for targeting specific amino acids for mutation, for the interpretation of our results and for identifying the role of specific amino acids in protein folding. X-ray crystallographic studies of the soluble portion of calnexin verify that the N-domain consisted of a globular β-sandwich domain with the P-domain forming an extended hairpin arm containing the repeat motifs (Schrag et al., 2001). Model predictions of calreticulin suggest that, similar to calnexin, the central P-domain of calreticulin also forms an elongated hairpin-like structure (Ellgaard et al., 2001b), with the N-domain composed of a globular β-sheet structure (Michalak et al., 2002b) (Figure 6- 1). This extended arm is curved, creating an opening which likely guides substrates to the peptide and oligosaccharide binding sites found in the globular N-domain (Ellgaard et al., 2001b). The P-domain together with this globular N-domain was previously identified as the functional folding unit in calreticulin (Michalak et al., 2002b; Nakamura et al., 2001b), as well as in calnexin (Leach et al., 2002).

Importantly, this model of the structure of calreticulin helps to visualize the location of amino acid residues investigated in this study (Figure 6- 1). The histidine residues postulated to interact with Zn^{2+}; His25, His82 and His128, are all found on the outer surface of the globular N-domain of the protein, away from the extended arm structure of the P-domain (Figure 6- 1) as well as from the substrate binding region in calreticulin and therefore, their mutation or deletion has no effect on the chaperone function of calreticulin. In contrast, His153 is localized on the top of a loop which is part of a short β-strand located at the interface between the globular N-domain and the hairpin P-domain (Figure 6- 1). Importantly, this loop containing His153 is predicted to be flexible with lateral movement towards the base of the P-domain. This flexibility may significantly influence the shape of the substrate (carbohydrate) binding pocket (Figure 6- 1). As well, observation of the cysteine residues forming the disulfide linkage (Cys88 and Cys120) demonstrates the dependence of the protein on this covalent linkage for proper conformation of the N-domain, specifically holding together two β-strands of the

N-domain. It is easy to see that if this bond is abolished the globular structure of the N-domain will be partially lost. The P-domain of calreticulin forms an unusual extended hairpin-like structure that loops back on itself with both ends in close proximity (Ellgaard et al., 2001b). This hairpin is stabilized by three pairs of short antiparallel β-sheets in calreticulin (Figure 6- 1), or four in calnexin. Three small hydrophobic clusters containing two tryptophan rings, including Trp244, provide additional stability (Ellgaard et al., 2001b) (Figure 6- 2A). As calreticulin and calnexin share a large degree of homology, we targeted several conserved amino acid residues for mutational analysis. The Glu351 amino acid is also located in the P-domain, not at the tip but along the one curved edge, however it is conserved between calreticulin and calnexin. The Trp428, also conserved, is located in a similar region in calnexin as compared to calreticulin. This loop containing the tryptophan appears to be flexible and may modulate the movement of the P-domain, thereby regulating the interactions of this domain with other substrates, including ERp57.

Amino Acid Residues Necessary for the Structure and Function of Calreticulin and Calnexin

We demonstrate that His153 is essential for chaperone function and is involved in the coordination of Zn^{2+} binding, necessary for structural stability of calreticulin, with the resultant effect on function. We also report identification of two tryptophan residues that are critical for the chaperone function of calreticulin; Trp302 located in the carbohydrate binding pocket and Trp244 found at the tip of the extended arm of the P-domain. Furthermore, we identify four other amino acid residues at the tip of the extended arm of the P-domain of calreticulin that are important in the binding interaction between ERp57 and calreticulin. We also determine that cysteine residue mutations are only able to recover chaperone function to approximately 40%. In calnexin, amino acid mutations, Glu351Arg and Trp428Ala, disrupted calnexin structure and function. Glu351Arg, found in the P-domain, caused subtle shifts in structure with minor changes in chaperone function, while Trp428Ala, located at the base of the P-domain, had more severe effects on structure and therefore function.

In Vivo and In Vitro Functional Analysis

We observe using functional assays such as bradykinin-dependent Ca^{2+} release (Nakamura et al., 2001b) and substrate aggregation (Saito et al., 1999) that specific amino acids, His153, Trp244 and Trp302 are directly responsible for calreticulin chaperone function, as when they are mutated, chaperone function is disrupted. Yet these mutants have no effect on the Ca^{2+} capacity of the ER stores, implying the functional effect is most likely dependent on the chaperone function and not the Ca^{2+} buffering capacity of calreticulin. Calnexin chaperone function was also disrupted with the two mutations, Glu351Arg and Trp428. Wild-type S-Cnx was able to prevent the thermal aggregation of IgY efficiently, while purified S-Cnx containing the Glu351Arg and Trp428Ala mutations lost most of its ability to prevent thermal aggregation. This result suggested that both the Glu351Arg mutation and the Trp428Ala mutation affect the chaperone activity of calnexin, presumably as a result of conformational changes. Interestingly, wild-type S-Cnx prevented the thermal aggregation of MDH with both mutations actually resulting in faster thermal aggregation of MDH. This demonstrated that S-Cnx was able to chaperone the non-glycosylated MDH substrate but that both mutations may be involved in protein interactions with substrate. The increase in aggregation may result from S-Cnx binding MDH and forming larger aggregates or directly precipitating the substrate. The important amino acids in calreticulin, His153, Trp244 and Trp302, as well as in calnexin, Glu351 and Trp428, demonstrated the dependence of chaperone function of calreticulin and calnexin on the specific amino acid sequence of the proteins.

Calreticulin and Calnexin Interaction with ERp57

Utilizing SPR analysis, we demonstrate a robust interaction between calreticulin and ERp57 and calnexin and ERp57. NMR structural studies in conjunction with biochemical analysis of the P-domain of calreticulin have demonstrated that the tip of the extended arm, comprised of residues 225-251, is responsible for the interaction with ERp57 (Ellgaard et al., 2002; Frickel et al., 2002; Leach et al., 2002). We examine several amino acid residues at the tip of the P-domain to identify what role they may play in ERp57-calreticulin interactions (for the location of specific residues see Figure 6- 1). Interestingly, site specific mutation of amino acids Asp241Arg and Trp244Ala found at the tip of the P-domain in calreticulin, abolish ERp57 interactions, mutations at Glu239Arg and Glu243Arg demonstrate reduced binding of ERp57, while mutation of

Glu238Arg do not effect ERp57 binding to calreticulin (Figure 6- 1). We conclude that the negatively charged amino acid residues Glu239, Asp241 and Glu243 and the residue Trp244 are critical for formation of the ERp57-calreticulin complex (Figure 6- 1). The residues Glu239, Asp241 and Glu243 are located on the inside curve at the tip of the P-domain, likely providing electrostatic forces important for the interaction of ERp57 and calreticulin (Figure 6- 1). The Trp244 amino acid residue may be vitally positioned to maintain the structural stability of the hairpin fold of the P-domain (Figure 6- 2). Our results also indicate that an interaction with ERp57 is not vital for the chaperone function of calreticulin as observed in our assays, as mutants Glu239Arg, Asp241Arg and Glu243Arg, which do not bind ERp57 efficiently, are able to fully restore the bradykinin-dependent Ca^{2+} release in calreticulin-deficient cells. ERp57 may still be necessary for the interaction of calreticulin with other substrates and this may be an exclusive result.

Recent studies using glutathione S-transferase (GST) pull down experiments demonstrate that ERp57, as well as interacting with calreticulin, also binds to the P-domain of calnexin (Leach et al., 2002). This interaction is further narrowed down using NMR analysis, which demonstrates that specific single amino acid mutations at the tip of the P-domain of calnexin have no significant effect on ERp57 binding; however, when two amino acids are mutated in unison, ERp57 binding is lost (Pollock et al., 2004). These sites are identified as Asp342, Asp344, Asp346, Asp348, Glu350 and Glu352, all involved in the interaction of calnexin with ERp57, with the amino acid residues Asp344 and Glu352 playing a central role in the interaction (Pollock et al., 2004). This supports our SPR data which implicates the conserved residues, Glu243 (calnexin Glu351 in our study, Glu352 in Pollock et al. (Pollock et al., 2004)) and Glu239 (calnexin Asp344 (Pollock et al., 2004)) as important residues for ERp57 binding to calreticulin. Similar to Pollock et al. (Pollock et al., 2004), SPR analysis of calnexin mutants, Glu351Arg and Trp428Ala, showed that a single site mutation in calnexin was not enough to abolish the interaction with ERp57. Wild-type S-Cnx interacted with ERp57, while mutation of Glu351Arg (our study, same as the Glu352 mutant (Pollock et al., 2004)) did not lead to a loss in the interaction with ERp57. The Trp428Ala mutation also did not abolish ERp57 binding, but actually enhanced the interaction with ERp57. This enhancement in binding may potentially be a result of exposure of several more ERp57 binding sites,

such as the Zn^{2+}-dependent ERp57 binding site found in the N-domain (Leach et al., 2002), or tighter interactions at the primary binding site. This was similar to what we observed for the conserved Trp302Ala mutation in calreticulin. These were interesting observations considering the tip of calreticulin and calnexin have a different shape and length. Calnexin P-domain contains a disulfide linkage creating a kink, bringing the tip of the P-domain back towards the globular N-domain. Recent work supports the interaction of ERp57 with calreticulin and calnexin involving the most distal set of conserved repeats (Leach et al., 2002), with ERp57 draping over this region and appearing to have a large amount of movement (Williams, 2006). This movement may be essential for the thiol reductase activity of ERp57, allowing the enzyme to access many regions of the substrate that is interacting with calreticulin or calnexin, generating numerous disulfide linkages in the least amount of time, energy and space. This flexibility may also allow ERp57 to interact with the globular N-domain of calreticulin or calnexin, potentially explaining the results observed with mutation of the tryptophan found at the base of the P-domain. Both calreticulin and calnexin contain a Zn^{2+}-dependent ERp57 binding site in the N-terminal globular domain (Leach et al., 2002). Trp302Ala (Trp428Ala in calnexin) may regulate the flexibility of the P-domain, swinging ERp57 closer to the globular domain, allowing further interactions to occur. As well, interaction of ERp57 with the P-domain of calreticulin and calnexin also appears to be mediated via the b′ domain of ERp57 (ERp57 contains four domains, a, a′, b and b′) (Williams, 2006), as well as through the positively charged C-terminus of ERp57 (Russell et al., 2004; Silvennoinen et al., 2004). This acidic tail is not modeled in our rendition of ERp57 (Figure 6- 1) and may interact with the globular N-domain, potentially responsible for the Zn^{2+}-dependent ERp57 binding observed in previous work (Leach et al., 2002). Further work needs to be done to identify the specific amino acids, potentially the conserved Trp350, similar to the calreticulin amino acid Trp244 (Trp351 in calnexin mouse/dog sequence), or the conserved Asp348, similar to the calreticulin amino acid Asp241 (Asp349 in calnexin mouse/dog amino acid sequence), which lead to complete abolishment of the interaction of calreticulin with ERp57, that may lead to complete loss of ERp57 binding to calnexin. Thus, it appears that clusters of negatively charged residues at the tip of the P-domain, in both calreticulin and calnexin, as well as a strategically positioned tryptophan residue in the globular domain, located at the base of

the P-domain, may play an important role in promoting and stabilizing the association with ERp57.

Site Specific Mutations of Calreticulin and Calnexin with Subsequent Modification of Conformation

Structural studies identify the His153Ala and the Trp244Ala mutations as responsible for significant modification of secondary and tertiary structure compared to the wild-type calreticulin. The His153Ala mutation results in decreasing intrinsic fluorescence and hydrophobicity, as well as increasing protease susceptibility and significant changes in secondary structure as observed by CD analysis. The other site specific mutation that affects the global conformation of calreticulin is the Trp244Ala mutation. This mutation leads to the loss of all Ca^{2+}-dependent resistance to protease digestion as well as having an alteration in secondary structure as measured by CD analysis, an indication of conformational changes in the structure of calreticulin. Clearly, the His153Ala mutation and the Trp244Ala mutation result in local conformational changes with a potential to significantly affect the function of calreticulin. Observation of the two calnexin mutations, Glu351Arg and Trp428Ala, demonstrated the importance of the tryptophan found in the globular N-domain for the structural conformation of S-Cnx. The Trp428Ala mutation resulted in major alterations in the conformation of the protein while the Glu351Arg mutation did not significantly affect the protein conformation.

ER Factors Responsible for Regulating the Conformation of Calreticulin and Calnexin

As the lumen of the ER is a dynamic and variable environment designed for the task of folding, it contains a high concentration of Ca^{2+} binding chaperones and an optimal concentration of ions and nucleotides necessary for proper protein folding, modification and assembly. Factors within the ER, such as Zn^{2+}, Ca^{2+} and ATP, are all necessary for a functioning cell and appear to regulate the conformation of calreticulin and calnexin. Using intrinsic fluorescence, CD analysis and limited proteolysis, we observed that addition of these factors significantly affected the structure of the two proteins, with resultant functional cost. As suggested previously (Corbett et al., 2000; Nigam et al., 1994; Ou et al., 1995; Saito et al., 1999), both calreticulin and calnexin bind Ca^{2+}, ATP and Zn^{2+}, with modification of the conformation of the proteins and

therefore the function. Similar to previous results (Corbett et al., 2000; Nigam et al., 1994; Ou et al., 1995; Saito et al., 1999), wild-type calreticulin is observed to be significantly resistant to protease digestion in the presence of Ca^{2+}. As well, wild-type calreticulin demonstrates a significant increase in intrinsic fluorescence intensity with the addition of Zn^{2+}, an indication of Zn^{2+}-dependent conformational changes in the protein. Importantly, these Zn^{2+}-dependent conformational changes, a signature of calreticulin behavior (Khanna et al., 1986), are compromised in the His153Ala mutant. It appears that His153Ala coordinates Zn^{2+} that is necessary for maintaining the proper conformation of calreticulin. This agrees with our previous observation that the N-domain histidine residues are involved in Zn^{2+} binding to calreticulin (Baksh et al., 1995b). As well, the Trp244Ala mutation in calreticulin demonstrates major alterations upon the addition of Zn^{2+}. Likely the Trp244Ala mutation disrupts the Zn^{2+} binding domain of calreticulin, with a subsequent conformational change. The Trp244Ala and the Glu243Arg mutation result in a loss of protection by Ca^{2+} in the presence of a protease. Calreticulin binds Ca^{2+} in a high affinity and low affinity manner, while calnexin binds only in a high affinity manner, with Ca^{2+} altering the conformation of the proteins. In calnexin, Zn^{2+} binding resulted in significant changes, appearing to lead to a less compact protein, potentially allowing a more flexible chaperone, able to interact with a variety of diverse substrates with different shapes and sizes. ATP appeared to partially relax domains of the protein as seen using limited digestion. ATP binding compressed other portions of the protein with an increase in the secondary structure and conformation of the protein, as observed using CD analysis and intrinsic fluorescence. Ca^{2+} appeared to have the contradictory effect, with compression of the conformation as observed by limited digestion and intrinsic fluorescence, but with a loss in secondary structure as seen using CD analysis. Chelation of this Ca^{2+} by EGTA abolished the global changes completely, with the protein completely non-responsive to Zn^{2+} or ATP. We suggest that the presence of the high affinity resident Ca^{2+} resulted in a global tightening of the conformation of calnexin, while the addition of Zn^{2+} and ATP only affected local domain conformation.

The ER lumen also contains ATP, required to support the correct folding of nascent proteins, as well as formation of disulfide linkages within these proteins. SPR analysis demonstrated that calreticulin and calnexin bound ATP and that the site specific

mutations generated in this study did not significantly affect this interaction. Previous observations demonstrate that ATP renders calreticulin more resistant to protease digestion and enhances the aggregation suppression activity of calreticulin and calnexin *in vitro* (Corbett et al., 2000; Ihara et al., 1999; Ou et al., 1995; Saito et al., 1999). While there is no obvious ATP binding region, Corbett et al. observes protection of the C-domain of calreticulin from proteolysis with the addition of ATP during protease digestion studies (Corbett et al., 2000), suggesting that the C-domain of calreticulin may be involved in the interaction with ATP. In the future, we will attempt to identify the ATP binding region of both calreticulin and calnexin by site specific mutation of a putative ATP binding site. Results indicate that calreticulin and calnexin interact with Ca^{2+}, Zn^{2+} and ATP, with a conformational requirement for these factors, modulating the chaperone function of the proteins.

Specific Amino Acid Mutations that Disrupt Function are Directly involved in Structure and Conformation of the Protein

As identified in this study, mutation of Trp244Ala results in the most severe effects on calreticulin function. The Trp244Ala mutant of calreticulin is unable to restore bradykinin-dependent Ca^{2+} release in calreticulin-deficient cells, it does not prevent thermally-induced aggregation of MDH or IgY and it does not bind ERp57. Biophysical studies of this calreticulin mutant suggest that conformational changes might be responsible for its loss of chaperone activity and lost ability to form a complex with ERp57. Tryptophan residues are a bulky amino acid containing an aromatic conjugated indole ring of unsaturated bonds. Mutation of this amino acid must significantly affect local conformation, similar to that observed in this study. The indole rings of Trp244 and Trp236 located at the tip of the P-domain (Figure 6- 2A and C), appear to stabilize this region of the P-domain, as modeling studies demonstrate the manifestation of an unstable cavity when amino acid Trp244Ala is mutated (Figure 6- 2B and D), as well as disrupting the interaction with ERp57. This, in turn, must have a significant effect on the ability of the substrate (carbohydrate) to bind to the globular N-domain of calreticulin. Interestingly, the Trp302Ala mutation also results in drastic abolishment of calreticulin function in a similar manner to the Trp244Ala mutation, with one exception. The Trp302Ala mutation, found in the globular domain at the base of the P-domain, actually

enhances the interaction with ERp57, potentially regulating the flexibility of the P-domain, or exposing a secondary ERp57 binding site. This enhancement was also observed during calnexin interaction with ERp57 (Trp428Ala), further verifying the importance of a single amino acid in the globular N-domain, with the ability to regulate another distant region of the protein.

Conformation of Calreticulin and Calnexin Regulates Function

The ability of calreticulin and calnexin to interact with a variety of factors and substrates demonstrates their dynamic nature. This adaptability is necessary to facilitate the binding and folding of these nascent substrates and factors. Results from this study demonstrate that calreticulin and calnexin are flexible proteins and their conformation is critical for the chaperone function. Alterations in the dynamics of the ER environment influence the structure of calreticulin and calnexin. These structural changes may explain how the ER luminal environment can influence and control the function of molecular chaperones. The likelihood of the two proteins being highly flexible in solution is consistent with the proteins being less amenable to crystallization. Previous experiments have demonstrated that protease digestion of either calreticulin or soluble calnexin in the presence of Ca^{2+} yields a protease resistant fragment (Corbett et al., 1999; Ou et al., 1995). However all attempts to crystallize the two proteins have been unsuccessful (Hahn et al., 1998) until only recently, with the crystallization and X-ray diffraction of the soluble portion of calnexin (Schrag et al., 2001). Crystallization of the protease resistant fragment of luminal calnexin, consisting of residues 47-468, with no density observed for residues 92-101 and 262-270, was only possible at 4°C and in the presence of 35 mM $CaCl_2$ (Schrag et al., 2001). Addition of Ca^{2+} must induce rigidity in the globular N-domain of the protein, while the lower temperature reduces the flexibility of the protein, with the resultant generation of a crystal suitable for X-ray diffraction and analysis. The same has not been acheived for calreticulin to date, potentially because of the lack of a similar Ca^{2+} binding site in the N-domain.

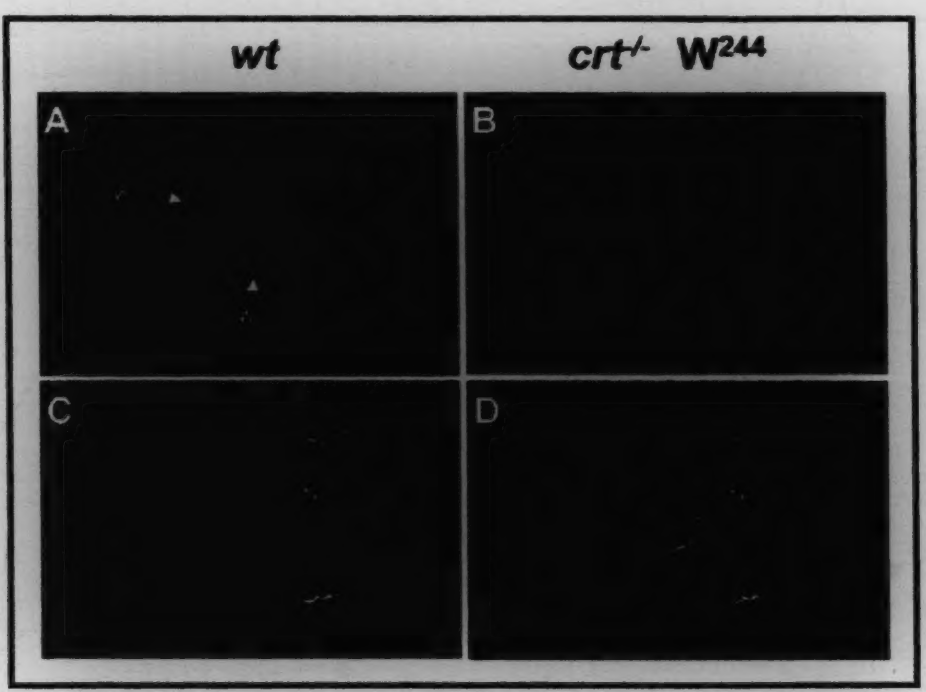

Figure 6- 2

Figure 6- 2 — Three-dimensional structure of the tip of the P-domain of calreticulin.

The structure of the tip of the P-domain of calreticulin is based on NMR studies (Ellgaard et al., 2001b). *A* and *C*, wild-type calreticulin; *B* and *D*, Trp244Ala calreticulin mutant. The location of the pair of interactive tryptophan residues Trp244Ala *(yellow)* and Trp236 *(green)* is indicated. *C* and *D*, a stereo view of the electron density around the Trp244Ala, indicating a cavity *(D)* in the P-domain with the mutated Trp244Ala.

Contrasts between Calreticulin and Calnexin

A family of lectin-like chaperones localized to the ER, calreticulin and calnexin perform an important role in the quality control of nascent glycoproteins, specifically interacting with monoglucosylated carbohydrates. There are a number of protein substrates which are exclusive to either calreticulin or calnexin (Michalak et al., 1999) and it is not clear what determines this substrate specificity. Based on our observations in this study and in previously published work, there are several major differences between calreticulin and calnexin. A Ca^{2+} binding site located in the N-domain of calnexin, composed of pairs of acidic amino acids (Tjoelker et al., 1994) that is not found in the N-domain of calreticulin, may potentially play a role during substrate specificity, as well as involved in structural stability. This Ca^{2+} binding site in calnexin has not been investigated. The flexibility of the P-domain of the two proteins may also affect substrate selection by the chaperone. It may also be possible that the histidine residues in the N-domain of the proteins are involved in substrate selectivity, as there are nine histidine residues in the globular N-terminal domain of calnexin (Schrag et al., 2001; Wada et al., 1991) with only two of these conserved in calreticulin. The conserved residues are His128Ala, which had no effect on calreticulin structure or function in this study and His153 (His237 in calnexin), that when mutated, disrupts structure and abolishes function in a Zn^{2+}-dependent manner. Although His153 is conserved in calnexin (His237), the amino acid sequence preceding this critical residue differs in the two proteins. Calnexin contains a larger N-domain with an additional short α-helix of 10 amino acid residues that is not found in calreticulin (Schrag et al., 2001), potentially involved in specific substrate recognition. The secondary structure of calnexin also differs in the length of the loop containing the conserved histidine residue. In calnexin, the loop is substantially longer and more flexible, while in calreticulin it appears to have much less flexibility. This upstream region, in addition to the conserved His237/His153, may contribute to substrate specificity of calreticulin and calnexin.

The data presented in this study provide ample evidence that mutation of these single amino acid residues in calreticulin drastically affects the secondary and tertiary structure of this protein, resulting in loss of function. Finally, evidence from this study demonstrates that the interaction between ERp57 and calreticulin and presumably with calnexin may not be a prerequisite for folding of some substrates. In summary,

experimental evidence reveals that a single amino acid mutation in calreticulin, an ER luminal chaperone, significantly affects protein folding. It follows that a mutation such as this in a molecular chaperone could possibly result in a genetic disorder of protein folding. As well, single site mutations may also be a therapeutic means to address folding diseases where the substrate is retained in the ER, but is still functional if eventually targeted to the endogenous site of residence. Specifically, a mutant CFTR protein, ΔF508, is retained in the ER with calnexin, but when induced to travel to the membrane, is still functional (Okiyoneda et al., 2004; Pind et al., 1994). Potentially, a single site mutation in calnexin may allow the release of this mutant CFTR, allowing it to localize to the plasma membrane where it functions to control chloride homeostasis. These findings have important implications in our understanding of protein folding diseases.

Calreticulin and Calnexin during Apoptosis

Calreticulin function is established to be vital throughout development (Mesaeli et al., 1999), ER Ca^{2+} homeostasis and protein folding (Nakamura et al., 2001b), however concerning the role of the ER and this molecular chaperone during apoptosis, not much is known. Calreticulin-deficient cells have a significant resistance to apoptosis, accompanied by a decrease in the level of released cytochrome *c* from the mitochondria and a low level of caspase 3 activity (Nakamura et al., 2000). It is correspondingly observed that cells that over expressed calreticulin have an increased sensitivity to apoptosis, possibly dependent on Ca^{2+} transfer between the ER and the mitochondria (Arnaudeau et al., 2002; Nakamura et al., 2000). The buffering capacity of calreticulin appears to be responsible for providing the Ca^{2+} necessary for the continuity of the apoptotic cascade. Ca^{2+} is firmly established as a vital part of the apoptotic cascade, with involvement of the mitochondria and activation of Ca^{2+}-dependent proteases to name just a few (Kim et al., 2005; Kong et al., 2005; Mattson and Chan, 2003; Rizzuto et al., 2004; Rizzuto et al., 2003; Szabadkai and Rizzuto, 2004; Tagliarino et al., 2003; Tantral et al., 2004). It appears that the ER might play an important role during the regulation of cellular sensitivity to apoptosis.

Prior to this study, the role of calnexin in the regulation of apoptosis has not been investigated. The function of calnexin during quality control may ultimately be responsible for maintaining cellular viability, first by recognizing and folding nascent

glycoproteins, but also by sensing an accumulation of misfolded proteins and specifically signaling apoptosis. Calnexin-deficient cells are demonstrated using apoptosis assays to be relatively resistant to ER-stress induced apoptosis as compared to wild-type cells. One central finding of this thesis was the identification of a complex between calnexin and ER associated apoptotic proteins, Bap31 and caspase 12, potentially linking ER stress resulting from accumulation of aggregated and misfolded proteins with triggering of apoptosis. Utilizing calnexin-deficient cells, we demonstrate that cleavage of Bap31 is significantly inhibited, an indication of potential communication between calnexin and Bap31. This communication may occur via the transmembrane domain of both proteins, or by the cytoplasmic tail of calnexin, coordinating the interaction of specific factors necessary for the cleavage of Bap31 (Chevet et al., 2000) such as caspase 12. The absence of calnexin prevents the efficient cleavage of Bap31, potentially by preventing the formation of the complex between Bap31, Bcl-2/Bcl-XL and caspase 8 or caspase 12. As Bap31 expression and function is altered in calnexin-deficient lymphoblasts, this demonstrates an involvement of calnexin in this ER stress-dependent cleavage event and may potentially form protein complexes necessary for this cleavage. Utilizing immunoprecipitation, calnexin is positively identified to interact with Bap31 in control lymphoblasts.

ER Membrane Protein Bap31 and Apoptosis

ER localized or integral membrane proteins play a critical role during apoptosis (Chami et al., 2001; Lam et al., 1994; Nakagawa et al., 2000; Ng et al., 1997; Zhu et al., 1996). Bap31, a polytopic membrane protein localized to the ER, appears to play an essential role during apoptosis. Bap31, a 28-kDa protein contains a "death effector" cytoplasmic domain that is cleaved during the apoptotic cascade producing two fragments, a p20 fragment that is the membrane portion of the protein and cytoplasmic fragment whose function is yet unidentified. Bap31 is found in complex with Bcl-2/Bcl-XL and caspase 8, with caspase 8 demonstrated to be responsible for the cleavage of Bap31 (Ng et al., 1997). When the p20 fragment is expressed ectopically, it is a potent inducer of cell death (Nguyen et al., 2000) with mitochondrial release of cytochrome *c* and activation of the apoptotic cascade. This suggests unforeseen crosstalk between the ER and the mitochondria (Nguyen et al., 2000). The p20 fragment generated by caspase

cleavage is identified to cause an early release of Ca^{2+} from the ER, potentially via an interaction with A4, a putative ER membrane ion channel (Wang et al., 2003), with resultant uptake of Ca^{2+} into the mitochondria and recruitment by the mitochondria of a dynamin-related protein involved in membrane scission, Drp1, resulting in fragmentation and fission of the mitochondrial membrane (Breckenridge et al., 2003b). Further evidence by inhibiting Drp1 or ER-mitochondrial Ca^{2+} signaling prevents this p20 induced fission of the mitochondrial membrane. It appears that p20 strongly sensitizes mitochondria to caspase 8-induced cytochrome *c* release, as demonstrated by overexpression of p20 ultimately inducing caspase activation and apoptosis via the mitochondrial apoptosome pathway. Therefore, caspase-8 cleavage of Bap31 at the ER membrane triggers Ca^{2+}-dependent mitochondrial fission, enhancing the release of cytochrome *c* in response to this initiator caspase (Breckenridge et al., 2003b). Identification of this ER localized complex may be involved in apoptosis signal transduction. It is further hypothesized that Bap31 may form a complex with calnexin, functioning as a sensing complex during ER stress (Ng et al., 1997). This hypothetical complex could work like the plasma membrane apoptotic receptors Fas and TNFR-1, recruiting other factors and autoactivating, triggering the apoptotic cascade (Nagata, 1997).

The Role of Caspase 12 during Apoptosis

As severe or prolonged ER stress eventually triggers apoptosis, caspase 12 is identified to play a central role during ER stress-induced apoptosis (Nakagawa et al., 2000; Szegezdi et al., 2003). Caspase 12 is localized to the cytoplasmic side of the ER membrane and is activated by specific triggers that disrupt the homeostasis of the ER, whether this is Ca^{2+} depletion or protein accumulation (Nakagawa and Yuan, 2000; Nakagawa et al., 2000). This is demonstrated by caspase 12-deficient mice being partially resistant to apoptosis induced by ER stress but not by other apoptotic stimuli (Nakagawa et al., 2000). Caspase 12 is found in complex with IRE1, a member of the UPR and TRAF2, an adaptor protein involved in the cytokine pathway (Yoneda et al., 2001). This complex has the ability to recruit ASK1, a proapoptotic kinase that triggers the activation of the JNK pathway, leading to the apoptotic cascade (Yoneda et al., 2001). Once caspase 12 forms a complex with these factors, the protease dimerizes and

autoactivates (Shi, 2004), with active caspase 12 able to activate downstream caspases such as caspase 9 (Morishima et al., 2002), which in turn cleaves the effector caspase 3 (Morishima et al., 2002; Rao et al., 2002), resulting in cellular damage and apoptosis. Interestingly, the cytoplasmic Ca^{2+}-activated protease m-calpain is able to cleave and activate caspase 12 in response to Ca^{2+} flux from the ER, which is often triggered by ER stress (Nakagawa and Yuan, 2000; Oubrahim et al., 2002).

Caspase 12 in Human Leukemic T-cells and Mouse Embryonic Fibroblasts

In this study, a caspase 12-like immunoreactive protein in human leukemic lymphoblast cell lines CEM (wild-type) and NKR (calnexin-deficient) is identified, with an approximate two fold increase in calnexin-deficient human lymphoblasts. Thapsigargin treatment results in processing of caspase 12 in both the control and the calnexin-deficient lymphoblasts, but with 40% less cleavage in the deficient cells. As well, there is 1.6 fold less caspase 3 in drug treated calnexin-deficient lymphoblasts as well as negligible processing of caspase 8. Direct evidence for an interaction between caspase 12 and Bap31 was demonstrated in the human lymphoblast cells using immunoprecipitation. Studies using caspase inhibitors demonstrate a hierarchical cascade, with caspase 8 inhibitor preventing Bap31 cleavage in control and calnexin-deficient lymphoblasts, while the caspase 3 inhibitor prevents cleavage in control cells, but not in calnexin-deficient cells. This confirms that caspase 3 is upstream of both caspase 8 and Bap31 in human lymphoblasts, but that calnexin is also necessary for the efficient cleavage of Bap31.

Recently, there is a controversy over the presence of caspase 12 in humans. Similar to Bitko et al. (Bitko and Barik, 2001), our evidence supports the presence of caspase 12 in human cells. The latest evidence determines that in the majority of humans, with the exception of 20% of the African American population, the caspase 12 gene has an early stop codon resulting in production of a truncated and non-functional caspase (Fischer et al., 2002; Saleh et al., 2004). With normal caspase 12 produced in mice, we sought to identify if the caspase 12-like protein identified in humans behaved in a similar manner and had comparable protein interactions occurring in mice. We generated calnexin-deficient and wild-type mouse embryonic fibroblasts (MEFs) and verified these protein interactions. A positive interaction between Bap31, caspase 12 and

calnexin was observed in MEFs with caspase 12, calnexin and Bap31 all localized to the ER.

A Functional Complex between Calnexin, Caspase 12 and Bap31, Regulating ER Stress-Induced Apoptosis

In the absence of calnexin, there is a major interruption in the transduction of the apoptosis signal from the ER to the mitochondria. Interestingly, even though thapsigargin-induced cell death is significantly reduced in calnexin-deficient cells, the activation of caspase 12 and caspase 3 is not altered. Thapsigargin treatment triggers mitochondrial apoptotic pathways normally (with the consequent release of cytochrome *c* from the mitochondria) in both CEM and calnexin-deficient NKR cell lines. Using immunoprecipitation, we demonstrated an interaction between Bap31, calnexin and caspase 12. Immunocytochemistry further verified that caspase 12, Bap31 and calnexin all colocalized to the ER membranes. We demonstrated by monitoring caspase 12 processing, that this protein is involved in apoptosis induced by specific ER stress in both human T-cells, as well as mouse cells. It appeared that the caspase 12-like protein identified in human lymphoblasts behaved in a similar manner to the caspase 12 found in mice. In MEFs, similar to human lymphoblasts, a deficiency in calnexin resulted in abolished cleavage of Bap31, as well as considerable resistance to apoptosis.

Together, these data indicate that the Bap31 complex (Ng and Shore, 1998) also includes calnexin and caspase 12, assisting in the performance of the signaling complex that triggers apoptosis in response to ER stress. Calnexin may also form a novel complex, particularly activated under conditions of ER stress, with calnexin actually sensing ER stress and transmitting this signal to the mitochondria via caspase 12-dependent cleavage of Bap31. This study supports the hypothesis that calnexin has another function besides molecular chaperone; potentially modulating cell sensitivity to apoptosis induced by ER stress, in conjunction with caspase 12 and Bap31. The formation of a caspase 12, Bap31 and calnexin membrane localized complex must be important in the apoptotic cascade stimulated by ER stress in two ways: first, in perception of the signal with the consequent activation of caspase 12; and second, in the cleavage of Bap31 followed by generation of the apoptotic p20 fragment and stimulation of the mitochondrial pathway. The human leukemic T-cells as well as the MEFs

perceived the signal that resulted from thapsigargin treatment and initiated the programmed cell death cascade, in particular activating the mitochondrial pathway. However, calnexin-deficiency disrupted this apoptotic cascade by blocking the cleavage of Bap31. Calnexin may be the link which allows activation of caspase 8 or 12 and the consequent cleavage of Bap31 to produce the apoptosis inducer fragment p20. It appeared that calnexin was necessary for the proper signaling of ER stress-induced apoptosis from the ER out, with formation of a complex between calnexin, Bap31 and caspase 12. Most significantly, we established a complex formed between caspase 12, Bap31 and calnexin, potentially involved in transmission of the apoptotic signal from the ER to the mitochondria. These findings further support the theory that apoptosis depends on the presence of external apoptosis-activating signals but also on internal factors, such as the ER and other intracellular organelles.

As calreticulin and calnexin are demonstrated to perform important functions within the ER, as molecular chaperones as well as Ca^{2+} buffering proteins, they may also perform other tasks, including modulation of apoptosis, specifically sensing ER stress and transmitting it to other signaling pathways. In conclusion, specific factors and interactions localized to the ER directly regulate the structural sensitivity of ER proteins, unequivocally affecting functionality and resultantly the efficiency and outcome of the cell or even the organism.

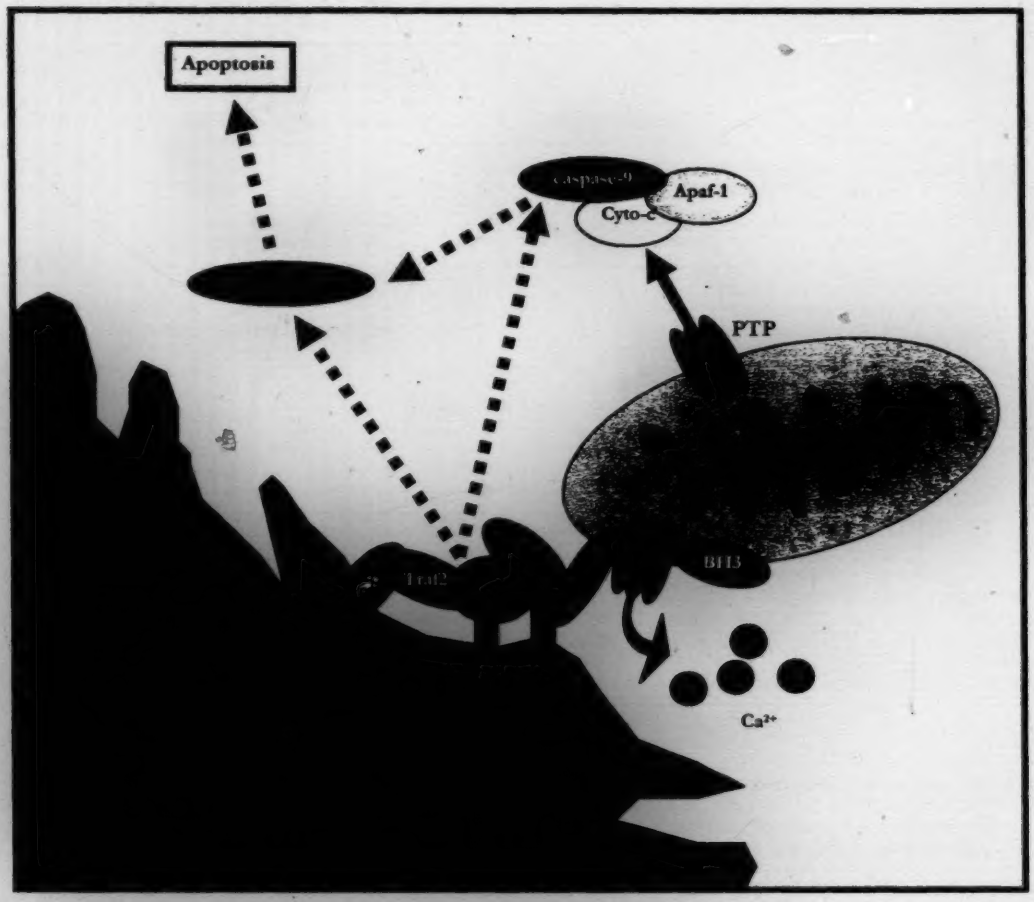

Figure 6- 3

Figure 6- 3 — Formation of a complex at the ER membrane between calnexin, Bap31 and caspase 12, in ER stress-induced apoptosis.

Calnexin and Bap31 form protein interaction at the ER membrane, with calnexin modulating the cleavage of Bap31 and production of the apoptotic fragment p20, involved in recruiting Drp1 at the mitochondrial membrane, allowing release of Ca^{2+} through the PTP. This Ca^{2+} release then triggers a cascade of events, including further Ca^{2+} release from the ER and mitochondria with specific activation of downstream caspases. Caspase 12 may potentially be recruited by calnexin for ER stress-dependent cleavage of Bap31. Apaf-1, apoptotic peptidase activating factor 1; cyto-*c*, cytochrome *c*; PTP, permeability transition pore; Drp1, dynamin related protein 1; IRE1, inositol requiring element 1; Traf2, TNF receptor-associated factor 2; Casp 12, caspase 12; Bap31, B-cell associated protein 31; BH3, BH3 containing protein; Cnx, calnexin.

References

Amaral, M. D. (2004). CFTR and chaperones: processing and degradation. J Mol Neurosci *23*, 41-48.

Amuthan, G., Biswas, G., Ananadatheerthavarada, H. K., Vijayasarathy, C., Shephard, H. M., and Avadhani, N. G. (2002). Mitochondrial stress-induced calcium signaling, phenotypic changes and invasive behavior in human lung carcinoma A549 cells. Oncogene *21*, 7839-7849.

Andrin, C., Corbett, E. F., Johnson, S., Dabrowska, M., Campbell, I. D., Eggleton, P., Opas, M., and Michalak, M. (2000). Expression and purification of mammalian calreticulin in *Pichia pastoris*. Protein Expr Purif *20*, 207-215.

Anfinsen, C. B., Haber, E., Sela, M., White, F.H.J. (1961). The kinetics of formation of native ribonuclease during oxidation of the reduced polypeptide chain. Proc Natl Acad Sci U S A *47*, 1309-1314.

Annis, M. G., Yethon, J. A., Leber, B., and Andrews, D. W. (2004). There is more to life and death than mitochondria: Bcl-2 proteins at the endoplasmic reticulum. Biochim Biophys Acta *1644*, 115-123.

Ardail, D., Popa, I., Bodennec, J., Louisot, P., Schmitt, D., and Portoukalian, J. (2003). The mitochondria-associated endoplasmic-reticulum subcompartment (MAM fraction) of rat liver contains highly active sphingolipid-specific glycosyltransferases. Biochem J *371*, 1013-1019.

Argon, Y., and Simen, B. B. (1999). GRP94, an ER chaperone with protein and peptide binding properties. Semin Cell Dev Biol *10*, 495-505.

Arnaudeau, S., Frieden, M., Nakamura, K., Castelbou, C., Michalak, M., and Demaurex, N. (2002). Calreticulin differentially modulates calcium uptake and release in the endoplasmic reticulum and mitochondria. J Biol Chem *277*, 46696-46705.

Arur, S., Uche, U. E., Rezaul, K., Fong, M., Scranton, V., Cowan, A. E., Mohler, W., and Han, D. K. (2003). Annexin I is an endogenous ligand that mediates apoptotic cell engulfment. Dev Cell *4*, 587-598.

Asai, A., Qiu, J., Narita, Y., Chi, S., Saito, N., Shinoura, N., Hamada, H., Kuchino, Y., and Kirino, T. (1999). High level calcineurin activity predisposes neuronal cells to apoptosis. J Biol Chem *274*, 34450-34458.

Ashby, M. C., and Tepikin, A. V. (2001). ER calcium and the functions of intracellular organelles. Semin Cell Dev Biol *12*, 11-17.

Ashkenazi, A. (2002). Targeting death and decoy receptors of the tumour-necrosis factor superfamily. Nat Rev Cancer *2*, 420-430.

Baksh, S., Burns, K., Andrin, C., and Michalak, M. (1995a). Interaction of calreticulin with protein disulfide isomerase. J Biol Chem *270*, 31338-31344.

Baksh, S., and Michalak, M. (1991). Expression of calreticulin in *Escherichia coli* and identification of its Ca^{2+} binding domains. J Biol Chem *266*, 21458-21465.

Baksh, S., Spamer, C., Heilmann, C., and Michalak, M. (1995b). Identification of the Zn^{2+} binding region in calreticulin. FEBS Lett *376*, 53-57.

Balasubramanian, K., and Schroit, A. J. (2003). Aminophospholipid asymmetry: A matter of life and death. Annu Rev Physiol *65*, 701-734.

Baumann, O., and Walz, B. (2001). Endoplasmic reticulum of animal cells and its organization into structural and functional domains. Int Rev Cytol *205*, 149-214.

Beard, N. A., Laver, D. R., and Dulhunty, A. F. (2004). Calsequestrin and the calcium release channel of skeletal and cardiac muscle. Prog Biophys Mol Biol *85*, 33-69.

Bedard, K., Szabo, E., Michalak, M., and Opas, M. (2005). Cellular functions of endoplasmic reticulum chaperones calreticulin, calnexin, and ERp57. Int Rev Cytol *245*, 91-121.

Ben-Chetrit, E. (1993). The molecular basis of the SSA/Ro antigens and the clinical significance of their autoantibodies. Br J Rheumatol *32*, 396-402.

Bergeron, J. J. M., Brenner, M. B., Thomas, D. Y., and Williams, D. B. (1994). Calnexin: a membrane-bound chaperone of the endoplasmic reticulum. Trends Biochem Sci *19*, 124-128.

Berninsone, P., and Hirschberg, C. B. (1998). Nucleotide sugars, nucleotide sulfate, and ATP transporters of the endoplasmic reticulum and Golgi apparatus. Ann N Y Acad Sci *842*, 91-99.

Berridge, M. J. (1995). Calcium signalling and cell proliferation. Bioessays *17*, 491-500.

Berridge, M. J. (2002). The endoplasmic reticulum: a multifunctional signaling organelle. Cell Calcium *32*, 235-249.

Berridge, M. J., Bootman, M. D., and Roderick, H. L. (2003). Calcium signalling: dynamics, homeostasis and remodelling. Nature Rev Mol Cell Biol *4*, 517-529.

Berridge, M. J., Lipp, P., and Bootman, M. D. (2000). The versatility and universality of calcium signalling. Nature Rev Mol Cell Biol *1*, 11-21.

Bertolotti, A., Zhang, Y., Hendershot, L. M., Harding, H. P., and Ron, D. (2000). Dynamic interaction of BiP and ER stress transducers in the unfolded-protein response. Nature Cell Biol *2*, 326-332.

Bitko, V., and Barik, S. (2001). An endoplasmic reticulum-specific stress-activated caspase (caspase-12) is implicated in the apoptosis of A549 epithelial cells by respiratory syncytial virus. J Cell Biochem *80*, 441-454.

Boatright, K. M., and Salvesen, G. S. (2003). Mechanisms of caspase activation. Curr Opin Cell Biol *15*, 725-731.

Boehning, D., Patterson, R. L., Sedaghat, L., Glebova, N. O., Kurosaki, T., and Snyder, S. H. (2003). Cytochrome c binds to inositol (1,4,5) trisphosphate receptors, amplifying calcium-dependent apoptosis. Nat Cell Biol *5*, 1051-1061.

Booth, C., and Koch, G. E. L. (1989). Perturbation of cellular calcium induces secretion of luminal ER proteins. Cell *59*, 729-737.

Bossy-Wetzel, E., Newmeyer, D. D., and Green, D. R. (1998). Mitochondrial cytochrome c release in apoptosis occurs upstream of DEVD-specific caspase activation and independently of mitochondrial transmembrane depolarization. EMBO J *17*, 37-49.

Bouvier, M. (2003). Accessory proteins and the assembly of human class I MHC molecules: a molecular and structural perspective. Mol Immunol *39*, 697-706.

Braakman, I., Helenius, J., and Helenius, A. (1992). Role of ATP and disulphide bonds during protein folding in the endoplasmic reticulum. Nature *356*, 260-262.

Bradford, M. M. (1976). A rapid and sensitive method for the quantitation of microgram quantities of protein utilizing the principle of protein-dye binding. Anal Biochem *72*, 248-254.

Breckenridge, D. G., Germain, M., Mathai, J. P., Nguyen, M., and Shore, G. C. (2003a). Regulation of apoptosis by endoplasmic reticulum pathways. Oncogene *22*, 8608-8618.

Breckenridge, D. G., Stojanovic, M., Marcellus, R. C., and Shore, G. C. (2003b). Caspase cleavage product of BAP31 induces mitochondrial fission through endoplasmic reticulum calcium signals, enhancing cytochrome c release to the cytosol. J Cell Biol *160*, 1115-1127.

Breuer, W., Klein, R. A., Hardt, B., Bartoschek, A., and Bause, E. (2001). Oligosaccharyltransferase is highly specific for the hydroxy amino acid in Asn-Xaa-Thr/Ser. FEBS Lett *501*, 106-110.

Brini, M., Bano, D., Manni, S., Rizzuto, R., and Carafoli, E. (2000). Effects of PMCA and SERCA pump overexpression on the kinetics of cell Ca(2+) signalling. Embo J *19*, 4926-4935.

Brooks, D. A. (1997). Protein processing: a role in the pathophysiology of genetic disease. FEBS Lett *409*, 115-120.

Brooks, D. A. (1999). Introduction: molecular chaperones of the ER: their role in protein folding and genetic disease. Semin Cell Dev Biol *10*, 441-442.

Brostrom, C. O., Prostko, C. R., Kaufman, R. J., and Brostrom, M. A. (1996). Inhibition of translational initiation by activators of the glucose-regulated stress protein and heat shock protein stress response systems. Role of the interferon-inducible double-stranded RNA-activated eukaryotic initiation factor 2alpha kinase. J Biol Chem *271*, 24995-25002.

Bukau, B., and Horwich, A. L. (1998). The Hsp70 and Hsp60 chaperone machines. Cell *92*, 351-366.

Buonanno, A., and Fields, R. D. (1999). Gene regulation by patterned electrical activity during neural and skeletal muscle development. Curr Opin Neurobiol *9*, 110-120.

Burns, K., Helgason, C. D., Bleackley, R. C., and Michalak, M. (1992). Calreticulin in T-lymphocytes. Identification of calreticulin in T- lymphocytes and demonstration that activation of T cells correlates with increased levels of calreticulin mRNA and protein. J Biol Chem *267*, 19039-19042.

Calfon, M., Zeng, H., Urano, F., Till, J. H., Hubbard, S. R., Harding, H. P., Clark, S. G., and Ron, D. (2002). IRE1 couples endoplasmic reticulum load to secretory capacity by processing the XBP-1 mRNA. Nature *415*, 92-96.

Camacho, P., and Lechleiter, J. D. (1995). Calreticulin inhibits repetitive intracellular Ca^{2+} waves. Cell *82*, 765-771.

Chami, M., Ferrari, D., Nicotera, P., Paterlini-Brechot, P., and Rizzuto, R. (2003). Caspase-dependent alterations of Ca2+ signaling in the induction of apoptosis by hepatitis B virus X protein. J Biol Chem *278*, 31745-31755.

Chami, M., Gozuacik, D., Lagorce, D., Brini, M., Falson, P., Peaucellier, G., Pinton, P., Lecoeur, H., Gougeon, M. L., le Maire, M., *et al.* (2001). Serca1 truncated proteins unable to pump calcium reduce the endoplasmic reticulum calcium concentration and induce apoptosis. J Cell Biol *153*, 1301-1314.

Chen, H., and Chan, D. C. (2005). Emerging functions of mammalian mitochondrial fusion and fission. Hum Mol Genet *14 Spec No. 2*, R283-289.

Chen, N. Q., Davis, A. T., Canbulat, E. C., Liu, Y. X., Goueli, S., McKenzie, B. A., Jr., Ahmed, K., and Holtzman, J. L. (1996). Evidence that casein kinase 2 phosphorylates hepatic microsomal calcium-binding proteins 1 and 2 but not 3. Biochemistry *35*, 8299-8306.

Chevet, E., Jakob, C. A., Thomas, D. Y., and Bergeron, J. J. (1999a). Calnexin family members as modulators of genetic diseases. Semin Cell Dev Biol *10*, 473-480.

Chevet, E., Nantel, A., Thomas, D., and Bergeron, J. J. M. (2000). Evidence for activation of calnexin signaling networks involved in ednoplasmic reticulum stress-induced apoptosis. Mol Biol Cell *11*, 417a.

Chevet, E., Wong, H. N., Gerber, D., Cochet, C., Fazel, A., Cameron, P. H., Gushue, J. N., Thomas, D. Y., and Bergeron, J. J. (1999b). Phosphorylation by CK2 and MAPK enhances calnexin association with ribosomes. Embo J *18*, 3655-3666.

Chin, E. R., Olson, E. N., Richardson, J. A., Yang, Q., Humphries, C., Shelton, J. M., Wu, H., Zhu, W., Bassel-Duby, R., and Williams, R. S. (1998). A calcineurin-dependent transcriptional pathway controls skeletal muscle fiber type. Genes Dev *12*, 2499-2509.

Choi, Y. H., Lee, S. J., Nguyen, P., Jang, J. S., Lee, J., Wu, M. L., Takano, E., Maki, M., Henkart, P. A., and Trepel, J. B. (1997). Regulation of cyclin D1 by calpain protease. J Biol Chem *272*, 28479-28484.

Chou, K. J., Fang, H. C., Chung, H. M., Cheng, J. S., Lee, K. C., Tseng, L. L., Tang, K. Y., and Jan, C. R. (2000). Effect of betulinic acid on intracellular-free Ca(2+) levels in Madin Darby canine kidney cells. Eur J Pharmacol *408*, 99-106.

Clairmont, C. A., De Maio, A., and Hirschberg, C. B. (1992). Translocation of ATP into the lumen of rough endoplasmic reticulum- derived vesicles and its binding to luminal proteins including BiP (GRP 78) and GRP 94. J Biol Chem *267*, 3983-3990.

Coppolino, M. G., and Dedhar, S. (1999). Ligand-specific, transient interaction between integrins and calreticulin during cell adhesion to extracellular matrix proteins is dependent upon phosphorylation/dephosphorylation events. Biochem J *340*, 41-50.

Corbett, E. F., Michalak, K. M., Oikawa, K., Johnson, S., Campbell, I. D., Eggleton, P., Kay, C., and Michalak, M. (2000). The conformation of calreticulin is influenced by the endoplasmic reticulum lumenal environment. J Biol Chem *275*, 27177-27185.

Corbett, E. F., and Michalak, M. (2000). Calcium, a signaling molecule in the endoplasmic reticulum? Trends Biochem Sci *25*, 307-311.

Corbett, E. F., Oikawa, K., Francois, P., Tessier, D. C., Kay, C., Bergeron, J. J., Thomas, D. Y., Krause, K. H., and Michalak, M. (1999). Ca2+ regulation of interactions between endoplasmic reticulum chaperones. J Biol Chem *274*, 6203-6211.

Cox, J. S., Shamu, C. E., and Walter, P. (1993). Transcriptional induction of genes encoding endoplasmic reticulum resident proteins requires a transmembrane protein kinase. Cell *73*, 1197-1206.

Crabtree, G. R. (1999). Generic signals and specific outcomes: signaling through Ca^{2+}, calcineurin, and NF-AT. Cell *96*, 611-614.

Creagh, E. M., Conroy, H., and Martin, S. J. (2003). Caspase-activation pathways in apoptosis and immunity. Immunol Rev *193*, 10-21.

Csermely, P., Miyata, Y., Schnaider, T., and Yahara, I. (1995). Autophosphorylation of grp94 (endoplasmin). J Biol Chem *270*, 6381-6388.

Csordas, G., Madesh, M., Antonsson, B., and Hajnoczky, G. (2002). tcBid promotes Ca(2+) signal propagation to the mitochondria: control of Ca(2+) permeation through the outer mitochondrial membrane. Embo J *21*, 2198-2206.

Danial, N. N., and Korsmeyer, S. J. (2004). Cell death: critical control points. Cell *116*, 205-219.

Darios, F., Lambeng, N., Troadec, J. D., Michel, P. P., and Ruberg, M. (2003). Ceramide increases mitochondrial free calcium levels via caspase 8 and Bid: role in initiation of cell death. J Neurochem *84*, 643-654.

de Alba, E., and Tjandra, N. (2004). Structural studies on the Ca2+-binding domain of human nucleobindin (calnuc). Biochemistry *43*, 10039-10049.

De Vos, K. J., Allan, V. J., Grierson, A. J., and Sheetz, M. P. (2005). Mitochondrial function and actin regulate dynamin-related protein 1-dependent mitochondrial fission. Curr Biol *15*, 678-683.

de Wet, H., McIntosh, D. B., Conseil, G., Baubichon-Cortay, H., Krell, T., Jault, J. M., Daskiewicz, J. B., Barron, D., and Di Pietro, A. (2001). Sequence requirements of the ATP-binding site within the C-terminal nucleotide-binding domain of mouse P-glycoprotein: structure-activity relationships for flavonoid binding. Biochemistry *40*, 10382-10391.

Delom, F., and Chevet, E. (2006). In vitro mapping of calnexin interaction with ribosomes. Biochem Biophys Res Commun *341*, 39-44.

Demaurex, N., and Distelhorst, C. (2003). Cell biology. Apoptosis--the calcium connection. Science *300*, 65-67.

Demaurex, N., and Frieden, M. (2003). Measurements of the free luminal ER Ca(2+) concentration with targeted "cameleon" fluorescent proteins. Cell Calcium *34*, 109-119.

Denault, J. B., and Salvesen, G. S. (2002). Caspases: keys in the ignition of cell death. Chem Rev *102*, 4489-4500.

Denzel, A., Molinari, M., Trigueros, C., Martin, J. E., Velmurgan, S., Brown, S., Stamp, G., and Owen, M. J. (2002). Early postnatal death and motor disorders in mice congenitally deficient in calnexin expression. Mol Cell Biol *22*, 7398-7404.

Di Jeso, B., Pereira, R., Consiglio, E., Formisano, S., Satrustegui, J., and Sandoval, I. V. (1998). Demonstration of a Ca2+ requirement for thyroglobulin dimerization and export to the golgi complex. Eur J Biochem *252*, 583-590.

Diaz-Horta, O., Kamagate, A., Herchuelz, A., and Van Eylen, F. (2002). Na/Ca exchanger overexpression induces endoplasmic reticulum-related apoptosis and caspase-12 activation in insulin-releasing BRIN-BD11 cells. Diabetes *51*, 1815-1824.

Dickson, K. M., Bergeron, J. J., Shames, I., Colby, J., Nguyen, D. T., Chevet, E., Thomas, D. Y., and Snipes, G. J. (2002). Association of calnexin with mutant peripheral myelin protein-22 *ex vivo*: A basis for "gain-of-function" ER diseases. Proc Natl Acad Sci USA *99*, 9852-9857.

Diedrich, G., Bangia, N., Pan, M., and Cresswell, P. (2001). A role for calnexin in the assembly of the MHC Class I loading complex in the endoplasmic reticulum. J Immunol *166*, 1703-1709.

Dierks, T., Volkmer, J., Schlenstedt, G., Jung, C., Sandholzer, U., Zachmann, K., Schlotterhose, P., Neifer, K., Schmidt, B., and Zimmermann, R. (1996). A microsomal ATP-binding protein involved in efficient protein transport into the mammalian endoplasmic reticulum. EMBO J *15*, 6931-6942.

Dissemond, J., Busch, M., Kothen, T., Mors, J., Weimann, T. K., Lindeke, A., Goos, M., and Wagner, S. N. (2004). Differential downregulation of endoplasmic reticulum-residing chaperones calnexin and calreticulin in human metastatic melanoma. Cancer Lett *203*, 225-231.

Distelhorst, C. W., and McCormick, T. S. (1996). Bcl-2 acts subsequent to and independent of Ca2+ fluxes to inhibit apoptosis in thapsigargin- and glucocorticoid-treated mouse lymphoma cells. Cell Calcium *19*, 473-483.

Distelhorst, C. W., and Roderick, H. L. (2003). Ins(1,4,5)P3-mediated calcium signals and apoptosis: is there a role for Bcl-2? Biochem Soc Trans *31*, 958-959.

Donepudi, M., Mac Sweeney, A., Briand, C., and Grutter, M. G. (2003). Insights into the regulatory mechanism for caspase-8 activation. Mol Cell *11*, 543-549.

Dorner, A. J., and Kaufman, R. J. (1994). The levels of endoplasmic reticulum proteins and ATP affect folding and secretion of selective proteins. Biologicals *22*, 103-112.

Dorner, A. J., Wasley, L. C., and Kaufman, R. J. (1990). Protein dissociation from GRP78 and secretion are blocked by depletion of cellular ATP levels. Proc Natl Acad Sci USA *87*, 7429-7432.

Draper, D. W., Harris, V. G., Culver, C. A., and Laster, S. M. (2004). Calcium and its role in the nuclear translocation and activation of cytosolic phospholipase A(2) in cells rendered sensitive to TNF-induced apoptosis by cycloheximide. J Immunol *172*, 2416-2423.

Duchen, M. R. (2000). Mitochondria and calcium: from cell signalling to cell death. J Physiol *529 Pt 1*, 57-68.

Dupuis, M., Schaerer, E., Krause, K.-H., and Tschopp, J. (1993). The calcium-binding protein calreticulin is a major constituent of lytic granules in cytolytic T lymphocytes. J Exp Med *177*, 1-7.

Dussmann, H., Rehm, M., Kogel, D., and Prehn, J. H. (2003). Outer mitochondrial membrane permeabilization during apoptosis triggers caspase-independent mitochondrial and caspase-dependent plasma membrane potential depolarization: a single-cell analysis. J Cell Sci *116*, 525-536.

Earnshaw, W. C., Martins, L. M., and Kaufmann, S. H. (1999). Mammalian caspases: structure, activation, substrates, and functions during apoptosis. Annu Rev Biochem *68*, 383-424.

Edman, J. C., Ellis, L., Blacher, R. W., Roth, R. A., and Rutter, W. J. (1985). Sequence of protein disulphide isomerase and implications of its relationship to thioredoxin. Nature *317*, 267-270.

Ellgaard, L., Bettendorff, P., Braun, D., Herrmann, T., Fiorito, F., Jelesarov, I., Guntert, P., Helenius, A., and Wuthrich, K. (2002). NMR structures of 36 and 73-residue fragments of the calreticulin P-domain. J Mol Biol *322*, 773-784.

Ellgaard, L., and Frickel, E. M. (2003). Calnexin, calreticulin, and ERp57: teammates in glycoprotein folding. Cell Biochem Biophys *39*, 223-247.

Ellgaard, L., and Helenius, A. (2003). Quality control in the endoplasmic reticulum. Nature Rev Mol Cell Biol *4*, 181-191.

Ellgaard, L., Riek, R., Braun, D., Herrmann, T., Helenius, A., and Wuthrich, K. (2001a). Three-dimensional structure topology of the calreticulin P-domain based on NMR assignment. FEBS Lett *488*, 69-73.

Ellgaard, L., Riek, R., Herrmann, T., Guntert, P., Braun, D., Helenius, A., and Wuthrich, K. (2001b). NMR structure of the calreticulin P-domain. Proc Natl Acad Sci USA *98*, 3133-3138.

Elliott, T., and Williams, A. (2005). The optimization of peptide cargo bound to MHC class I molecules by the peptide-loading complex. Immunol Rev *207*, 89-99.

Enari, M., Sakahira, H., Yokoyama, H., Okawa, K., Iwamatsu, A., and Nagata, S. (1998). A caspase-activated DNase that degrades DNA during apoptosis, and its inhibitor ICAD. Nature *391*, 43-50.

Eriksson, K. K., Vago, R., Calanca, V., Galli, C., Paganetti, P., and Molinari, M. (2004). EDEM contributes to maintenance of protein folding efficiency and secretory capacity. J Biol Chem *279*, 44600-44605.

Ermak, G., and Davies, K. J. (2002). Calcium and oxidative stress: from cell signaling to cell death. Mol Immunol *38*, 713-721.

Felder, C. C., Poulter, M. O., and Wess, J. (1992). Muscarinic receptor-operated Ca^{2+} influx in transfected fibroblast cells is independent of inositol phosphates and release of intracellular Ca^{2+}. Proc Natl Acad Sci USA *89*, 509-513.

Fernandez, F., DAlessio, C., Fanchiotti, S., and Parodi, A. J. (1998). A misfolded protein conformation is not a sufficient condition for *in vivo* glucosylation by the UDP-Glc:glycoprotein glucosyltransferase. EMBO J *17*, 5877-5886.

Ferrari, D., Pinton, P., Szabadkai, G., Chami, M., Campanella, M., Pozzan, T., and Rizzuto, R. (2002). Endoplasmic reticulum, Bcl-2 and Ca2+ handling in apoptosis. Cell Calcium *32*, 413-420.

Ferraro, E., Corvaro, M., and Cecconi, F. (2003). Physiological and pathological roles of Apaf1 and the apoptosome. J Cell Mol Med *7*, 21-34.

Fink, A. L. (1999). Chaperone-mediated protein folding. Physiol Rev *79*, 425-449.

Fischer, H., Koenig, U., Eckhart, L., and Tschachler, E. (2002). Human caspase 12 has acquired deleterious mutations. Biochem Biophys Res Commun *293*, 722-726.

Fliegel, L., Burns, K., MacLennan, D. H., Reithmeier, R. A. F., and Michalak, M. (1989). Molecular cloning of the high affinity calcium-binding protein (calreticulin) of skeletal muscle sarcoplasmic reticulum. J Biol Chem *264*, 21522-21528.

Fontanini, A., Chies, R., Snapp, E. L., Ferrarini, M., Fabrizi, G. M., and Brancolini, C. (2005). Glycan-independent role of calnexin in the intracellular retention of Charcot-Marie-tooth 1A Gas3/PMP22 mutants. J Biol Chem *280*, 2378-2387.

Foyouzi-Youssefi, R., Arnaudeau, S., Borner, C., Kelley, W. L., Tschopp, J., Lew, D. P., Demaurex, N., and Krause, K. H. (2000). Bcl-2 decreases the free Ca2+ concentration within the endoplasmic reticulum. Proc Natl Acad Sci U S A *97*, 5723-5728.

Franzini-Armstrong, C., and Protasi, F. (1997). Ryanodine receptors of striated muscles: a complex channel capable of multiple interactions. Physiol Rev *77*, 699-729.

Frenkel, Z., Gregory, W., Kornfeld, S., and Lederkremer, G. Z. (2003). ER-associated degradation of mammalian glycoproteins involves sugar chain trimming to Man6 - 5 GlcNAc2. J Biol Chem.

Frickel, E. M., Frei, P., Bouvier, M., Stafford, W. F., Helenius, A., Glockshuber, R., and Ellgaard, L. (2004). ERp57 is a multifunctional thiol-disulfide oxidoreductase. J Biol Chem.

Frickel, E. M., Riek, R., Jelesarov, I., Helenius, A., Wuthrich, K., and Ellgaard, L. (2002). TROSY-NMR reveals interaction between ERp57 and the tip of the calreticulin P-domain. Proc Natl Acad Sci USA *99*, 1954-1959.

Gahmberg, C. G., and Tolvanen, M. (1996). Why mammalian cell surface proteins are glycoproteins. Trends Biochem Sci *21*, 308-311.

Gao, B., Adhikari, R., Howarth, M., Nakamura, K., Gold, M. C., Hill, A. B., Knee, R., Michalak, M., and Elliott, T. (2002). Assembly and Antigen-Presenting Function of MHC Class I Molecules in Cells Lacking the ER Chaperone Calreticulin. Immunity *16*, 99-109.

Gething, M. J. (1999). Role and regulation of the ER chaperone BiP. Sem Cell Dev Biol *10*, 465-472.

Ghaemmaghami, S., Huh, W. K., Bower, K., Howson, R. W., Belle, A., Dephoure, N., O'Shea, E. K., and Weissman, J. S. (2003). Global analysis of protein expression in yeast. Nature *425*, 737-741.

Goldberger, R. F., Epstein, C. J., and Anfinsen, C. B. (1963). Acceleration of reactivation of reduced bovine pancreatic ribonuclease by a microsomal system from rat liver. J Biol Chem *238*, 628-635.

Goldstein, J. C., Waterhouse, N. J., Juin, P., Evan, G. I., and Green, D. R. (2000). The coordinate release of cytochrome c during apoptosis is rapid, complete and kinetically invariant. Nature Cell Biol *2*, 156-162.

Graf, G. A., Cohen, J. C., and Hobbs, H. H. (2004). Missense mutations in ABCG5 and ABCG8 disrupt heterodimerization and trafficking. J Biol Chem *279*, 24881-24888.

Granville, D. J., Carthy, C. M., Jiang, H., Shore, G. C., McManus, B. M., and Hunt, D. W. (1998). Rapid cytochrome c release, activation of caspases 3, 6, 7 and 8 followed by Bap31 cleavage in HeLa cells treated with photodynamic therapy. FEBS Lett *437*, 5-10.

Greber, U. F., and Gerace, L. (1995). Depletion of calcium from the lumen of endoplasmic reticulum reversibly inhibits passive diffusion and signal-mediated transport into the nucleus. J Cell Biol *128*, 5-14.

Greeb, J., and Shull, G. E. (1989). Molecular cloning of a third isoform of the calmodulin-sensitive plasma membrane Ca^{2+}-transporting ATPase that is expressed predominantly in brain and skeletal muscle. J Biol Chem *264*, 18569-18576.

Green, D. R., and Evan, G. I. (2002). A matter of life and death. Cancer Cell *1*, 19-30.

Grenert, J. P., Johnson, B. D., and Toft, D. O. (1999). The importance of ATP binding and hydrolysis by hsp90 in formation and function of protein heterocomplexes. J Biol Chem *274*, 17525-17533.

Griffiths, G., Ericsson, M., Krijnse-Locker, J., Nilsson, T., Goud, B., Soling, H. D., Tang, B. L., Wong, S. H., and Hong, W. (1994). Localization of the Lys, Asp, Glu, Leu tetrapeptide receptor to the Golgi complex and the intermediate compartment in mammalian cells. J Cell Biol *127*, 1557-1574.

Groenendyk, J., Lynch, J., and Michalak, M. (2004). Calreticulin, Ca2+, and calcineurin - signaling from the endoplasmic reticulum. Mol Cells *17*, 383-389.

Groenendyk, J., and Michalak, M. (2005). Endoplasmic reticulum quality control and apoptosis. Acta Biochim Pol *52*, 381-395.

Gross, A., McDonnell, J. M., and Korsmeyer, S. J. (1999). BCL-2 family members and the mitochondria in apoptosis. Genes Dev *13*, 1899-1911.

Guo, L., Groenendyk, J., Papp, S., Dabrowska, M., Knoblach, B., Kay, C., Parker, J. M. R., Opas, M., and Michalak, M. (2003). Identification of an N-domain histidine essential for chaperone function in calreticulin. J Biol Chem *278*, 50645-50653.

Guo, L., Nakamura, K., Lynch, J., Opas, M., Olson, E. N., Agellon, L. B., and Michalak, M. (2002). Cardiac-specific expression of calcineurin reverses embryonic lethality in calreticulin-deficient mouse. J Biol Chem *277*, 50776-50779.

Guthapfel, R., Gueguen, P., and Quemeneur, E. (1996). ATP binding and hydrolysis by the multifunctional protein disulfide isomerase. J Biol Chem *271*, 2663-2666.

Haas, I. G., and Wabl, M. (1983). Immunoglobulin heavy chain binding protein. Nature *306*, 387-389.

Hahn, M., Borisova, S., Schrag, J. D., Tessier, D. C., Zapun, A., Tom, R., Kamen, A. A., Bergeron, J. J., Thomas, D. Y., and Cygler, M. (1998). Identification and crystallization of a protease-resistant core of calnexin that retains biological activity. J Struct Biol *123*, 260-264.

Hajnoczky, G., Davies, E., and Madesh, M. (2003). Calcium signaling and apoptosis. Biochem Biophys Res Commun *304*, 445-454.

Hammond, C., Braakman, I., and Helenius, A. (1994). Role of N-linked oligosaccharide recognition, glucose trimming, and calnexin in glycoprotein folding and quality control. Proc Natl Acad Sci USA *91*, 913-917.

Harding, H. P., Zhang, Y., and Ron, D. (1999). Protein translation and folding are coupled by an endoplasmic-reticulum- resident kinase. Nature *397*, 271-274.

Harris, M. R., Yu, Y. Y., Kindle, C. S., Hansen, T. H., and Solheim, J. C. (1998). Calreticulin and calnexin interact with different protein and glycan determinants during the assembly of MHC class I. J Immunol *160*, 5404-5409.

Hebert, D. N., Zhang, J. X., Chen, W., Foellmer, B., and Helenius, A. (1997). The number and location of glycans on influenza hemagglutinin determine folding and association with calnexin and calreticulin. J Cell Biol *139*, 613-623.

Helenius, A., and Aebi, M. (2001). Intracellular functions of N-linked glycans. Science *291*, 2364-2369.

Helenius, A., and Aebi, M. (2004). Roles of N-linked glycans in the endoplasmic reticulum. Annu Rev Biochem *73*, 1019-1049.

Helenius, A., Trombetta, E. S., Hebert, D. N., and Simons, J. F. (1997). Calnexin, calreticulin and the folding of glycoproteins. Trends Cell Biol *7*, 193-200.

High, S., Lecomte, F. J., Russell, S. J., Abell, B. M., and Oliver, J. D. (2000). Glycoprotein folding in the endoplasmic reticulum: a tale of three chaperones? FEBS Lett *476*, 38-41.

Hirano, N., Shibasaki, F., Sakai, R., Tanaka, T., Nishida, J., Yazaki, Y., Takenawa, T., and Hirai, H. (1995). Molecular cloning of the human glucose-regulated protein ERp57/GRP58, a thiol-dependent reductase. Identification of its secretory form and inducible expression by the oncogenic transformation. Eur J Biochem *234*, 336-342.

Hirota, J., Furuichi, T., and Mikoshiba, K. (1999). Inositol 1,4,5-Trisphosphate receptor type 1 is a substrate for caspase- 3 and is cleaved during apoptosis in a caspase-3-dependent manner. J Biol Chem *274*, 34433-34437.

Hirschberg, C. B., Robbins, P. W., and Abeijon, C. (1998). Transporters of nucleotide sugars, ATP, and nucleotide sulfate in the endoplasmic reticulum and Golgi apparatus. Annu Rev Biochem *67*, 49-69.

Ho, S. N., Hunt, H. D., Horton, R. M., Pullen, J. K., and Pease, L. R. (1989). Site-directed mutagenesis by overlap extension using the polymerase chain reaction. Gene *77*, 51-59.

Hochstenbach, F., David, V., Watkins, S., and Brenner, M. B. (1992). Endoplasmic reticulum resident protein of 90 kilodaltons associates with the T- and B-cell antigen receptors and major histocompatibility complex antigens during their assembly. Proc Natl Acad Sci U S A *89*, 4734-4738.

Hofmann, K., Bucher, P., and Tschopp, J. (1997). The CARD domain: a new apoptotic signalling motif. Trends Biochem Sci *22*, 155-156.

Hong, M., Luo, S., Baumeister, P., Huang, J. M., Gogia, R. K., Li, M., and Lee, A. S. (2004). Underglycosylation of ATF6 as a novel sensing mechanism for activation of the unfolded protein response. J Biol Chem *279*, 11354-11363.

Hosokawa, N., Wada, I., Hasegawa, K., Yorihuzi, T., Tremblay, L. O., Herscovics, A., and Nagata, K. (2001). A novel ER alpha-mannosidase-like protein accelerates ER-associated degradation. EMBO Rep *2*, 415-422.

Howell, D. N., Andreotti, P. E., Dawson, J. R., and Cresswell, P. (1985). Natural killing target antigens as inducers of interferon: studies with an immunoselected, natural killing-resistant human T lymphoblastoid cell line. J Immunol *134*, 971-976.

Hughes, E. A., and Cresswell, P. (1998). The thiol oxidoreductase ERp57 is a component of the MHC class I peptide-loading complex. Curr Biol *8*, 709-712.

Ihara, Y., Cohen-Doyle, M. F., Saito, Y., and Williams, D. B. (1999). Calnexin discriminates between protein conformational states and functions as a molecular chaperone *in vitro*. Molecular Cell *4*, 331-341.

Jackson, M. R., Nilsson, T., and Peterson, P. A. (1990). Identification of a consensus motif for retention of transmembrane proteins in the endoplasmic reticulum. Embo J *9*, 3153-3162.

Jakob, C. A., Bodmer, D., Spirig, U., Battig, P., Marcil, A., Dignard, D., Bergeron, J. J., Thomas, D. Y., and Aebi, M. (2001a). Htm1p, a mannosidase-like protein, is involved in glycoprotein degradation in yeast. EMBO Rep *2*, 423-430.

Jakob, C. A., Burda, P., te Heesen, S., Aebi, M., and Roth, J. (1998). Genetic tailoring of N-linked oligosaccharides: the role of glucose residues in glycoprotein processing of *Saccharomyces cerevisiae in vivo*. Glycobiology *8*, 155-164.

Jakob, C. A., Chevet, E., Thomas, D. Y., and Bergeron, J. J. (2001b). Lectins of the ER quality control machinery. Results Probl Cell Differ *33*, 1-17.

Jarosch, E., Lenk, U., and Sommer, T. (2003). Endoplasmic reticulum-associated protein degradation. Int Rev Cytol *223*, 39-81.

Jayaraman, T., and Marks, A. R. (1997). T cells deficient in inositol 1,4,5-trisphosphate receptor are resistant to apoptosis. Mol Cell Biol *17*, 3005-3012.

Jeffery, J., Kendall, J. M., and Campbell, A. K. (2000). Apoaequorin monitors degradation of endoplasmic reticulum (ER) proteins initiated by loss of ER Ca(2+). Biochem Biophys Res Commun *268*, 711-715.

Johnson, A. E., and van Waes, M. A. (1999). The translocon: a dynamic gateway at the ER membrane. Annu Rev Cell Dev Biol *15*, 799-842.

Johnson, S., Michalak, M., Opas, M., and Eggleton, P. (2001). The ins and outs of calreticulin: from the ER lumen to the extracellular space. Trends Cell Biol *11*, 122-129.

Jones, L. R., Suzuki, Y. J., Wang, W., Kobayashi, Y. M., Ramesh, V., Franzini-Armstrong, C., Cleemann, L., and Morad, M. (1998). Regulation of Ca^{2+} signaling in transgenic mouse cardiac myocytes overexpressing calsequestrin. J Clin Invest *101*, 1385-1393.

Joseph, S. K., Boehning, D., Bokkala, S., Watkins, R., and Widjaja, J. (1999). Biosynthesis of inositol trisphosphate receptors: selective association with the molecular chaperone calnexin. Biochem J *342*, 153-161.

Kageyama, K., Ihara, Y., Goto, S., Urata, Y., Toda, G., Yano, K., and Kondo, T. (2002). Overexpression of Calreticulin Modulates Protein Kinase B/Akt Signaling to Promote Apoptosis during Cardiac Differentiation of Cardiomyoblast H9c2 Cells. J Biol Chem *277*, 19255-19264.

Kalz-Fuller, B., Bieberich, E., and Bause, E. (1995). Cloning and expression of glucosidase we from human hippocampus. Eur J Biochem *231*, 344-351.

Kam, P. C., and Ferch, N. I. (2000). Apoptosis: mechanisms and clinical implications. Anaesthesia *55*, 1081-1093.

Kapoor, M., Ellgaard, L., Gopalakrishnapai, J., Schirra, C., Gemma, E., Oscarson, S., Helenius, A., and Surolia, A. (2004). Mutational analysis provides molecular insight into the carbohydrate-binding region of calreticulin: pivotal roles of tyrosine-109 and aspartate-135 in carbohydrate recognition. Biochemistry *43*, 97-106.

Karplus, M. (1997). The Levinthal paradox: yesterday and today. Fold Des *2*, S69-75.

Katiyar, S., Joshi, S., and Lennarz, W. J. (2005). The retrotranslocation protein Derlin-1 binds peptide:N-glycanase to the endoplasmic reticulum. Mol Biol Cell *16*, 4584-4594.

Katoh, I., Tomimori, Y., Ikawa, Y., and Kurata, S. (2004). Dimerization and processing of procaspase-9 by redox stress in mitochondria. J Biol Chem *279*, 15515-15523.

Keller, S. H., Lindstrom, J., and Taylor, P. (1998). Inhibition of glucose trimming with castanospermine reduces calnexin association and promotes proteasome degradation of the alpha-subunit of the nicotinic acetylcholine receptor. J Biol Chem *273*, 17064-17072.

Khanna, N. C., Tokuda, M., and Waisman, D. M. (1986). Conformational changes induced by binding of divalent cations to calregulin. J Biol Chem *261*, 8883-8887.

Kim, M. J., Jo, D. G., Hong, G. S., Kim, B. J., Lai, M., Cho, D. H., Kim, K. W., Bandyopadhyay, A., Hong, Y. M., Kim do, H., *et al.* (2002). Calpain-dependent cleavage of cain/cabin1 activates calcineurin to mediate calcium-triggered cell death. Proc Natl Acad Sci U S A *99*, 9870-9875.

Kim, R., Emi, M., and Tanabe, K. (2005). Role of mitochondria as the gardens of cell death. Cancer Chemother Pharmacol, 1-9.

Kluck, R. M., Bossy-Wetzel, E., Green, D. R., and Newmeyer, D. D. (1997). The release of cytochrome c from mitochondria: a primary site for Bcl-2 regulation of apoptosis. Science *275*, 1132-1136.

Knauer, R., and Lehle, L. (1999). The oligosaccharyltransferase complex from yeast. Biochim Biophys Acta *1426*, 259-273.

Knee, R., Ahsan, I., Mesaeli, N., Kaufman, R. J., and Michalak, M. (2003). Compromised calnexin function in calreticulin deficient cells. Biochem Biophys Res Commun *304*, 661-666.

Knoblach, B., Keller, B. O., Groenendyk, J., Aldred, S., Zheng, J., Lemire, B. D., Li, L., and Michalak, M. (2003). ERp19 and ERp46, new members of the thioredoxin family of endoplasmic reticulum proteins. Mol Cell Proteomics *2*, 1104-1119.

Kobrinsky, E. M., and Kirchberger, M. A. (2001). Evidence for a role of the sarcoplasmic/endoplasmic reticulum Ca(2+)-ATPase in thapsigargin and Bcl-2 induced changes in Xenopus laevis oocyte maturation. Oncogene *20*, 933-941.

Koch, G., Smith, M., Macer, D., Webster, P., and Mortara, R. (1986). Endoplasmic reticulum contains a common, abundant calcium-binding glycoprotein, endoplasmin. J Cell Sci *86*, 217-232.

Koivunen, P., Helaakoski, T., Annunen, P., Veijola, J., Raisanen, S., Pihlajaniemi, T., and Kivirikko, K. I. (1996). ERp60 does not substitute for protein disulphide isomerase as the beta- subunit of prolyl 4-hydroxylase. Biochem J *316*, 599-605.

Kong, D., Xu, L., Yu, Y., Zhu, W., Andrews, D. W., Yoon, Y., and Kuo, T. H. (2005). Regulation of Ca2+-induced permeability transition by Bcl-2 is antagonized by Drpl and hFis1. Mol Cell Biochem *272*, 187-199.

Kono, T., Jones, K. T., Bos-Mikich, A., Whittingham, D. G., and Carroll, J. (1996). A cell cycle-associated change in Ca2+ releasing activity leads to the generation of Ca2+ transients in mouse embryos during the first mitotic division. J Cell Biol *132*, 915-923.

Koyasu, S., Nishida, E., Miyata, Y., Sakai, H., and Yahara, I. (1989). HSP100, a 100-kDa heat shock protein, is a Ca^{2+}-calmodulin-regulated actin-binding protein. J Biol Chem *264*, 15083-15087.

Kozutsumi, Y., Segal, M., Normington, K., Gething, M. J., and Sambrook, J. (1988). The presence of malfolded proteins in the endoplasmic reticulum signals the induction of glucose-regulated proteins. Nature *332*, 462-464.

Krebs, J. (1998). The role of calcium in apoptosis. Biometals *11*, 375-382.

Kuznetsov, G., Chen, L. B., and Nigam, S. K. (1997). Multiple molecular chaperones complex with misfolded large oligomeric glycoproteins in the endoplasmic reticulum. J Biol Chem *272*, 3057-3063.

Kwon, M. S., Park, C. S., Choi, K., Ahnn, J., Kim, J. I., Eom, S. H., Kaufman, S. J., and Song, W. K. (2000). Calreticulin couples calcium release and calcium influx in integrin-mediated calcium signaling. Mol Biol Cell *11*, 1433-1443.

Laemmli, U. K. (1970). Cleavage of structural proteins during the assembly of the head of bacteriophage T4. Nature *227*, 680-685.

Lai, M. M., Burnett, P. E., Wolosker, H., Blackshaw, S., and Snyder, S. H. (1998). Cain, a novel physiologic protein inhibitor of calcineurin. J Biol Chem *273*, 18325-18331.

Lai, M. M., Luo, H. R., Burnett, P. E., Hong, J. J., and Snyder, S. H. (2000). The calcineurin-binding protein cain is a negative regulator of synaptic vesicle endocytosis. J Biol Chem *275*, 34017-34020.

Lam, M., Dubyk, G., Chen, L., Nunez, G., Miesfeld, R. L., and Distelhorst, C. W. (1994). Evidence that Bcl-2 represses apoptosis by regulating endoplasmic reticulum-associated Ca^{2+} fluxes. Proc Natl Acad Sci USA *91*, 6569-6573.

Lanctot, P. M., Leclerc, P. C., Escher, E., Guillemette, G., and Leduc, R. (2006). Role of N-glycan-dependent quality control in the cell-surface expression of the AT1 receptor. Biochem Biophys Res Commun *340*, 395-402.

Leach, M. R., Cohen-Doyle, M. F., Thomas, D. Y., and Williams, D. B. (2002). Localization of the Lectin, ERp57 Binding, and Polypeptide Binding Sites of Calnexin and Calreticulin. J Biol Chem *277*, 29686-29697.

Leach, M. R., and Williams, D. B. (2004). Lectin-deficient calnexin is capable of binding class I histocompatibility molecules in vivo and preventing their degradation. J Biol Chem *279*, 9072-9079.

Lebeche, D., Lucero, H. A., and Kaminer, B. (1994). Calcium binding properties of rabbit liver protein disulfide isomerase. Biochem Biophys Res Commun *202*, 556-561.

Lee, G. J., Roseman, A. M., Saibil, H. R., and Vierling, E. (1997). A small heat shock protein stably binds heat-denatured model substrates and can maintain a substrate in a folding-competent state. EMBO J *16*, 659-671.

Lee, K., Tirasophon, W., Shen, X., Michalak, M., Prywes, R., Okada, T., Yoshida, H., Mori, K., and Kaufman, R. J. (2002). IRE1-mediated unconventional mRNA splicing and S2P-mediated ATF6 cleavage merge to regulate XBP1 in signaling the unfolded protein response. Genes Dev *16*, 452-466.

Levinthal., C. (1968). Are there pathways for protein folding? . J Chim Phys *65*, 44–45.

Li, F., Mandal, M., Barnes, C. J., Vadlamudi, R. K., and Kumar, R. (2001a). Growth factor regulation of the molecular chaperone calnexin. Biochem Biophys Res Commun *289*, 725-732.

Li, L., Guerini, D., and Carafoli, E. (2000). Calcineurin controls the transcription of Na+/Ca2+ exchanger isoforms in developing cerebellar neurons. J Biol Chem *275*, 20903-20910.

Li, W. W., Alexandre, S., Cao, X., and Lee, A. S. (1993). Transactivation of the grp78 promoter by Ca^{2+} depletion. A comparative analysis with A23187 and the

endoplasmic reticulum Ca^{2+}-ATPase inhibitor thapsigargin. J Biol Chem *268*, 12003-12009.

Li, Y., and Camacho, P. (2004). Ca2+-dependent redox modulation of SERCA2b by ERp57. J Cell Biol *164*, 35-46.

Li, Z., and Srivastava, P. K. (1993). Tumor rejection antigen gp96/grp94 is an ATPase: implications for protein folding and antigen presentation. Embo J *12*, 3143-3151.

Li, Z., Stafford, W. F., and Bouvier, M. (2001b). The metal ion binding properties of calreticulin modulate its conformational flexibility and thermal stability. Biochemistry *40*, 11193-11201.

Lievremont, J. P., Rizzuto, R., Hendershot, L., and Meldolesi, J. (1997). BiP, a major chaperone protein of the endoplasmic reticulum lumen, plays a direct and important role in the storage of the rapidly exchanging pool of Ca^{2+}. J Biol Chem *272*, 30873-33089.

Lilley, B. N., and Ploegh, H. L. (2004). A membrane protein required for dislocation of misfolded proteins from the ER. Nature *429*, 834-840.

Lilley, B. N., and Ploegh, H. L. (2005). Multiprotein complexes that link dislocation, ubiquitination, and extraction of misfolded proteins from the endoplasmic reticulum membrane. Proc Natl Acad Sci U S A *102*, 14296-14301.

Linden, T., Doutheil, J., and Paschen, W. (1998). Role of calcium in the activation of erp72 and heme oxygenase-1 expression on depletion of endoplasmic reticulum calcium stores in rat neuronal cell culture. Neurosci Lett *247*, 103-106.

Liu, J., Farmer, J. D., Jr., Lane, W. S., Friedman, J., Weissman, I., and Schreiber, S. L. (1991). Calcineurin is a common target of cyclophilin-cyclosporin A and FKBP-FK506 complexes. Cell *66*, 807-815.

Liu, X., Kim, C. N., Yang, J., Jemmerson, R., and Wang, X. (1996). Induction of apoptotic program in cell-free extracts: requirement for dATP and cytochrome c. Cell *86*, 147-157.

Llewellyn, D. H., Kendall, J. M., Sheikh, F. N., and Campbell, A. K. (1996). Induction of calreticulin expression in HeLa cells by depletion of the endoplasmic reticulum Ca^{2+} store and inhibition of N-linked glycosylation. Biochem J *318*, 555-560.

Llewellyn, D. H., and Roderick, H. L. (1998). Overexpression of calreticulin fails to abolish its induction by perturbation of normal ER function. Biochem Cell Biol *76*, 875-880.

Lodish, H. F., and Kong, N. (1990). Perturbation of cellular calcium blocks exit of secretory proteins from the rough endoplasmic reticulum. J Biol Chem *265*, 10893-10899.

Lodish, H. F., Kong, N., and Wikstrom, L. (1992). Calcium is required for folding of newly made subunits of the asialoglycoprotein receptor within the endoplasmic reticulum. J Biol Chem *267*, 12753-12760.

Lu, K. P., and Means, A. R. (1993). Regulation of the cell cycle by calcium and calmodulin. Endocr Rev *14*, 40-58.

Lucero, H. A., and Kaminer, B. (1999). The role of calcium on the activity of ERcalcistorin/protein-disulfide isomerase and the significance of the C-terminal and its calcium binding. A comparison with mammalian protein-disulfide isomerase. J Biol Chem *274*, 3243-3251.

Lucero, H. A., Lebeche, D., and Kaminer, B. (1998). ERcalcistorin/protein-disulfide isomerase acts as a calcium storage protein in the endoplasmic reticulum of a living cell. Comparison with calreticulin and calsequestrin. J Biol Chem *273*, 9857-9863.

Lynch, J., Guo, L., Gelebart, P., Chilibeck, K., Xu, J., Molkentin, J. D., Agellon, L. B., and Michalak, M. (2005). Calreticulin signals upstream of calcineurin and MEF2C in a critical Ca(2+)-dependent signaling cascade. J Cell Biol *170*, 37-47.

Lynch, J., and Michalak, M. (2003). Calreticulin is an upstream regulator of calcineurin. Biochem Biophys Res Commun *311*, 1173-1179.

Ma, T. S., Mann, D. L., Lee, J. H., and Gallinghouse, G. J. (1999). SR compartment calcium and cell apoptosis in SERCA overexpression. Cell Calcium *26*, 25-36.

Ma, Y., and Hendershot, L. M. (2004). ER chaperone functions during normal and stress conditions. J Chem Neuroanat *28*, 51-65.

Maatta, J., Hallikas, O., Welti, S., Hilden, P., Schroder, J., and Kuismanen, E. (2000). Limited caspase cleavage of human BAP31. FEBS Lett *484*, 202-206.

MacLennan, D. H., and Wong, P. T. (1971). Isolation of a calcium-sequestering protein from sarcoplasmic reticulum. Proc Natl Acad Sci U S A *68*, 1231-1235.

Malyguine, A. M., Scott, J. E., and Dawson, J. R. (1998). The role of calnexin in NK-target cell interaction. Immunol Lett *61*, 67-71.

Mann, C. L., Bortner, C. D., Jewell, C. M., and Cidlowski, J. A. (2001). Glucocorticoid-induced plasma membrane depolarization during thymocyte apoptosis: association with cell shrinkage and degradation of the Na(+)/K(+)-adenosine triphosphatase. Endocrinology *142*, 5059-5068.

Manna, T., Sarkar, T., Poddar, A., Roychowdhury, M., Das, K. P., and Bhattacharyya, B. (2001). Chaperone-like activity of tubulin. binding and reactivation of unfolded substrate enzymes. J Biol Chem *276*, 39742-39747.

Mansuy, I. M., Mayford, M., Jacob, B., Kandel, E. R., and Bach, M. E. (1998). Restricted and regulated overexpression reveals calcineurin as a key component in the transition from short-term to long-term memory. Cell *92*, 39-49.

Mao, C., Tai, W. C., Bai, Y., Poizat, C., and Lee, A. S. (2006). In vivo regulation of GRP78/BiP transcription in the embryonic heart: Role of the ERSE and GATA-4. J Biol Chem.

Margolese, L., Waneck, G. L., Suzuki, C. K., Degen, E., Flavell, R. A., and Williams, D. B. (1993). Identification of the region on the class I histocompatibility molecule that interacts with the molecular chaperone, p88 (calnexin, IP90). J Biol Chem *268*, 17959-17966.

Martin, V., Groenendyk, J., Steiner, S. S., Guo, L., Dabrowska, M., Parker, J. M., Muller-Esterl, W., Opas, M., and Michalak, M. (2006). Identification by mutational analysis of amino acid residues essential in the chaperone function of calreticulin. J Biol Chem *281*, 2338-2346.

Marzo, I., Brenner, C., Zamzami, N., Jurgensmeier, J. M., Susin, S. A., Vieira, H. L., Prevost, M. C., Xie, Z., Matsuyama, S., Reed, J. C., and Kroemer, G. (1998). Bax and adenine nucleotide translocator cooperate in the mitochondrial control of apoptosis. Science *281*, 2027-2031.

Matsukawa, J., Matsuzawa, A., Takeda, K., and Ichijo, H. (2004). The ASK1-MAP kinase cascades in mammalian stress response. J Biochem (Tokyo) *136*, 261-265.

Mattson, M. P. (2000). Apoptosis in neurodegenerative disorders. Nat Rev Mol Cell Biol *1*, 120-129.

Mattson, M. P., and Chan, S. L. (2003). Calcium orchestrates apoptosis. Nat Cell Biol *5*, 1041-1043.

Matulis, D., Baumann, C. G., Bloomfield, V. A., and Lovrien, R. E. (1999). 1-anilino-8-naphthalene sulfonate as a protein conformational tightening agent. Biopolymers *49*, 451-458.

Matulis, D., and Lovrien, R. (1998). 1-Anilino-8-naphthalene sulfonate anion-protein binding depends primarily on ion pair formation. Biophys J *74*, 422-429.

Mayer, M. P., and Bukau, B. (2005). Hsp70 chaperones: cellular functions and molecular mechanism. Cell Mol Life Sci *62*, 670-684.

McClintock, D. S., Santore, M. T., Lee, V. Y., Brunelle, J., Budinger, G. R., Zong, W. X., Thompson, C. B., Hay, N., and Chandel, N. S. (2002). Bcl-2 family members and functional electron transport chain regulate oxygen deprivation-induced cell death. Mol Cell Biol *22*, 94-104.

Meier, P., Finch, A., and Evan, G. (2000). Apoptosis in development. Nature *407*, 796-801.

Meldolesi, J., and Pozzan, T. (1998). The endoplasmic reticulum Ca^{2+} store: a view from the lumen. Trends Biochem Sci *23*, 10-14.

Melnick, J., Dul, J. L., and Argon, Y. (1994). Sequential interaction of the chaperones BiP and GRP94 with immunoglobulin chains in the endoplasmic reticulum. Nature *370*, 373-375.

Menzel, R., Vogel, F., Kargel, E., and Schunck, W. H. (1997). Inducible membranes in yeast: relation to the unfolded-protein-response pathway. Yeast *13*, 1211-1229.

Mery, L., Mesaeli, N., Michalak, M., Opas, M., Lew, D. P., and Krause, K.-H. (1996). Overexpression of calreticulin increases intracellular Ca^{2+} storage and decreases store-operated Ca^{2+} influx. J Biol Chem *271*, 9332-9339.

Mesaeli, N., Nakamura, K., Opas, M., and Michalak, M. (2001). Endoplasmic reticulum in the heart, a forgotten organelle? Mol Cell Biochem *224*, 1-6.

Mesaeli, N., Nakamura, K., Zvaritch, E., Dickie, P., Dziak, E., Krause, K.-H., Opas, M., MacLennan, D. H., and Michalak, M. (1999). Calreticulin is essential for cardiac development. J Cell Biol *144*, 857-868.

Meunier, L., Usherwood, Y. K., Chung, K. T., and Hendershot, L. M. (2002). A subset of chaperones and folding enzymes form multiprotein complexes in endoplasmic reticulum to bind nascent proteins. Mol Biol Cell *13*, 4456-4469.

Meusser, B., Hirsch, C., Jarosch, E., and Sommer, T. (2005). ERAD: the long road to destruction. Nat Cell Biol *7*, 766-772.

Michalak, M., Corbett, E. F., Mesaeli, N., Nakamura, K., and Opas, M. (1999). Calreticulin: one protein, one gene, many functions. Biochem J *344*, 281-292.

Michalak, M., Lynch, J., Groenendyk, J., Guo, L., Robert Parker, J. M., and Opas, M. (2002a). Calreticulin in cardiac development and pathology. Biochim Biophys Acta *1600*, 32-37.

Michalak, M., Robert Parker, J. M., and Opas, M. (2002b). Ca^{2+} signaling and calcium binding chaperones of the endoplasmic reticulum. Cell Calcium *32*, 269-278.

Milner, R. E., Busaan, J., and Michalak, M. (1992a). Isolation and characterization of different C-terminal fragments of dystrophin expressed in *Escherichia coli*. Biochem J *288*, 1037-1044.

Milner, R. E., Famulski, K. S., and Michalak, M. (1992b). Calcium binding proteins in the sarcoplasmic/endoplasmic reticulum of muscle and nonmuscle cells. Mol Cell Biochem *112*, 1-13.

Molinari, M., Eriksson, K. K., Calanca, V., Galli, C., Cresswell, P., Michalak, M., and Helenius, A. (2004). Contrasting functions of calreticulin and calnexin in glycoprotein folding and ER quality control. Mol Cell *13*, 125-135.

Molinari, M., and Helenius, A. (1999). Glycoproteins form mixed disulphides with oxidoreductases during folding in living cells. Nature *402*, 90-93.

Molinari, M., and Helenius, A. (2000). Chaperone selection during glycoprotein translocation into the endoplasmic reticulum. Science *288*, 331-333.

Molkentin, J. D., Lu, J. R., Antos, C. L., Markham, B., Richardson, J., Robbins, J., Grant, S. R., and Olson, E. N. (1998). A calcineurin-dependent transcriptional pathway for cardiac hypertrophy. Cell *93*, 215-228.

Mori, K., Kawahara, T., Yoshida, H., Yanagi, H., and Yura, T. (1996). Signalling from endoplasmic reticulum to nucleus: transcription factor with a basic-leucine zipper motif is required for the unfolded protein- response pathway. Genes Cells *1*, 803-817.

Morishima, N., Nakanishi, K., Takenouchi, H., Shibata, T., and Yasuhiko, Y. (2002). An endoplasmic reticulum stress-specific caspase cascade in apoptosis. Cytochrome c-independent activation of caspase-9 by caspase-12. J Biol Chem *277*, 34287-34294.

Morrice, N. A., and Powis, S. J. (1998). A role for the thiol-dependent reductase ERp57 in the assembly of MHC class I molecules. Curr Biol *8*, 713-716.

Munro, S., and Pelham, H. R. (1987). A C-terminal signal prevents secretion of luminal ER proteins. Cell *48*, 899-907.

Nagata, S. (1997). Apoptosis by death factor. Cell *88*, 355-365.

Naismith, J. H., and Sprang, S. R. (1998). Modularity in the TNF-receptor family. Trends Biochem Sci *23*, 74-79.

Nakagawa, T., and Yuan, J. (2000). Cross-talk between two cysteine protease families. Activation of caspase-12 by calpain in apoptosis. J Cell Biol *150*, 887-894.

Nakagawa, T., Zhu, H., Morishima, N., Li, E., Xu, J., Yankner, B. A., and Yuan, J. (2000). Caspase-12 mediates endoplasmic-reticulum-specific apoptosis and cytotoxicity by amyloid-beta. Nature *403*, 98-103.

Nakamura, K., Bossy-Wetzel, E., Burns, K., Fadel, M., Lozyk, M., Goping, I. S., Opas, M., Bleackley, R. C., Green, D. R., and Michalak, M. (2000). Changes in endoplasmic reticulum luminal environment affect cell sensitivity to apoptosis. J Cell Biol *150*, 731-740.

Nakamura, K., Robertson, M., Liu, G., Dickie, P., Guo, J. Q., Duff, H. J., Opas, M., Kavanagh, K., and Michalak, M. (2001a). Complete heart block and sudden death in mouse over-expressing calreticulin. J Clin Invest *107*, 1245-1253.

Nakamura, K., Zuppini, A., Arnaudeau, S., Lynch, J., Ahsan, I., Krause, R., Papp, S., De Smedt, H., Parys, J. B., Müller-Esterl, W., *et al.* (2001b). Functional specialization of calreticulin domains. J Cell Biol *154*, 961-972.

Nakamura, M., Michikawa, Y., Baba, T., Okinaga, S., and Arai, K. (1992a). Calreticulin is present in the acrosome of spermatids of rat testis. Biochem Biophys Res Commun *186*, 668-673.

Nakamura, M., Oshio, S., Tamura, A., Okinaga, S., and Arai, K. (1992b). Antisera to calreticulin inhibits sperm motility in mice. Biochem Biophys Res Commun *186*, 984-990.

Nath, R., Raser, K. J., McGinnis, K., Nadimpalli, R., Stafford, D., and Wang, K. K. (1996). Effects of ICE-like protease and calpain inhibitors on neuronal apoptosis. Neuroreport *8*, 249-255.

Nauseef, W. M. (1999). Quality control in the endoplasmic reticulum: lessons from hereditary myeloperoxidase deficiency. J Lab Clin Med *134*, 215-221.

Nelson, M. R., and Chazin, W. J. (1998). Structures of EF-hand Ca(2+)-binding proteins: diversity in the organization, packing and response to Ca2+ binding. Biometals *11*, 297-318.

Ng, F. W., Nguyen, M., Kwan, T., Branton, P. E., Nicholson, D. W., Cromlish, J. A., and Shore, G. C. (1997). p28 Bap31, a Bcl-2/Bcl-XL- and procaspase-8-associated protein in the endoplasmic reticulum. J Cell Biol *139*, 327-338.

Ng, F. W. H., and Shore, G. C. (1998). Bcl-X_L cooperatively associates with the Bap31 complex in the endoplasmic reticulum, dependent on procaspase-8 and Ced-4 adaptor. J Biol Chem *273*, 3140-3143.

Nguyen, M., Breckenridge, D. G., Ducret, A., and Shore, G. C. (2000). Caspase-resistant BAP31 inhibits fas-mediated apoptotic membrane fragmentation and release of cytochrome c from mitochondria. Mol Cell Biol *20*, 6731-6740.

Nguyen, T. O., Capra, J. D., and Sontheimer, R. D. (1996). Calreticulin is transcriptionally upregulated by heat shock, calcium and heavy metals. Mol Immunol *33*, 379-386.

Nichols, J., Evans, E. P., and Smith, A. G. (1990). Establishment of germ-line-competent embryonic stem (ES) cells using differentiation inhibiting activity. Development *110*, 1341-1348.

Nicholson, D. W., and Thornberry, N. A. (1997). Caspases: killer proteases. Trends Biochem Sci *22*, 299-306.

Nigam, S. K., Goldberg, A. L., Ho, S., Rohde, M. F., Bush, K. T., and Sherman, M. (1994). A set of endoplasmic reticulum proteins possessing properties of molecular chaperones includes Ca^{2+}-binding proteins and members of the thioredoxin superfamily. J Biol Chem *269*, 1744-1749.

Nika, J., Rippel, S., and Hannig, E. M. (2001). Biochemical analysis of the eIF2beta gamma complex reveals a structural function for eIF2alpha in catalyzed nucleotide exchange. J Biol Chem *276*, 1051-1056.

Nilsson, T., and Warren, G. (1994). Retention and retrieval in the endoplasmic reticulum and the Golgi apparatus. Curr Opin Cell Biol *6*, 517-521.

Noiva, R. (1999). Protein disulfide isomerase: the multifunctional redox chaperone of the endoplasmic reticulum. Sem Cell Dev Biol *10*, 481-493.

Norbury, C. J., and Zhivotovsky, B. (2004). DNA damage-induced apoptosis. Oncogene *23*, 2797-2808.

Oakes, S. A., Opferman, J. T., Pozzan, T., Korsmeyer, S. J., and Scorrano, L. (2003). Regulation of endoplasmic reticulum Ca2+ dynamics by proapoptotic BCL-2 family members. Biochem Pharmacol *66*, 1335-1340.

Oda, Y., Hosokawa, N., Wada, I., and Nagata, K. (2003). EDEM as an acceptor of terminally misfolded glycoproteins released from calnexin. Science *299*, 1394-1397.

Oda, Y., Okada, T., Yoshida, H., Kaufman, R. J., Nagata, K., and Mori, K. (2006). Derlin-2 and Derlin-3 are regulated by the mammalian unfolded protein response and are required for ER-associated degradation. J Cell Biol *172*, 383-393.

Ohsako, S., Hayashi, Y., and Bunick, D. (1994). Molecular cloning and sequencing of calnexin-t. An abundant male germ cell-specific calcium-binding protein of the endoplasmic reticulum. J Biol Chem *269*, 14140-14148.

Okiyoneda, T., Harada, K., Takeya, M., Yamahira, K., Wada, I., Shuto, T., Suico, M. A., Hashimoto, Y., and Kai, H. (2004). Delta F508 CFTR pool in the endoplasmic reticulum is increased by calnexin overexpression. Mol Biol Cell *15*, 563-574.

Olivari, S., Galli, C., Alanen, H., Ruddock, L., and Molinari, M. (2005). A novel stress-induced EDEM variant regulating endoplasmic reticulum-associated glycoprotein degradation. J Biol Chem *280*, 2424-2428.

Oliver, J. D., Roderick, H. L., Llewellyn, D. H., and High, S. (1999). ERp57 Functions as a Subunit of Specific Complexes Formed with the ER Lectins Calreticulin and Calnexin. Mol Biol Cell *10*, 2573-2582.

Oliver, J. D., van der Wal, F. J., Bulleid, N. J., and High, S. (1997). Interaction of the thiol-dependent reductase ERp57 with nascent glycoproteins. Science *275*, 86-88.

Ostwald, T. J., and MacLennan, D. H. (1974). Isolation of a high affinity calcium-binding protein from sarcoplasmic reticulum. J Biol Chem *249*, 974-979.

Otteken, A., and Moss, B. (1996). Calreticulin interacts with newly synthesized human immunodeficiency virus type 1 envelope glycoprotein, suggesting a chaperone function similar to that of calnexin. J Biol Chem *271*, 97-103.

Ou, W. J., Bergeron, J. J., Li, Y., Kang, C. Y., and Thomas, D. Y. (1995). Conformational changes induced in the endoplasmic reticulum luminal domain of calnexin by Mg-ATP and Ca2+. J Biol Chem *270*, 18051-18059.

Ou, W. J., Thomas, D. Y., Bell, A. W., and Bergeron, J. J. (1992). Casein kinase II phosphorylation of signal sequence receptor alpha and the associated membrane chaperone calnexin. J Biol Chem *267*, 23789-23796.

Oubrahim, H., Chock, P. B., and Stadtman, E. R. (2002). Manganese(II) induces apoptotic cell death in NIH3T3 cells via a caspase-12-dependent pathway. J Biol Chem *277*, 20135-20138.

Pariat, M., Carillo, S., Molinari, M., Salvat, C., Debussche, L., Bracco, L., Milner, J., and Piechaczyk, M. (1997). Proteolysis by calpains: a possible contribution to degradation of p53. Mol Cell Biol *17*, 2806-2815.

Parodi, A. J. (2000). Protein glucosylation and its role in protein folding. Annu Rev Biochem *69*, 69-93.

Peaper, D. R., Wearsch, P. A., and Cresswell, P. (2005). Tapasin and ERp57 form a stable disulfide-linked dimer within the MHC class I peptide-loading complex. Embo J *24*, 3613-3623.

Pind, S., Riordan, J. R., and Williams, D. B. (1994). Participation of the endoplasmic reticulum chaperone calnexin (p88, IP90) in the biogenesis of the cystic fibrosis transmembrane conductance regulator. J Biol Chem *269*, 12784-12788.

Pinton, P., Ferrari, D., Magalhaes, P., Schulze-Osthoff, K., Di Virgilio, F., Pozzan, T., and Rizzuto, R. (2000). Reduced loading of intracellular Ca^{2+} stores and downregulation of capacitative Ca^{2+} influx in Bcl-2-overexpressing cells. J Cell Biol *148*, 857-862.

Pinton, P., Ferrari, D., Rapizzi, E., Di Virgilio, F., Pozzan, T., and Rizzuto, R. (2002). A role for calcium in Bcl-2 action? Biochimie *84*, 195-201.

Pipe, S. W., Morris, J. A., Shah, J., and Kaufman, R. J. (1998). Differential interaction of coagulation factor VIII and factor V with protein chaperones calnexin and calreticulin. J Biol Chem *273*, 8537-8544.

Pitts, K. R., Yoon, Y., Krueger, E. W., and McNiven, M. A. (1999). The dynamin-like protein DLP1 is essential for normal distribution and morphology of the

endoplasmic reticulum and mitochondria in mammalian cells. Mol Biol Cell *10*, 4403-4417.

Pollock, S., Kozlov, G., Pelletier, M. F., Trempe, J. F., Jansen, G., Sitnikov, D., Bergeron, J. J., Gehring, K., Ekiel, I., and Thomas, D. Y. (2004). Specific interaction of ERp57 and calnexin determined by NMR spectroscopy and an ER two-hybrid system. Embo J *23*, 1020-1029.

Popov, M., Tam, L. Y., Li, J., and Reithmeier, R. A. (1997). Mapping the ends of transmembrane segments in a polytopic membrane protein. Scanning N-glycosylation mutagenesis of extracytosolic loops in the anion exchanger, band 3. J Biol Chem *272*, 18325-18332.

Porat, A., and Elazar, Z. (2000). Regulation of intra-Golgi membrane transport by calcium. J Biol Chem *275*, 29233-29237.

Porcellini, S., Traggiai, E., Schenk, U., Ferrera, D., Matteoli, M., Lanzavecchia, A., Michalak, M., and Grassi, F. (2006). Regulation of peripheral T cell activation by calreticulin. J Exp Med *203*, 461-471.

Portzehl, H., Caldwell, P. C., and Rueegg, J. C. (1964). The Dependence of Contraction and Relaxation of Muscle Fibres from the Crab Maia Squinado on the Internal Concentration of Free Calcium Ions. Biochim Biophys Acta *79*, 581-591.

Potter, D. A., Tirnauer, J. S., Janssen, R., Croall, D. E., Hughes, C. N., Fiacco, K. A., Mier, J. W., Maki, M., and Herman, I. M. (1998). Calpain regulates actin remodeling during cell spreading. J Cell Biol *141*, 647-662.

Pozzan, T., Rizzuto, R., Volpe, P., and Meldolesi, J. (1994). Molecular and cellular physiology of intracellular calcium stores. Physiol Rev *74*, 595-636.

Prakash, S., and Matouschek, A. (2004). Protein unfolding in the cell. Trends Biochem Sci *29*, 593-600.

Prasad, S. A., Yewdell, J. W., Porgador, A., Sadasivan, B., Cresswell, P., and Bennink, J. R. (1998). Calnexin expression does not enhance the generation of MHC class I-peptide complexes. Eur J Immunol *28*, 907-913.

Primm, T. P., Walker, K. W., and Gilbert, H. F. (1996). Facilitated protein aggregation. Effects of calcium on the chaperone and anti-chaperone activity of protein disulfide-isomerase. J Biol Chem *271*, 33664-33669.

Prostko, C. R., Dholakia, J. N., Brostrom, M. A., and Brostrom, C. O. (1995). Activation of the double-stranded RNA-regulated protein kinase by depletion of endoplasmic reticular calcium stores. J Biol Chem *270*, 6211-6215.

Provencher, S. W., and Glöckner, J. (1981). Estimation of globular protein secondary structure from circular dichroism. Biochemistry *20*, 33-37.

Rajagopalan, S., Xu, Y., and Brenner, M. B. (1994). Retention of unassembled components of integral membrane proteins by calnexin. Science *263*, 387-390.

Rao, R. V., Castro-Obregon, S., Frankowski, H., Schuler, M., Stoka, V., del Rio, G., Bredesen, D. E., and Ellerby, H. M. (2002). Coupling endoplasmic reticulum stress to the cell death program. An Apaf-1-independent intrinsic pathway. J Biol Chem *277*, 21836-21842.

Rao, R. V., Ellerby, H. M., and Bredesen, D. E. (2004). Coupling endoplasmic reticulum stress to the cell death program. Cell Death Differ *11*, 372-380.

Rao, R. V., Hermel, E., Castro-Obregon, S., del Rio, G., Ellerby, L. M., Ellerby, H. M., and Bredesen, D. E. (2001). Coupling endoplasmic reticulum stress to the cell death program. Mechanism of caspase activation. J Biol Chem *276*, 33869-33874.

Rapoport, T. A., Rolls, M. M., and Jungnickel, B. (1996). Approaching the mechanism of protein transport across the ER membrane. Curr Opin Cell Biol *8*, 499-504.

Ray, M. K., Yang, J., Sundaram, S., and Stanley, P. (1991). A novel glycosylation phenotype expressed by Lec23, a Chinese hamster ovary mutant deficient in alpha-glucosidase I. J Biol Chem *266*, 22818-22285.

Remillard, C. V., and Yuan, J. X. (2004). Activation of K+ channels: an essential pathway in programmed cell death. Am J Physiol Lung Cell Mol Physiol *286*, L49-67.

Rizzuto, R., Duchen, M. R., and Pozzan, T. (2004). Flirting in little space: the ER/mitochondria Ca2+ liaison. Sci STKE *2004*, re1.

Rizzuto, R., Pinton, P., Ferrari, D., Chami, M., Szabadkai, G., Magalhaes, P. J., Di Virgilio, F., and Pozzan, T. (2003). Calcium and apoptosis: facts and hypotheses. Oncogene *22*, 8619-8627.

Roderick, H. L., Lechleiter, J. D., and Camacho, P. (2000). Cytosolic phosphorylation of calnexin controls intracellular Ca^{2+} oscillations via an interaction with SERCA2b. J Cell Biol *149*, 1235-1248.

Rokeach, L. A., Haselby, J. A., Meilof, J. F., Smeenk, R. J., Unnasch, T. R., Greene, B. M., and Hoch, S. O. (1991). Characterization of the autoantigen calreticulin. J Immunol *147*, 3031-3039.

Rosenbaum, E. E., Hardie, R. C., and Colley, N. J. (2006). Calnexin is essential for rhodopsin maturation, Ca2+ regulation, and photoreceptor cell survival. Neuron *49*, 229-241.

Rudd, P. M., Elliott, T., Cresswell, P., Wilson, I. A., and Dwek, R. A. (2001). Glycosylation and the immune system. Science *291*, 2370-2376.

Rudner, J., Lepple-Wienhues, A., Budach, W., Berschauer, J., Friedrich, B., Wesselborg, S., Schulze-Osthoff, K., and Belka, C. (2001). Wild-type, mitochondrial and ER-restricted Bcl-2 inhibit DNA damage-induced apoptosis but do not affect death receptor-induced apoptosis. J Cell Sci *114*, 4161-4172.

Russell, S. J., Ruddock, L. W., Salo, K. E., Oliver, J. D., Roebuck, Q. P., Llewellyn, D. H., Roderick, H. L., Koivunen, P., Myllyharju, J., and High, S. (2004). The primary substrate binding site in the b' domain of ERp57 is adapted for endoplasmic reticulum lectin association. J Biol Chem *279*, 18861-18869.

Rutkowski, D. T., and Kaufman, R. J. (2004). A trip to the ER: coping with stress. Trends Cell Biol *14*, 20-28.

Sadasivan, B., Lehner, P. J., Ortmann, B., Spies, T., and Cresswell, P. (1996). Roles for calreticulin and a novel glycoprotein, tapasin, in the interaction of MHC class I molecules with TAP. Immunity *5*, 103-114.

Sadasivan, B. K., Cariappa, A., Waneck, G. L., and Cresswell, P. (1995). Assembly, peptide loading, and transport of MHC class I molecules in a calnexin-negative cell line. Cold Spring Harb Symp Quant Biol *60*, 267-275.

Saito, Y., Ihara, Y., Leach, M. R., Cohen-Doyle, M. F., and Williams, D. B. (1999). Calreticulin functions *in vitro* as a molecular chaperone for both glycosylated and non-glycosylated proteins. EMBO J *18*, 6718-6729.

Sakahira, H., Enari, M., and Nagata, S. (1998). Cleavage of CAD inhibitor in CAD activation and DNA degradation during apoptosis. Nature *391*, 96-99.

Saleh, M., Vaillancourt, J. P., Graham, R. K., Huyck, M., Srinivasula, S. M., Alnemri, E. S., Steinberg, M. H., Nolan, V., Baldwin, C. T., Hotchkiss, R. S., *et al.* (2004). Differential modulation of endotoxin responsiveness by human caspase-12 polymorphisms. Nature *429*, 75-79.

Salomons, G. S., Brady, H. J., Verwijs-Janssen, M., Van Den Berg, J. D., Hart, A. A., Van Den Berg, H., Behrendt, H., Hahlen, K., and Smets, L. A. (1997). The Bax alpha:Bcl-2 ratio modulates the response to dexamethasone in leukaemic cells and is highly variable in childhood acute leukaemia. Int J Cancer *71*, 959-965.

Salvesen, G. S., and Renatus, M. (2002). Apoptosome: the seven-spoked death machine. Dev Cell *2*, 256-257.

Saraste, A., and Pulkki, K. (2000). Morphologic and biochemical hallmarks of apoptosis. Cardiovasc Res *45*, 528-537.

Sarkar, G., and Sommer, S. S. (1990). The "megaprimer" method of site-directed mutagenesis. Biotechniques *8*, 404-407.

Sartorius, U., Schmitz, I., and Krammer, P. H. (2001). Molecular mechanisms of death-receptor-mediated apoptosis. Chembiochem *2*, 20-29.

Scaffidi, C., Medema, J. P., Krammer, P. H., and Peter, M. E. (1997). FLICE is predominantly expressed as two functionally active isoforms, caspase-8/a and caspase-8/b. J Biol Chem *272*, 26953-26958.

Scheper, W., Thaminy, S., Kais, S., Stagljar, I., and Romisch, K. (2003). Coordination of N-glycosylation and protein translocation across the endoplasmic reticulum membrane by Sss1 protein. J Biol Chem *278*, 37998-38003.

Schinzel, A., Kaufmann, T., and Borner, C. (2004). Bcl-2 family members: intracellular targeting, membrane-insertion, and changes in subcellular localization. Biochim Biophys Acta *1644*, 95-105.

Schrag, J. D., Bergeron, J. J. M., Li, Y., Borisova, S., Hahn, M., Thomas, D. Y., and Cygler, M. (2001). The structure of calnexin, an ER chaperone involved in quality control of protein folding. Mol Cell *8*, 633-644.

Schroder, M., and Kaufman, R. J. (2005a). ER stress and the unfolded protein response. Mutat Res *569*, 29-63.

Schroder, M., and Kaufman, R. J. (2005b). The mammalian unfolded protein response. Annu Rev Biochem *74*, 739-789.

Schroder, M., and Kaufman, R. J. (2006). Divergent Roles of IRE1alpha and PERK in the Unfolded Protein Response. Curr Mol Med *6*, 5-36.

Schulz, R. A., and Yutzey, K. E. (2004). Calcineurin signaling and NFAT activation in cardiovascular and skeletal muscle development. Dev Biol *266*, 1-16.

Scott, J. E., and Dawson, J. R. (1995). MHC class I expression and transport in a calnexin-deficient cell line. J Immunol *155*, 143-148.

Shames, I., Fraser, A., Colby, J., Orfali, W., and Snipes, G. J. (2003). Phenotypic differences between peripheral myelin protein-22 (PMP22) and myelin protein zero (P0) mutations associated with Charcot-Marie-Tooth-related diseases. J Neuropathol Exp Neurol *62*, 751-764.

Shchepina, L. A., Pletjushkina, O. Y., Avetisyan, A. V., Bakeeva, L. E., Fetisova, E. K., Izyumov, D. S., Saprunova, V. B., Vyssokikh, M. Y., Chernyak, B. V., and Skulachev, V. P. (2002). Oligomycin, inhibitor of the F0 part of H+-ATP-synthase, suppresses the TNF-induced apoptosis. Oncogene *21*, 8149-8157.

Shen, J., Chen, X., Hendershot, L., and Prywes, R. (2002). ER stress regulation of ATF6 localization by dissociation of BiP/GRP78 binding and unmasking of Golgi localization signals. Dev Cell *3*, 99-111.

Sherman, M. Y., and Goldberg, A. L. (2001). Cellular defenses against unfolded proteins: a cell biologist thinks about neurodegenerative diseases. Neuron *29*, 15-32.

Shi, Y. (2002). Mechanisms of caspase activation and inhibition during apoptosis. Mol Cell *9*, 459-470.

Shi, Y. (2004). Caspase activation: revisiting the induced proximity model. Cell *117*, 855-858.

Shibasaki, F., and McKeon, F. (1995). Calcineurin functions in Ca(2+)-activated cell death in mammalian cells. J Cell Biol *131*, 735-743.

Shibatani, T., David, L. L., McCormack, A. L., Frueh, K., and Skach, W. R. (2005). Proteomic analysis of mammalian oligosaccharyltransferase reveals multiple subcomplexes that contain Sec61, TRAP, and two potential new subunits. Biochemistry *44*, 5982-5992.

Siegel, R. M., Muppidi, J., Roberts, M., Porter, M., and Wu, Z. (2003). Death receptor signaling and autoimmunity. Immunol Res *27*, 499-512.

Silberstein, S., and Gilmore, R. (1996). Biochemistry, molecular biology, and genetics of the oligosaccharyltransferase. Faseb J *10*, 849-858.

Silvennoinen, L., Myllyharju, J., Ruoppolo, M., Orru, S., Caterino, M., Kivirikko, K. I., and Koivunen, P. (2004). Identification and characterization of structural domains of human ERp57. Association with calreticulin requires several domains. J Biol Chem.

Sipione, S., Ewen, C., Shostak, I., Michalak, M., and Bleackley, R. C. (2005). Impaired cytolytic activity in calreticulin-deficient CTLs. J Immunol *174*, 3212-3219.

Sitia, R., and Braakman, I. (2003). Quality control in the endoplasmic reticulum protein factory. Nature *426*, 891-894.

Slee, E. A., Adrain, C., and Martin, S. J. (1999). Serial killers: ordering caspase activation events in apoptosis. Cell Death Differ *6*, 1067-1074.

Smith, M. J., and Koch, G. L. E. (1989). Multiple zones in the sequence of calreticulin (CRP55, calregulin, HACBP), a major calcium binding ER/SR protein. EMBO J *8*, 3581-3586.

Smyth, M. J., Kelly, J. M., Sutton, V. R., Davis, J. E., Browne, K. A., Sayers, T. J., and Trapani, J. A. (2001). Unlocking the secrets of cytotoxic granule proteins. J Leukoc Biol *70*, 18-29.

Sorensen, S., Ranheim, T., Bakken, K. S., Leren, T. P., and Kulseth, M. A. (2006). Retention of mutant low density lipoprotein receptor in endoplasmic reticulum (ER) leads to ER stress. J Biol Chem *281*, 468-476.

Soti, C., and Csermely, P. (2002). Chaperones and aging: role in neurodegeneration and in other civilizational diseases. Neurochem Int *41*, 383-389.

Spiro, R. G. (2004). Role of N-linked polymannose oligosaccharides in targeting glycoproteins for endoplasmic reticulum-associated degradation. Cell Mol Life Sci *61*, 1025-1041.

Stevens, F. J., and Argon, Y. (1999). Protein folding in the ER. Sem Cell Dev Biol *10*, 443-454.

Strasser, A., O'Connor, L., and Dixit, V. M. (2000). Apoptosis signaling. Annu Rev Biochem *69*, 217-245.

Studier, F. W., Rosenberg, A. H., Dunn, J. J., and Dubendorff, J. W. (1990). Use of T7 RNA polymerase to direct expression of cloned genes. Methods Enzymol *185*, 60-89.

Sun, L., Youn, H. D., Loh, C., Stolow, M., He, W., and Liu, J. O. (1998). Cabin 1, a negative regulator for calcineurin signaling in T lymphocytes. Immunity *8*, 703-711.

Swanson, C. A., Arkin, A. P., and Ross, J. (1997). An endogenous calcium oscillator may control early embryonic division. Proc Natl Acad Sci U S A *94*, 1194-1199.

Swanton, E., High, S., and Woodman, P. (2003). Role of calnexin in the glycan-independent quality control of proteolipid protein. Embo J *22*, 2948-2958.

Szabadkai, G., and Rizzuto, R. (2004). Participation of endoplasmic reticulum and mitochondrial calcium handling in apoptosis: more than just neighborhood? FEBS Lett *567*, 111-115.

Szabadkai, G., Simoni, A. M., and Rizzuto, R. (2003). Mitochondrial Ca2+ uptake requires sustained Ca2+ release from the endoplasmic reticulum. J Biol Chem *278*, 15153-15161.

Szegezdi, E., Fitzgerald, U., and Samali, A. (2003). Caspase-12 and ER-stress-mediated apoptosis: the story so far. Ann N Y Acad Sci *1010*, 186-194.

Tagliarino, C., Pink, J. J., Reinicke, K. E., Simmers, S. M., Wuerzberger-Davis, S. M., and Boothman, D. A. (2003). Mu-calpain activation in beta-lapachone-mediated apoptosis. Cancer Biol Ther *2*, 141-152.

Tanaka, Y., Nakamura, M., Matsui, T., Iizuka, N., Kondo, H., Tohma, S., Masuko, K., Yudoh, K., Nakamura, H., Nishioka, K., *et al.* (2006). Proteomic surveillance of autoantigens in relapsing polychondritis. Microbiol Immunol *50*, 117-126.

Tantral, L., Malathi, K., Kohyama, S., Silane, M., Berenstein, A., and Jayaraman, T. (2004). Intracellular calcium release is required for caspase-3 and -9 activation. Cell Biochem Funct *22*, 35-40.

Tatu, U., and Helenius, A. (1997). Interactions between newly synthesized glycoproteins, calnexin and a network of resident chaperones in the endoplasmic reticulum. J Cell Biol *136*, 555-565.

Taylor, C. W., and Laude, A. J. (2002). IP3 receptors and their regulation by calmodulin and cytosolic Ca2+. Cell Calcium *32*, 321-334.

Thammavongsa, V., Mancino, L., and Raghavan, M. (2005). Polypeptide substrate recognition by calnexin requires specific conformations of the calnexin protein. J Biol Chem *280*, 33497-33505.

Thatte, U., and Dahanukar, S. (1997). Apoptosis: clinical relevance and pharmacological manipulation. Drugs *54*, 511-532.

Thomson, S. P., and Williams, D. B. (2005). Delineation of the lectin site of the molecular chaperone calreticulin. Cell Stress Chaperones *10*, 242-251.

Thornberry, N. A., and Lazebnik, Y. (1998). Caspases: enemies within. Science *281*, 1312-1316.

Tirasophon, W., Welihinda, A. A., and Kaufman, R. J. (1998). A stress response pathway from the endoplasmic reticulum to the nucleus requires a novel bifunctional protein kinase/endoribonuclease (Ire1p) in mammalian cells. Genes Dev *12*, 1812-1824.

Tjoelker, L. W., Seyfried, C. E., Eddy, R. L., Jr., Byers, M. G., Shows, T. B., Calderon, J., and Gray, P. W. (1994). Human, mouse, and rat calnexin cDNA cloning: identification of potential calcium binding motifs and gene localization to human chromosome 5. Biochemistry *33*, 3229-3236.

Towbin, H., Staehelin, T., and Gordon, J. (1979). Electrophoretic transfer of proteins from polyacrylamide gels to nitrocellulose sheets: procedure and some applications. Proc Natl Acad Sci USA *76*, 4350-4354.

Tran, H., Pankov, R., Tran, S. D., Hampton, B., Burgess, W. H., and Yamada, K. M. (2002). Integrin clustering induces kinectin accumulation. J Cell Sci *115*, 2031-2040.

Trombetta, E. S., and Helenius, A. (2000). Conformational requirements for glycoprotein reglucosylation in the endoplasmic reticulum. J Cell Biol *148*, 1123-1130.

Tsai, B., Ye, Y., and Rapoport, T. A. (2002). Retro-translocation of proteins from the endoplasmic reticulum into the cytosol. Nat Rev Mol Cell Biol *3*, 246-255.

Turksen K, E. S. C., Humana Press.

Urano, F., Wang, X., Bertolotti, A., Zhang, Y., Chung, P., Harding, H. P., and Ron, D. (2000). Coupling of stress in the ER to activation of JNK protein kinases by transmembrane protein kinase IRE1. Science *287*, 664-666.

Van Delden, C., Favre, C., Spat, A., Cerny, E., Krause, K.-H., and Lew, D. P. (1992). Purification of an inositol 1,4,5-trisphosphate-binding calreticulin-containing intracellular compartment of HL-60 cells. Biochem J *281*, 651-656.

Van, P. N., Peter, F., and Soling, H.-D. (1989). Four intracisternal calcium-binding glycoproteins from rat liver microsomes with high affinity for calcium. No indication for calsequestrin-like proteins in inositol 1,4,5-trisphosphate-sensitive calcium sequestering rat liver vesicles. J Biol Chem *264*, 17494-17501.

Vance, J. E. (1990). Phospholipid synthesis in a membrane fraction associated with mitochondria. J Biol Chem *265*, 7248-7256.

Vangheluwe, P., Raeymaekers, L., Dode, L., and Wuytack, F. (2005). Modulating sarco(endo)plasmic reticulum Ca2+ ATPase 2 (SERCA2) activity: cell biological implications. Cell Calcium *38*, 291-302.

Vassilakos, A., Michalak, M., Lehrman, M. A., and Williams, D. B. (1998). Oligosaccharide binding characteristics of the molecular chaperones calnexin and calreticulin. Biochemistry *37*, 3480-3490.

Veinger, L., Diamant, S., Buchner, J., and Goloubinoff, P. (1998). The small heat-shock protein IbpB from *Escherichia coli* stabilizes stress-denatured proteins for subsequent refolding by a multichaperone network. J Biol Chem *273*, 11032-11037.

Wada, I., Rindress, D., Cameron, P. H., Ou, W. J., Doherty, J. J., 2nd, Louvard, D., Bell, A. W., Dignard, D., Thomas, D. Y., and Bergeron, J. J. (1991). SSR alpha and associated calnexin are major calcium binding proteins of the endoplasmic reticulum membrane. J Biol Chem *266*, 19599-19610.

Wanamaker, C. P., and Green, W. N. (2005). N-linked glycosylation is required for nicotinic receptor assembly but not for subunit associations with calnexin. J Biol Chem *280*, 33800-33810.

Wang, B., Nguyen, M., Breckenridge, D. G., Stojanovic, M., Clemons, P. A., Kuppig, S., and Shore, G. C. (2003). Uncleaved BAP31 in association with A4 protein at the endoplasmic reticulum is an inhibitor of Fas-initiated release of cytochrome c from mitochondria. J Biol Chem *278*, 14461-14468.

Wang, K. K. (2000). Calpain and caspase: can you tell the difference? Trends Neurosci *23*, 20-26.

Wang, X. (2001). The expanding role of mitochondria in apoptosis. Genes Dev *15*, 2922-2933.

Ware, F. E., Vassilakos, A., Peterson, P. A., Jackson, M. R., Lehrman, M. A., and Williams, D. B. (1995). The molecular chaperone calnexin binds Glc1Man9GlcNAc2 oligosaccharide as an initial step in recognizing unfolded glycoproteins. J Biol Chem *270*, 4697-4704.

Waser, M., Mesaeli, N., Spencer, C., and Michalak, M. (1997). Regulation of calreticulin gene expression by calcium. J Cell Biol *138*, 547-557.

Webb, S. E., and Miller, A. L. (2003). Calcium signalling during embryonic development. Nature Rev Mol Cell Biol *4*, 539-551.

Wei, J., Gaut, J. R., and Hendershot, L. M. (1995). *In vitro* dissociation of BiP-peptide complexes requires a conformational change in BiP after ATP binding but does not require ATP hydrolysis. J Biol Chem *270*, 26677-26682.

Whitaker, J. E., Haugland, R. P., Moore, P. L., Hewitt, P. C., and Reese, M. (1991). Cascade blue derivatives: water soluble, reactive, blue emission dyes evaluated as fluorescent labels and tracers. AnalŽ Biochem *198*, 119-130.

Whitley, P., Nilsson, I. M., and von Heijne, G. (1996). A nascent secretory protein may traverse the ribosome/endoplasmic reticulum translocase complex as an extended chain. J Biol Chem *271*, 6241-6244.

Widlak, P., and Garrard, W. T. (2005). Discovery, regulation, and action of the major apoptotic nucleases DFF40/CAD and endonuclease G. J Cell Biochem *94*, 1078-1087.

Williams, D. B. (2006). Beyond lectins: the calnexin/calreticulin chaperone system of the endoplasmic reticulum. J Cell Sci *119*, 615-623.

Williams, D. B., and Watts, T. H. (1995). Molecular chaperones in antigen presentation. Curr Opin Immunol *7*, 77-84.

Winder, D. G., Mansuy, I. M., Osman, M., Moallem, T. M., and Kandel, E. R. (1998). Genetic and pharmacological evidence for a novel, intermediate phase of long-term potentiation suppressed by calcineurin. Cell *92*, 25-37.

Wong, H. N., Ward, M. A., Bell, A. W., Chevet, E., Bains, S., Blackstock, W. P., Solari, R., Thomas, D. Y., and Bergeron, J. J. (1998). Conserved in vivo phosphorylation of calnexin at casein kinase II sites as well as a protein kinase C/proline-directed kinase site. J Biol Chem *273*, 17227-17235.

Wood, D. E., and Newcomb, E. W. (1999). Caspase-dependent activation of calpain during drug-induced apoptosis. J Biol Chem *274*, 8309-8315.

Wright, C. A., Kozik, P., Zacharias, M., and Springer, S. (2004). Tapasin and other chaperones: models of the MHC class I loading complex. Biol Chem *385*, 763-778.

Wu, H., Naya, F. J., McKinsey, T. A., Mercer, B., Shelton, J. M., Chin, E. R., Simard, A. R., Michel, R. N., Bassel-Duby, R., Olson, E. N., and Williams, R. S. (2000). MEF2 responds to multiple calcium-regulated signals in the control of skeletal muscle fiber type. EMBO J *19*, 1963-1973.

Yamamoto, K., Yoshida, H., Kokame, K., Kaufman, R. J., and Mori, K. (2004). Differential contributions of ATF6 and XBP1 to the activation of endoplasmic reticulum stress-responsive cis-acting elements ERSE, UPRE and ERSE-II. J Biochem (Tokyo) *136*, 343-350.

Yang, J., Liu, X., Bhalla, K., Kim, C. N., Ibrado, A. M., Cai, J., Peng, T. I., Jones, D. P., and Wang, X. (1997). Prevention of apoptosis by Bcl-2: release of cytochrome c from mitochondria blocked. Science *275*, 1129-1132.

Ye, Y., Shibata, Y., Kikkert, M., van Voorden, S., Wiertz, E., and Rapoport, T. A. (2005). Inaugural Article: Recruitment of the p97 ATPase and ubiquitin ligases to the site of retrotranslocation at the endoplasmic reticulum membrane. Proc Natl Acad Sci U S A *102*, 14132-14138.

Ye, Y., Shibata, Y., Yun, C., Ron, D., and Rapoport, T. A. (2004). A membrane protein complex mediates retro-translocation from the ER lumen into the cytosol. Nature *429*, 841-847.

Yoneda, T., Imaizumi, K., Oono, K., Yui, D., Gomi, F., Katayama, T., and Tohyama, M. (2001). Activation of caspase-12, an endoplastic reticulum (ER) resident caspase,

through tumor necrosis factor receptor-associated factor 2-dependent mechanism in response to the ER stress. J Biol Chem *276*, 13935-13940.

Yoon, Y., Pitts, K. R., and McNiven, M. A. (2001). Mammalian dynamin-like protein DLP1 tubulates membranes. Mol Biol Cell *12*, 2894-2905.

Yoshida, H., Haze, K., Yanagi, H., Yura, T., and Mori, K. (1998). Identification of the cis-acting endoplasmic reticulum stress response element responsible for transcriptional induction of mammalian glucose-regulated proteins - Involvement of basic leucine zipper transcription factors. J Biol Chem *273*, 33741-33749.

Yoshida, H., Matsui, T., Yamamoto, A., Okada, T., and Mori, K. (2001). XBP1 mRNA is induced by ATF6 and spliced by IRE1 in response to ER stress to produce a highly active transcription factor. Cell *107*, 881-891.

Zapun, A., Darby, N. J., Tessier, D. C., Michalak, M., Bergeron, J. J., and Thomas, D. Y. (1998). Enhanced catalysis of ribonuclease B folding by the interaction of calnexin or calreticulin with ERp57. J Biol Chem *273*, 6009-6012.

Zapun, A., Petrescu, S. M., Rudd, P. M., Dwek, R. A., Thomas, D. Y., and Bergeron, J. J. M. (1997). Conformation-independent binding of monoglucosylated ribonuclease B to calnexin. Cell *88*, 29-38.

Zhu, W., Cowie, A., Wasfy, G. W., Penn, L. Z., Leber, B., and Andrews, D. W. (1996). Bcl-2 mutants with restricted subcellular location reveal spatially distinct pathways for apoptosis in different cell types. EMBO J *15*, 4130-4141.

Zhuo, M., Zhang, W., Son, H., Mansuy, I., Sobel, R. A., Seidman, J., and Kandel, E. R. (1999). A selective role of calcineurin aalpha in synaptic depotentiation in hippocampus. Proc Natl Acad Sci USA *96*, 4650-4655.

Zong, W. X., Li, C., Hatzivassiliou, G., Lindsten, T., Yu, Q. C., Yuan, J., and Thompson, C. B. (2003). Bax and Bak can localize to the endoplasmic reticulum to initiate apoptosis. J Cell Biol *162*, 59-69.

Zuppini, A., Groenendyk, J., Cormack, L. A., Shore, G., Opas, M., Bleackley, R. C., and Michalak, M. (2002). Calnexin deficiency and endoplasmic reticulum stress-induced apoptosis. Biochemistry *41*, 2850-2858.